MCR-76-166

Contract NAS8-31535

Final Report

March 1976

ANALYTICAL TRADE STUDY OF THE STS PAYLOAD ENVIRONMENT

MARTIN MARIETTA

MCR-76-166

ANALYTICAL TRADE STUDY
OF THE
STS PAYLOAD ENVIRONMENT

By: W. P. Rader
Stan Barrett
John Baratono
Ken Payne

Prepared Under Contract No. NAS8-31535 by

Martin Marietta Corporation
Denver Division
Denver, Colorado

for

NATIONAL AERONAUTICS AND SPACE ADMINISTRATION

FOREWORD

This report presents the results of a study performed for the Marshall Space Flight Center under Contract NAS8-31535. The primary objective of this study was to develop, through design and cost effectiveness trade studies, conceptual noise suppression device designs, payload environmental impact/benefit data and a payload design and test philosophy, with an ultimate goal of reducing payload test costs.

The authors gratefully acknowledge the cooperation and contributions of Mr. Lester D. Saint of the Marshall Space Flight Center throughout this study.

CONTENTS

ILLUSTRATIONS

ILLUSTRATIONS (continued)

ILLUSTRATIONS (continued)

TABLES

INTRODUCTION

The current predicted acoustic environment for the shuttle orbiter payload bay will produce random vibration environments for payload components and subsystems which potentially will result in design, weight and cost penalties if means of protecting the payloads are not developed. This study was performed to define conceptual payload noise suppression devices, estimate the noise reduction achievable, and perform trade studies to determine the impact/benefit for shuttle payloads. The study consisted of six tasks as follows:

a. Define generic payload classes,

b. Establish STS payload test philosophy (for study purposes),

c. Estimate STS payload test costs,

d. Develop STS payload noise suppression devices,

e. Generate payload cost matrices,

f. Establish STS payload environmental requirements rationale and test philosophy.

The tasks were performed in a sequence of interrelated steps as shown in the flow chart in Figure 1.

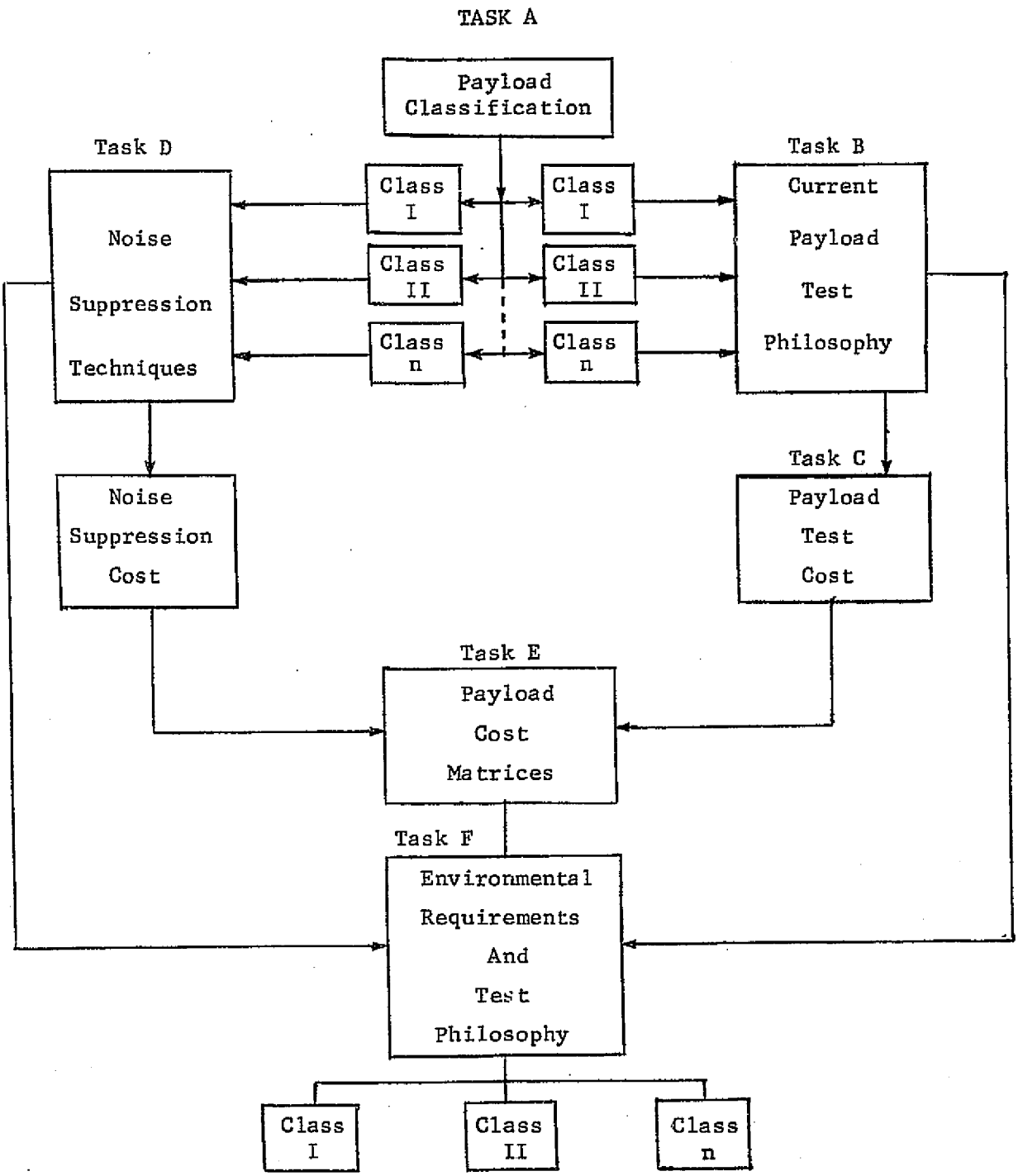

Figure 1. Task Flow and Interrelationships

Each of these tasks are described in detail in this report. Initial efforts were directed towards obtaining information on proposed payload characteristics and categorizing these payloads according to configuration, mission requirements and commonality of experiments and components. Current test philosophies used throughout the industry were collected in order to form a basis for estimating payload test costs.

The primary emphasis during this study was the development of noise suppression concepts for the different payload configurations and the evaluation of cost, weight and impact on the payload. Two model shroud configurations were fabricated and tested and the results are compared to other types of shroud configurations developed by other companies and NASA centers. This information was used to form a basis for cost effectiveness trade studies to assess the impact of noise suppression on environmental levels and associated test costs, and on test philosophy for the various payload classes.

A. PAYLOAD CLASSIFICATIONS

Knowledge of proposed payload characteristics and mission requirements which might require different design and test philosophies was essential in evaluating the need for noise suppression and establishing a basis and rationale for overall payload cost reduction. Information available from the Space Shuttle Payload Documents (References 1 through 3) was used to establish payload classes based on structural characteristics and mission requirements. In this report, the classification is based on the characteristics of individual experiments. The majority of payloads are comprised of multiple experiments; however, in some cases, the payload consists of a single experiment.

Structural Characteristics

From the viewpoint of providing noise protection shrouds, the experiments fall into three major categories:

1. pallet mounted,
2. IUS-TUG,
3. direct mounted.

For each major category, the experiments are listed along with their weights, dimensions and other pertinent information in the tables in Appendix A. In order to assess the number and sizes of shrouds required, the distribution of experiment dimensions for each of the major categories was determined.

a. Pallet Mounted - The distribution of lengths (in 3-meter increments) of pallet mounted experiments is shown in Figure 2. Of a total of 80 payloads identified, 55% can be protected by shrouds on a single 3-meter

pallet, and 85% can be protected by shrouds 9 meters or less in length.

b. IUS-TUG - The distribution of IUS-TUG experiment lengths is shown in Figure 3. From these data, it was determined that 92.5% of the experiment population could be protected by shrouds of various lengths of up to 9 meters (~30 feet). The distribution of the experiment population suggests that a modular type shroud concept would be weight effective.

There were a total of 52 experiments (for which dimensions were available) identifiable as flown in conjunction with TUG. Of this total, 8 (15.4%) have a diameter of 4.6 meters, and it was assumed that it would not be practical to provide a shroud for these because of space limitations within the payload bay. Of the remaining experiments, the distributions of lengths and diameters are shown in Figure 4, and 95.5% of these could be protected by shrouds of up to 6 meters long. Therefore, 80% of the experiments flown in conjunction with IUS-TUG could be protected by shrouds up to 6 meters long.

c. Direct Mounted - This class of experiments includes those such as the Space Telescope (ST) which are mounted directly to the payload bay structure. Of this class of experiments, 46.4% have diameters of 4.6 meters. Of the remaining population, 77% could be protected by shrouds of up to 5 meters long, as indicated by the data in Figure 5.

Therefore, noise protection could be provided for at least 41% of the total population of direct mounted experiments.

Mission Requirements

The tables (Appendix A) of experiment characteristics were examined to determine the distribution of the total number of flights for experiments

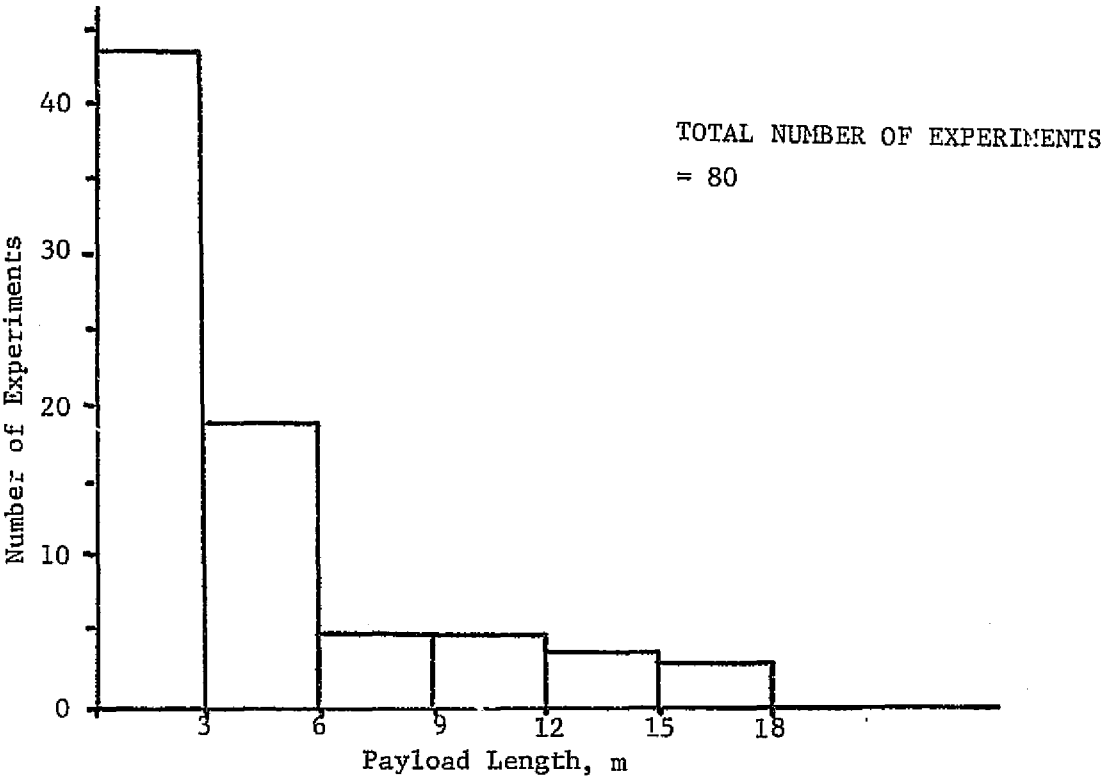

Figure 2. Distribution of Lengths of Pallet Mounted Experiments

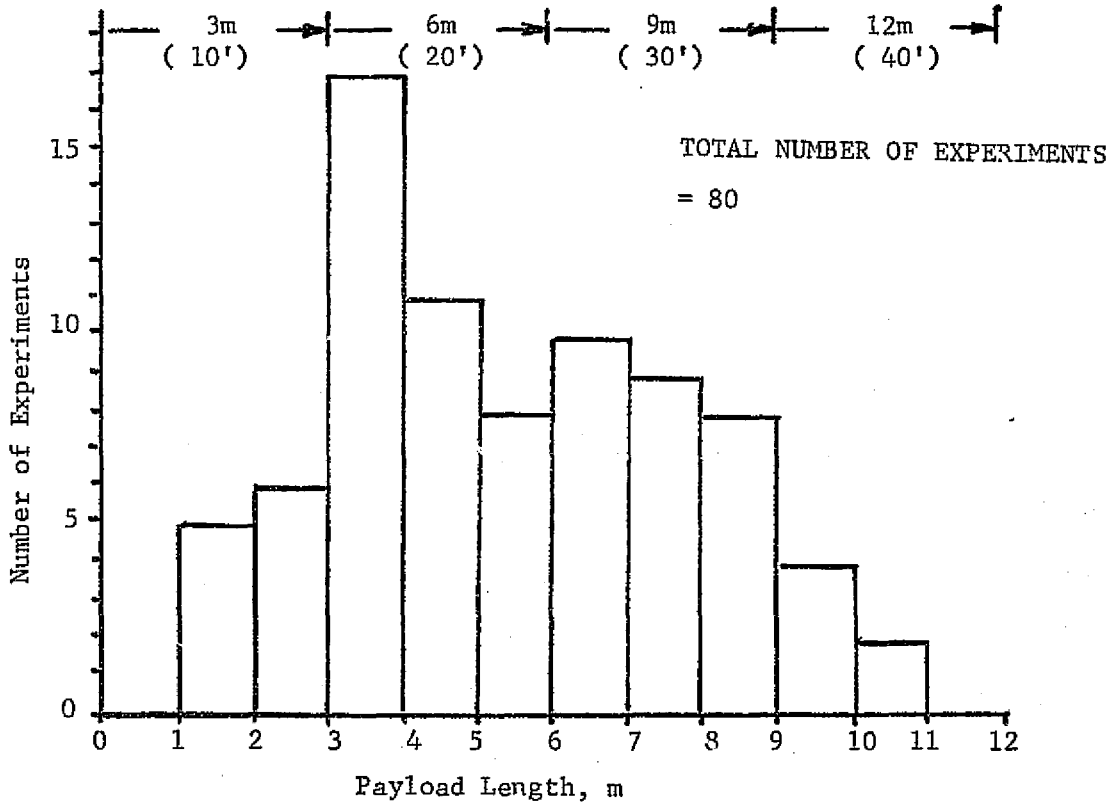

Figure 3. Distribution of Lengths of IUS-TUG Experiments

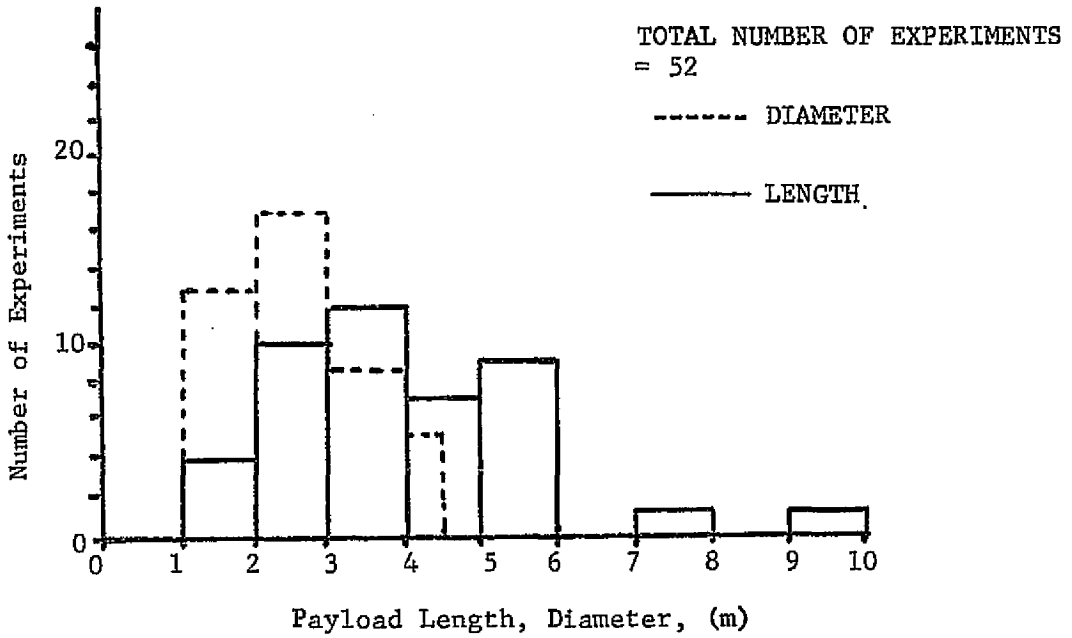

Figure 4. Distribution of Lengths and Diameters for Experiments Flown in Conjunction with IUS-TUG (Diameters Less Than 4.6 Meters)

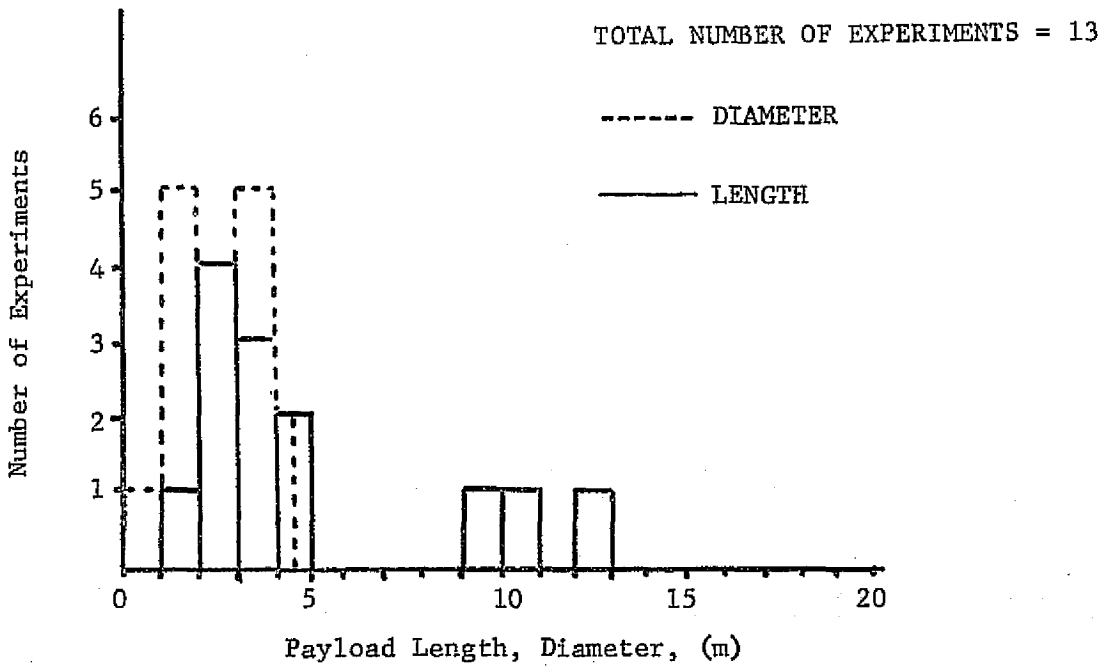

Figure 5. Distribution of Lengths and Diameters For Module (Self-Contained Experiments) with Diameters Less Than 4.6 Meters

of various lengths. These distributions are shown in Figures 6 and 7. These data, when combined with the previous distribution of number of experiments (Figures 2 through 5), provide an assessment of the percentages of total number of experiments for which shrouds of various lengths could provide protection. For pallet mounted experiments, this distribution is shown in Figure 8. The distributions for experiments flown in conjunction with IUS-TUG and for direct-mounted payloads are presented in Figure 9.

For pallet mounted experiments (Figure 8), it is significant to note that 95.6% of the total number of experiments to be flown could be protected by shrouds of lengths of 3 meters and 6 meters. An examination of Figure 9 indicates that 99.7% of the experiments flown in conjunction with IUS are 6 meters or less in length, and for the direct mounted experiments, 67.8% of the total experiments flown could be protected by shrouds of up to 5 meters long.

From the available information, contained in the tables in Appendix A, an evaluation of the structural characteristics and mission requirements of experiments in each major category can be summarized as follows.

a. Pallet Mounted - There are a total of 2762 experiment/flights for which information is available. Of these, 2641 (95.6%) can be covered by shrouds of 3 or 6 meters in length.

b. IUS-TUG - 80 payloads have been identified of which 74 (92.5%) could be protected by shrouds 9 meters long or less.

Experiments Flown in Conjunction with IUS - 365 (97.3%) of a total of 375 experiment/flights can be protected by shrouds 6 meters or less in length.

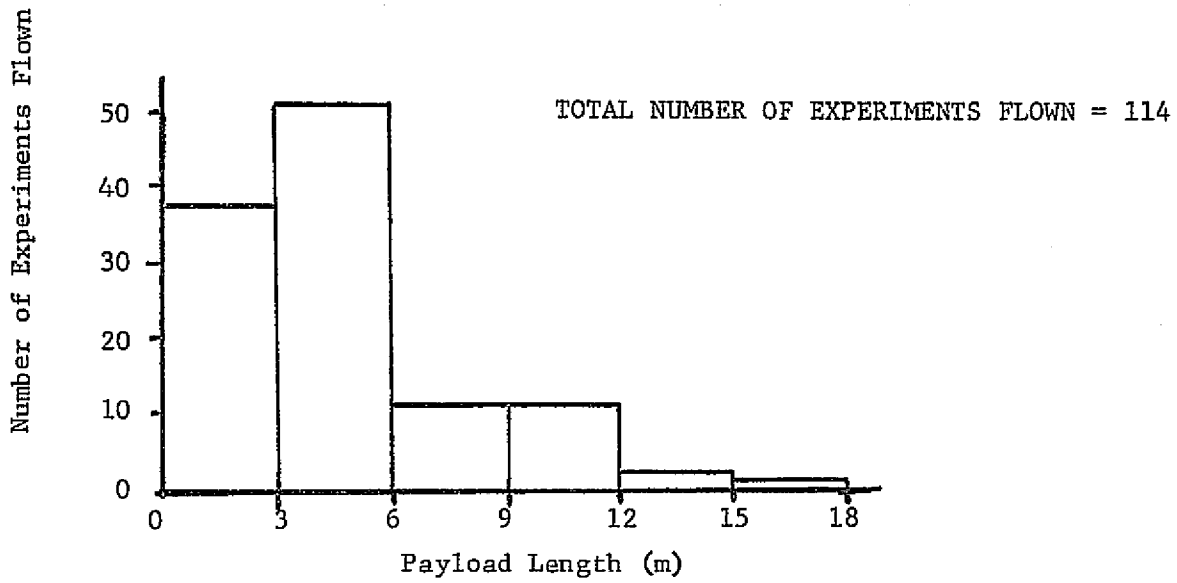

Figure 6. Distribution of Numbers of Experiments Flown as a Function of Length for Pallet Mounted Payloads

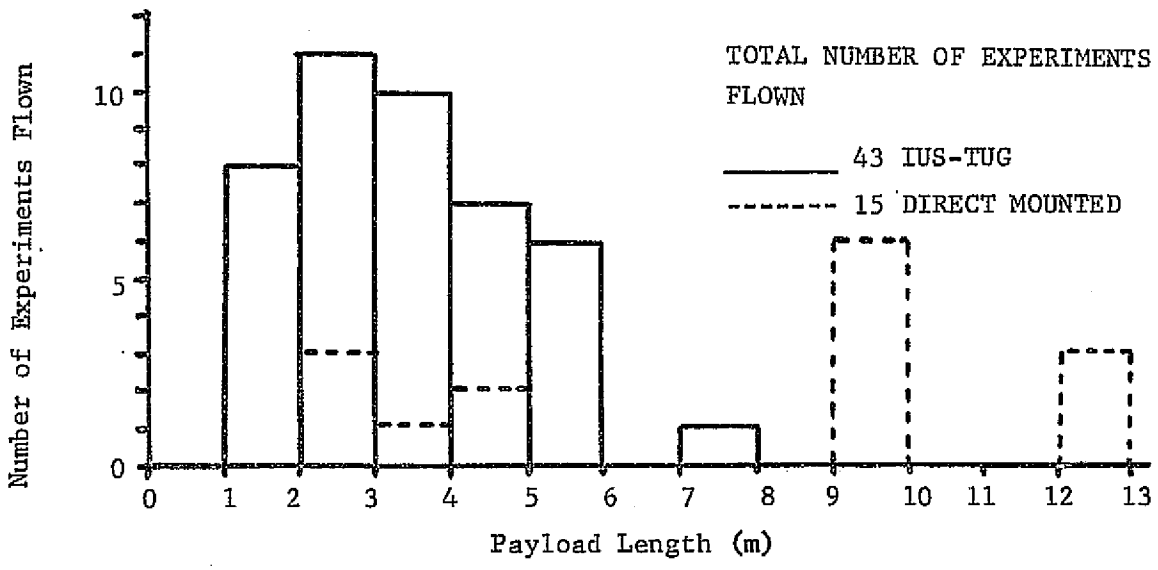

Figure 7. Distribution of Number of Experiments Flown as a Function of Length for Experiments in Conjunction with IUS-TUG and for Direct Mounted Payloads (Diameters Less Than 4.6 Meters)

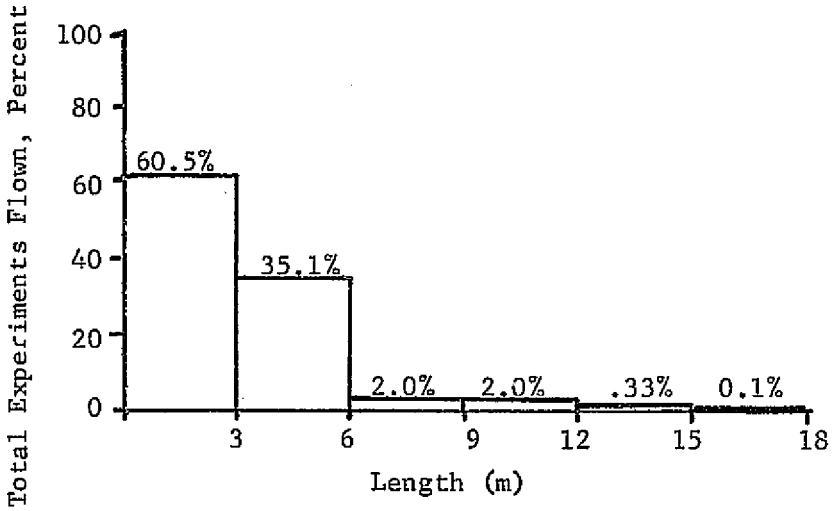

Figure 8. Distribution of Total Number of Experiments Flown Versus Length For Pallet Mounted Payloads

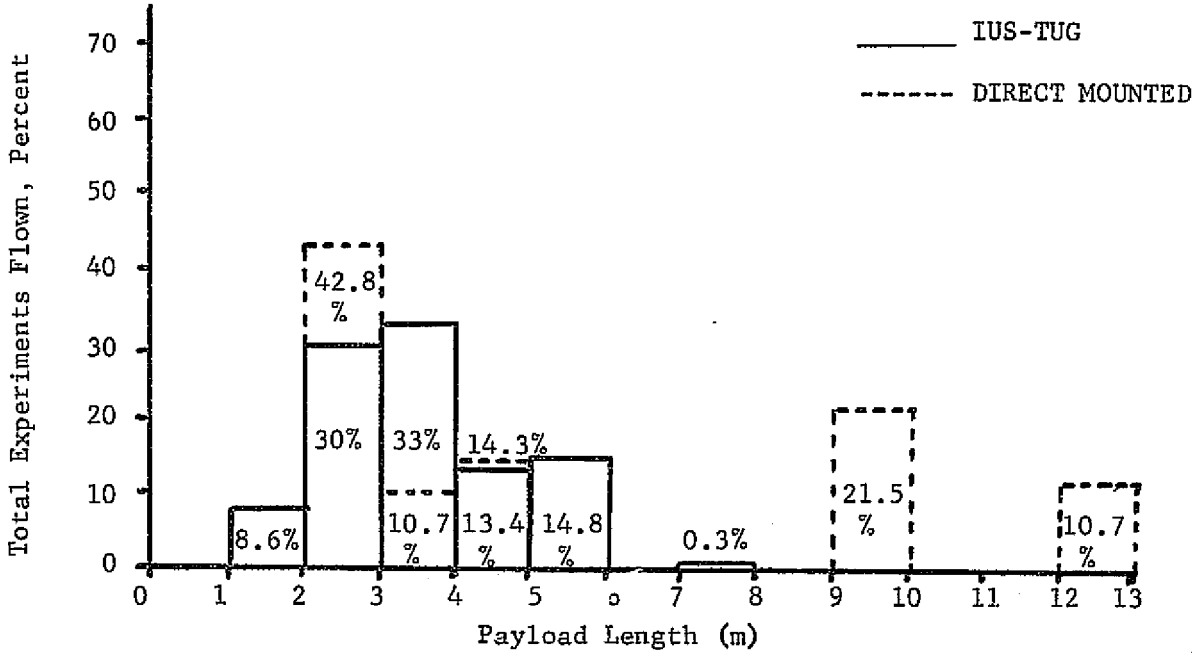

Figure 9. Distribution of Total Number of Experiments Flown as a Function of Length For Experiments in Conjunction With IUS-TUG and For Direct Mounted Payloads (Diameter Less Than 4.6 Meters)

c. Direct Mounted Payloads - Of a total of 42 experiment/flight combinations, 20 (47.6%) could be protected by shroud lengths of up to 5 meters.

Considering the total payload population, there is a total of 3259 experiment flights for which information is available, and 3100 (95%) of these could be provided noise protection by shrouds of up to 9 meters long. The remaining 5% include those experiments which have diameters of 4.6 meters and adequate space is not available to provide a shroud, a relatively small population requiring long shroud lengths, and a few payloads for which weight is not available for a shroud. In these cases, other noise reduction techniques such as end absorbers or baffles in the payload interior might provide a more cost-effective approach to noise protection.

Reliability Requirements

Single mission, planetary exploration experiments will require an extensive test program including component, subsystem and system level tests in order to achieve the high reliability required for this type of mission. On the other hand, it may be cost effective to assign a lower reliability requirement to multi-mission experiments such as those associated with Spacelab, earth resources exploration, and others which can be returned, repaired and reflown. For example, the single mission, planetary exploration experiments might require a 97.5% confidence level, whereas an 80% confidence level might be adequate for the multi-mission type experiments. Based on a Gaussian distribution of the random vibration environment, the difference between the 97.5% and 80% confidence

levels could result in approximately a factor of 2 decrease in test level for the multi-mission experiments. The reduction in test failures resulting from the lower test levels can produce significant test program cost savings as described later in Section C, STS PAYLOAD COST ESTIMATES, under the Effect of Current Philosophy on Test Costs. There is, of course, an associated increase in risk of flight failure.

In the experiment classification tables in Appendix A, there are 141 experiments for which the mission requirements information was available. Of this total, 122 are single mission experiments, including the 80 IUS payloads which are assumed to be single mission experiments. Therefore, a high reliability requirement should be assigned to the majority (86.5%) of shuttle experiments.

Experiment Complexity - The available information on payloads was reviewed to attempt to formulate sub-classes on the basis of complexity. Unfortunately, sufficient information was not available on which to make definitive classifications. Therefore, for purposes of analyzing test program costs, we have defined two arbitrary payload classifications: i.e., "simple" and "complex". A "simple" payload is comprised of 20 components and subsystems, whereas a "complex" payload is made up of 100 components and subsystems.

Experiment/Component Commonality

Experiment/component commonality matrices are presented in Appendix A, Tables A-6, A-7 and A-8. These matrices, which identify components/subsystems which are common to 2 or more experiments, when combined with the number of flights per experiment identified in Tables A-2, A-4 and

A-5, provide information on which to base fatigue considerations and test philosophy.

The distribution of components (in percent) with number of experiments is as follows.

	Number of Experiments										
	2	3	4	5	8	9	11	12	13	14	19
Percentage of Components	71	13.3	4.4	2.8	1.6	0.4	0.8	0.4	2.0	0.8	2.4

Of the total number of experiments identified in the tables in Appendix A, information on the number of missions was not available for 41.3%. For those experiments for which the number of flights could be identified, the distribution of the number of components with experiment/missions is as follows.

	Number of Missions							
	1	2	3	5	8	10	11	15
Percentage of Components	68.3	5.2	.42	3.5	1.9	14.2	3.3	3.1

If this distribution can be considered to be representative of the total component population, then increased test exposure time for fatigue need only be considered for 31.7% of the components to be flown on Shuttle payloads.

To obtain an assessment of the distribution of components with

experiments and number of missions, the following chart was prepared.

Number of Missions	Number of Experiments										
	2	3	4	5	8	9	11	12	13	14	19
	Percentage of Components										
1	15.24	9.81			3.34	1.25	1.67	2.10	13.78	2.30	18.79
2	2.71	.63					.21		.21	.21	1.25
3					.42						
5	2.3										1.25
8		1.88									
10	12.5	.62	.62				.42				
11	1.46	1.88									
15	1.25	1.88									
TOTALS	35.5	16.7	.6		3.8	1.3	2.3	2.1	14.0	2.5	21.3

In this chart, 14% of the components are common to 13 different experiments and 21.3% are common to 19 experiments. Referring to Tables A-7 and A-8 in Appendix A, components SS001 through SS009, it is evident that these components are associated with propulsion and control of IUS TUG experiments and may warrant special consideration for reliability and fatigue aspects.

B. STS PAYLOAD TEST PHILOSOPHY

An industry and literature survey was conducted to collect and compare the various test philosophies used throughout the industry in order to form a basis for estimating payload test costs. Significant differences in test requirements and dynamic test practices for spacecraft exist among the military, NASA and commercial programs. These differences exist in not only the confidence level bases and test factors used, but also in where the emphasis is placed in verifying spacecraft design capability. For example, at Goddard Space Flight Center, the "general philosophy is to develop a spacecraft that passes the required system level test requirements as modified by flight loads analysis" (Reference 4), whereas the Air Force requires extensive environmental testing at both the component and system level. At the Marshall Space Flight Center, the emphasis is placed on component testing using an early acoustic development test to establish component test criteria.

The bases for establishing test levels and range of test factors used are summarized in Figure 10. In this figure, the confidence levels and test factors used are assumed to be based on the same flight data and normalized to a mean flight vibration level of 1.0. On this basis, MSFC would establish the qualification test requirement as the 97.5% confidence level of the flight data, whereas the Air Force, in accordance with MIL STD 1540A, would establish an acceptance test requirement at the 95% confidence level with a 6 dB margin for qualification testing, a factor of 3.36 times higher than the MSFC qualification requirement.

The concept of the "proto-flight" vehicle has gained considerable

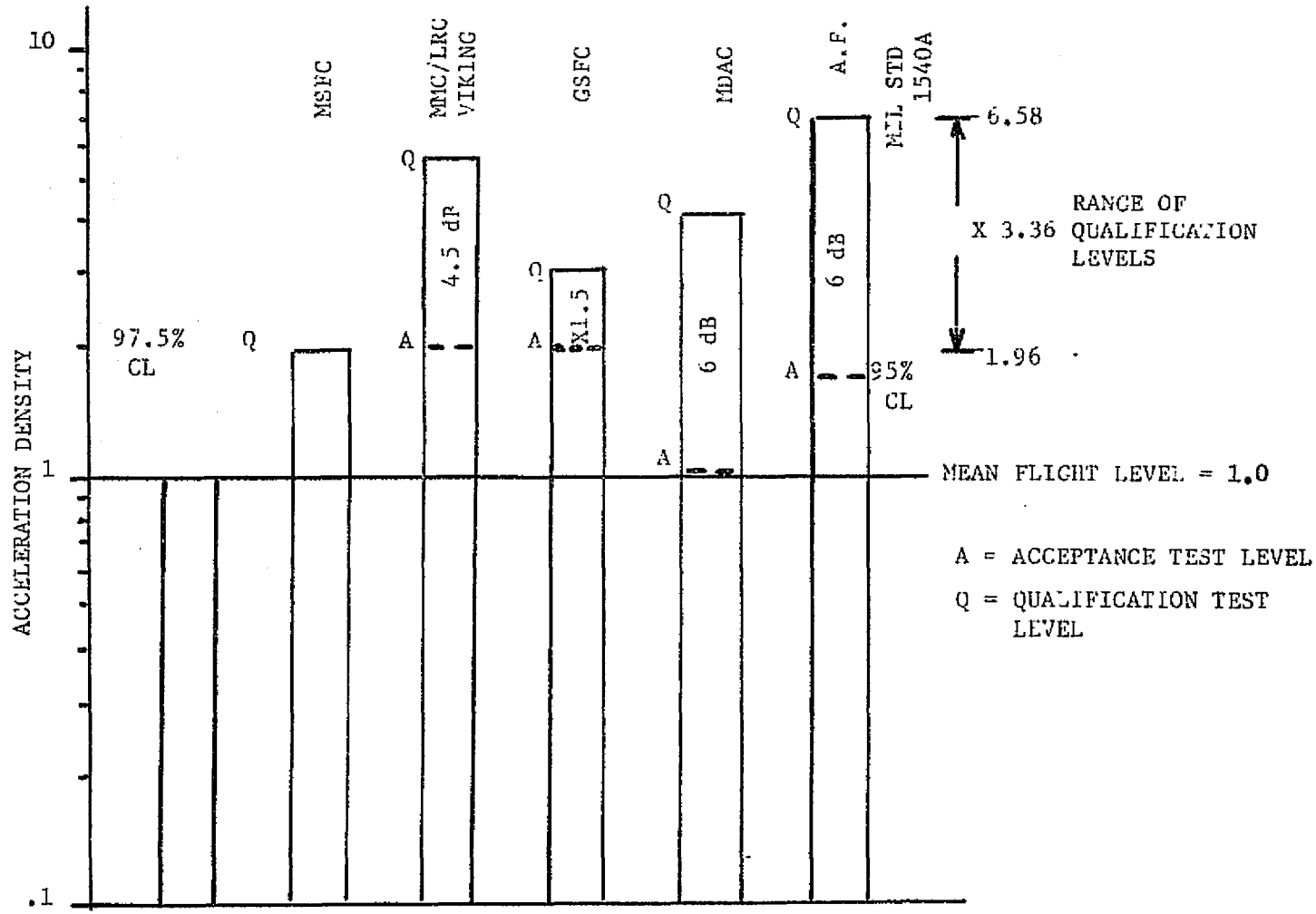

Figure 10. Comparison of Bases for Test Requirements

importance with the current emphasis on reducing test costs. Developed initially at the Goddard Space Flight Center, where a number of one-of-a-kind spacecraft have been built, the proto-flight vehicle approach should be cost effective for many of the major Shuttle experiments. It is estimated that approximately 86% of the Shuttle experiments would fall into this category, based on the information discussed in Section A, PAYLOAD CLASSIFICATIONS.

Although the established GSFC policy had required that a prototype vehicle, used for qualification testing, would precede the flight spacecraft, escalating costs forced an examination of alternatives to this policy. One alternative was to omit the test on the prototype vehicle, and an evaluation of the cost effectiveness of performing a system level vibration test on a prototype spacecraft was conducted by Stahle (Reference 5). Major factors considered included the severity of the vibration environment, the complexity of the spacecraft (as indicated by its weight), the costs of the spacecraft and the test, and reliability requirements. Stahle showed that the system level test provides a significant cost reduction if the environment is severe, the spacecraft is complex and a large number of operational spacecraft are required. If the opposite conditions apply, the test would increase the total expected program cost. Thus, in the present application, a very effective shroud would increase the feasibility of omitting the system level test. However, although many of the Shuttle payloads will be very complex, in the majority of cases they will be "one-of-a-kind", so that the overall situation is not clear-cut, and more work is required in order to establish guidelines applicable to the Shuttle test philosophy.

The proto-flight concept was another alternative which appeared to offer a reduction in test program costs. Consequently, in both the Interplanetary Monitoring Platform (IMP) and Radio Astronomy Explorer (RAE) projects, a single spacecraft was taken through a proto-flight test program and then successfully launched. A study of the cost effectiveness of the proto-flight approach was performed by Boeckel and Timmins (Reference 6) at GSFC. It was found that the most economical way to conduct an evaluation program on a one-of-a-kind payload is to use a test plan that requires one flight article with two sets of components. A large number of interacting factors were considered, including variability of hardware quality, the probability of failure at both component and system test level, the ratio of component-to-system test effectiveness and three different test plans.

From the results of the GSFC study, it is concluded that the proto-flight approach should be investigated for use in Shuttle payload testing and will probably be cost effective in a majority of cases. Since considerable commonality between components and even subsystems exists in the Shuttle program, it may be desirable on certain payloads to select a level of assembly for testing which is lower than the all-up system level. For example, in a payload consisting of several experiments using common components which have been qualified at the component level, it may be feasible to perform qualification testing on the individual experiments, as they become available, in lieu of a full system test. Interfaces between experiments would normally be minimal, and scheduling of the test program would be simplified. As the full system became available its testing could then be limited to a final functional check.

In order to estimate payload test costs, a baseline test philosophy was established, incorporating the following assumptions:

1. the acoustic environment during liftoff will be as currently defined in NASA document JSC 07700, with an overall level of 145 dB;
2. input spectrum shapes for component and system level tests will be conventional; therefore, the cost of a particular test will not be directly affected by the test level;
3. since the qualification test levels will be relatively high, it is assumed for present purposes that all payloads will be tested;
4. the number of failures experienced during test will be proportional to the test level and, therefore, directly related to the test factor applied;
5. finally, it is assumed that a payload or experiment which fails its initial test will be refurbished by having its failed components removed, modified and replaced, and will then be retested. A single cycle of modify/retest is assumed to be sufficient, so that a modified unit will always pass the retest.

C. STS PAYLOAD TEST COST ESTIMATES

A cost model was formulated to evaluate test costs for different payload classes based on current test philosophy, and to provide a rational mathematical basis for examining cost effectiveness of using acoustic shrouds over selected payloads in order to attenuate the acoustic environment. Factors affecting the decision of whether or not to use a shroud are indicated below:

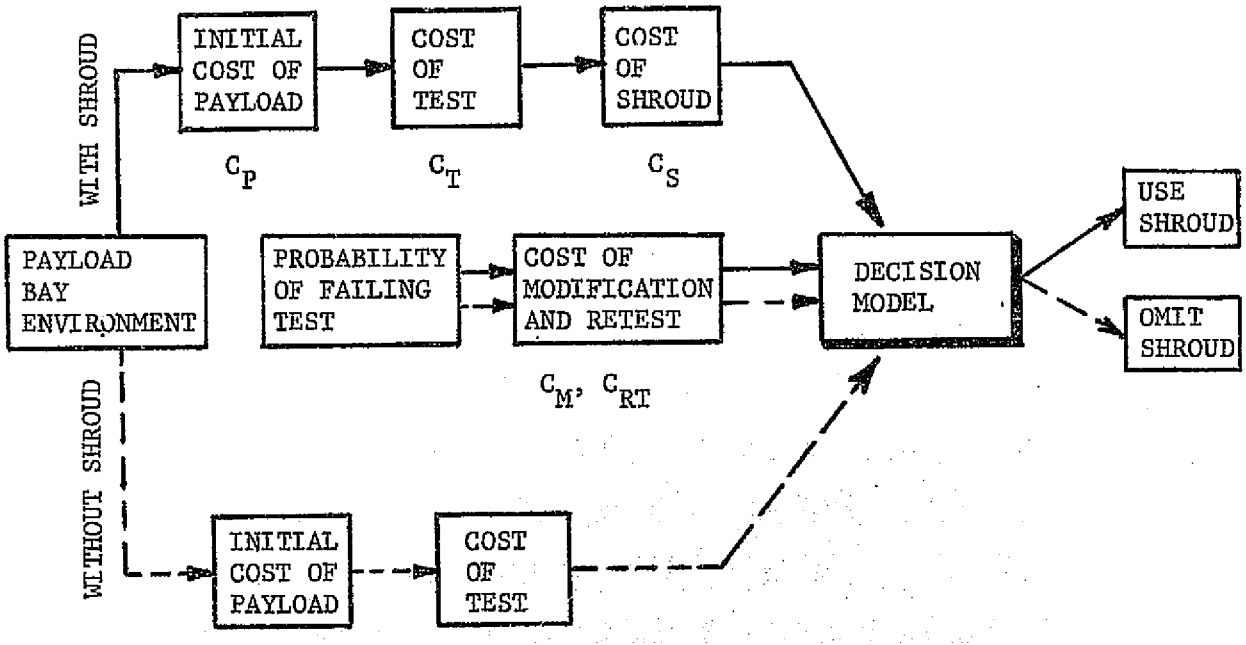

Figure 11. Elements of Decision Model

The cost model is intended to be flexible enough to be applicable to system, subsystem and component level tests. As outlined in Figure 11, the approach is quite simple, and does not include all of the factors contributing to total payloads costs, such as the integration costs which would be involved in a system test, or costs associated with the actual launch. However, since the emphasis is on investigating the difference

in costs related to shroud usage, the omissions are not considered to be important. The model could be applied to a complex multipath test program, such as the proto-flight approach, without major revision.

A literature and industry survey was conducted to obtain information on which to base a practical assessment of potential cost impact if payload shrouds are used. The primary parameters of interest were the range of test costs and the failure rate (or percentage of failures) as a function of acoustically induced vibration. The data obtained indicates a range of costs of system level acoustic tests as follows:

Cost*	Spacecraft Type
$10-$25K	a. Pioneer, Vela
$35-$50K	b. Delta Second Stage
$50-$100K	c. ATS-F, ERTS

* cost range is dependent upon amount of instrumentation

We feel that, in general, the ranges of costs for the three types of spacecraft (a, b and c) will be applicable to pallet mounted experiments, IUS payloads and direct mounted, self-contained payloads, respectively.

One of the major cost drivers in a spacecraft test program is the testing of components. A survey was made of the component qualification test files at the Martin Marietta Corporation to determine the cost of random vibration tests in recent years. Information on 44 components was obtained, and the distribution of test costs is shown in Figure 12. The average test cost was $4737, and approximately 66% of the component tests cost less than $5000. The average test cost of approximately $5000 was substantiated by the survey of companies and agencies.

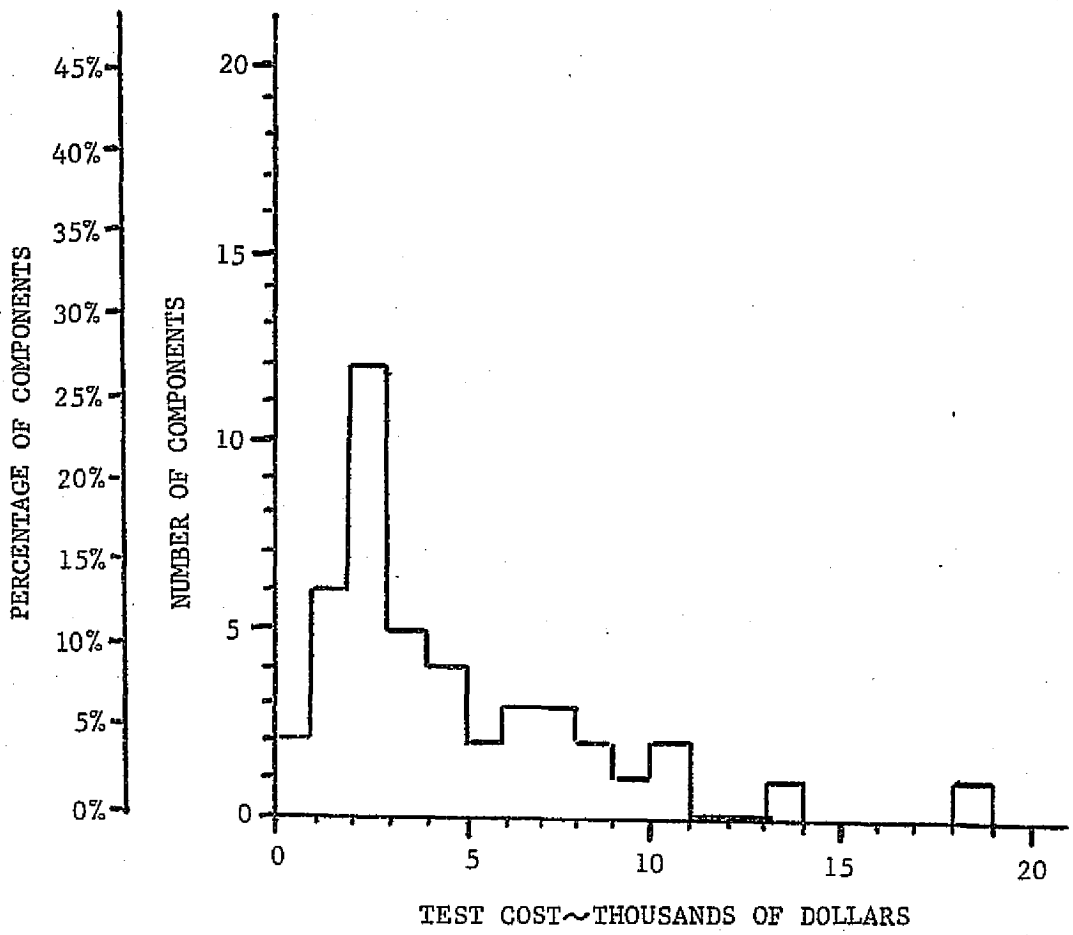

Figure 12. Distribution of Test Cost

The relationship between failure rate and vibration level was a much more difficult parameter to determine, but was necessary if the effects of noise attenuation were to be evaluated. The factor used in our cost model was based primarily on data obtained from Reference 7, where it was possible to determine the change in failure rate as a function of vibration level for 638 components of 9 different types as shown in Figure 13. With the exception of solenoid valves, these data indicate that for the range of vibration levels from 5 to 30 g's rms, the change in failure rate is approximately linearly related to the change in vibration level. It should be recognized that the Saturn failure rate data presented in Figure 13 are based on tests of valves, connectors, switches, etc., and may not be representative of electronic "black boxes". During this study, an extensive survey of the industry was conducted to obtain information relative to failure rate as a function of vibration level for all types of components. The very limited information obtained was inconclusive, and our cost analyses are based on the Saturn failure rate data. Since the reduction in vibration level is directly related to the noise attenuation, the cost model assumes that the change in failure rate is directly proportional to the noise reduction factor, i.e., reducing the noise level and associated vibration by 6 dB will result in 50% fewer failures for a particular payload.

If a test were performed at the payload bay level G_P a maximum of N_P component failures would be expected to occur in time T, whereas if the test were performed at a reduced level G_R (corresponding to the environment inside a shroud) a smaller number of failures N_R would be predicted.

65 V_S - Valves, Solenoid
98 V_{VR} - Valves, Vent & Relief
62 V_{SO} - Valves, Shut-Off
61 P - Pumps
64 R_P - Regulators, Pressure

36 C_e - Connectors, Electrical
136 S_e - Switches, Electrical
63 S_P - Switches, Pressure
53 T_t - Transducers, Temp.

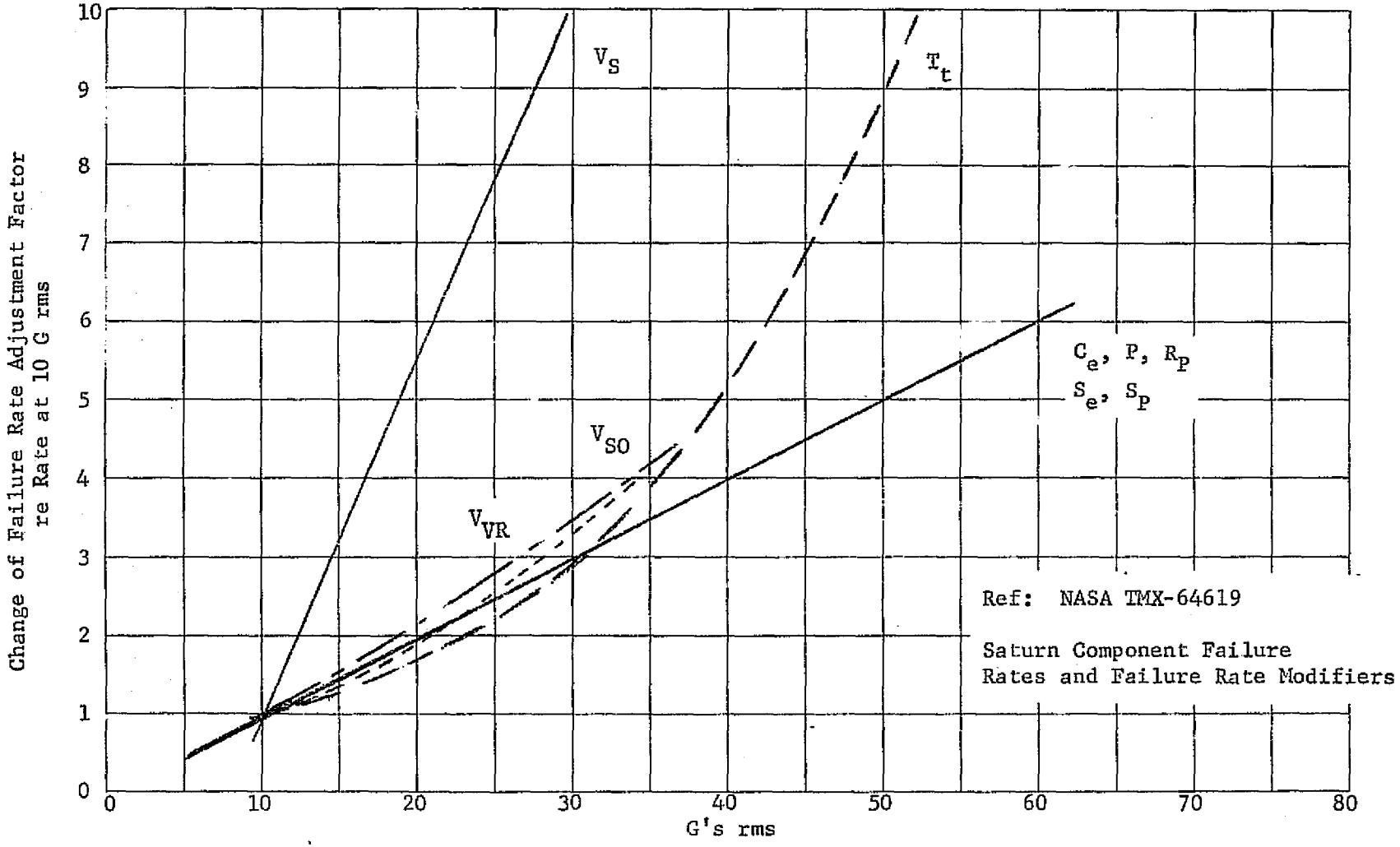

Figure 13. Change in Failure Rate as a Function of Vibration Level

Assume that the attenuation provided by the shroud reduces the number of test-induced failures by a constant factor, k, so that

$$N_R = k\, N_P \qquad (0 \leq k \leq 1) \tag{1}$$

Note that k=1 indicates zero noise reduction, while k=0 would correspond to 100% noise reduction. Intermediate values are

k=0.1 ..... 20 dB reduction,
0.31..... 10 dB reduction,
0.5 ..... 6 dB reduction,
0.71..... 3 dB reduction.

Let C_S = total cost of shroud,
C_P = initial cost of payload,
C_T = cost of initial test,
C_M = average cost of modifying and replacing a component
C_{RT} = cost of retesting the refurbished payload

The resulting development costs would be $N_P C_M + C_{RT}$ for the payload bay test and $k\, N_P C_M + C_{RT}$ for the inshroud test. The expected total cost, if a shroud is <u>not</u> used is

$$E\left\{C\right\} = C_P + C_T + N_P C_M + C_{RT} \tag{2}$$

If a shroud <u>is</u> used the expected total cost becomes

$$E\left\{C^*\right\} = C_P + C_T + C_S + k\, N_P C_M + C_{RT} \tag{3}$$

The expected cost savings due to using a shroud is

$$\left[\text{total cost without shroud}\right] - \left[\text{total cost with shroud}\right]$$

$$\text{i.e., } \Delta C = E\left\{C\right\} - E\left\{C^*\right\}$$
$$= C_P + C_T + N_P C_M + C_{RT} - C_P - C_T - C_S - k\,N_P C_M - C_{RT}$$
$$= N_P C_M\,(1-k) - C_S$$

Thus, the generalized cost model is

$$\Delta C = N_P C_M\,(1-k) - C_S \qquad (4)$$

The cost of the shroud C_S is obviously affected by the value of k achieved, and can be subdivided into the cost of the basic structure C_o (including tooling and setup costs) plus the cost of that part of the assembly which provides the noise reduction (absorbent material, double-walled shell, etc.).

The first part, C_0, is a fixed cost which will be present even if the shroud has virtually no attenuation properties; i.e., before insulation is added. The second part of the total cost will be some function of the noise reduction achieved, depending on the technique used. It seems likely that, although initially the reduction achieved will be a fairly linear function of this cost, eventually a "diminishing returns" effect will take over so that to achieve additional attenuation becomes very costly. A convenient representation of this behavior is

$$C_S = C_0\,A(k) \qquad (5)$$

where A(k) is a function of the noise reduction properties of the shroud, such that $C_S \to C_0$ as $k \to 1$ and $C_S \to \infty$ as $k \to 0$. One suitable function which satisfies these end point requirements is the form

$$A(k) = e^{n(1/k-1)} \tag{6}$$

where n is a constant which controls the slope of the curve.

Information relating shroud cost to noise reduction properties was obtained from a Martin Marietta Corporation noise reduction study performed in 1966 for the Vela satellite payload (Reference 8) and is shown in Figure 14. These data were normalized and plotted as a function of k in Figure 15, then used to evaluate n in equation (6). It was found that n=0.122 provides a very good match to the Vela shroud data, as indicated in Figure 16, where the function $C_S/C_0 = A(k) = e^{0.122(1/k-1)}$ is compared with the envelope of the Vela data. Using this value, the cost model becomes

$$\Delta C = N_P C_M (1-k) - C_0 e^{0.122(1/k-1)} \tag{7}$$

This equation can be divided by the shroud fixed cost C_0 to obtain a normalized cost model:

$$\frac{\Delta C}{C_0} = \frac{N_P C_M}{C_0} (1-k) - e^{0.122(1/k-1)} . \tag{8}$$

The normalized model is plotted in Figure 17 using k as a parameter, and cross-plotted in Figure 18 using the quantity $N_P C_M/C_0$ as a parameter.

In order to investigate the maximum cost savings achievable, the cost model was optimized. First differentiate (7) with respect to k:

$$\frac{d(\Delta C)}{dk} = -N_P C_M + 0.122\ C_0\ \frac{e^{0.122(1/k-1)}}{k^2} \tag{9}$$

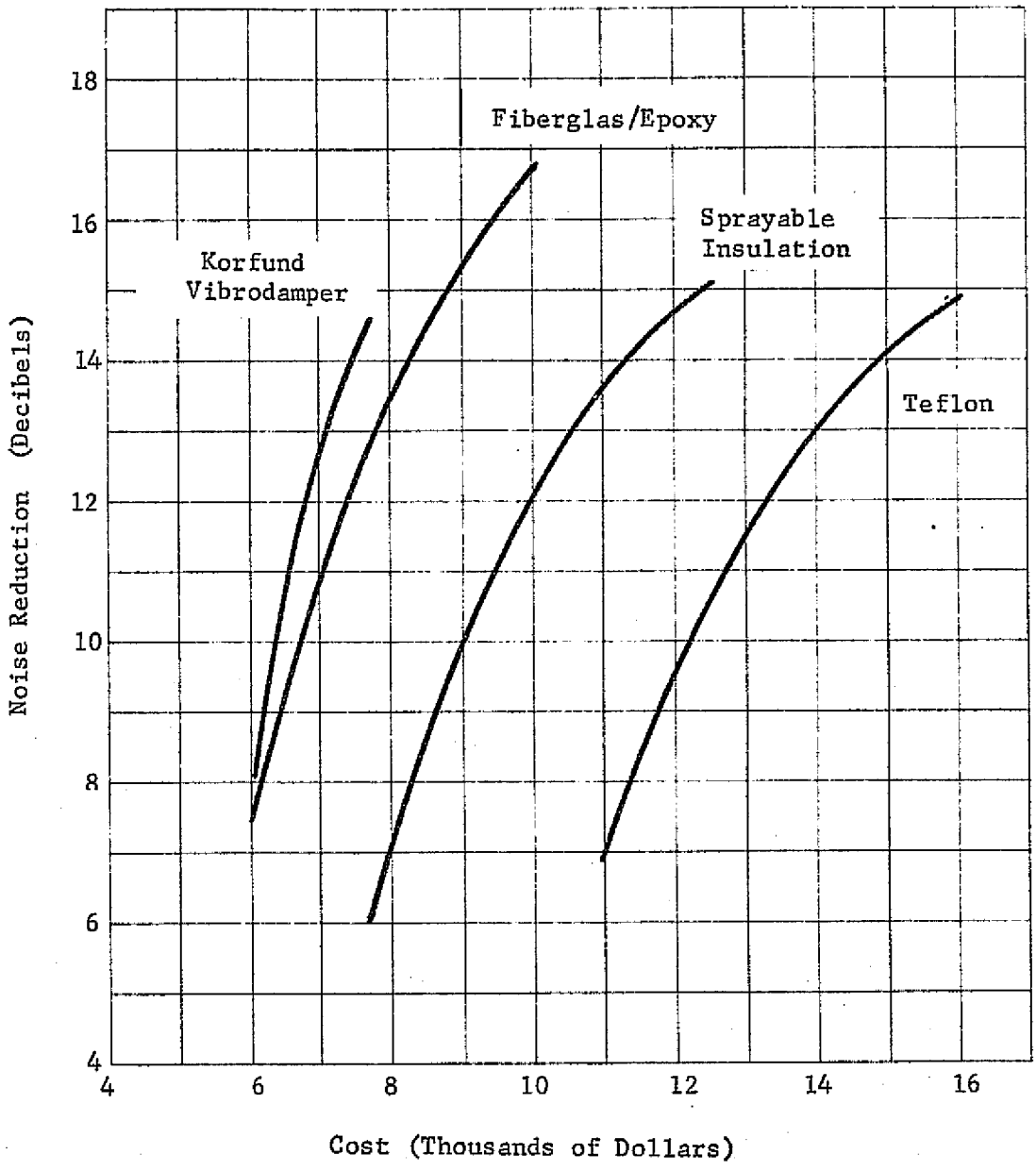

Figure 14. Noise Reduction Versus Cost for Candidate Materials for the Vela Payload Shroud

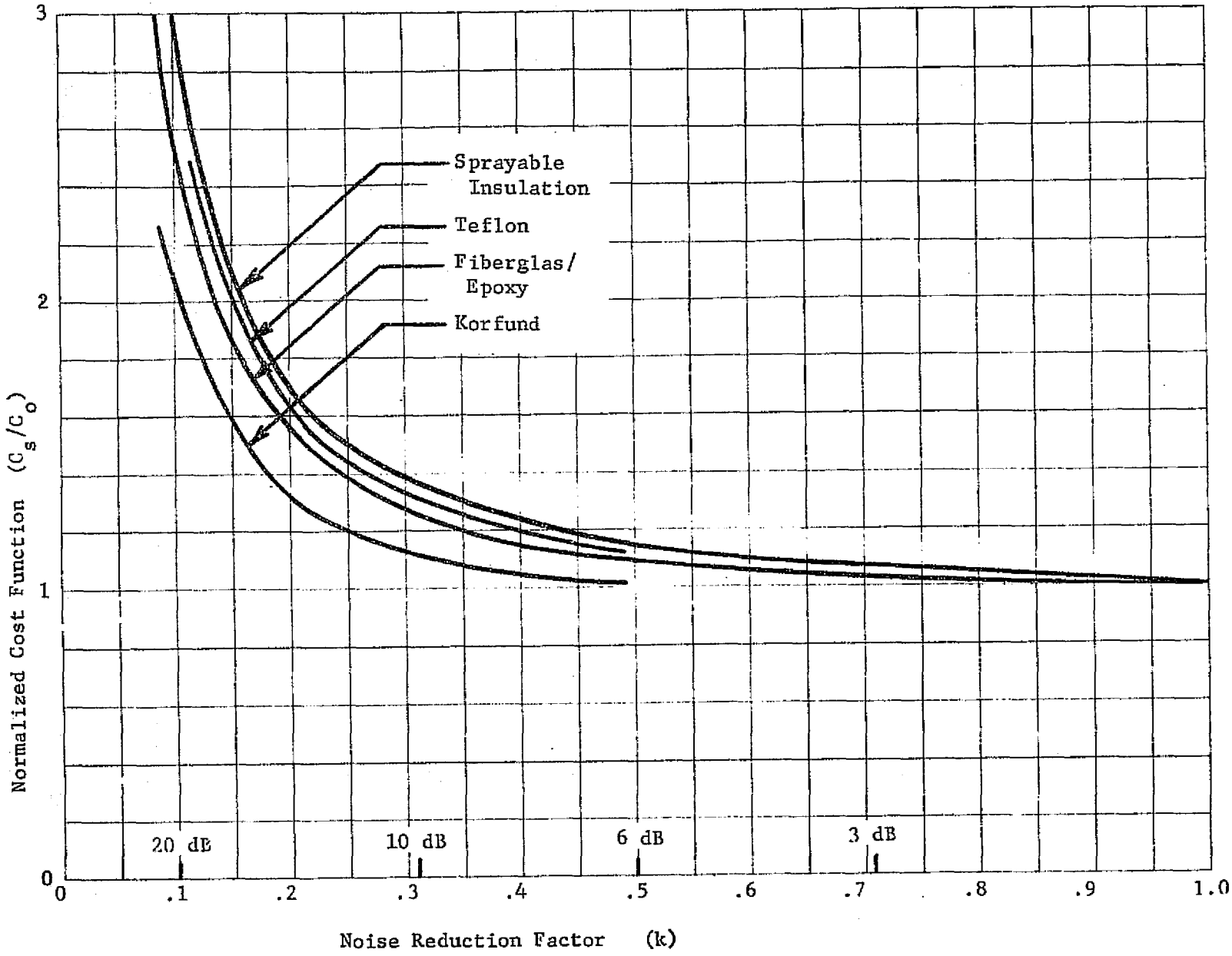

Figure 15. Normalized Cost as a Function of Noise Reduction Factor (k)

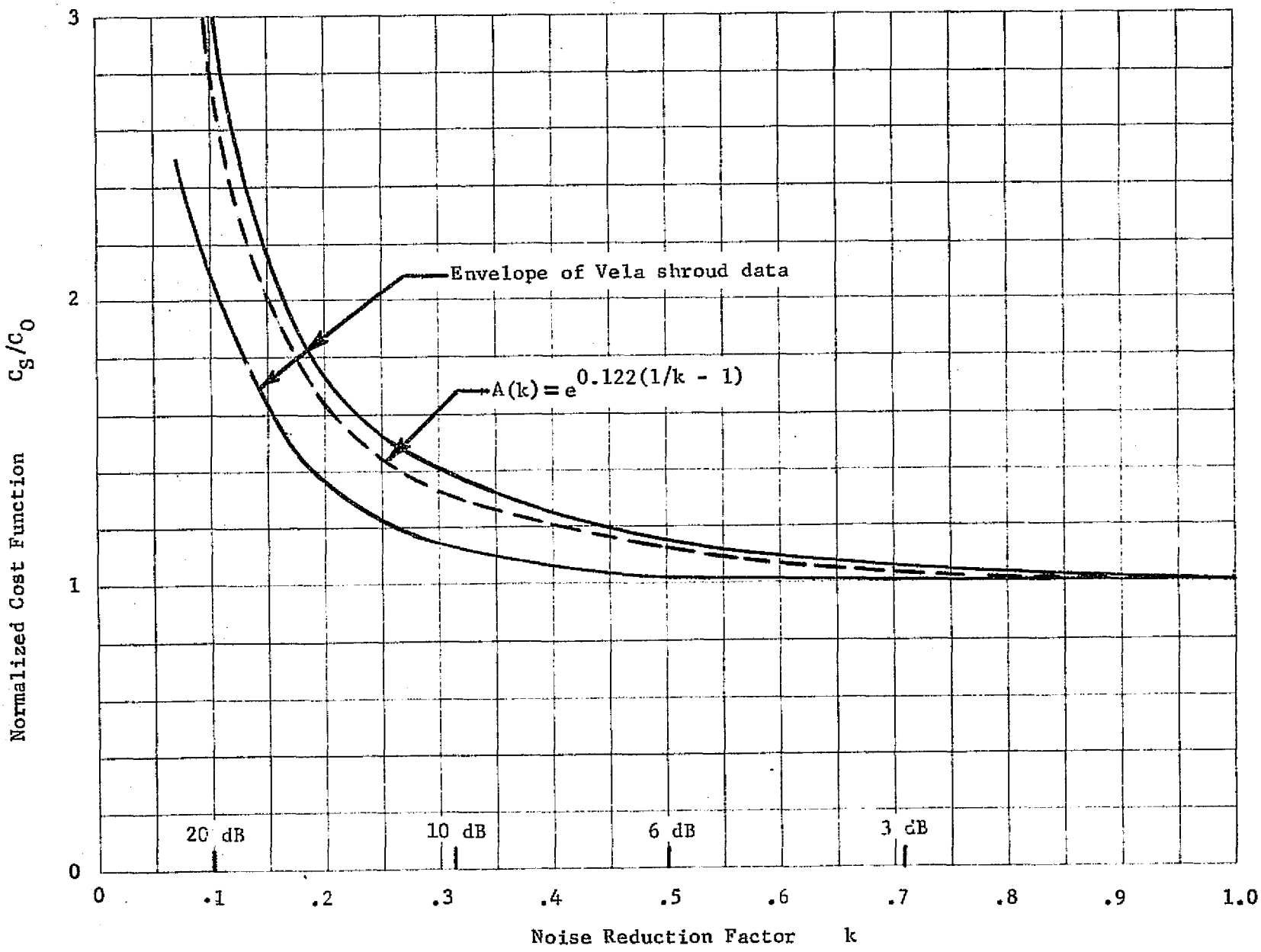

Figure 16. Comparison of Vela Shroud Data Envelope With Theoretical Normalized Cost Function

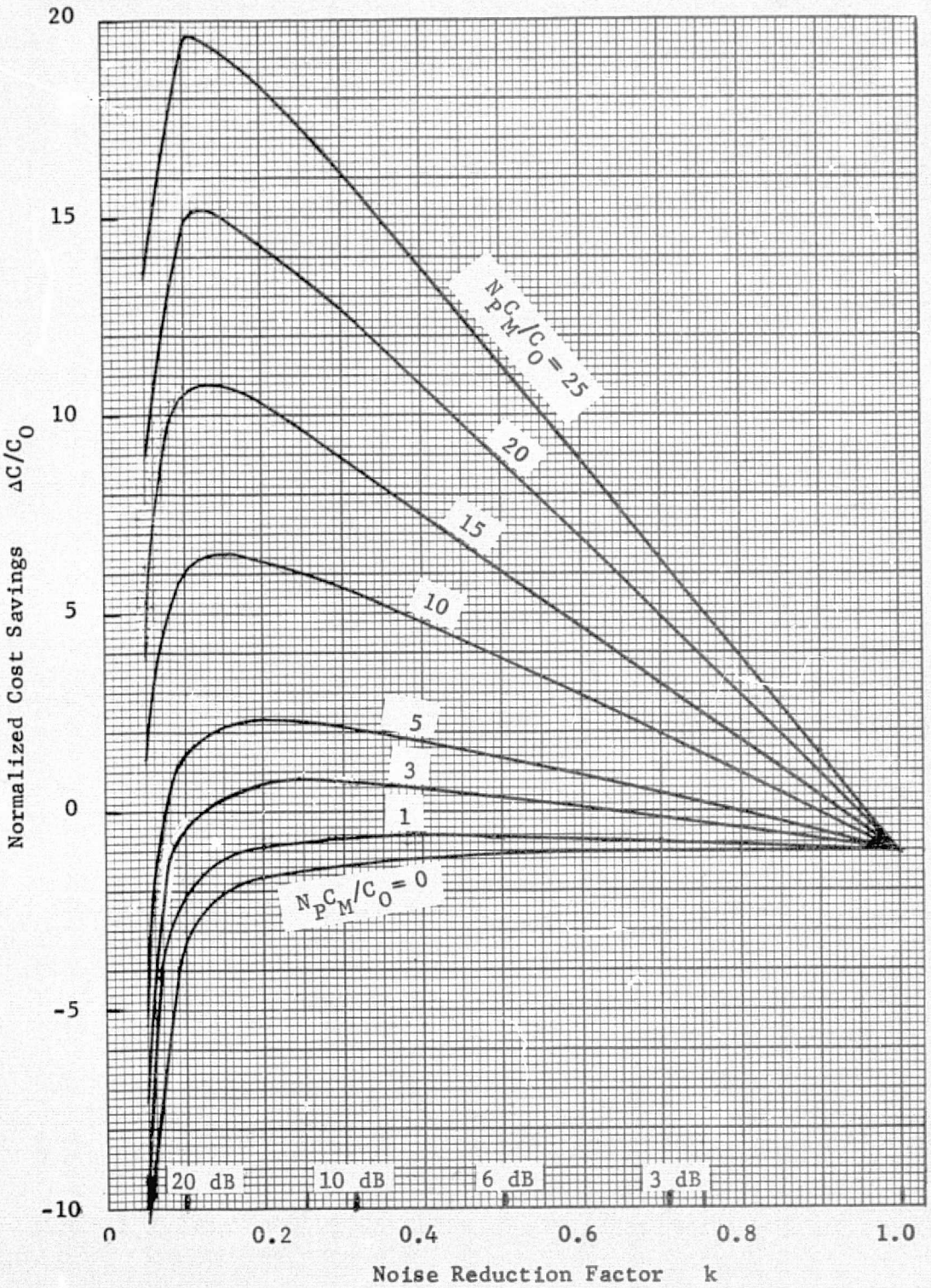

Figure 17. Normalized Cost Savings as a Function of Noise Reduction Factor for Various Values of Cost Ratio

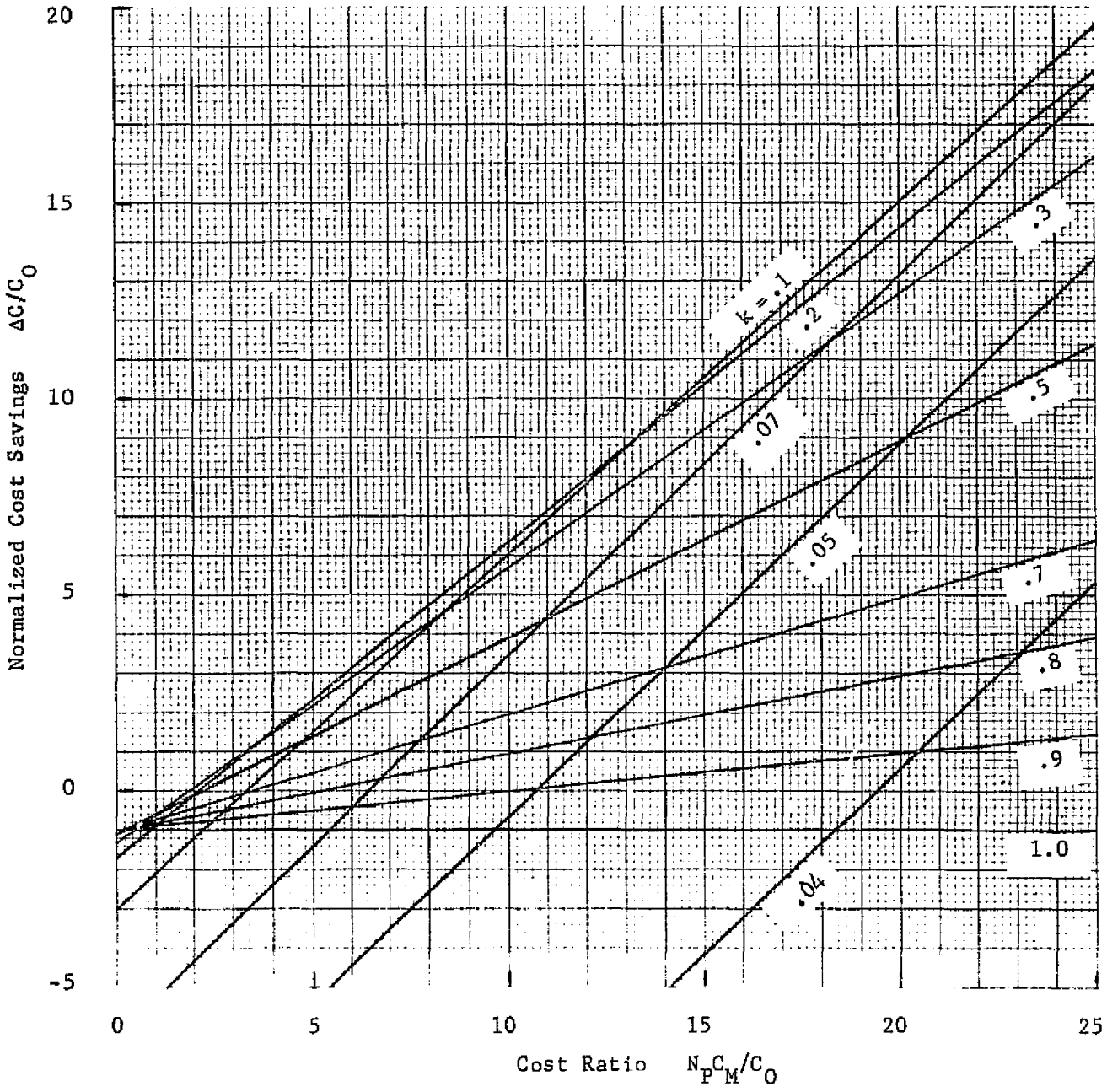

Figure 18. Normalized Cost Savings as a Function of Cost Ratio for Various Noise Reduction Factors

$= 0$ for maximum/minimum values of ΔC

$$\therefore \quad e^{0.122(1/k-1)} = \frac{k^2}{.122}\left[\frac{N_P C_M}{C_0}\right] \qquad (9)$$

continued

This equation must now be solved for k. The solution (denoted by $\hat{k}$) is the optimum value of k, which maximizes the cost savings ΔC. In order to ensure that $\hat{k}$ maximizes rather than minimizes ΔC, we must inspect the sign of the second derivative:

$$\frac{d^2(\Delta C)}{dk^2} = -0.122\ C_0\left[0.122\ k^{-4} + 2k^{-3}\right] e^{0.122(1/k-1)}$$

— this is always negative, since C_0 and k must be positive, proving that $\hat{k}$ maximizes ΔC.

Equation (9) was solved graphically using a range of values of the cost parameter $N_P C_M/C_0$. The result is shown in Figure 19. The values of $\hat{k}$ were then used to calculate the maximum cost savings as a function of $N_P C_M/C_0$, and plotted in Figure 20. Finally, for purposes of illustration, a three-dimensional isometric plot of $\Delta C/C_0$ versus $N_P C_M/C_0$ and $\hat{k}$ was drawn, with the locus of $\hat{k}$ indicated, as shown in Figure 21.

In order to apply the cost model to a particular payload, the expected number of failures N_P must be estimated, using failure rate data for the components making up the payload. The average cost of modifying and replacing the failed components, C_M, must then be determined from historic data. For the shroud under consideration we need an estimate of the fixed cost C_0 so that the quantity $N_P C_M/C_0$ may be calculated. If the noise reduction factor k is known for the shroud, the cost savings resulting from using the shroud over the payload installation can be

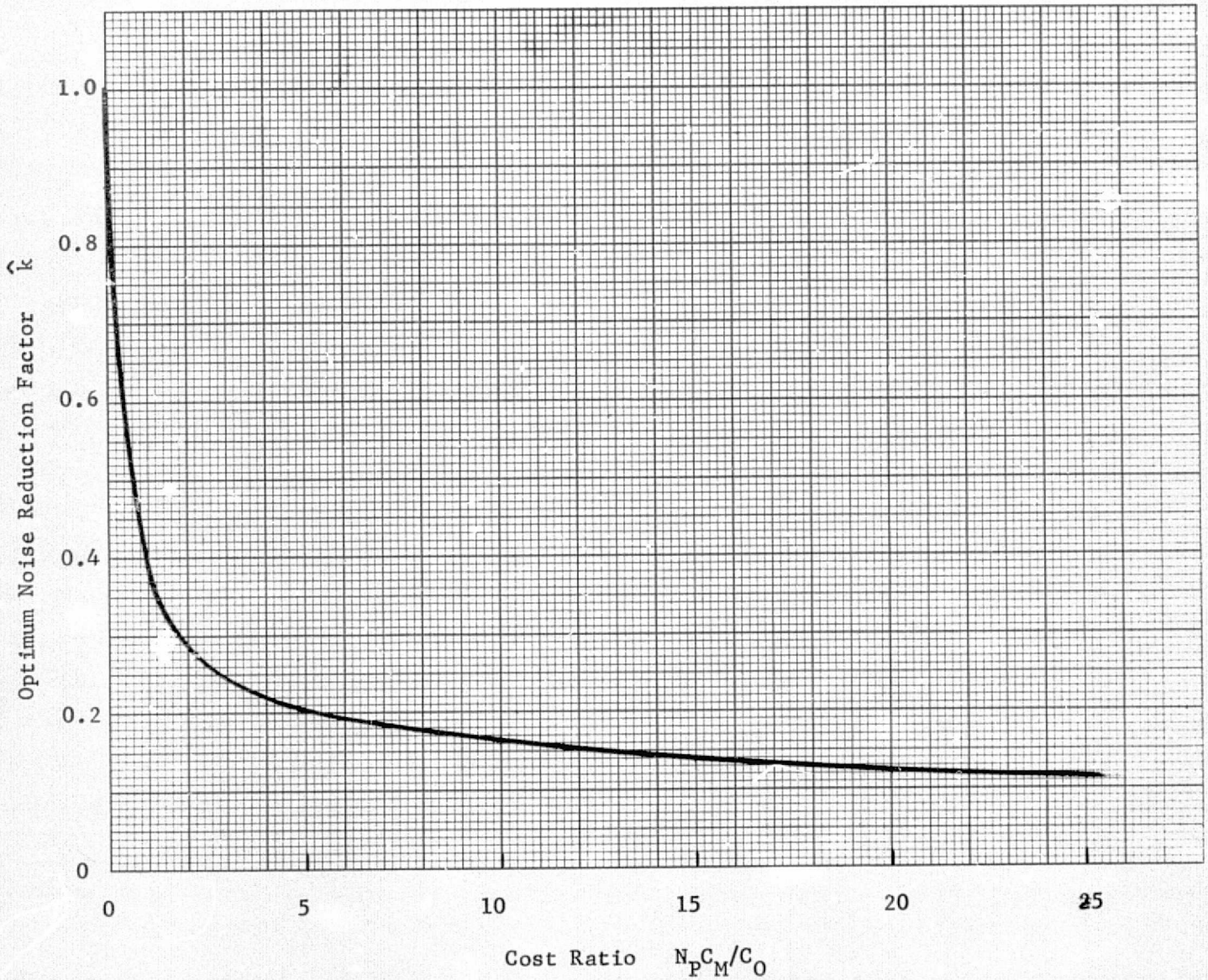

Figure 19. Optimum Noise Reduction Factor, $\hat{k}$ as a Function of Cost Ratio

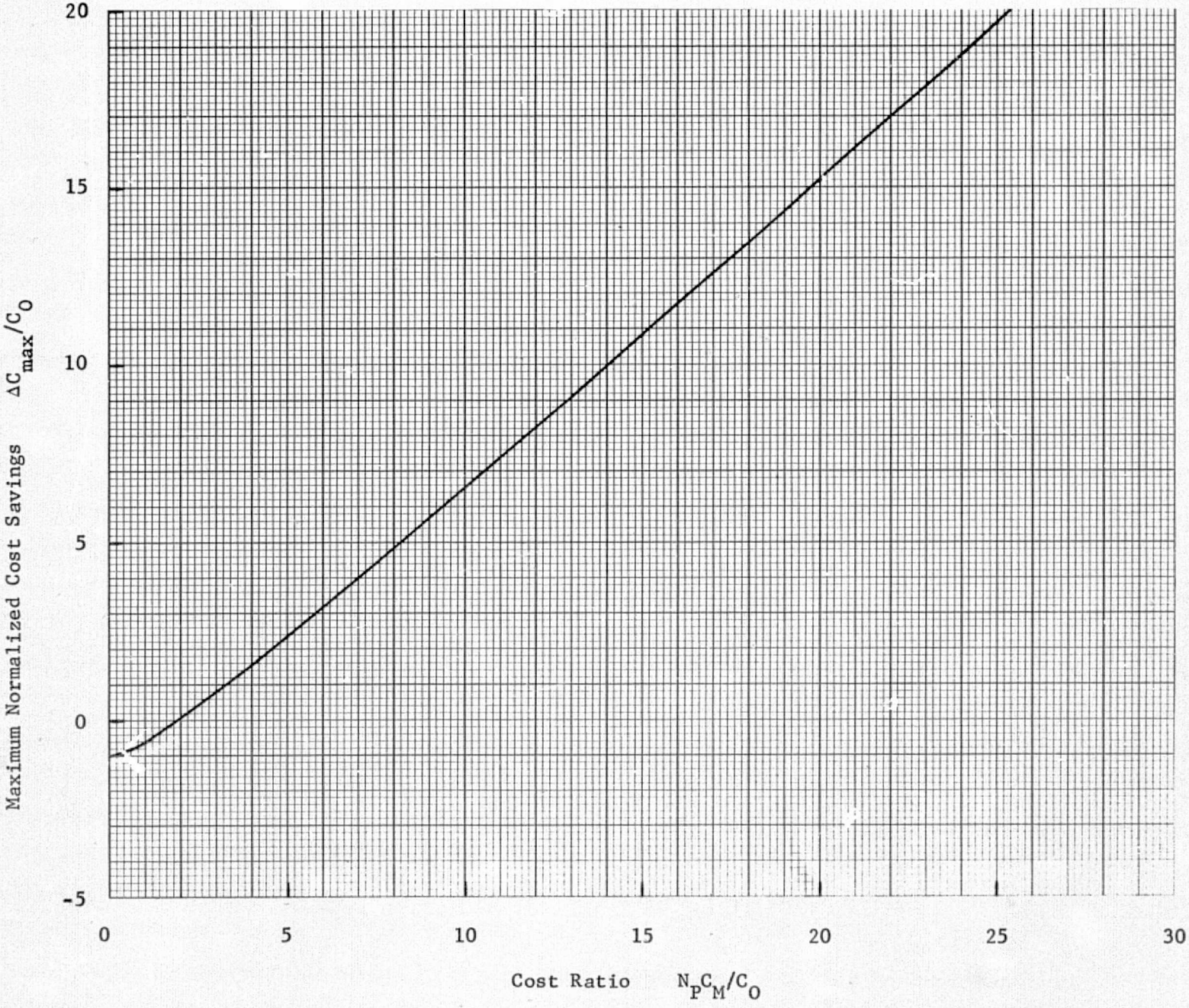

Figure 20. Maximum Normalized Cost Savings Versus Cost Ratio When $k=\hat{k}$

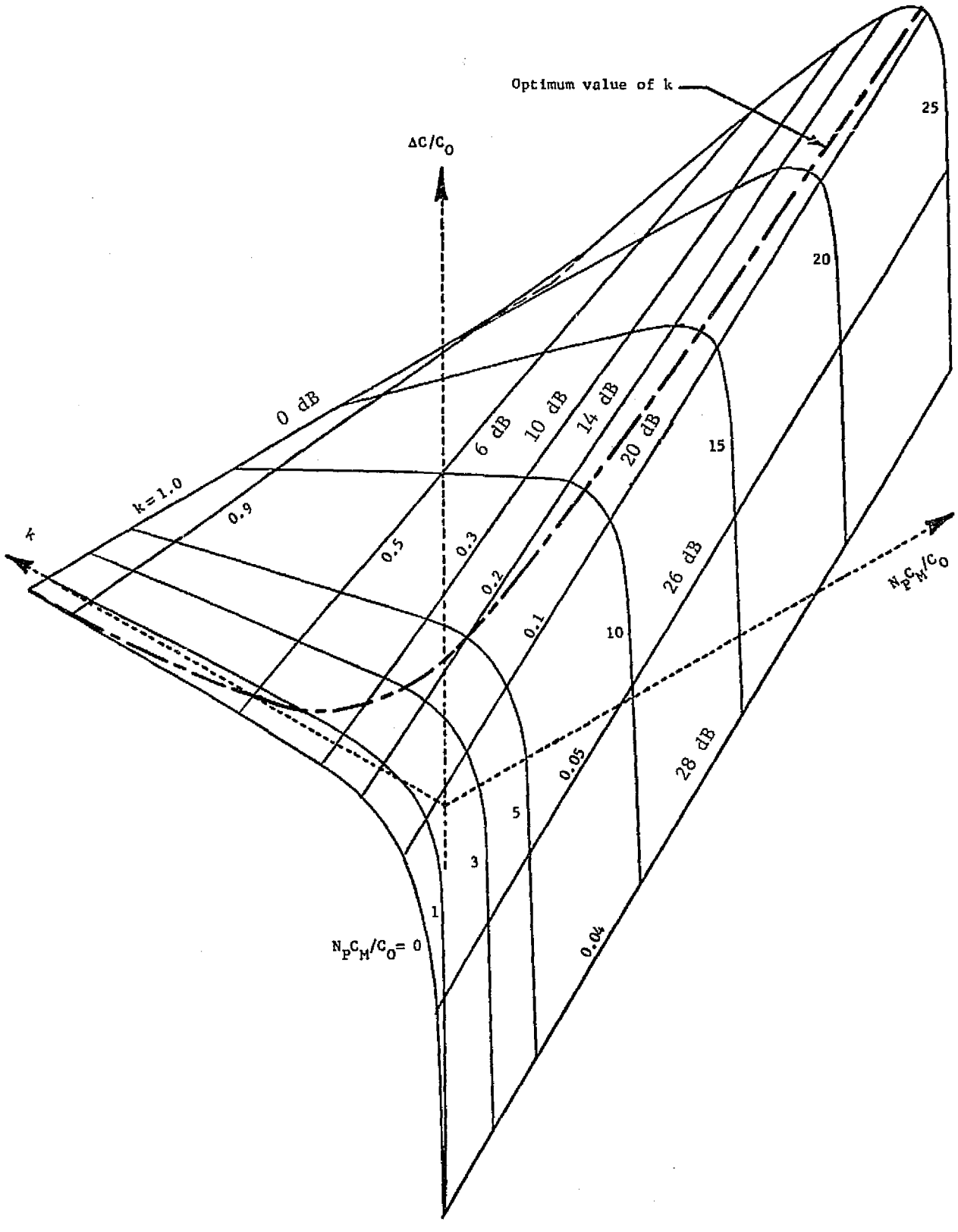

Figure 21. Normalized Cost Savings as a Function of Cost Ratio and Noise Reduction Factor

found. Alternatively, the optimum amount of noise reduction and the corresponding maximum savings can be calculated. This information can be used to finalize the shroud design requirements and make the decision of whether to use the shroud or not.

One contribution to the shroud cost which has not been addressed so far is the cost of flying the shroud in the mission. Available data on experiments currently planned to be flown on the first 20 missions were reviewed in an attempt to assess the significance of this omission. It was found that if shrouds were provided wherever possible on the first 20 missions, the ratio of shroud weight to total payload weight would range from 5 to 16 percent, with an average of 9 percent. This is based on an assumed shroud surface density of 7.34 kg/m^2(1.5 lb/ft^2). The cost per pound of flying hardware on Shuttle missions is not known, since it will depend on the particular mission being flown, total payload weight, frequency of launches, etc. However, very preliminary estimates indicate that the cost of flying a shroud will be comparable with the cost of manufacturing the shroud, assuming a simple composite-type design and a fairly large production run (10 units or more) in each shroud size. Thus, it appears that this contribution to the total shroud cost could be very significant, and should be taken into account when the necessary cost information becomes available.

Effect of Current Philosophy on Test Costs

Until recently, testing philosophy has required the fabrication of 2 or more complete sets of hardware, of which one set is dedicated to the qualification test program. Continuously rising costs caused a reevaluation of this approach, however, and several additional approaches to

investigate the cost effectiveness of testing at various assembly levels have been advanced and techniques published in recent years, as discussed in Section B. The payload complexity and severity of the environment are primary factors influencing test costs.

The study by Stahle (Reference 5), discussed earlier, examined the cost effectiveness of performing system level vibration qualification tests using a dedicated qualification test spacecraft. An example from his results is shown in Figure 22. The results indicate that the prototype qualification test produces increasing cost savings as the required number of operational spacecraft (N) increases. In addition, the family of break-even curves for N=1, 2, 3 and 4 indicates that if the vibration level could be reduced to a low enough level, the qualification test will always increase the program costs and should not be performed. For those conditions of spacecraft complexity and vibration levels for which the qualification test would increase the program cost, the "proto-flight" test would appear to be a logical alternative.

Under the proto-flight philosophy, the system level test of a flight spacecraft is performed at qualification levels and flight acceptance durations. The problem then becomes one of determining a test level which does not compromise the integrity of the flight hardware, such that the spacecraft cannot perform its mission. Young (Reference 9) examined the test level as related to the total cost of the environmental test portion of a spacecraft program under the proto-flight concept. His results indicate that the optimum test factor ranges from approximately 1.1 to 1.4 for the most likely range of the ratio of the cost of test failure to the cost of flight failure. In the following paragraphs we

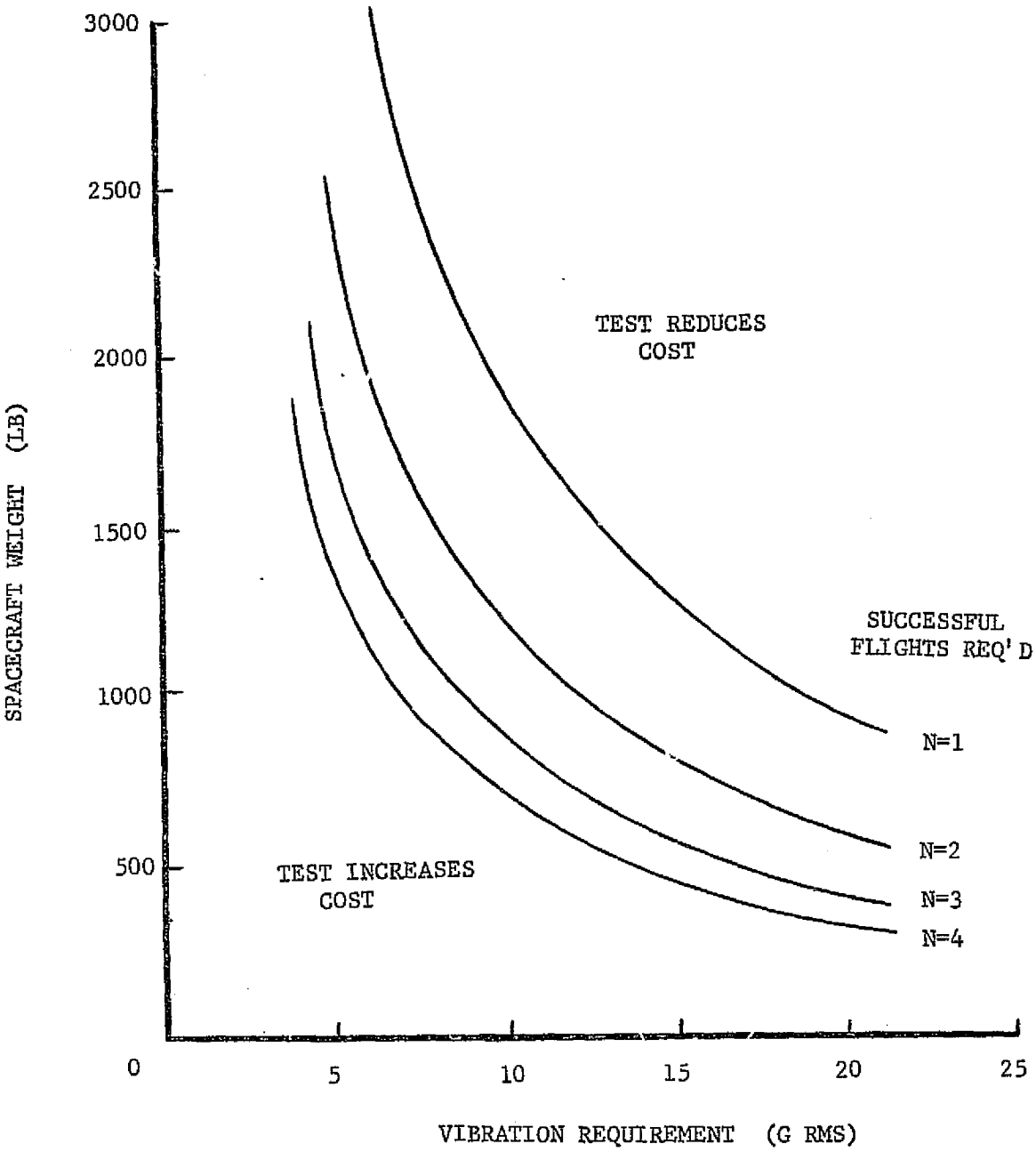

Figure 22. Breakeven Boundary for Space Exploration System (Source: Reference 5, p. 3-76)

will examine the effect of test factors on test program costs. The analysis is directed primarily towards component test programs, but the technique is applicable to a test at any level of assembly.

Assume that a payload may be tested either at a nominal qualification test level G or at an increased qualification test level rG, where r is a factor equal to or greater than unity;

$$r \geq 1.0$$

Expected total cost if test level G is used is

$$E\left\{C\right\} = C_P + C_T + N_G\, C_M + C_{RT} \tag{10}$$

where C_P = cost of payload, including cost of shroud if used,

C_T = cost of test,

N_G = expected number of component failures at test level G,

C_M = average cost of modifying and replacing a component,

C_{RT} = cost of retesting modified payload.

Since, as discussed earlier, the number of component failures is proportional to test level, we can also write an expression for the expected total cost if test level rG is used:

$$E\left\{C'\right\} = C_P + C_T + r\, N_G\, C_M + C_{RT} \tag{11}$$

The cost penalty caused by testing at the increased level is thus

$$\begin{aligned} \delta C &= E\left\{C'\right\} - E\left\{C\right\} \\ &= r\, N_G\, C_M - N_G\, C_M \\ &= N_G\, C_M\, (r-1) \end{aligned}$$

or $$\frac{\delta C}{C_M} = N_G\, (r-1) \tag{12}$$

Now assume that the payload contains a total number of components N_T with which we can associate an average constant failure rate λ_G when the payload is tested at level G. Then the expected number of failed components after a test duration T will be $N_G = \lambda_G T N_T$ so that equation (12) takes the form

$$\frac{\delta C}{C_M} = \lambda_G T N_T (r-1) \qquad (13)$$

From Reference 7 we know that λ_G/G is constant. As reported by Peverly (Reference 10), failure data were collected from a large number of vibration tests performed on Apollo components and subsystems. As discussed in Section C, STS PAYLOAD TEST COST ESTIMATES, definitive failure rate data werenot available for electrical, electronic, or optical components (block boxes), and for purposes of this study, it is assumed that these types of components will follow the same trend as the Saturn data shown in Figure 13. With this assumption, these data can be used to calculate a value for failure rate which is probably reasonably representative of STS payload components.

A total of 11,467 units were tested at a level of 6 g_{rms} for 1 minute per axis, resulting in 559 failures.

Failure rate is calculated at a 90% confidence level using a chi-squared table, as follows:

Total test exposure T = 3 x 11,467 = 34,401 minutes

Number of statistical degrees of freedom

$$\nu = 2 \text{ (no. of failures} + 1)$$

$$= 2 \times 560$$

$$= 1120 \text{ d.o.f.}$$

$$\chi^2_{(.1,\nu)} \approx 1222 \text{ from chi-squared table}$$

$$\lambda = \frac{\chi^2}{2T} = \frac{1222}{2 \times 34{,}401}$$

$$= 0.01776 \text{ failures/minute}$$

Since this resulted from a 6 g_{rms} test level, we have $\frac{\lambda 6}{6} = \frac{0.01776}{6}$

$\simeq 0.003 = \frac{\lambda G}{G}$

$$\therefore \quad \lambda_G = 0.003\ G$$

Equation (13) becomes

$$\frac{\delta C}{C_M} = 0.003\ G\ T\ N_T\ (r-1) \qquad (14)$$

From Figure 10 we can calculate a "normalized qualification test factor" (NQTF) on a basis of RMS acceleration for the various agencies, using the definition

$$NQTF = \sqrt{\frac{\text{Qualification Test Level in } g^2/Hz}{\text{Mean Flight Level in } g^2/Hz}}$$

Agency	Qual Test Level for Mean Flight Level of 1 g^2/Hz	NQTF
MSFC	1.96 g^2/Hz	1.40
GSFC	2.94	1.71
MDAC	4.0	2.00
LRC/MMC	5.44	2.33
USAF	6.58	2.57

If we now define the nominal qualification test level G to be equal to 1 g_{rms}, then NQTF is the factor r and equation (14) may be written as

$$\frac{\delta C}{N_T C_M} = 0.003\ T\ (r-1) \qquad (15)$$

This equation is plotted in Figure 23 for a range of values of r covering the agencies listed and for test durations ranging from 5 minutes to 30 minutes.

As an example of the effect of the difference in test factors used, assume a reasonably complex multi-mission payload comprising $N_T = 100$ components/subsystems which will be tested for a duration of 30 minutes. Further assume that the average cost (C_M) of modifying and replacing a component is \$10,000. From Figure 23, the cost ratio for the USAF test factor is 0.14, whereas for the MSFC philosophy, the cost ratio is 0.036. The difference in the delta cost is then \$140,000 - \$36,000 or \$104,000 added cost to the test program if the Air Force test factor is used, excluding the effects of flight failures, if any.

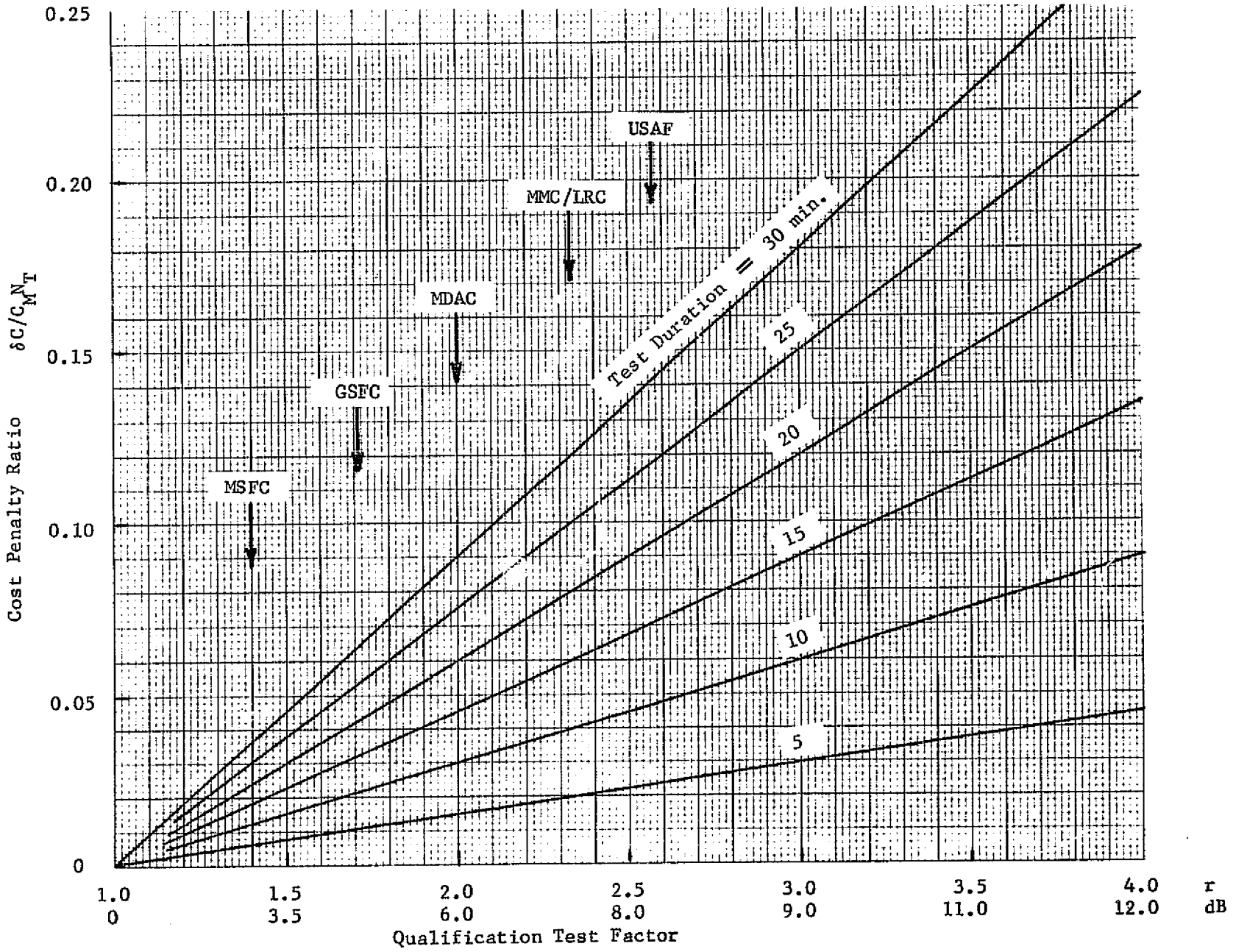

Figure 23. Effect of Qualification Test Level Philosophy on Test Costs

D. STS PAYLOAD NOISE SUPPRESSION DEVICES

The primary emphasis during this study was the development of noise suppression concepts for various classes of payloads, and estimating the noise reduction achievable as related to weight, cost and operational impacts. Previous investigations as well as our own experience have indicated that conventional shroud/blanket treatments impose significant volume and weight penalties to achieve adequate low and mid-frequency noise suppression. Consequently, the approach here has been directed towards developing light weight, stiff shroud configurations in order to minimize the weight impact.

It is recognized that an extremely effective noise reduction concept can be compromised by noise leakage paths at umbilical/duct interface points, or by the noise reduction of the pallet and IUS upper stage structure. There are potential problems which must be addressed in the final design. For example, it will not be cost effective to design a shroud to achieve 20 dB noise reduction if the pallet itself provides only 10 dB attenuation. Analyses and/or tests of the pallets and IUS upper stage structure will need to be performed to define the effective goal for noise reduction for payload shrouds.

In this section, noise reduction concepts for the major payload classes defined under Task A are described, analyses and test results related to two specific shroud designs are presented, and comparisons of these shrouds with others developed by MDAC, GSFC and MSFC are made. Finally, the thermal, contamination and payload interference/deployment considerations are discussed.

Noise Reduction Concepts

Under Task A, three major payload classes were defined and statistical distributions of the numbers of payloads of various sizes were

determined. The results indicated that modular shroud configurations would be weight effective. Figures 24 and 25 are sketches of potential modular shroud configurations for pallet and IUS payloads, respectively. The distribution of lengths of direct mounted payloads indicates that shrouds 3 meters and 5 meters long would provide protection for approximately 70% of the payloads with diameters less than 4.6 meters. For the remaining payloads, for which space is not available for a shroud, end absorbers and baffles represent a more feasible approach to noise reduction.

In order to utilize absorbers/baffles with maximum effectiveness and minimum weight penalty, it is necessary to determine the frequencies and mode shapes of acoustic modes of the orbiter payload bay. The equation for the analysis of cylindrical enclosures described by Morse (Reference 11) was programmed for a digital computer to determine acoustic modes of the orbiter bay and of the different shroud configurations. The resonant frequencies are given by:

$$f(\ell,m,n) = \frac{c}{2} \left[\left(\frac{\alpha_{m,n}}{A} \right)^2 + \left(\frac{\ell}{B} \right)^2 \right]^{\frac{1}{2}} \qquad (1)$$

where f = frequency of the (ℓ,m,n) th mode (Hz)

ℓ,m,n = mode numbers, each taking values 0,1,2,3,... etc. ℓ,m,n are associated with wave motion in the axial, circumferential and radial directions respectively.

c = speed of sound in air, assumed to be 344 m/sec (1128.6 ft/sec)

$\alpha_{m,n}$ = characteristic values, which are the roots of the equation obtained by setting the derivative of the mth order Bessel function J_m to zero; tabulated in Reference 11.

A = cylinder radius (m)

B = cylinder length (m).

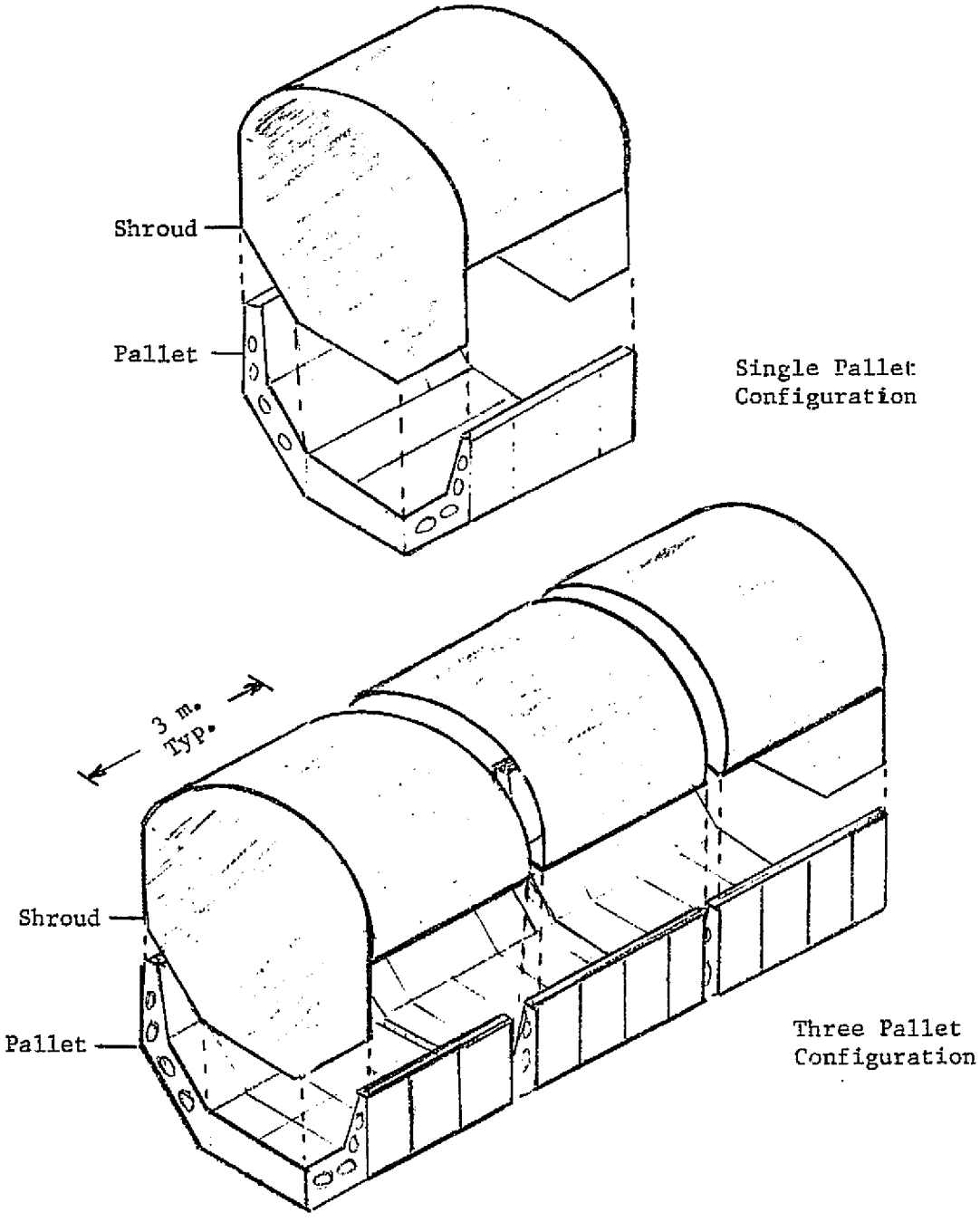

Figure 24. Modular Shroud Configurations
For Pallet Mounted Payloads.

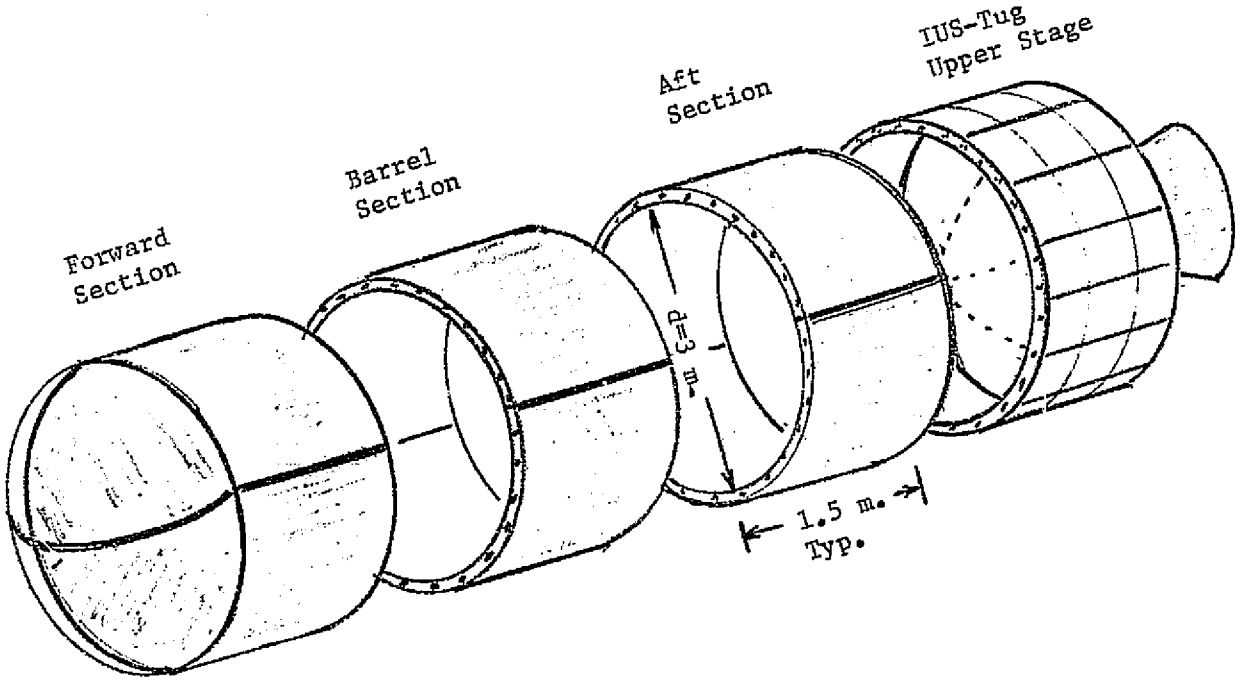

Figure 25 . Modular Shroud Configurations For IUS-Tug Payloads.

The internal acoustic resonances of the empty payload bay were computed and are summarized in the following table, which shows the first 30 modes in order of increasing frequency.

Table 1. Payload Bay Acoustic Modes

Mode No.	Frequency (Hz)	Mode No.	Frequency (Hz)
1,0,0	9.4	1,2,0	73.8
2,0,0	18.8	8,0,0	75.2
3,0,0	28.2	2,2,0	75.5
4,0,0	37.6	3,2,0	78.4
0,1,0	44.1	7,1,0	79.2
1,1,0	45.1	4,2,0	82.3
5,0,0	47.0	9,0,0	84.6
2,1,0	47.9	5,2,0	87.0
3,1,0	52.4	8,1,0	87.2
6,0,0	56.4	0,0,1	91.8
4,1,0	58.0	1,0,1	92.3
5,1,0	64.5	6,2,0	92.4
7,0,0	68.5	2,0,1	93.6
6,1,0	71.6	9,1,0	95.4
0,2,0	73.2	3,0,1	96.0

The mode shapes are very complex for any but the simplest combinations of modes, and absorbing material applied to the curved surface would only be effective in reducing the circumferential modes. Examination of the lower frequency mode shapes indicates that the optimum location for applying absorbers is at the flat ends of the cylinder. Additional studies (References 12 and 13) are currently in progress to evaluate this concept as well as the effect of payload configurations on the

internal acoustic environment; therefore, the emphasis in this study has been on the evaluation of shroud concepts.

Shroud Designs

Two specific shroud configurations were developed. The first of these, a double-walled aluminum structure with reduced pressure between the walls, was designed to take advantage of the effects of increased skin panel stiffness due to membrane tension forces resulting from the static pressure load. The design would incorporate mis-matched panel sizes in the inner and outer skins to avoid coincident panel frequencies, with an associated decrease in noise reduction. The second configuration considered consisted of fiberglass/epoxy face sheets with various thicknesses of polyurethane foam core. Conceptual views of the two configurations are shown in Figure 26.

For the double walled aluminum concept, a parametric study of the frequencies of various panel sizes under different pressure loading conditions was conducted to determine a range of practical panel sizes and reduced pressure conditions from a weight viewpoint. The analytical effort consisted of the development of a finite element model for curved panels and the evaluation of the effects of pressure on the in-plane stiffness of the panel to determine whether or not the concept is valid for practical panel sizes and pressure ranges for full scale shrouds.

A standard eigensolution routine was utilized to determine the mode shapes and frequencies for each panel and pressure condition. The results, for the range of parameters given in Table 2, are presented in Figures 27 through 29, and indicate that the shroud concept is feasible

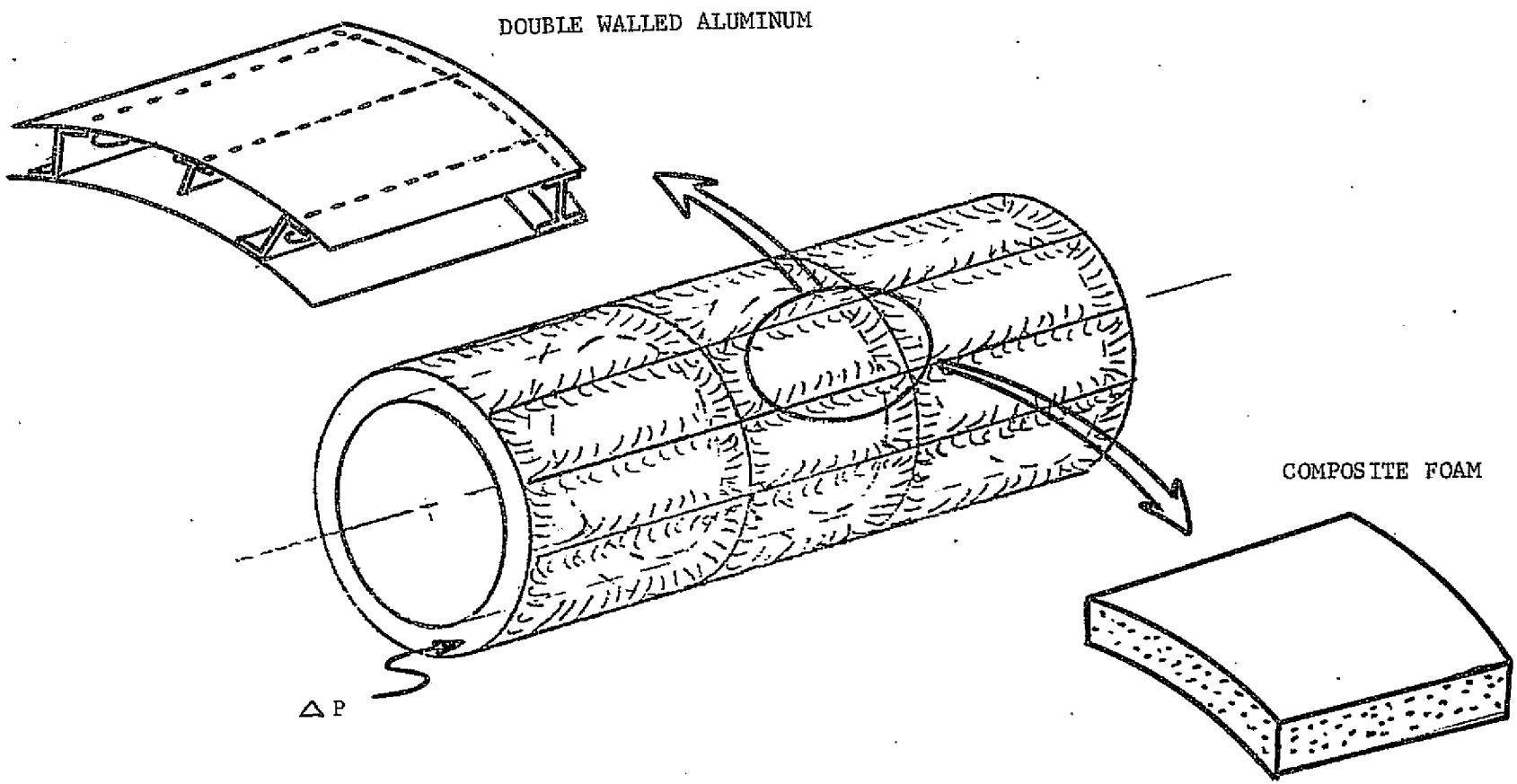

Figure 26 . Payload Shroud Concepts

Table 2. Shroud Panel Parameters

Aspect Ratio	Panel Thickness	Radius of Curvature	Pressure
2:1	.0254 cm. (.010 in.)	152.4 cm. (60 in.)	0
			3.401×10^3 N/m^2 (0.5 psi)
1:1	.0508 cm. (.020 in.)	203.2 cm. (80 in.)	1.361×10^4 N/m^2 (2.0 psi)
3:2	.0762 cm. (.030 in.)		3.401×10^4 N/m^2 (5.0 psi)

from the viewpoint of practical panel sizes and differential pressure range requirements. To eliminate the problems of panel buckling, the concentric cylinders of the shroud could be constructed as shown in Figure 30. By constructing the shroud in this manner the curved panels will always be in a state of positive pressure, and the buckling condition is eliminated.

The second type of shroud design considered was a composite urethane foam/fiberglass epoxy construction because of its inherent light weight and stiffness characteristics. An additional advantage is the relative ease of fabrication of different shapes to fit a variety of payload configurations. Although the fiberglass/epoxy face sheets were considered originally because of the stiffness and damping characteristics, aluminum or steel face sheets could be used if the former material presents a problem from a thermal or contamination standpoint.

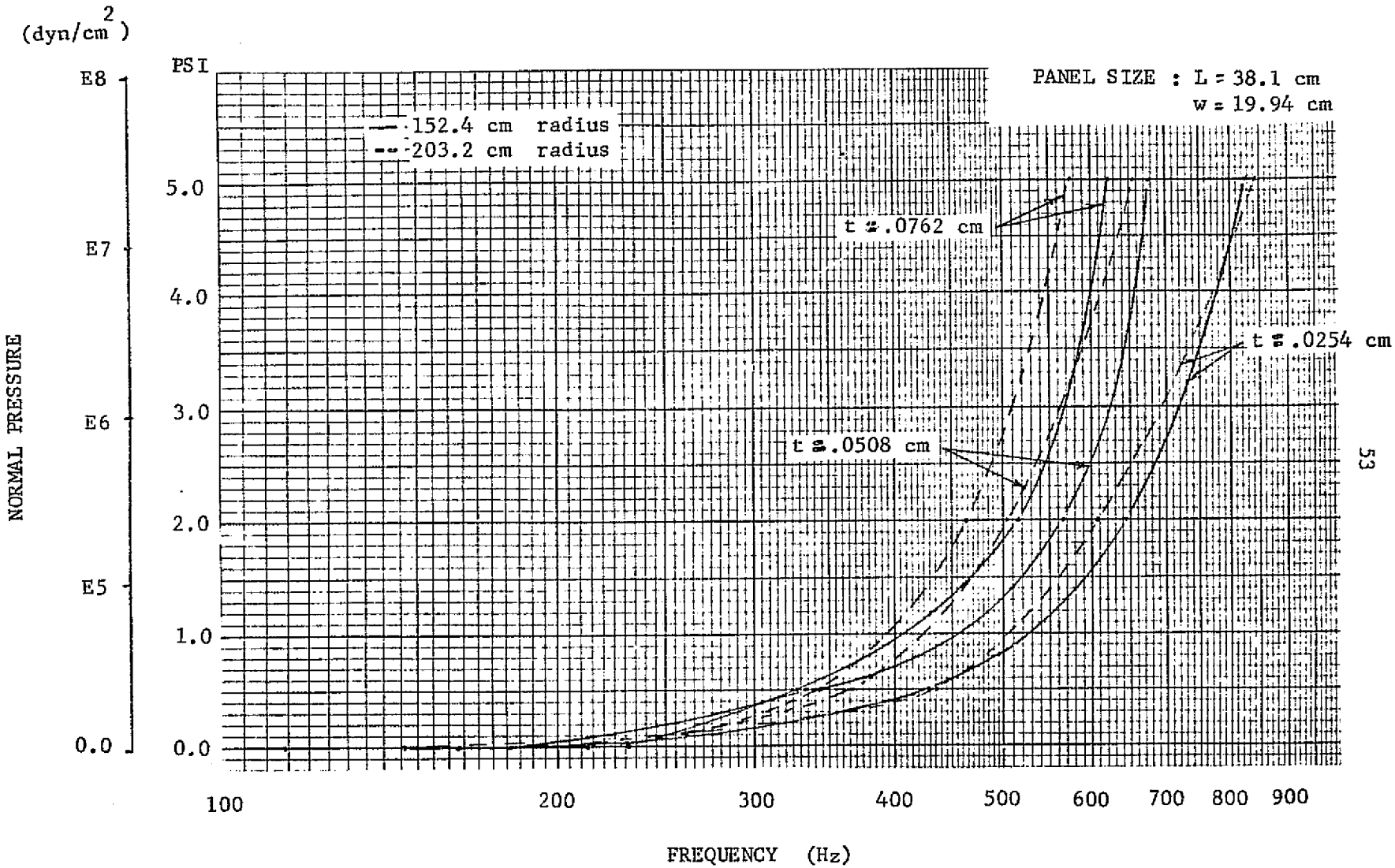

Figure 27 . First Mode Frequencies for Curved Panel With Aspect Ratio of 2 to 1

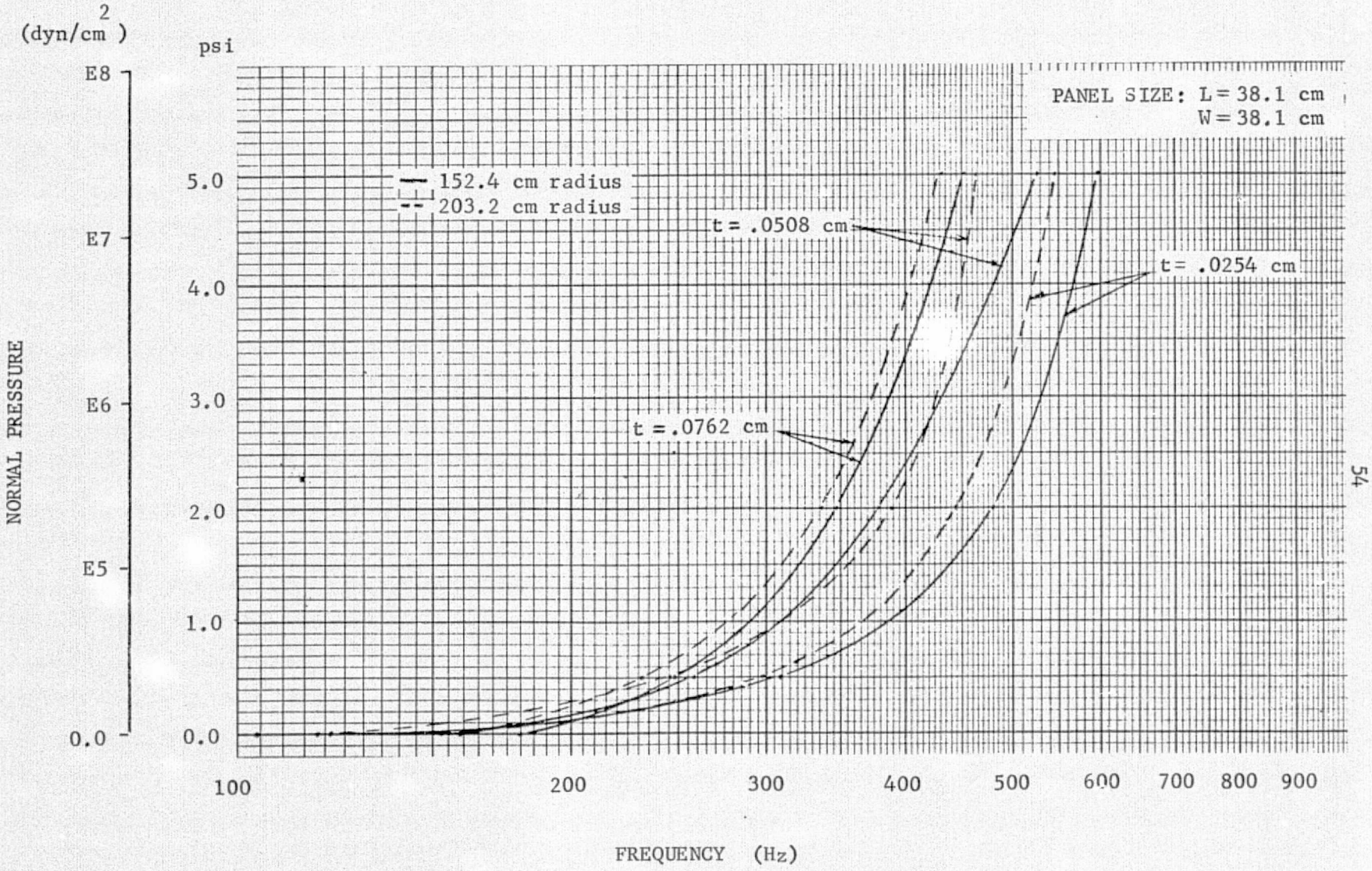

Figure 28. First Mode Frequencies for Curved Panel With Aspect Ratio of 1 to 1

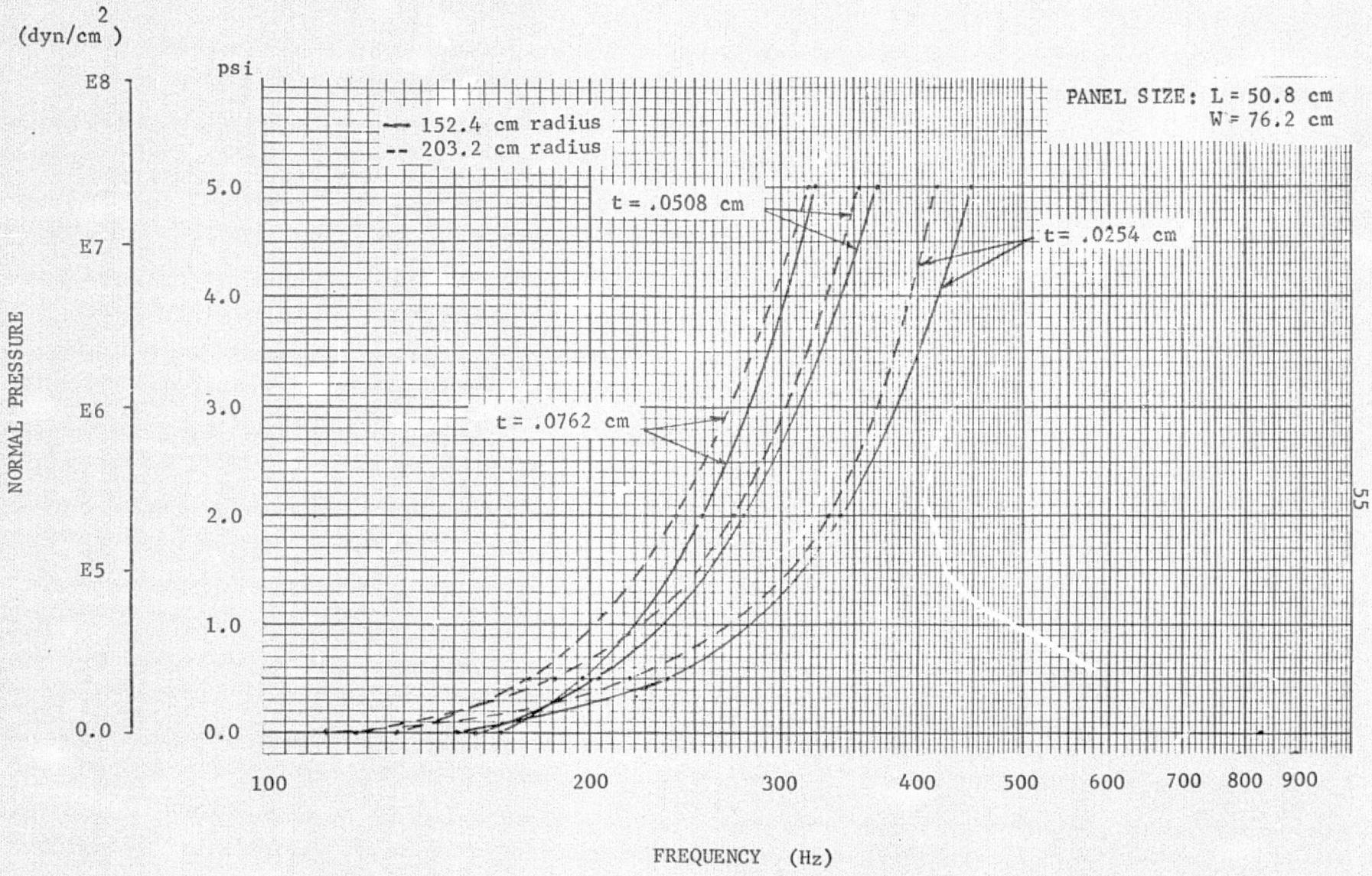

Figure 29. First Mode Frequencies for Curved Panel With Aspect Ratio of 3 to 2

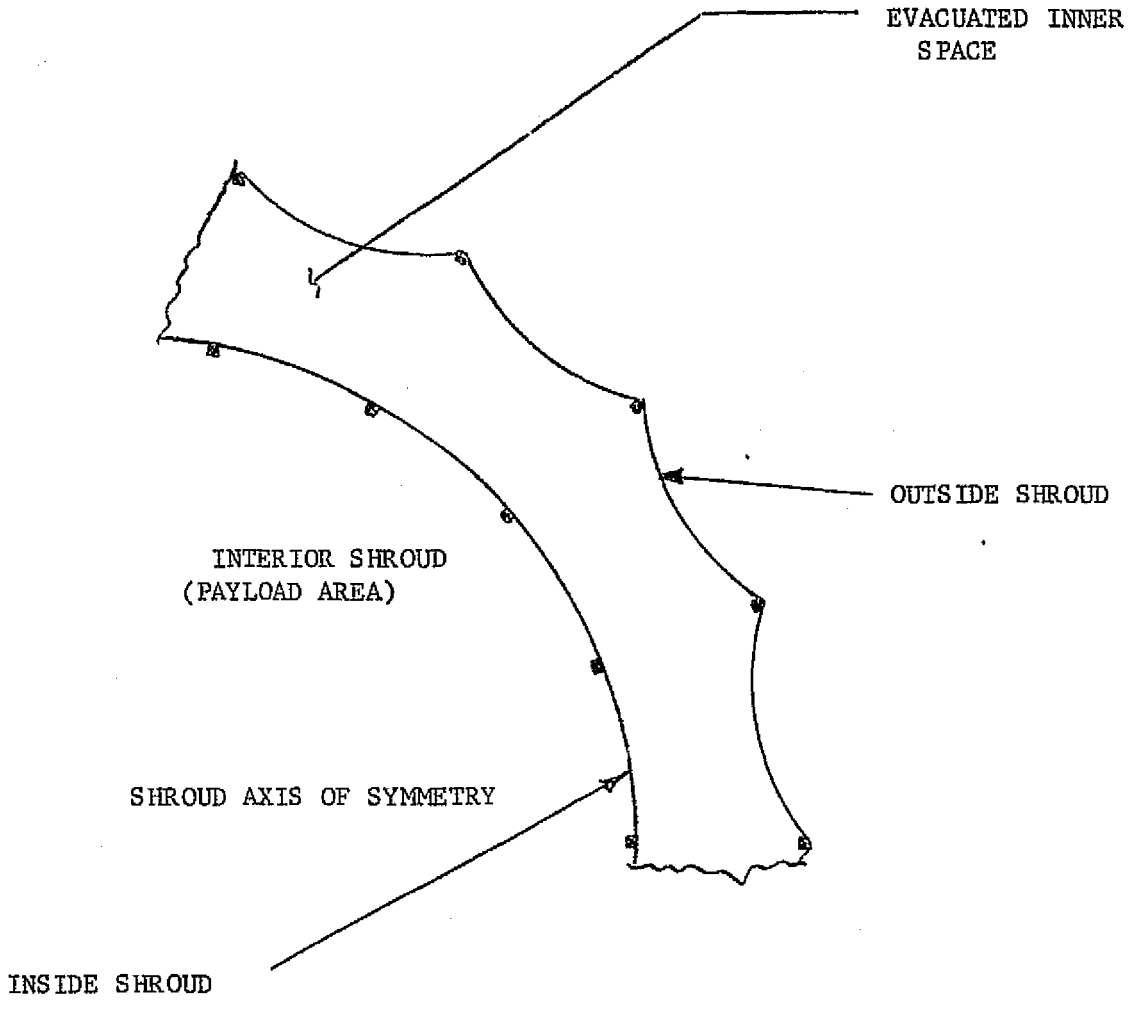

Figure 30 . Schematic of Proposed Curved Panel Configuration for Shuttle Payload Shroud

Scale-Model Shroud Tests

Models of the two candidate shroud configurations were constructed and tested to determine noise reduction and structural response characteristics as a basis for comparison with other shroud designs and extrapolation of analyses to full scale shroud configurations. The general characteristics and test conditions for the two model shrouds are listed in Table 3.

The noise reduction achieved for the different test conditions are presented in Figures 31 through 34 . A comparison of the ranges of the noise reduction achieved by the two different types of shrouds at ambient conditions is shown in Figure 35 . The double walled aluminum shroud produces approximately 5 to 10 dB more noise reduction than does the composite shroud in the frequency range from 20 to 1000 Hz. To evaluate the effects of reduced pressure and helium between the walls of the aluminum shroud, the change in noise reduction was determined at each of the internal microphone locations. The results are shown in Figures 36 and 37. For the configurations/conditions tested, the helium produced a more significant change in noise reduction over a broader frequency range.

The composite shroud was instrumented with accelerometers and biaxial strain gages were installed on the inner and outer skin panels of the double walled aluminum shroud. Narrow band (8 Hz bandwidth) analyses of these measurements and of the internal microphone data were performed to correlate with the characteristics of the noise reduction spectra, and with the analytically calculated frequencies of the acoustic modes of the cylinder. A complete description of the model tests and data obtained are contained in Appendix B. A comparison of calculated and measured fre-

Table 3. Characteristics and Test Conditions for Model Shrouds

Double Walled Aluminum					
Length	Diameter	Inner Skin	Outer Skin	Core Material	Core Thickness
1.83 m. (6.0 ft.)	0.914 m. (3.0 ft.)	Aluminum .04 cm (.016 in.)	Aluminum .04 cm (.016 in.)	Air	5.08 cm. (2.0 in.)
Test Conditions: 1. Ambient 2. Reduced Pressure Between Skins $p = -4827\ N/m^2$ (-0.7 psi) 3. Helium Gas Between Skins $p = +1379\ N/m^2$ (+0.2 psi)					

Composite Shroud							
Length	Diameter	Inner Skin	Outer Skin	Core Material	Core Thickness	Core Density	Face Sheet Density
1.83 m. (6.0 ft.)	0.914 m. (3.0 ft.)	.043 cm. (.017 in.) Fiberglass Cloth #181 /Epoxy	.0216 cm. (.0085 in.) Fiberglass Cloth #181 /Epoxy	Polyurethane Foam	2.54 cm. (1.0 in)	26.4 $Kg/m.^3$ (1.65 $lb./ft.^3$)	2076 $Kg/m.^3$ (.075 $lb./in.^3$)
Test Conditions: 1. Ambient 2. Reduced Pressure Internal to Shroud $p = -17930\ N/m^2$ (-2.6 psi)							

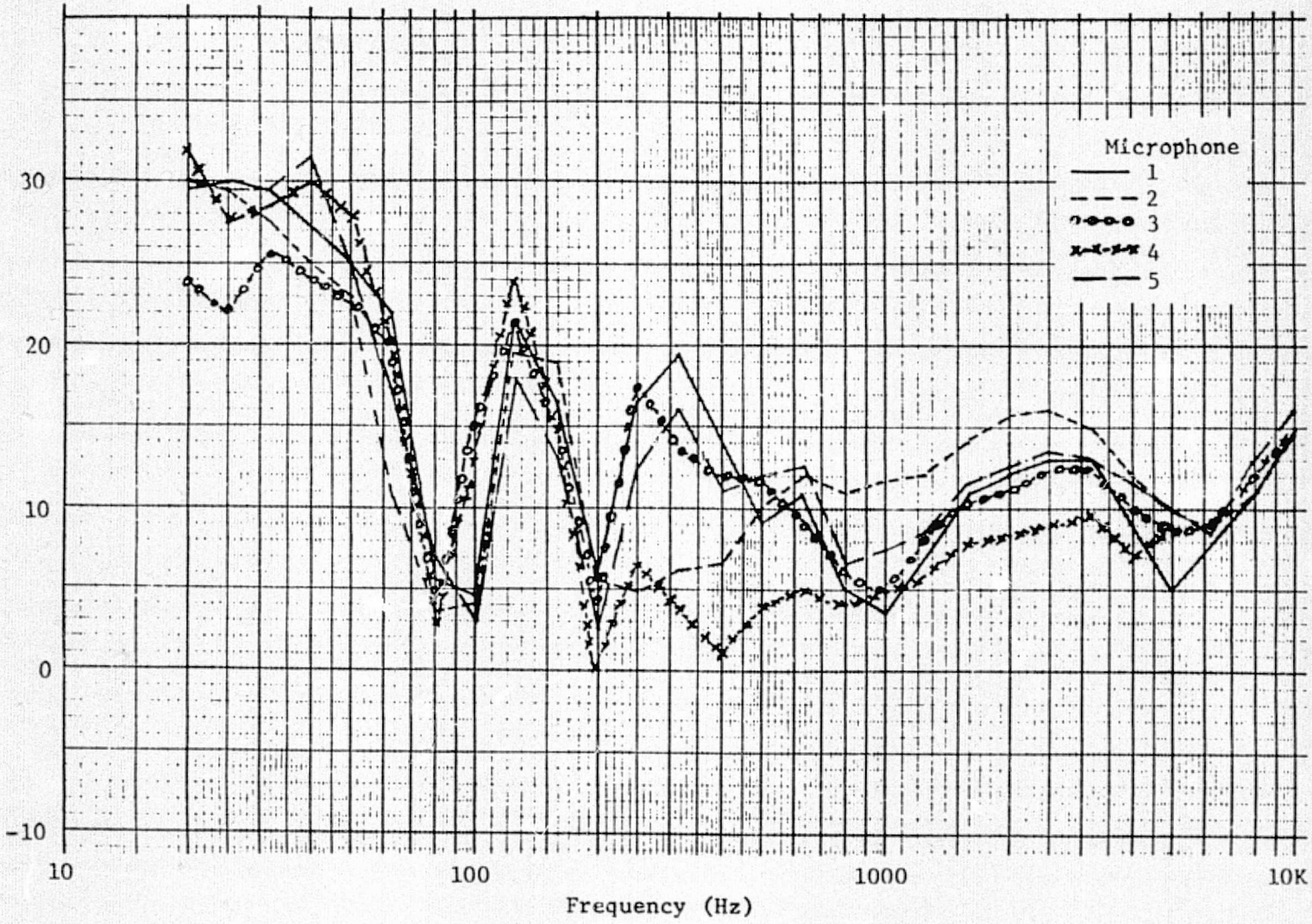

Figure 31. Noise Reduction for Composite Shroud -- Ambient Conditions

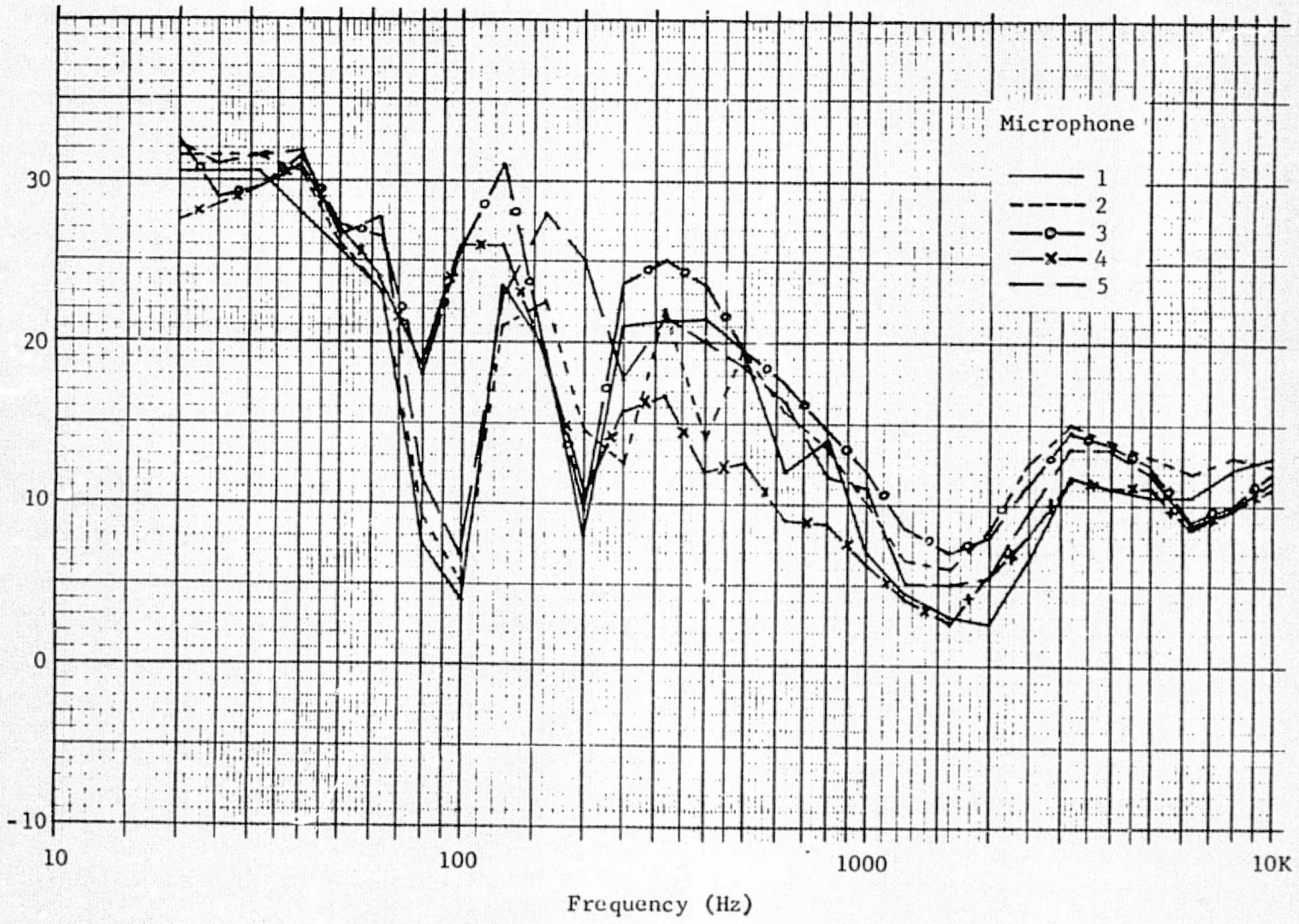

Figure 32. Noise Reduction for Aluminum Shroud - Ambient Conditions

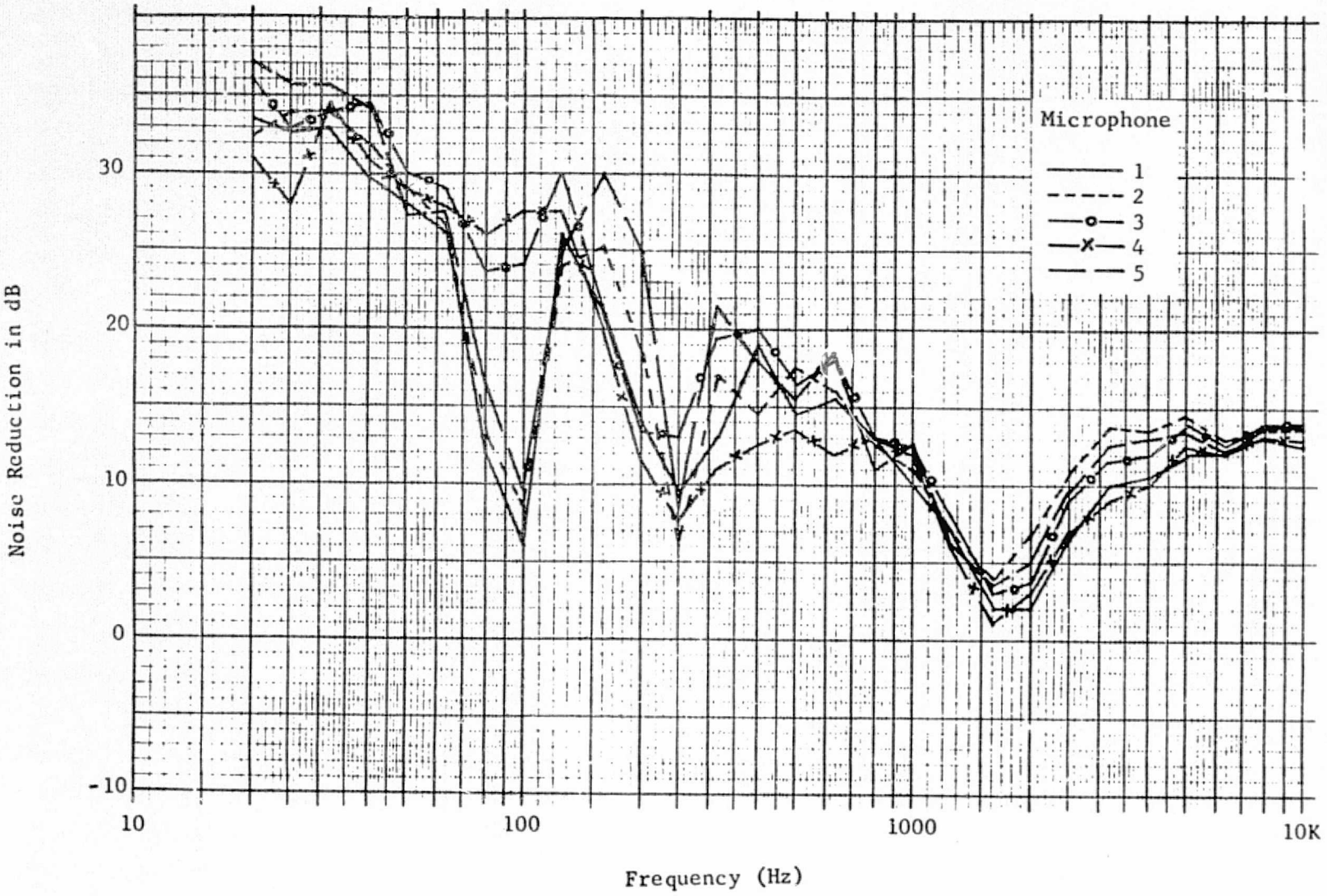

Figure 33. Noise Reduction for Aluminum Shroud - ΔP = 4827 N/m^2 (0.7 psi)

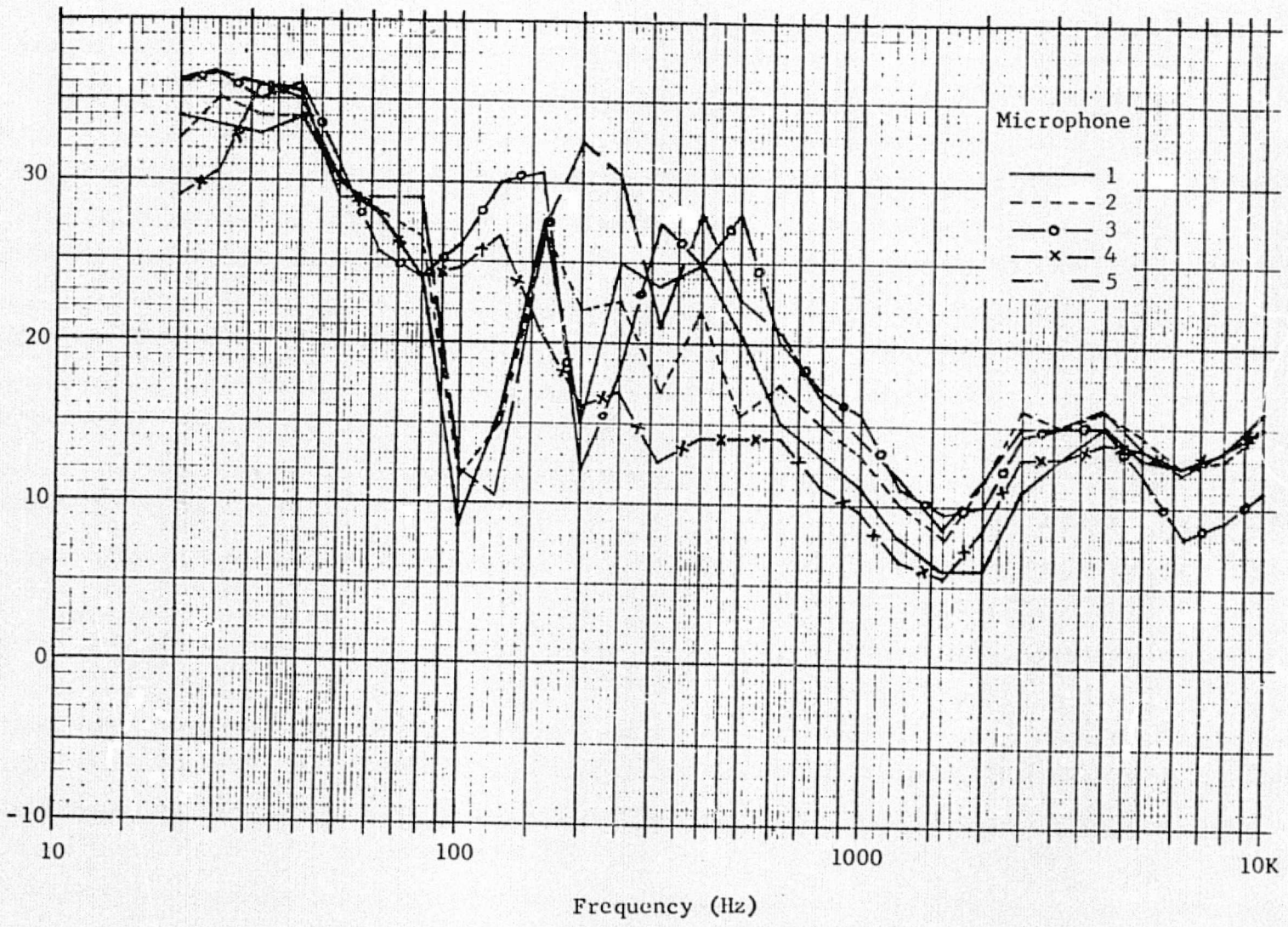

Figure 34. Noise Reduction for Aluminum Shroud --1379 N/m^2 (0.2 psi) Helium Condition

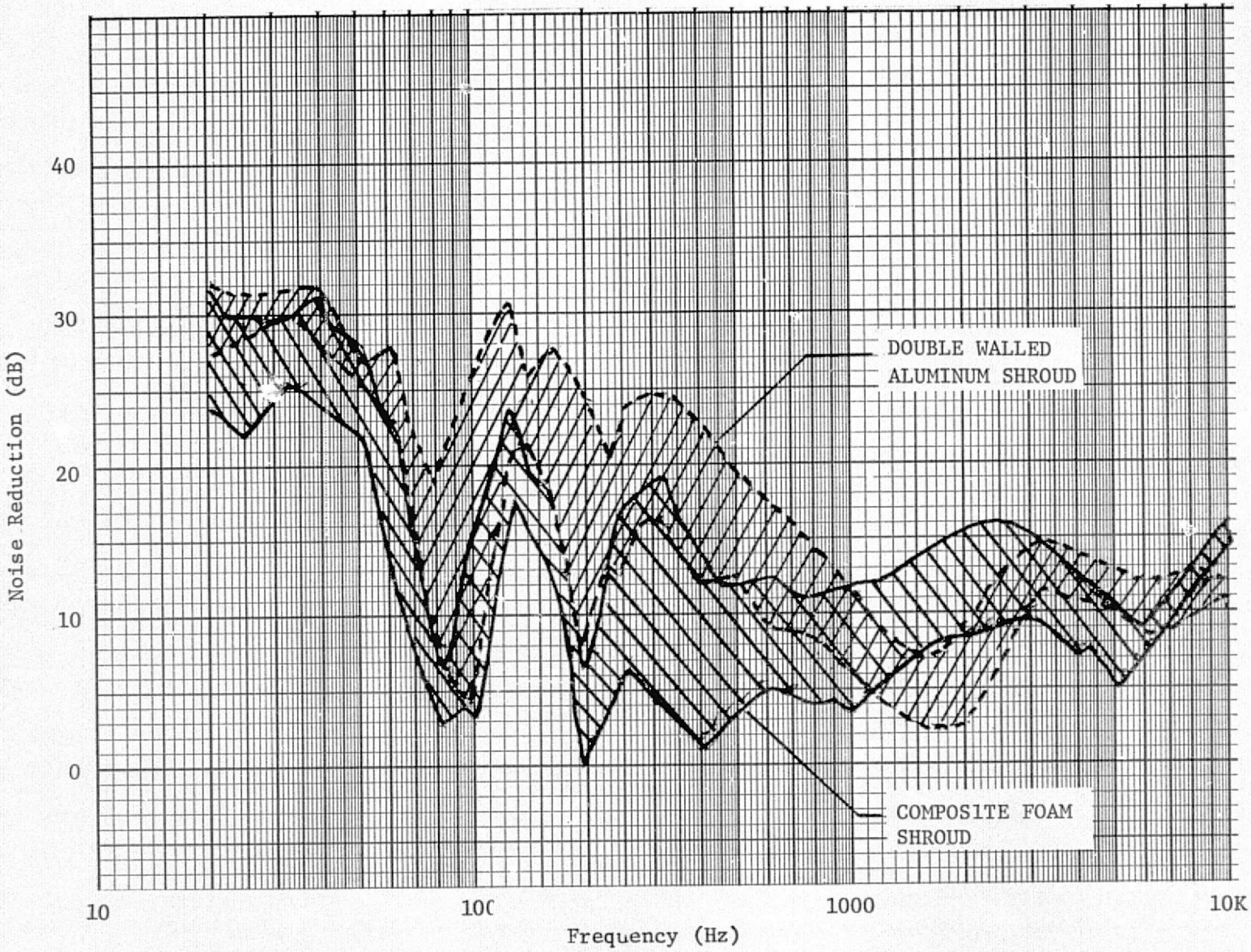

Figure 35. Comparison of Noise Reduction for Shrouds at Ambient Conditions.

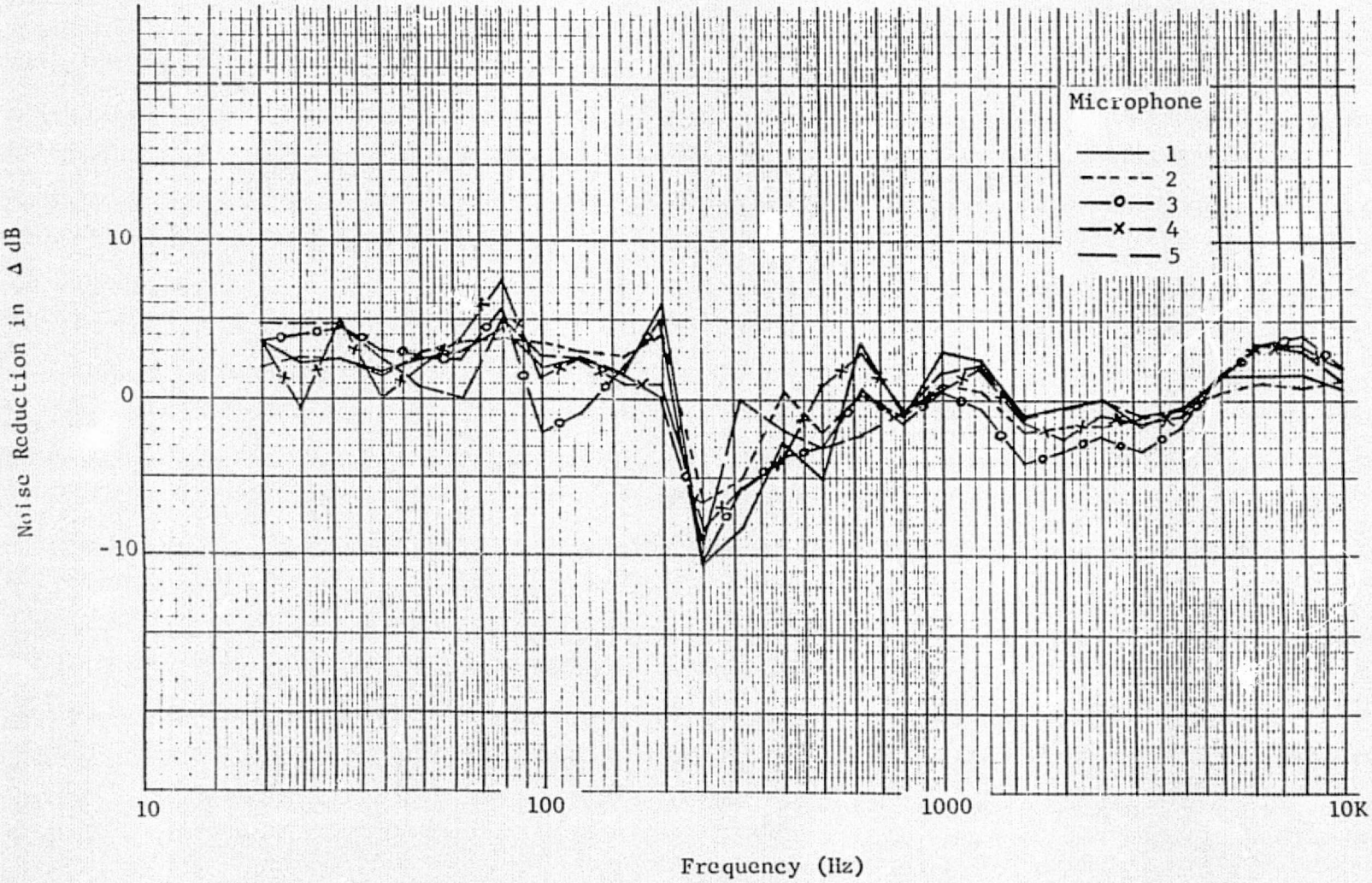

Figure 36 Comparison of Aluminum Shroud Noise Reduction Data - (4827 N/m^2 (0.7 psi) Minus Ambient Condition Data)

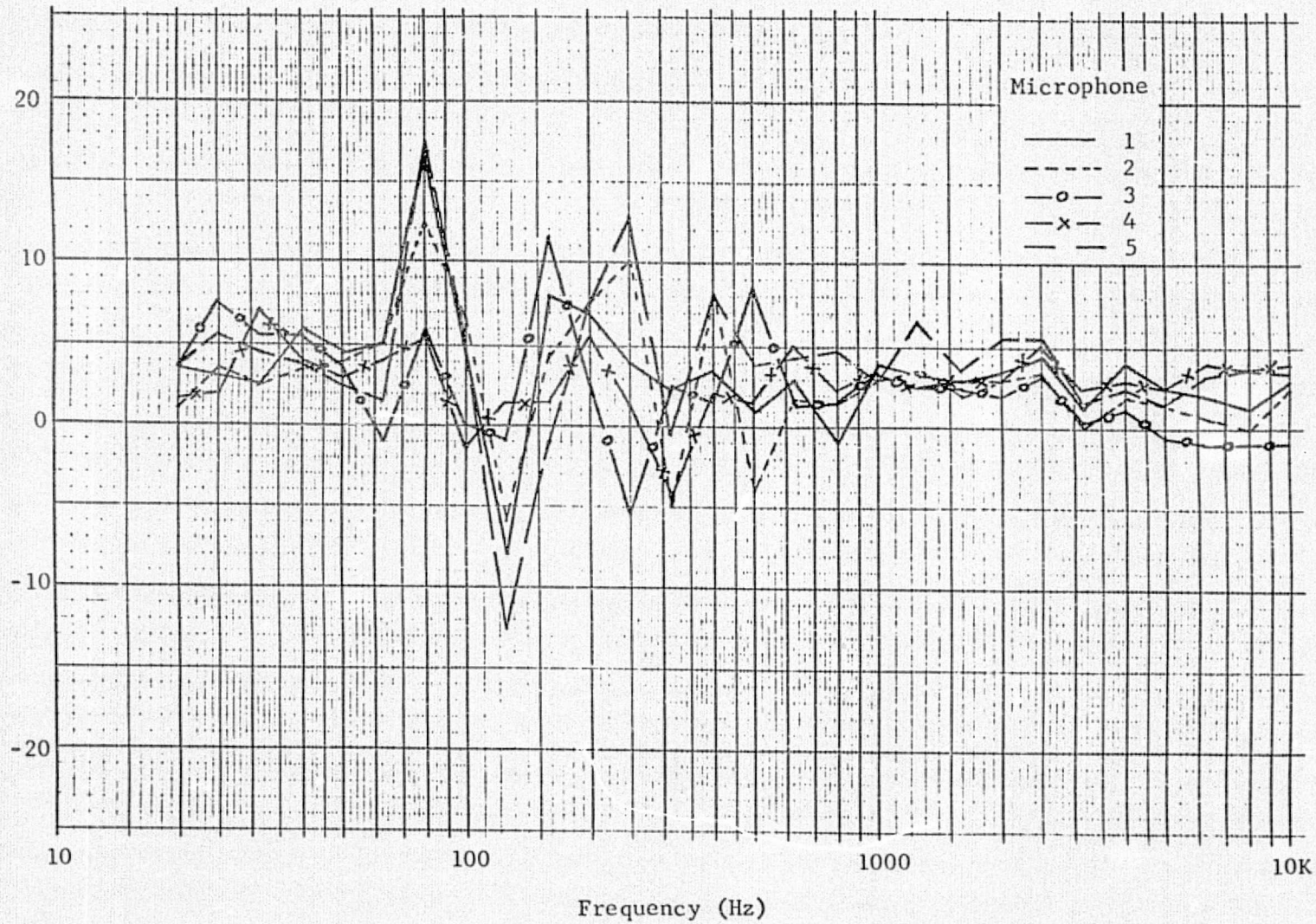

Figure 37. Comparison of Aluminum Shroud Noise Reduction Data - (1379 N/m^2 (0.2 psi) Helium Minus Ambient Condition Data)

quencies (as determined from narrow band analyses of internal microphones) is shown in Table 4. The internal acoustic modes of the model shrouds were calculated using the equation by Morse as described earlier in this section under Noise Reduction Concepts. In general, excellent agreement was obtained between the analytical and measured frequencies. The noise reduction curves exhibit rather sharp notches in the 80 and 200 Hz bands as shown in Figure 38 by the spectra obtained at microphone location 3 located at the center of the shrouds. These notches are produced by the first and second internal acoustic modes and are expected to be modified by the presence of a payload within the shroud.

Another region exhibiting minimum noise reduction is associated with the ring frequency regions of the spectrum. The ring frequencies were calculated by the following equation:

$$f_R = \frac{C_L}{2\pi R}$$

where f_R = ring frequency, Hz

C_L = longitudinal wave velocity, m/sec.

R = radius of the cylinder, m.

The analytically derived ring frequencies for the double-walled aluminum and composite shrouds were 1720 Hz and 1130 Hz respectively. Again, good correlation with the measured noise reduction spectra is shown in Figure 38.

The results of the model shroud tests and the excellent correlation with analytical results form a basis for comparison with other shroud configurations studied, and for prediction of noise reduction characteristics of full scale shrouds.

TABLE 4. ACOUSTIC FREQUENCIES IN MODEL (COMPOSITE) SHROUD

Mode Number (ℓ, m, n)	1,0,0	2,0,0	0,1,0	1,1,0	3,0,0	2,1,0	3,1,0	0,2,0 4,0,0	1,2,0	2,2,0	4,1,0	3,2,0 5,0,0	0,0,1	2,0,1
Calculated Frequency (Hz)	94	188	227	246	282	295	362	376	388	421	439	470	472	508
	Measured Frequency (Hz.)													
Microphone #1	96	192			280			376					472	496
#2	96	192	216	240		296	356		384		432		472	
#3	80 104	192	216	256		296		376			432	456		496
#4	80 104	192	216			296		376			432	456		
#5	96	192		240	280			376				464		496

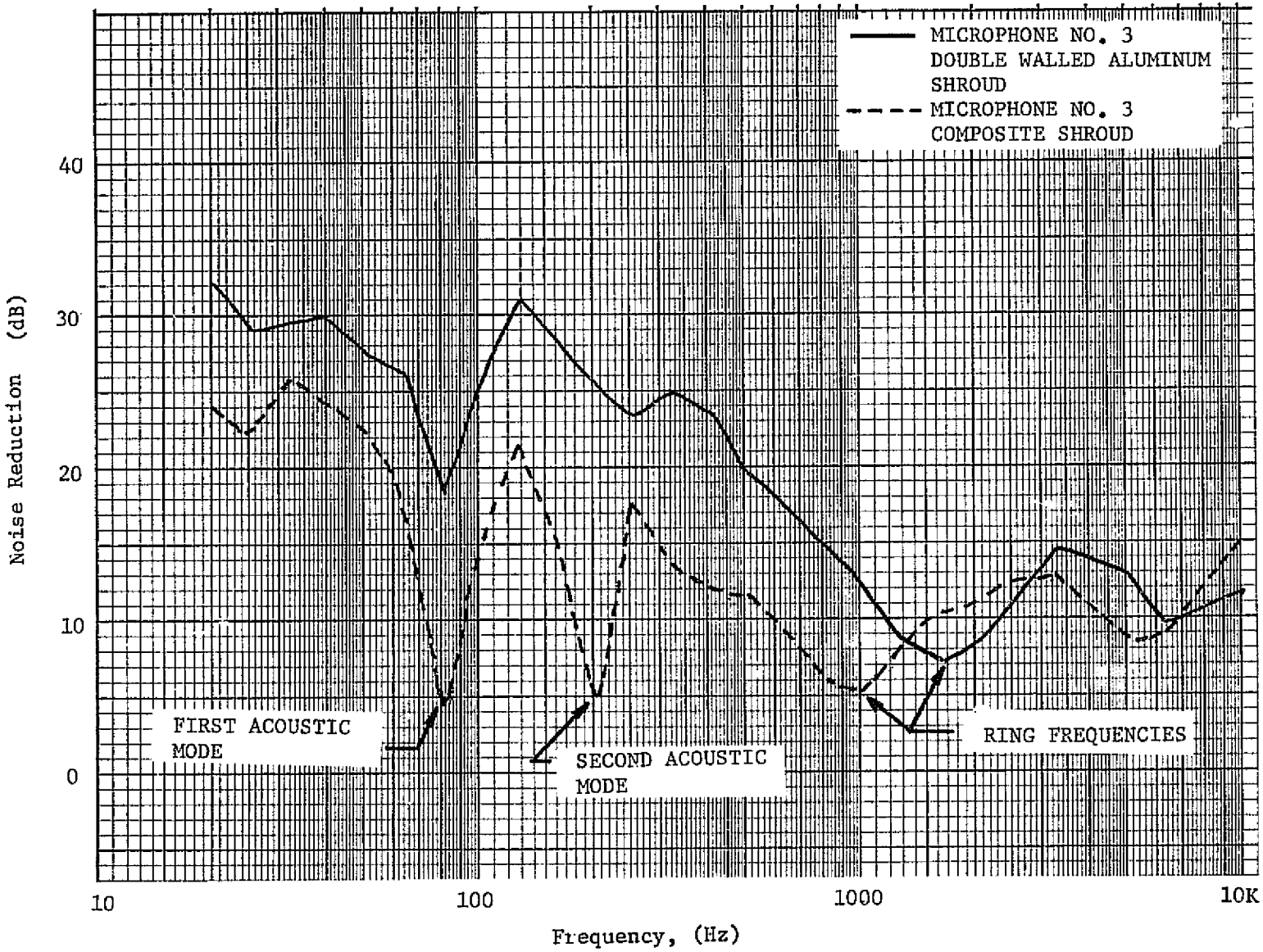

Figure 38 . Comparison of Noise Reduction Measured
At Microphone Location 3.

Shroud Comparisons

Noise Reduction

The average noise reduction values obtained from tests of the two scale model shrouds described in the previous section are compared to data obtained from the GSFC model shroud in Figure 39. The GSFC shroud described in Reference 14 was constructed of viscoelastic laminated material, and was approximately 0.914 m. (3.0 ft.) in diameter by 0.914 m. (3.0 ft.) long. The acoustic modes in the 80 Hz band, associated with the longitudinal dimension of the MMC shrouds, did not occur in the GSFC shroud due to its length to diameter ratio of 1:1. Tests were conducted on the GSFC shroud with and without a 2.54 cm. (1.0 inch) thick fiberglass liner, and the results are compared in Figure 40.

The results of the model shroud tests were used to estimate the noise reduction of full scale shroud configurations for comparison with proposed configurations developed by MSFC, GSFC and MDAC. The full scale shroud configurations are as follows:

Double-Walled Aluminum

Ring frame/longeron inner frame 5.08 cm (2.0 inch) thickness

Face sheets: 0.0406 cm (.016 inch) thickness
Diameter: 3.05 m (10.0 feet)
Length: 6.1 m (20.0 feet)

Foam/Fiberglass Epoxy

Face sheets: 0.065 cm (.0256 inch) thickness
Urethane foam core: 5.08 cm (2.0 inch) thickness
Diameter: 3.05 m (10.0 feet)
Length: 6.1 m (20.0 feet)

The estimated noise reduction spectra for these configurations are compared with other shroud configurations in Figure 41. The

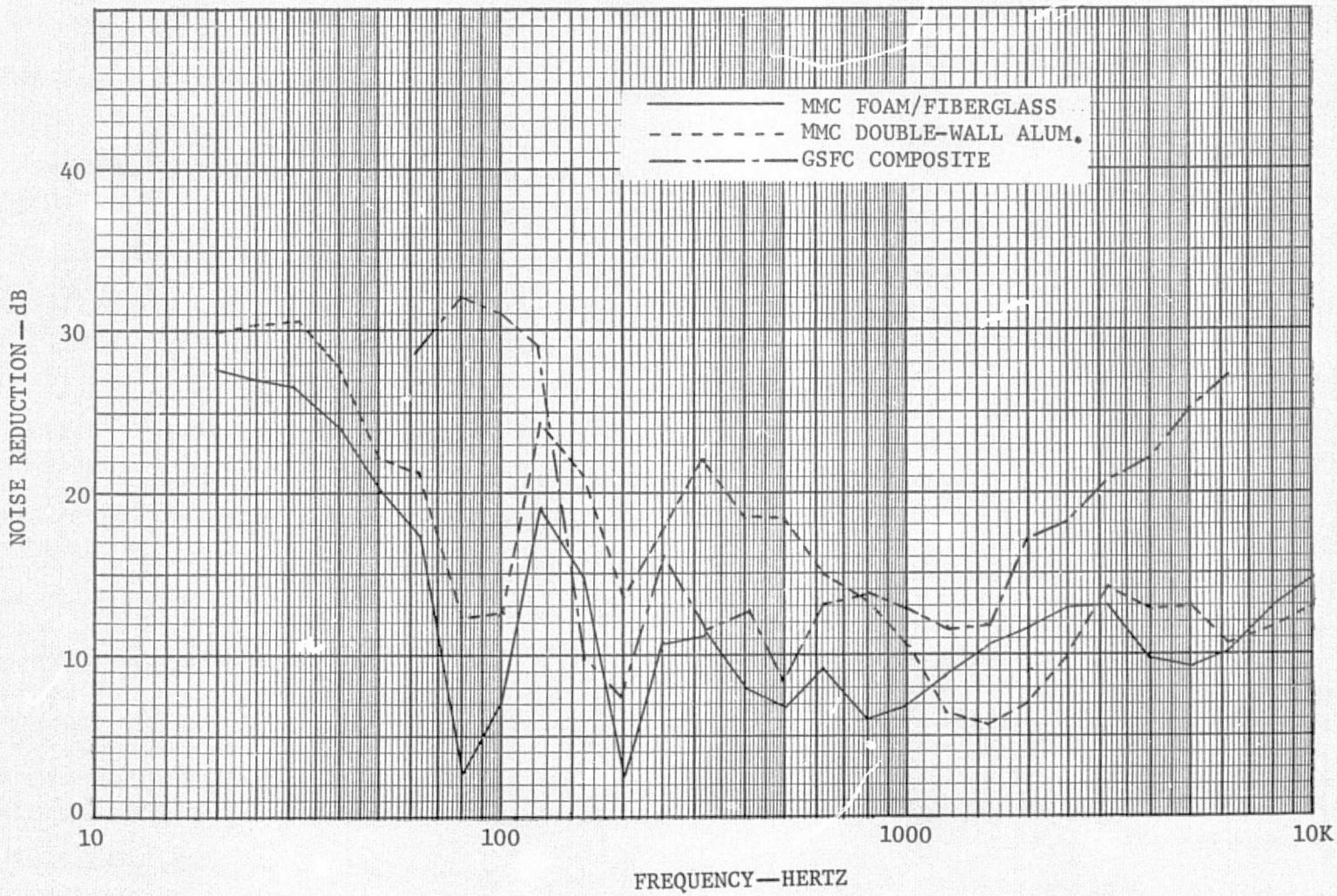

Figure 39. Comparison of Measured Noise Reduction Between MMC and GSFC 0.914m(3.0FT.) Diameter Test Shrouds.

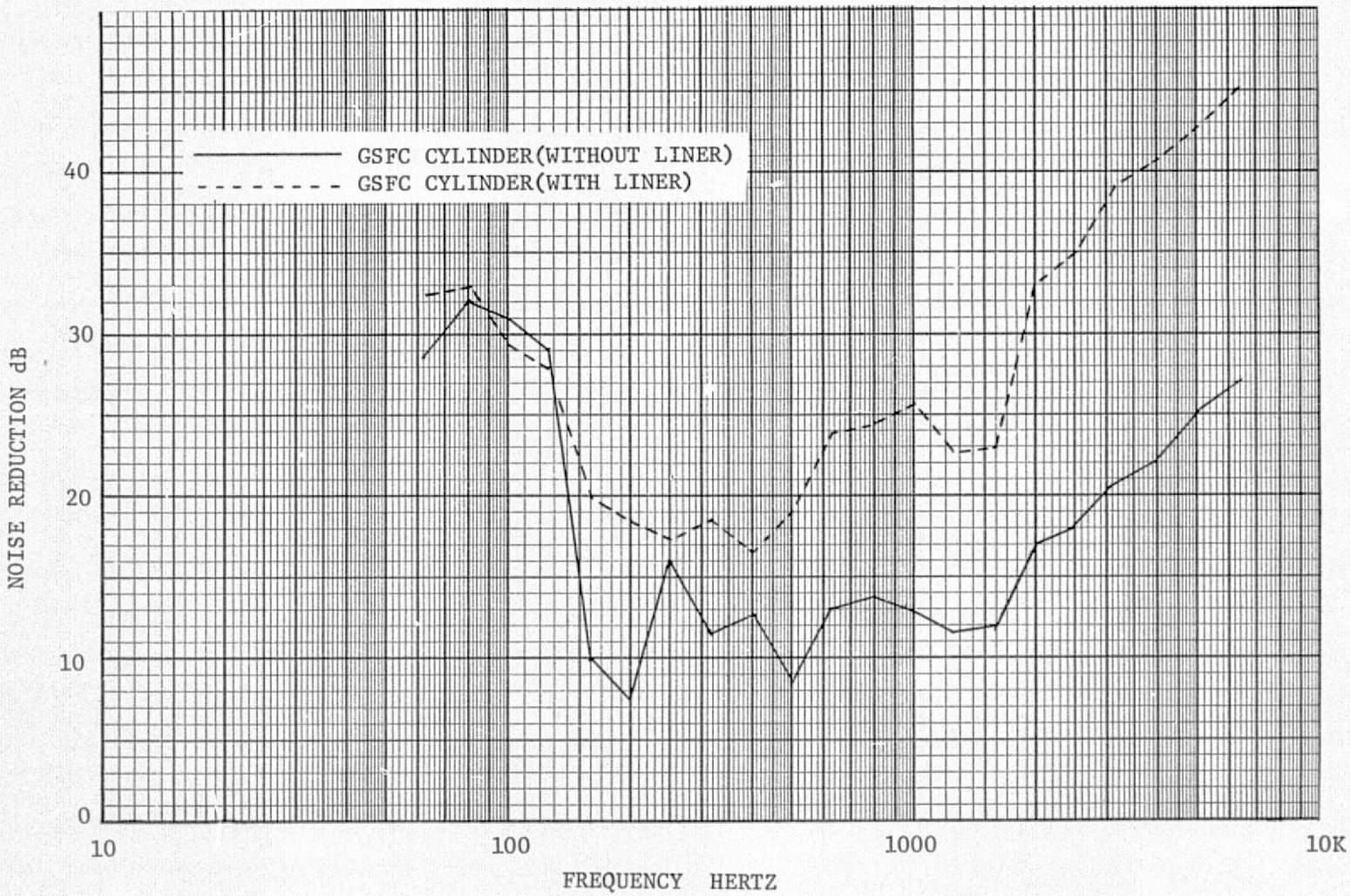

Figure 40. Comparison of GSFC Measured Noise Reduction With and Without Fiberglass Liner.

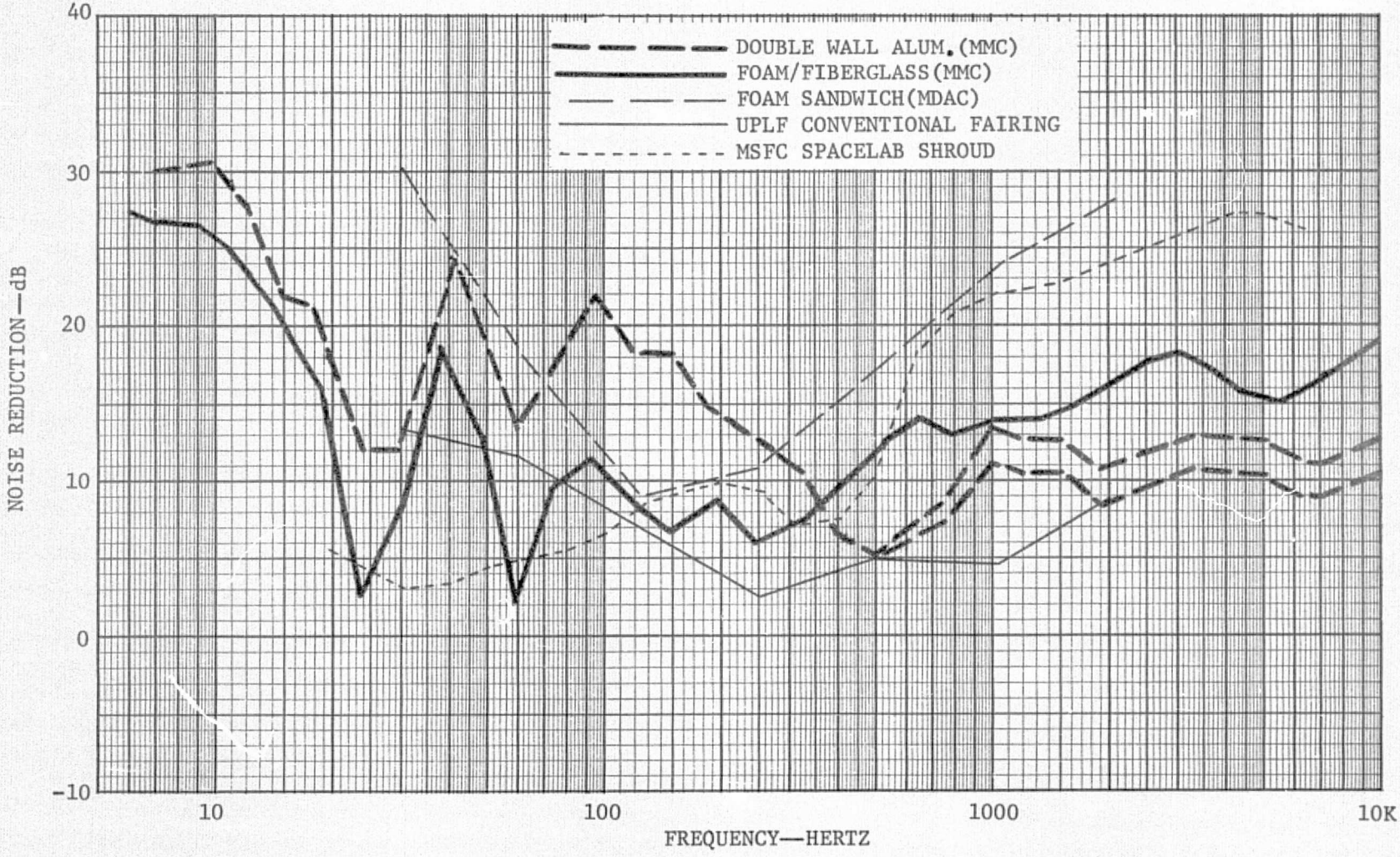

Figure 41. Comparison of Estimated Full-Scale Noise Reduction Spectra for MMC, MDAC, UPLF, and MSFC Shrouds.

significant material properties and configuration definitions are listed in Table 5 . The data and information relative to the MDAC and UPLF shrouds were obtained from Reference 15 , whereas data on the MSFC shroud were obtained from Reference 16 . As shown in Figure 41 , the notches in the noise reduction spectra which occurred in the 80 and 200 Hz bands for the model shrouds, have been shifted to the 25 and 63 Hz bands for the full scale configurations. Analytical calculations of the ring frequencies and surface weight considerations were used in the estimates of noise reduction for the full scale configurations. We feel that the estimates of noise reduction in the notch regions corresponding to internal modes are conservatively low because the installation of payloads within the shrouds will tend to eliminate certain of these modes and increase the noise reduction in these regions. Since these internal acoustic modes are a function of the shroud geometry, the first 10 modes were calculated for several different configurations and are presented in Table 6.

The noise reduction values (Figure 41) were applied to the orbiter internal bay acoustic levels (Figure 42) as specified in JSC 07700, Volume XIV, and as predicted by Rockwell International. The resulting predicted payload environments are presented in Figures 43 and 44.

Table 5. Comparison of the Properties of Different Shroud Configurations

Description	Weight/Area kg/m^2 (lb/ft^2)	Noise Reduction (O.A. SPL, dB) R.I. (149.4 dB)	Noise Reduction (O.A. SPL, dB) JSC-07700, (145 dB)
1. MMC Double-Wall Alum. Shroud 0.0406 m (.016 in.) Face Sheets 5.08 cm (2.0 in.) Core (Stringer-O-Rings) 3.05 m (10.0 ft) Diam.x6.1 m (20.0 ft) Long.	6.7 (1.37)	11.6	9.5
2. MMC Foam/Fiberglass Epoxy Shroud 0.065 cm (.0256 in.) Face Sheets 5.08 cm (2.0 in.) Foam Core 3.05 m (10.0 ft) Diam.x6.1 m (20.0 ft) Long.	6.35 (1.3)	7.1	8.3
3. MDAC Foam/Aluminum Sandwich Shroud 0.063 cm (.025 in.) Face Sheets 15.2 cm (6.0 in.) Foam Core 4.6 m (15.0 ft) Diam.x7.6 m (25.0 ft) Long.	8.4 (1.72)	13.7	9.6
4. Universal Payload Fairing (UPLF) Conventional Alum. Skin/Stringer 3.048 m (10.0 ft) Diameter	6.83 (1.4)	7.8	4.9
5. MSFC - Skin/Stringer with Liner 0.1524 cm (.06 in.) Al. Skin, 5.08 cm (2.0 in.) Stringer 3.81 cm (1.5 in.) Thick Liner	6.5 (1.332)	6.6	9.8

Table 6. Calculated Acoustic Modes for Full-Size Shrouds

Radius	LENGTH = 3.048m(10 FT.)		LENGTH = 6.096m(20 FT.)		LENGTH = 9.144m(30 FT.)	
	Mode No.	Freq. (Hz)	Mode No.	Freq. (Hz)	Mode No.	Freq. (Hz)
1.524m (5.0 FT.)	1,0,0	56.4	1,0,0	28.2	1,0,0	18.2
	0,1,0	66.2	2,0,0	56.4	2,0,0	37.6
	1,1,0	87.0	0,1,0	66.2	3,0,0	56.4
	0,2,0	109.7	1,1,0	71.9	0,1,0	66.2
	2,0,0	112.9	3,0,0	84.6	1,1,0	68.8
	2,1,0	130.8	2,1,0	87.0	4,0,0	75.2
	0,0,1	137.7	3,1,0	107.4	2,1,0	76.1
	1,0,1	148.8	0,2,0	109.7	3,1,0	87.0
	0,3,0	150.9	4,0,0	112.9	5,0,0	94.1
	2,2,0	157.4	1,2,0	113.3	4,1,0	100.2
2.286 m (7.5 FT.)	0,1,0	44.1	1,0,0	28.2	1,0,0	18.8
	1,0,0	56.4	0,1,0	44.1	2,0,0	37.6
	1,1,0	71.6	1,1,0	52.4	0,1,0	44.1
	0,2,0	73.2	2,0,0	56.4	1,1,0	47.9
	0,0,1	91.8	2,1,0	71.6	3,0,0	56.4
	1,2,0	92.4	0,2,0	73.2	2,1,0	58.0
	0,3,0	100.6	1,2,0	78.4	3,1,0	71.6
	1,0,0	107.7	3,0,0	84.6	0,2,0	73.2
	2,0,0	112.9	0,0,1	91.8	4,0,0	75.2
	1,3,0	115.4	2,2,0	92.4	1,2,0	75.5

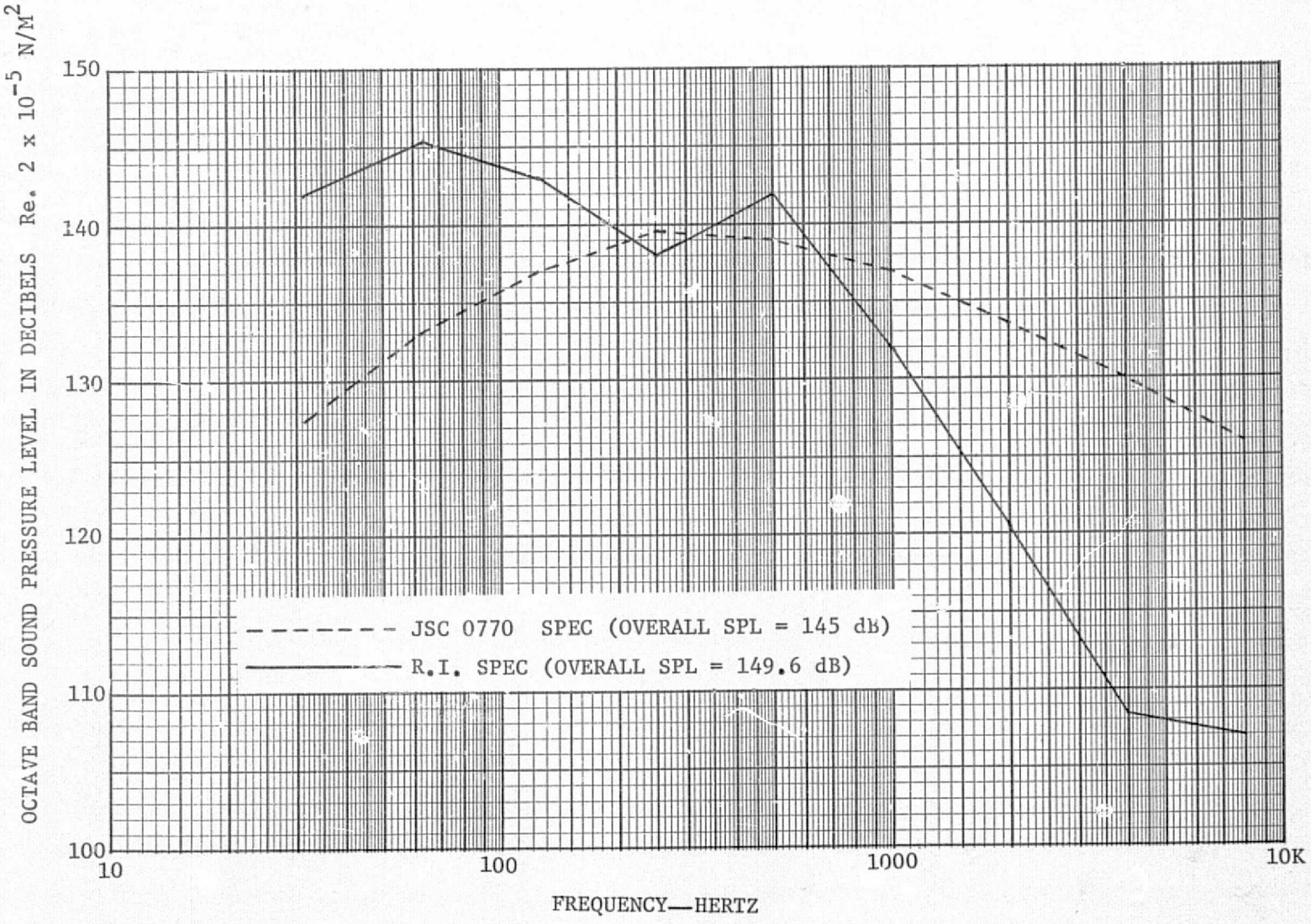

Figure 42. Orbiter Internal Bay Acoustic Levels.

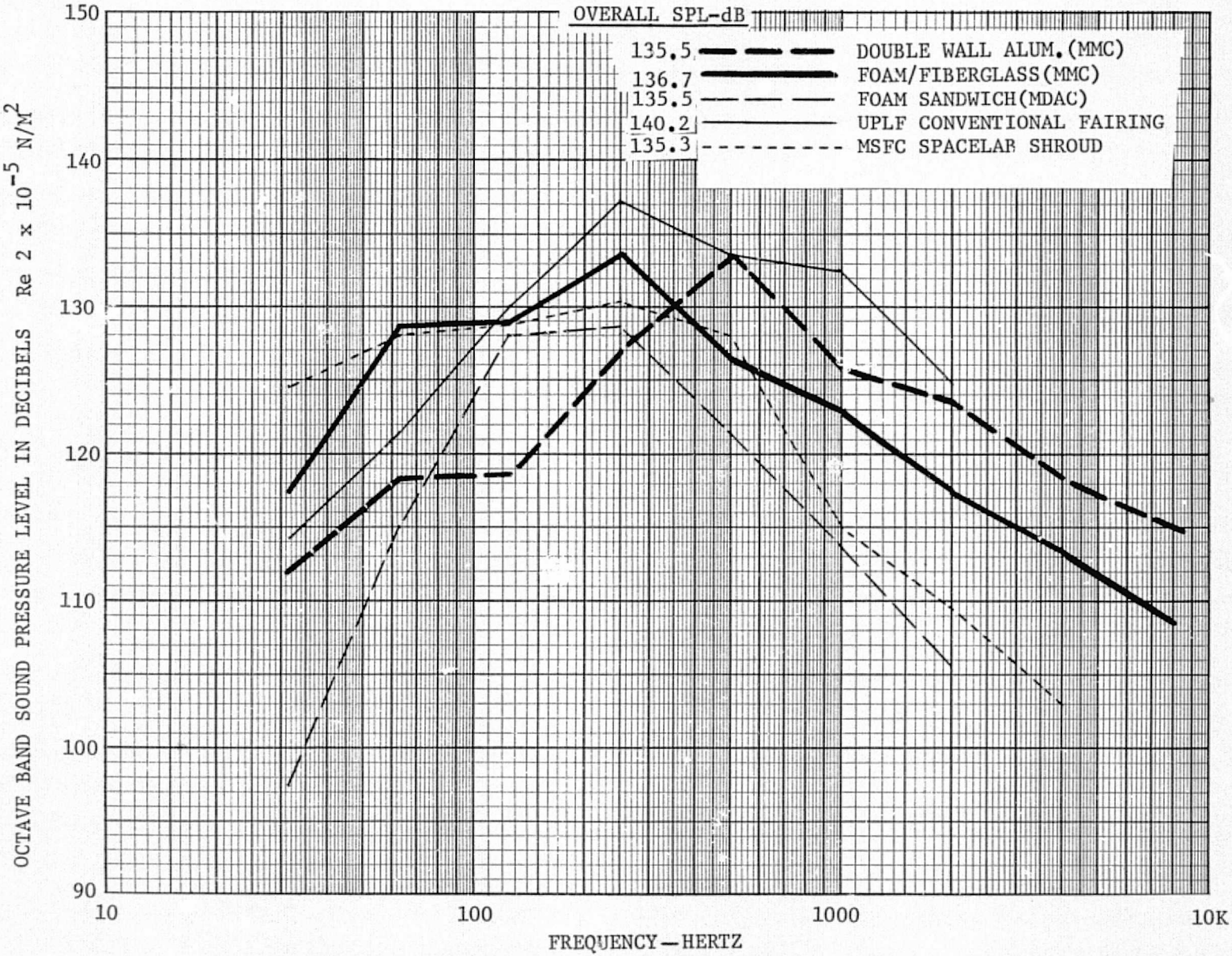

Figure 43. Predicted Payload Sound Pressure Levels Based Upon JSC 0770 Acoustic Levels.

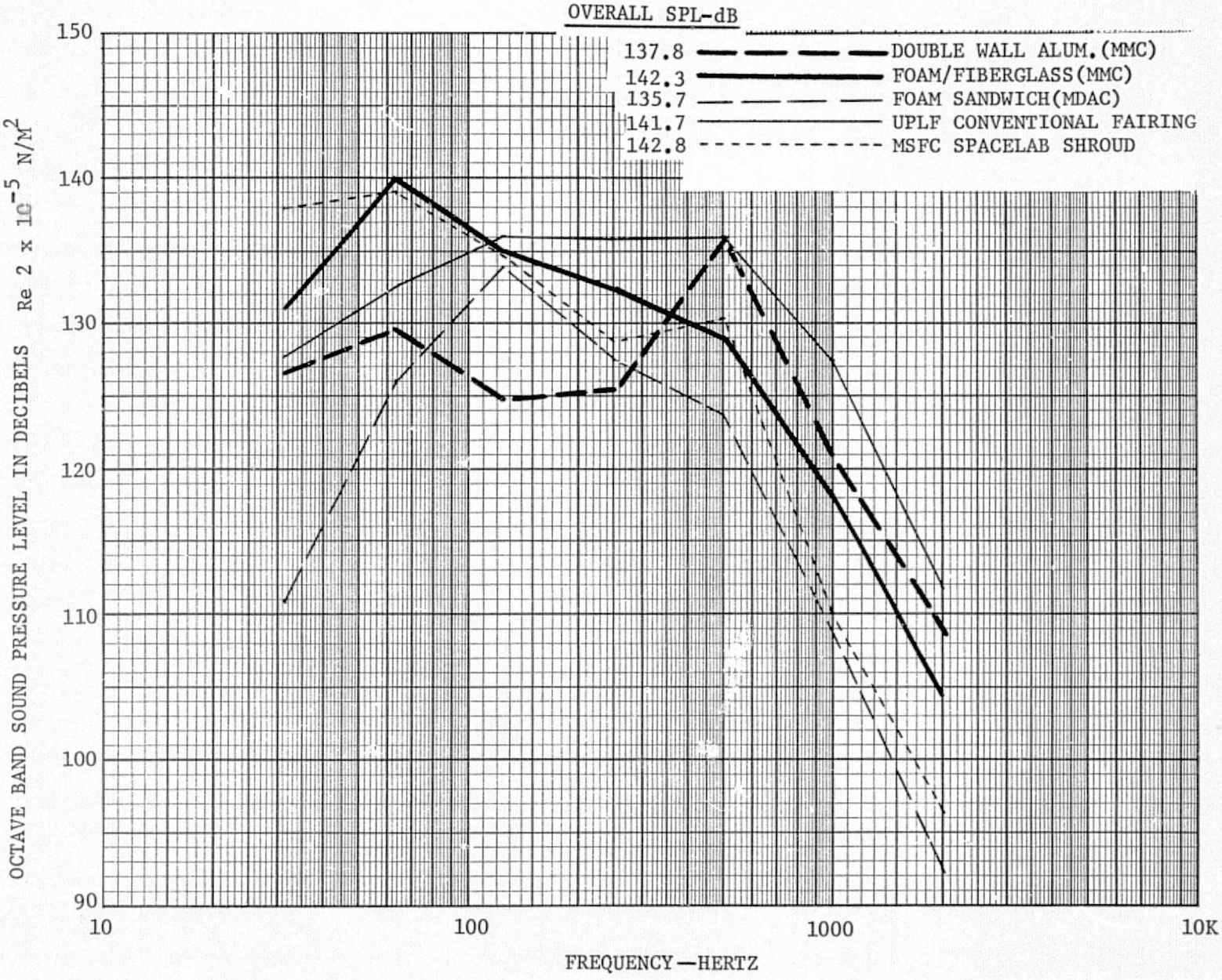

Figure 44. Predicted Payload Sound Pressure Levels Based Upon Rockwell International Acoustic Levels.

Payload Impact Considerations

Thermal

If thermal requirements are not considered, the impact of the incorporation of acoustic shrouds on payload thermal control would range from negligible to severe, depending upon the individual payload involved. This is true whether the double wall metallic or the composite wall shroud construction is used.

In order to avoid compromising the basic utility of the shuttle with respect to handling payloads with a wide variety of thermal environment requirements, it is desirable that the acoustic shroud be made thermally "invisible" to the greatest extent possible, regardless of the payload involved. The following paragraphs are a discussion of the thermal control impact of acoustic shrouds as seen during the various shuttle mission phases.

Presumably, the acoustic shrouds will not be added to the payload until it is in the process of being mated to the shuttle payload bay. Once in the cargo bay, however, the payload designer expects his creation to be in a compartment containing an atmosphere conditioned to specified temperature limits. The designer may also depend on a specified throughput of conditioned air/GN_2 to carry away energy generated within his spacecraft, thus preventing overheating during prelaunch checkout. This situation will prevail until just prior to launch.

The acoustic shroud must not materially interfere with the flow of conditioned air/GN_2 past a payload. This requirement may be met by making the shroud permeable to the surrounding atmosphere through an appropriate acoustic energy blocking medium. A more positive approach would be to

provide ducts from the payload bay conditioned gas source to the interior of the shroud(s) with an appropriate shroud vent that provides acoustic blocking.

The boost phase is a thermally short term situation during which the payload makes the transition from convective mode heat rejection to radiant mode heat rejection. The presence of the acoustic shroud will have little impact during this phase because it will be thermally equivalent to the payload bay and walls as far as a payload is concerned.

Unless an internal heat sink is provided, any thermally active payload must be provided with a radiant "view" of space at some point in time after orbit is achieved. The time delay allowable is of course inversely proportional to the heat rejection rate of the payload. The acoustic shroud will serve to shorten this allowable delay time because it constitutes a radiation barrier between the payload and the payload bay walls which are presumably cooling down. As a general policy, then, the acoustic shroud should be removed from the payload as soon as possible after orbit is achieved.

It is thermally desirable, however, to allow all or parts of the acoustic shroud to be retained for as long as individual mission requirements may dictate. For instance, a payload destined for later deployment might require shielding from space and/or heating while payload bay doors are open for retrieval or deployment of another payload. In this situation, retaining the acoustic shield around the inert payload may conserve energy and/or simplify payload design.

Contamination

The incorporation of an acoustical shroud system into the Orbiter

payload bay necessitates that its impact upon the contamination control of the Space Transportation System and its payloads must be considered and completely evaluated. The shroud system will not only provide additional contamination protection while it is in place, but it may also introduce new contaminant sources in the near vicinity of the enclosed payloads and influence other contamination related phenomena taking place within the payload bay volume. These items are discussed in further detail in the following paragraphs.

Once the acoustical shroud has been assembled around a particular payload, it will inherently provide contamination protection during all ensuing ground, launch and on orbit operations. This will include attenuation of particulate and non-volatile residue deposition during ground operations as well as minimizing contamination impacts during the launch phase. The launch phase contaminants result from such sources as launch generated plasma sheath effluents ingested through the active payload bay vents due to imbalances in pressure differentials across them, particulate matter migration within the payload bay under the influence of gravity and inertia, and exhaust products ingested through the active vents generated during Solid Rocket Booster separation rocket operation. Prior to discarding the shroud on orbit, it will provide additional protection when the payload bay doors have been opened from Orbiter outgassing, offgassing, cabin atmosphere leakage, Vernier Control System, Reaction Control System, Orbital Maneuvering System, and evaporator vent impacts as well as any other Orbiter sources incurred during this phase.

In addition to the apparent benefits that the acoustical shroud system will provide to payload contamination control, several disadvan-

tages or areas of concern arise which must be dealt with to effectively insure payload sensitive surface cleanliness integrity and minimum interference with mission operations. Any non-metallic materials used in the construction of the shroud system will introduce additional contaminant sources to the enclosed Orbiter payloads in the form of outgassing (bulk material mass loss) and offgassing (desorption of adsorbed and absorbed gases, liquids, and volatiles). Therefore, proper selection of construction materials is very critical in the shroud designs. Materials used must meet the criteria set forth in SP-R-0022A (Reference 17) or have already been qualified under 50M02442 (Reference 18). In addition, materials that are generally high outgassing but are enclosed or sealed such as the BX-250 polyurethane foam configuration option should be tested for outgassing in the design configuration to the aforementioned criteria. Construction materials must also be selected on the basis of minimum production of particulate contamination. The entire shroud system must be designed and constructed to meet the program criteria established in "Payload Contamination Control Requirements for STS Induced Environments", MSFC, 22 July 1975.

The presence of the acoustical shroud around the payload on orbit will tend to extend the enclosed materials high offgassing period due to limiting the vent down period for encapsulated payloads. This extension of the offgassing period will lengthen the on orbit time for payloads to become operational to avoid potential pressure induced corona arc-over damage to high voltage power systems. This is especially true for the IUS-Tug shroud configuration which will not be discarded until after Orbiter/IUS separation. The pallet mounted shroud should be deployed as early as

possible to minimize these required delay times.

The acoustical shroud system must be designed with interface provisions for the Class 5000 clean air ground purge system and must have the ability to be held at a Class 100K or better. The deployment operation on orbit must be such that Orbiter payload bay purge capability is maintained due to the fact that the system is required for environmental control 30 minutes after Orbiter landing.

Deployment/Interface Considerations

Deployment of the shroud system should impart minimum impact to the payloads and Orbiter. No pyrotechnic systems should be utilized on Orbiter attached equipment (i.e., pallet mounted shroud), therefore, consideration should be given to incorporating a spring release system or to deploying the shroud with the Remote Manipulator System and pulling away by use of the Orbiter Reaction Control System. Deployment of the IUS-Tug shroud system could be by pyrotechnics if operations are timelined properly. An example of a type of non-explosive initiator which could be utilized to release a spring latch system is shown in Figure 45 . This configuration consists of a molded ceramic split spool with spring-temper stainless steel wire, one end of which is held in position on the spool by a link wire. The link wire, which is short and of small diameter, is terminated by two electrical contacts contained in the same spool half. The spool halves are joined and the restraining wire is hooked into the link wire loop and then wound onto the spool. The winding is accomplished under a specific tensile load and is completed by tying off the restraining wire at the spool end opposite the link wire.

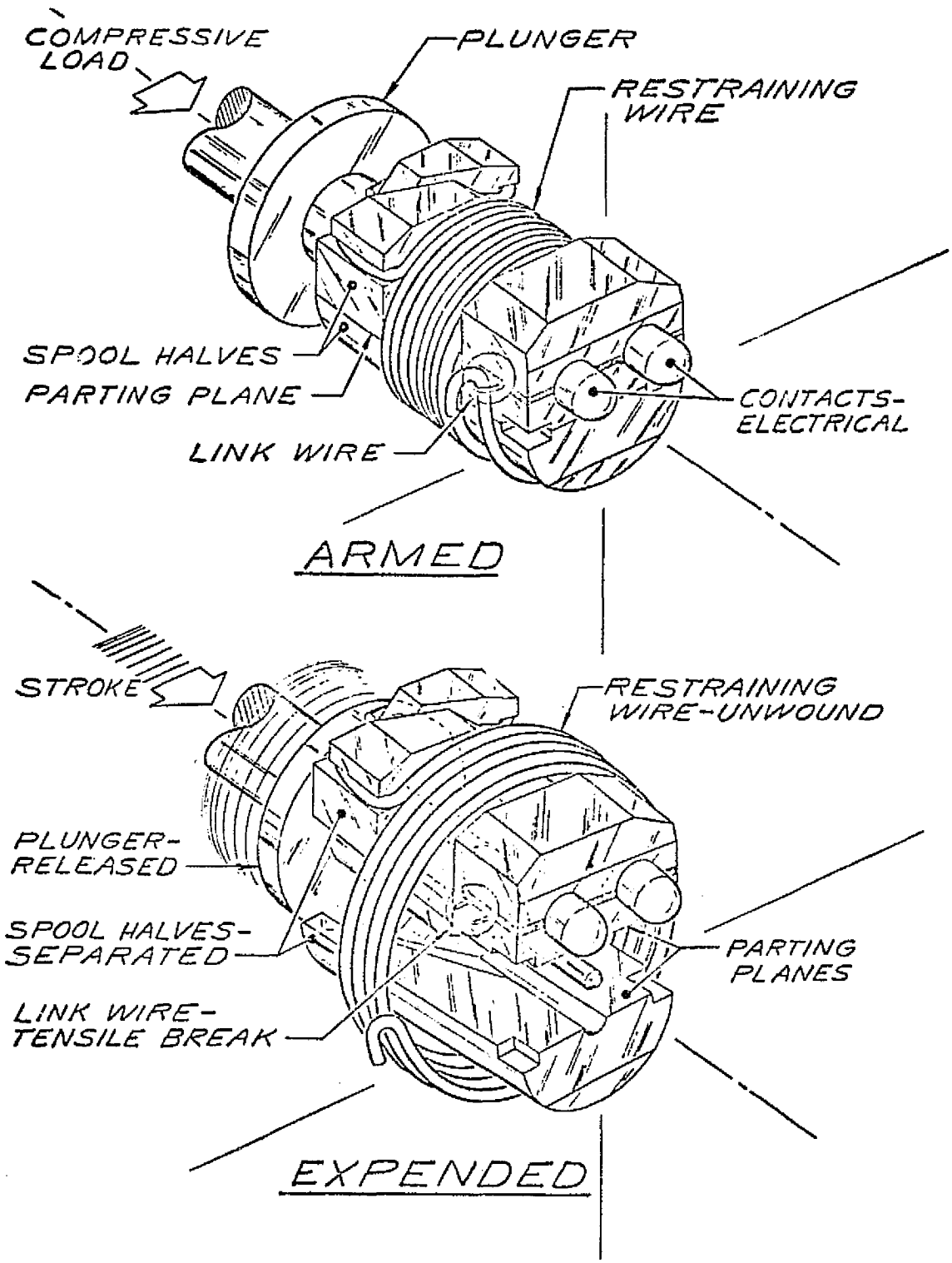

Figure 45. Typical Non-Explosive Initiator Utilized To Release a Spring Latch System.

The spool is configured to permit compressive axial loading such as to cause the spool halves to separate when not restrained by the wrapped wire. NOTE: the specific device indicated in Figure 45 is patented by G&H Technology, Inc. Electrical current is passed through the link wire causing it to heat up. As the wire temperature increases, its tensile strength decreases, until it falls below the tensile stress applied by the restrainin ire. The link wire fails in tension, freeing the restraining wire. The restraining wire uncoils, permitting the spool halves to separate.

One end of the spool (link wire end) is flat, the other end is configured to receive plunger which is spring loaded toward the flat spool end. When the restraining wire is released by the link wire breaking, the spring loaded plunger drives in between the spool halves. It is this plunger movement which performs the end function or initiates a follow-on function.

A major consideration will be the design of umbilical and thermal control duct interfaces as well as attachment hardware for the pallet and/or payload bay interface connections in order to minimize acoustic flanking or leakage paths.

Weight Comparisons

Estimates were made of the weights of several configurations of both the double walled aluminum and of the composite/foam shrouds. These data are presented in Tables 7 through 10 , and plotted in Figures 46 and 47 . The weight estimates were based on the modular type shroud concepts described previously in this section and are not necessarily optimum for any of the shroud sizes.

For the double walled aluminum shroud, the weights were calculated based on a typical aerospace ring frame/stringer construction comprised of the following elements:

2 End Closures: Channel (C) sections
5.08 x 2.54 x 0.318 cm.
(2.0 x 1.0 x 0.125 in.)

3 Ring Frames: I-sections
5.08 x 2.54 x 0.254 cm.
(2.0 x 1.0 x 0.10 in.)

24 Stringers: Zee sections
5.08 x 1.9 x 0.254 cm.
(2.0 x 0.75 x 0.10 in.)

24 Intercostals: Tee sections
2.54 x 2.54 x 0.127 cm.
(1.0 x 1.0 x 0.050 in.)

2 Skins: 0.041 cm. (0.016 in.) thickness.

Table 7. IUS/TUG Double Walled Shroud Weights in Kilograms (pounds) (Shroud Diameter = 3.048 m)

	Shroud Length m (ft)				
	3.048 m (10.0 ft)	4.67 m (15.0 ft)	6.1 m (20.0 ft)	7.62 m (25.0 ft)	9.15 m (30.0 ft)
Double Walled Aluminum Cylinder	243 Kg (535 lbs)	340 Kg (749 lbs)	437 Kg (963 lbs)	534 Kg (1177 lbs)	631 Kg (1391 lbs)

Table 8. Pallet Double Walled Shroud Weights in Kilograms (pounds) (Shroud Diameter = 4.46 m)

	Shroud Length m (ft)		
	3.048 m (10.0 ft)	6.1 m (20.0 ft)	9.15 m (30.0 ft)
Double Walled Aluminum Cylinder	356 Kg (786 lbs)	496 Kg (1094 lbs)	636 Kg (1402 lbs)

Table 9. IUS/TUG Composite Shroud Weights - kg (lbs) (Shroud Diameter = 3.048 m)

Core Thickness cm (in.)	Shroud Length m (ft)				
	3.048 m (10.0 ft)	4.67 m (15.0 ft)	6.1 m (20.0 ft)	7.62 m (25.0 ft)	9.15 m (30.0 ft)
2.54 (1.0)	193 (425)	270 (595)	347 (764)	424 (934)	500 (1103)
5.08 (2.0)	231 (510)	324 (714)	416 (918)	509 (1122)	602 (1327)
7.62 (3.0)	269 (593)	376 (830)	484 (1067)	591 (1304)	699 (1541)
10.16 (4.0)	306 (675)	429 (945)	551 (1215)	674 (1485)	796 (1755)

Table 10. Pallet Composite Shroud Weights kg (lbs) (Shroud Diameter = 4.46 m)

Core Thickness cm (in.)	Shroud Length m (ft)		
	3.048 m (10.0 ft)	6.1 m (20.0 ft)	9.15 m (30.0 ft)
2.54 (1.0)	283.5 (625)	395 (870)	506 (1115)
5.08 (2.0)	341 (752)	474 (1046)	608 (1340)
7.62 (3.0)	396 (873)	551 (1215)	706 (1557)
10.16 (4.0)	451 (995)	628 (1384)	804 (1773)

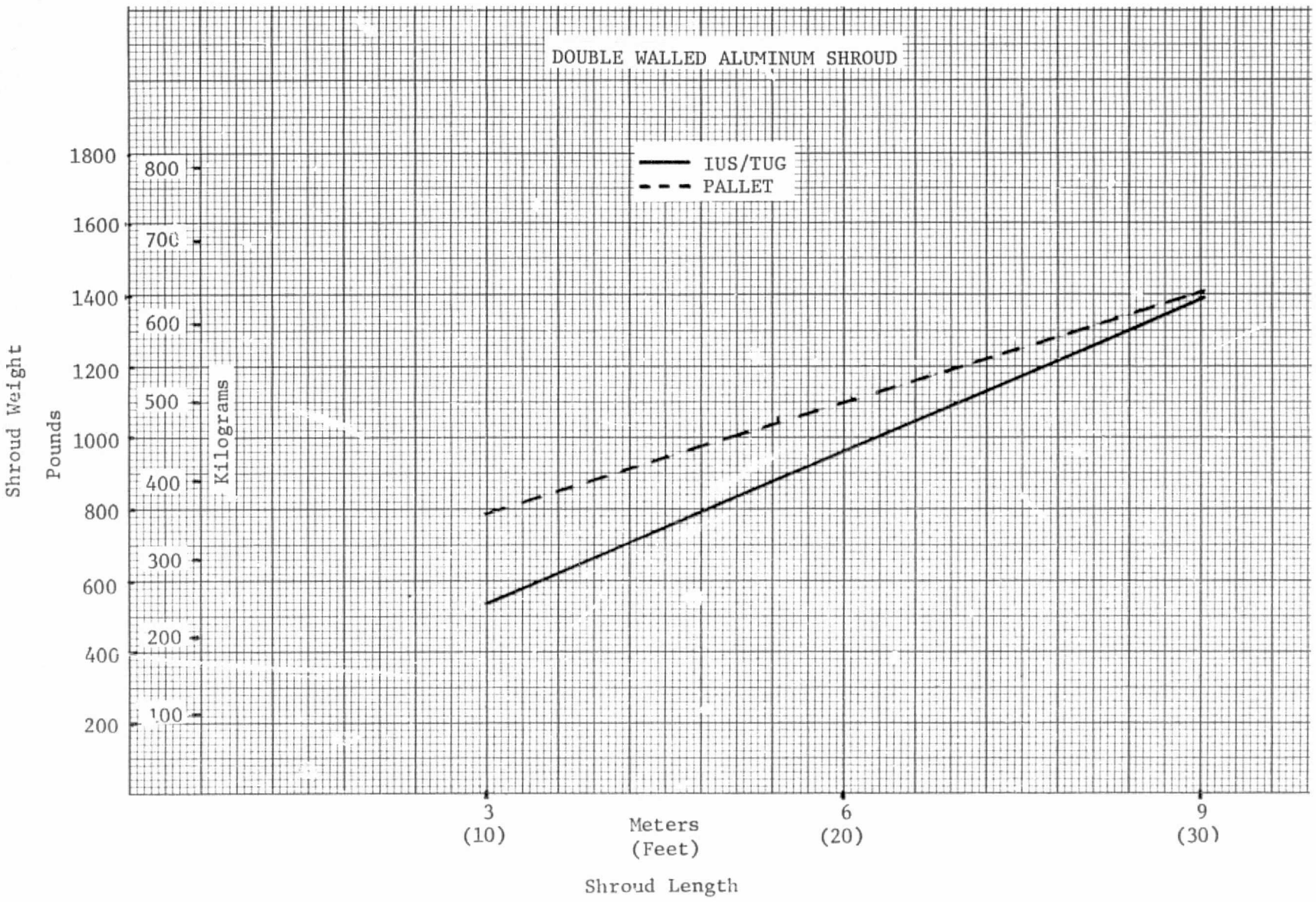

Figure 46. Weights of Double Walled Aluminum Shrouds as a Function of Length.

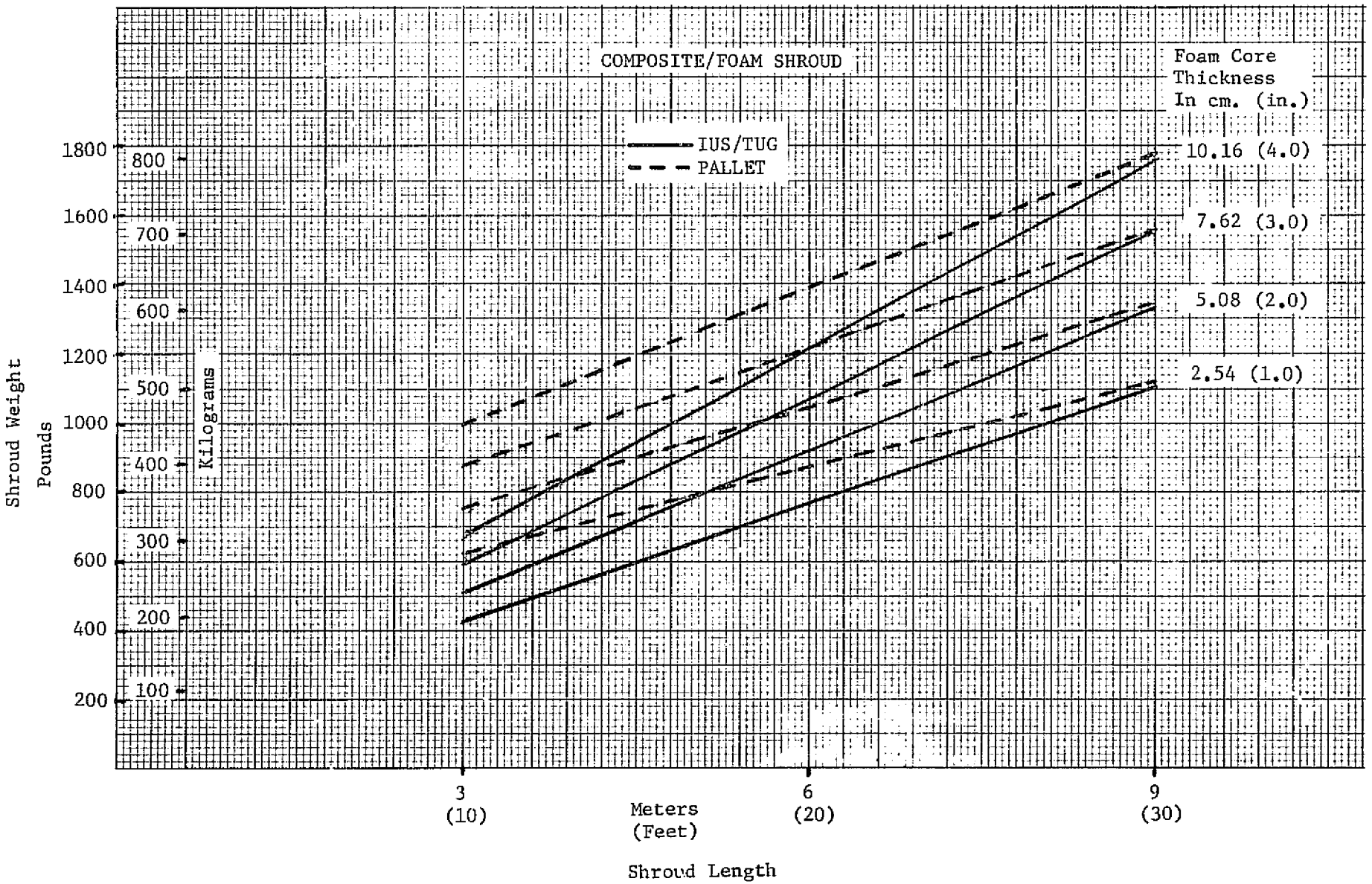

Figure 47. Weights of Composite/Foam Shrouds as a Function of Length.

Weights for the composite/foam shrouds were based on the use of inner and outer skin thicknesses of 0.065 cm (.025 in.) and foam core thicknesses as indicated in Tables 9 and 10.

Comparisons of the weights of these shrouds with configurations developed by MSFC, MDAC and GSFC can be made only approximately, since the shroud geometries and noise reduction characteristics are different for each configuration. The configurations and pertinent data for all of the shroud configurations are listed in Table 11. To obtain an approximate comparison of weights of the different shrouds, a 3 meter diameter x 6 meter long (IUS-TUG) configuration was selected, and weights of the various shroud configurations were normalized to this size, based on the assumption that the surface weights remained constant. The results are summarized in Table 12.

Table 11. Weight Comparisons of Full-Scale Shrouds

	Weight kg (lb)	Shell Thickness cm (in.)	Face Sheet Th. cm (in.)	Wt./Area kg/m^2 (lb/ft^2)
MMC D.W. Alum. Pallet 4.46 m diam. x 3.0 m long. (14.6 ft x 9.84 ft)	357 (786)	5.08 (2.0)	0.041 (0.016)	6.64 (1.36)
MMC D.W. Alum. IUS/TUG 3.048 m diam. x 3.048 m long. (10.0 ft x 10.0 ft)	243 (535)	5.08 (2.0)	0.041 (0.016)	6.64 (1.36)
MMC Composite Pallet 4.46 m diam. x 3.0 m long. (14.6 ft x 9.84 ft)	341 (752)	5.08 (2.0)	0.065 (0.0255)	6.35 (1.3)
MMC Composite IUS/TUG 3.048 m diam. x 3.048 m long. (10.0 ft x 10.0 ft)	231 (510)	5.08 (2.0)	0.065 (0.0255)	6.35 (1.3)
MDAC Composite Cylinder 3.4 m diam. x 3.6 m long. (11.0 ft x 12.0 ft)	340 (750)	7.6 (3.0)	0.041 (0.016)	3.86 (0.79)
MDAC Composite Cylinder 4.6 m diam. x 7.6 m long. (15.0 ft x 25.0 ft)	1509 (3328)	15.2 (6.0)	0.064 (0.025)	8.4 (1.72)
MSFC Spacelab Pallet 4.46 m diam. x 3.0 m long. (14.6 ft x 9.84 ft)	316 (696)	5.08 (2.0)	0.1524 (0.060)	6.5 (1.331)
GSFC Viscoelastic Cylinder 3.048 m diam. x 3.048 m long. (10.0 ft x 10.0 ft)	173 (382)	5.08 (2.0)	0.051 (0.020)	3.7 (0.75)

Table 12. Comparison of Weights for Different Shroud Configurations (3 m diameter x 6 m long., IUS-TUG)

Shroud Type	Shroud Weight in kg (lbs)
MMC Double Walled Aluminum	483 (963)
MMC Composite/Foam (5.08 cm thick)	416 (918)
MSFC (IUS-TUG)	481 (1060)
MDAC (7.62 cm thick)	472 (1040)
MDAC (15.24 cm thick)	787 (1736)

Cost Comparisons

Estimates of the cost to design and fabricate both the double-walled aluminum shroud and the composite foam shroud were made for a number of lengths and production run volumes. These data are presented in Tables 13 and 14 , and selected configurations are compared in Figures 48 and 49 .

Estimated costs of the MDAC shrouds were available from Reference 15. However, cost figures were not available for the MSFC and GSFC shrouds, and no meaningful comparison of costs could be made for the different shroud configurations.

Table 13. Estimated Unit Costs of Double Walled Aluminum Shroud in Thousands of Dollars

IUS/TUG Configurations (diameter = 3.048 m (10.0 ft))

Per Unit Costs	Shroud Length				
	3.048 m (10.0 ft)	4.67 m (15.0 ft)	6.1 m (20.0 ft)	7.62 m (25.0 ft)	9.15 m (30.0 ft)
1 Shroud	$2552.2	$2945.0	$3194.8	$3587.8	$3837.4
10 Shrouds	482.3	671.0	770.5	959.1	1058.7
50 Shrouds	254.0	398.5	473 1	614.4	686.9
100 Shrouds	213.6	344.2	407.9	538.7	602.4

Pallet Configurations (Shroud Diameter = 4.46 m (14.6 ft))

Per Unit Costs	Shroud Length		
	3 m (9.84 ft)	6 m (19.68 ft)	9 m (29.53 ft)
1 Shroud	$2865.6	$3357.4	$3870.4
10 Shrouds	567.5	817.3	1069.3
50 Shrouds	308.2	497.3	686.8
100 Shrouds	261.9	433.4	605.2

Table 14. Estimated Unit Costs of Composite Shrouds in Thousands of Dollars

IUS/TUG Configuration - Diameter = 3.048 m (10.0 ft)

	Core Thickness cm (in.)	Shroud Length				
		3.048 m (10.0 ft)	4.67 m (15.0 ft)	6.1 m (20.0 ft)	7.62 m (25.0 ft)	9.15 m (30.0 ft)
1 unit	2.54(1.0)	$1346.8	$1462.8	$1578.9	$1695.0	$1809.6
	5.08(2.0)	1347.1	1463.2	1579.4	1695.5	1811.7
	7.62(3.0)	1347.4	1463.6	1579.9	1696.2	1812.5
	10.2(4.0)	1347.7	1464.0	1580.4	1696.7	1813.0
10 units	2.54(1.0)	$141.3	$154.7	$168.2	$181.7	$193.8
	5.08(2.0)	141.5	155.1	168.6	182.2	195.7
	7.62(3.0)	141.8	155.5	169.1	182.7	196.4
	10.2(4.0)	142.1	155.8	169.5	183.3	196.9
100 units	2.54(1.0)	$20.1	$23.1	$26.1	$29.1	$31.0
	5.08(2.0)	20.3	23.4	26.5	29.6	32.6
	7.62(3.0)	20.5	23.7	26.9	30.1	33.2
	10.2(4.0)	20.8	24.0	27.3	30.5	33.8

Pallet Configuration - Diameter = 4.46 m (14.6 ft)

	Core Thickness cm (in.)	Shroud Length		
		3.0 m (9.84 ft)	6.0 m (19.68 ft)	9.0 m (29.53 ft)
1 unit	2.54(1.0)	$1482.0	$1567.3	$1663.0
	5.08(2.0)	1482.4	1567.7	1663.5
	7.62(3.0)	1482.8	1568.2	1664.1
	10.2(4.0)	1483.2	1568.6	1664.5
10 units	2.54(1.0)	$155.9	$167.5	$180.2
	5.08(2.0)	156.3	167.8	180.6
	7.62(3.0)	156.6	168.3	181.1
	10.2(4.0)	157.0	168.7	181.5
100 units	2.54(1.0)	$22.5	$26.5	$30.6
	5.08(2.0)	22.8	26.8	30.9
	7.62(3.0)	23.2	27.2	31.4
	10.2(4.0)	23.5	27.6	31.8

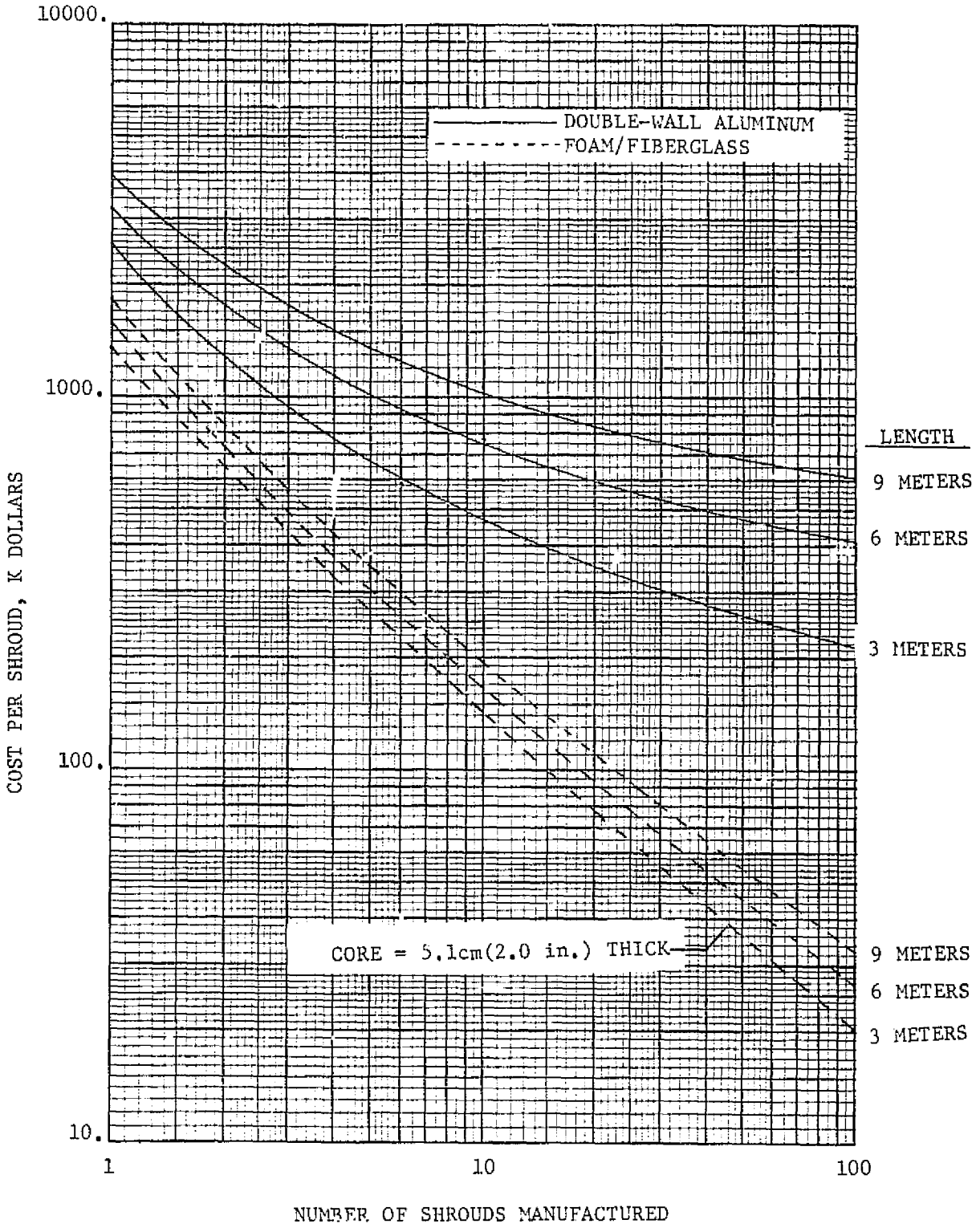

Figure 48. IUS/TUG ROM Cost Comparisons--Double-wall Aluminum vs Composite.

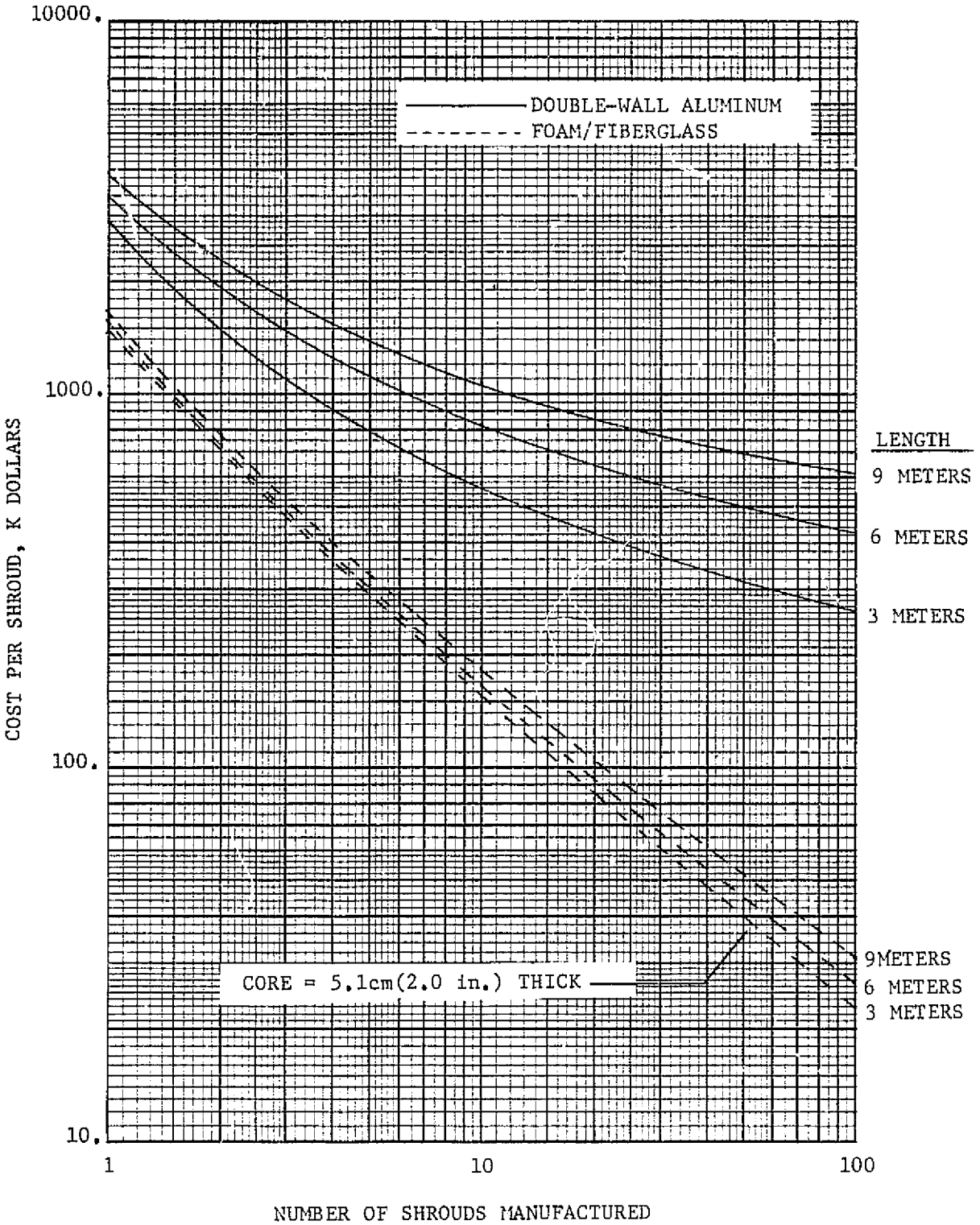

Figure 49. Pallet ROM Cost Comparisons--Double-wall Aluminum vs Composite.

E. PAYLOAD COST MATRICES

The cost model developed under Task C is utilized in this section to estimate potential cost savings for payload classifications developed under Task A. Specifically, payload cost matrices have been developed for IUS/TUG and pallet mounted payloads. The normalized cost model defined in Task C is:

$$\frac{\Delta C}{C_o} = \frac{N_P C_M}{C_o} (1-k) - e^{0.122 \left(\frac{1}{k} - 1\right)}$$

where: ΔC = cost savings,

C_o = fixed cost of shroud,

N_P = number of component failures expected at unsuppressed levels,

C_M = average cost of modifying a component

k = noise suppression factor.

Cost savings have been estimated for two values of noise suppression, 5 dB (k=0.562) and 10 dB (k=0.316), for different mission requirements, and for "simple" and "complex" payloads. In this analysis, a "simple" payload is defined as being made up of 20 components/subsystems of which 10 (50%) would be expected to fail during the vibration test program; i.e., $N_P = 10$. The 50% factor used here represents an "average" of failure rates obtained during the industry survey. The information obtained indicated that, for acceptance and qualification test programs, the number of failures ranged from 10% to 75% of the components tested, depending upon the payload/launch vehicle program. For a complex payload, $N_P = 50$, and C_M is assumed to be \$10,000 for either case. It is further assumed that the fixed cost of the shroud (C_o) is \$1,000,000 based on shroud cost data described in Section D. When these values are substituted into the cost model with the appropriate values of k, the equation

simplifies to the following form:

$$\text{5 dB Shroud:} \quad \Delta C = N_P \, C_M \, (0.438) - 1.1 \, C_o,$$

$$\text{10 dB Shroud:} \quad \Delta C = N_P \, C_M \, (0.684) - 1.3 \, C_o.$$

The cost savings as a function of number of payload test programs is shown in Figure 50. Under the assumed conditions, a loss will be incurred until a minimum number of payload test programs are completed. For example, the "break even" point for complex payloads using a 10 dB shroud is 4 payload test programs, after which significant cost savings will be realized as the number of payload test programs increases. As the number of shrouds increases and the unit shroud cost decreases, the cost savings will increase proportionately.

An estimate of the potential savings to the shuttle program can be made using the cost model, the assumptions described above, and information on payloads derived from Task A. There are 240 individual payloads/experiments listed in the payload classification tables in Appendix A. Of these, 194 can be protected by shrouds. If we assume that 30% (58) of these are classified as "complex", and the remaining 136 are "simple", then the cost savings (based on a 10 dB shroud) is as follows:

$$\Delta C = N_P \, C_M \, (0.684) = 1.3 \, C_o$$

For "simple" payloads,

$$\Delta C = 136 \, (\$0.1 \times 10^6) \, (0.684) - 1.3 \, (\$1 \times 10^6)$$

$$\Delta C = \$8 \times 10^6$$

For 58 "complex" payloads,

$$\Delta C = 58 \, (\$0.5 \times 10^6) \, (0.684) - 1.3 \, (\$1 \times 10^6)$$

$$\Delta C = \$18.5 \times 10^6$$

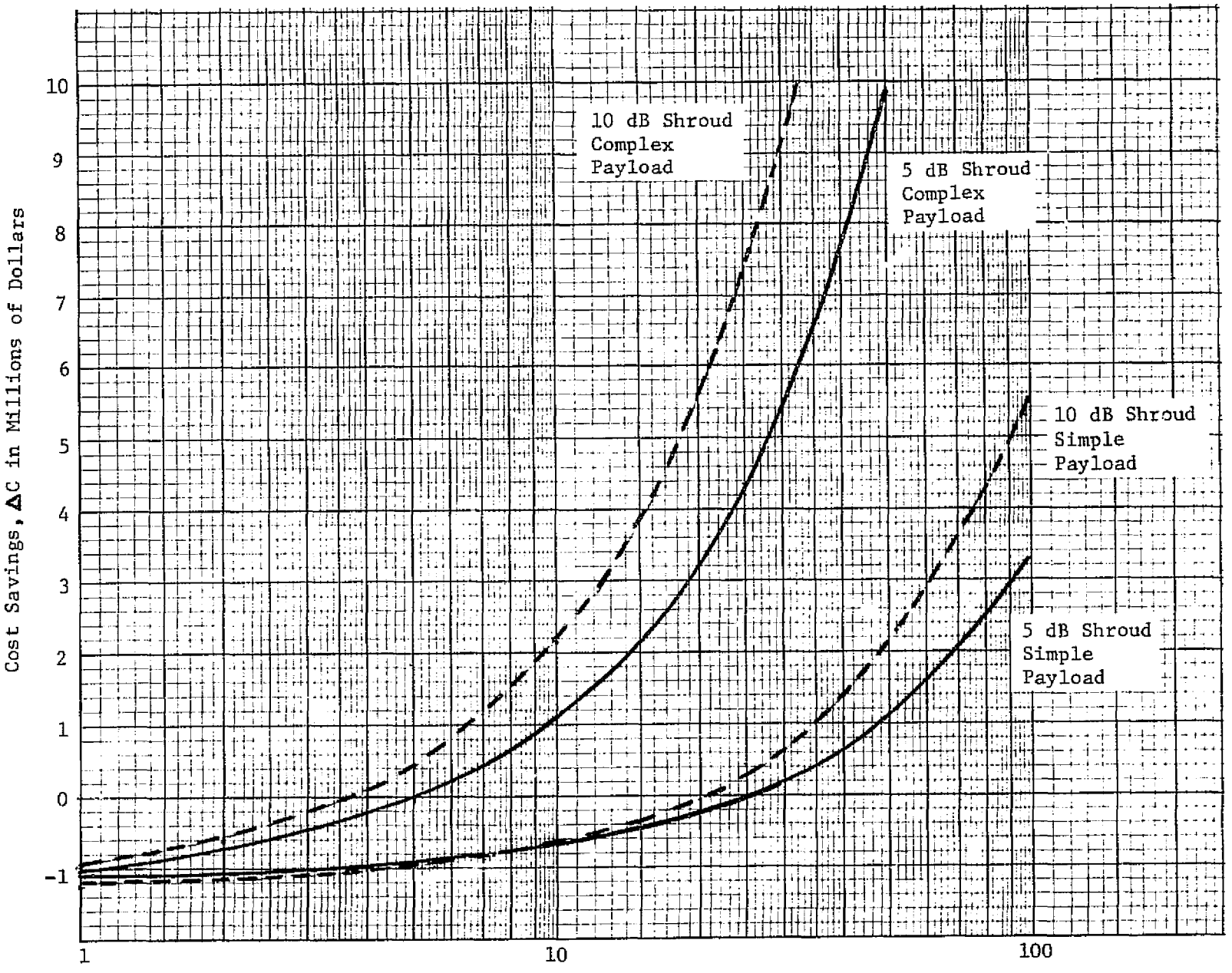

Figure50 . Cost Savings as a Function of Number of Payload Test Programs For Different Values of Noise Suppression.

The total program cost savings is then 26.5 million dollars from the test program alone and does not include the savings resulting from decreased flight failures as a result of using the shrouds.

To determine the range of test program cost savings for the different shroud configuration and numbers of missions, the cost model was used to form the payload cost savings matrices presented in Tables 15 through 18. In these tables the noise suppression costs were based on the composite foam shroud configuration only since the costs of the double-walled aluminum shroud were significantly greater. The cost savings estimates were made for both reusable shrouds (Tables 15 and 16) and expandable shrouds (Tables 17 and 18).

Table 15. Payload Cost Matrices for Pallet Mounted Payloads Based on Composite/Foam Shroud (Reusable)

Payload Classification	Noise Suppression Costs (Millions of Dollars)		Payload Cost Savings (Millions of Dollars)	
	140 dB	135 dB	140 dB	135 dB
3 Meter Pallet				
Simple Payload*				
1 Mission	1.255	1.483	-1.337	-1.860
10 Missions	0.133	0.157	0.292	0.480
100 Missions	0.020	0.024	4.358	6.810
Complex Payload*				
1 Mission	1.255	1.483	-1.162	-1.605
10 Missions	0.133	0.157	2.044	3.216
100 Missions	0.020	0.024	21.878	34.170
6 Meter Pallet				
Simple Payload				
1 Mission	1.330	1.569	-1.417	-1.971
10 Missions	0.143	0.169	0.281	0.465
100 Missions	0.023	0.028	4.354	6.804
Complex Payload				
1 Mission	1.330	1.569	-1.241	-1.700
10 Missions	0.143	0.169	2.033	3.200
100 Missions	0.023	0.028	21.874	34.164
9 Meter Pallet				
Simple Payload				
1 Mission	1.409	1.665	-1.506	-2.096
10 Missions	0.154	0.182	0.209	0.448
100 Missions	0.027	0.032	4.350	6.799
Complex Payload				
1 Mission	1.409	1.665	-1.330	-1.822
10 Missions	0.154	0.182	2.021	1.256
100 Missions	0.027	0.032	21.870	34.170

* Simple payload (20 components/subsystems); complex payload (100 components/subsystems)

Table 16. Payload Cost Matrices for IUS-TUG Payloads Based on Composite/Foam Shroud (Reusable)

Payload Classification	Noise Suppression Costs (Millions of Dollars)		Payload Cost Savings (Millions of Dollars)	
	5 dB	10 dB	140 dB	135 dB
3 Meter Shroud				
Simple Payload				
1 Mission	1.140	1.348	-1.210	-1.68
10 Missions	0.120	0.142	+0.306	+0.5
100 Missions	0.018	0.021	+4.360	+6.81
Complex Payload				
1 Mission	1.140	1.368	-1.035	-1.41
10 Missions	0.120	0.142	+2.060	+3.24
100 Missions	0.018	0.021	+21.88	+34.17
6 Meter Shroud				
Simple Payload				
1 Mission	1.337	1.580	-1.43	-1.99
10 Missions	0.144	0.17	+0.28	+0.46
100 Missions	0.023	0.027	+4.355	+6.80
Complex Payload				
1 Mission	1.337	1.580	-1.25	-1.71
10 Missions	0.144	0.17	+2.03	+3.20
100 Missions	0.023	0.027	+21.875	+34.16
9 Meter Shroud				
Simple Payload				
1 Mission	1.532	1.810	-1.64	-2.28
10 Missions	0.167	0.197	+0.254	+0.43
100 Missions	0.029	0.034	+4.348	+6.80
Complex Payload				
1 Mission	1.532	1.810	-1.47	-2.01
10 Missions	0.167	0.197	+2.01	+3.16
100 Missions	0.029	0.034	+21.868	+34.16

Table 17. Payload Cost Matrices for Pallet Mounted Payloads Based on Composite/Foam Shrouds (Expendable)

Payload Classification	Noise Suppression Costs (Millions of Dollars)		Payload Cost Savings (Millions of Dollars)	
	140 dB	135 dB	140 dB	135 dB
3 Meter Pallet				
Simple Payload				
1 Mission	1.225	1.483	-1.337	-1.860
10 Missions	1.328	1.570	-1.023	-1.357
100 Missions	1.988	2.350	+2.193	+3.785
Complex Payload				
1 Mission	1.255	1.483	-1.162	-1.586
10 Missions	1.328	1.570	+0.729	+1.379
100 Missions	1.988	2.350	+19.710	+31.145
6 Meter Pallet				
Simple Payload				
1 Mission	1.328	1.569	-1.417	-1.971
10 Missions	1.427	1.687	-1.132	-1.509
100 Missions	2.335	2.760	+1.812	+3.252
Complex Payload				
1 Mission	1.328	1.569	-1.241	-1.698
10 Missions	1.427	1.687	+0.620	+1.227
100 Missions	2.335	2.760	+19.332	+30.612
9 Meter Pallet				
Simple Payload				
1 Mission	1.409	1.665	-1.506	-2.096
10 Missions	1.537	1.816	-1.252	-1.677
100 Missions	2.691	3.180	+1.420	+2.706
Complex Payloads				
1 Mission	1.409	1.665	-1.330	-1.822
10 Missions	1.537	1.816	+0.500	+1.059
100 Missions	2.691	3.180	+18.940	+30.070

Table 18. Payload Cost Matrices for IUS-TUG Payloads Based on Composite/Foam Shrouds (Expendable)

Payload Classification	Noise Suppression Costs (Millions of Dollars)		Payload Cost Savings (Millions of Dollars)	
	140 dB	135 dB	140 dB	135 dB
3 Meter Shroud				
Simple Payload				
1 Mission	1.140	1.348	-1.210	-1.684
10 Missions	1.200	1.421	-0.882	-1.164
100 Missions	1.810	2.084	+2.389	+4.131
Complex Payload				
1 Mission	1.140	1.348	-1.035	-1.410
10 Missions	1.200	1.421	+0.870	+1.572
100 Missions	1.810	2.084	+19.910	+31.500
6 Meter Shroud				
Simple Payload				
1 Mission	1.337	1.580	-1.426	-1.986
10 Missions	1.440	1.696	-1.146	-1.520
100 Missions	2.300	2.732	+1.85	+3.290
Complex Payload				
1 Mission	1.337	1.580	-1.252	-1.712
10 Missions	1.440	1.696	+0.606	+1.216
100 Missions	2.300	2.732	+19.370	+30.650
9 Meter Shroud				
Simple Payload				
1 Mission	1.532	1.813	-1.641	-2.289
10 Missions	1.670	1.970	-1.399	-1.877
100 Missions	2.900	3.380	+1.190	+2.446
Complex Payload				
1 Mission	1.532	1.813	-1.466	-2.015
10 Missions	1.670	1.970	-0.353	+0.860
100 Missions	2.900	3.380	+18.710	+29.806

F. STS ENVIRONMENTAL REQUIREMENTS AND TEST PHILOSOPHY

The results of Tasks A, C and E were studied to evaluate environmental requirements and test philosophy as related to test program costs for shuttle payloads. Early definition of the acoustic and random vibration environments through a relatively extensive flight measurement program on the early shuttle flights is needed to obtain statistical confidence in the definition of these environments, thus minimizing the uncertainty factors that are currently applied in the definition of vibration specifications. When sufficient flight data are acquired to establish statistical confidence in the flight environments, it should be possible to reduce the qualification margins, depending upon the data scatter and degree of statistical confidence achieved.

Early payloads will not benefit from the flight measurement programs and it is assumed that current requirements and test philosophy will be applied in the test programs for these payloads. However, it would be advantageous to both the government and the payload community if a common basis and qualification test factor could be used for the establishment of test criteria. As a suggested compromise to the broad range of qualification levels shown in Figure 10 of Section B, it is proposed that flight acceptance levels be based on the mean expected flight level, with a +6 dB margin for qualification tests of single mission payloads.

As shown in Figure 23 of Section C, for a given test factor, r , increased exposure time results in increased test program cost according to the equation

$$\frac{\delta C}{N_T C_M} = 0.003\ T\ (r - 1).$$

If there is to be no increase in cost penalty associated with increasing test duration, T, then T(r-1) must remain constant. Using the 6 dB

margin, (r = 2.0 on rms levels), for exposure times of up to, for example, 5 minutes per axis, then T (r =1) = 5. Corresponding values of the test factor, r, for various exposure times are as follows:

Exposure Time, T	Test Factor, r
10 minutes	1.5
20 minutes	1.25
30 minutes	1.17

It should be recognized that the test factors shown are not recommended values, but are merely presented as an example to indicate how the test factor should change with increasing exposure time if there is to be no increase in cost penalty associated with increasing test duration. It is recommended that the qualification test factor used be reduced as a function of the test exposure time down to a minimum value represented by the maximum expected flight level, e.g. the 97.5% confidence level of the flight data. This approach would tend to alleviate the problem of overly conservative stresses applied to a multiple mission payload, which would result from the nonlinearity of the stress-life (S/N) curve if the same factor used for a single mission were applied.

With this approach, the test requirements for early shuttle payloads might be of the form shown in Table 19.

Table 19. Proposed Test Requirements for Early Shuttle Payloads.

Test Type	No. of Missions		
	1-5	6-10	10
Acceptance	Mean Flight Level	Mean Flight Level	Mean Flight Level
Qualification Test Factor	+6 dB	+4.5 dB	+3 dB (maximum expected flight level)

For the early payloads, the "mean" flight level in the table necessarily is an estimate which must be based on the data spread which exists in the data banks from previous programs. It is further recommended that acoustic tests be performed on initial payloads as early in the programs as possible in order to acquire data with which to establish realistic criteria and obtain vibroacoustic transfer functions for comparison with flight data as it is acquired. These data are necessary to refine criteria predictions for future payloads and determine efficiency factors for the acoustic facilities used for ground tests.

For common/standardized components and subsystems, extensive testing at the highest practical common level of assembly is recommended. The qualification test environment should be at the highest level/test duration for any payload used, thus qualifying the component for all payloads for which it is common. Where components are common to both a single mission and a "long life payload, multiple qualification tests may be required.

The use of shrouds to reduce the vibracoustic environment has a number of potential cost savings benefits which were not addressed specifically in this study. Achieving sufficient noise reduction will allow qualification of components by similarity from previous flight usage or qualification on current launch vehicle programs. In the case of large numbers of common/standardized components, the potential cost benefits from eliminating re-qualification tests are obvious.

If the vibration level can be reduced sufficiently, the previous work by Stahle (reference 5), figure 22, indicates that the system level qualification test could be eliminated. Certainly, as the vibration

requirement is reduced, the area under the curves in which the separate qualification test increases program cost is increased, making the protoflight concept more attractive through elimination of the cost of separate hardware for the qualification test vehicle.

Different reliability requirements should be assigned for different types of payloads. For the single mission, planetary exploration spacecraft, the results of this study indicate that a relatively high test margin should be applied to achieve the high reliability required without a severe cost penalty. For multi-mission experiments which can be repaired and re-flown, a reduced reliability factor can be applied, and testing performed at lower levels resulting in cost savings through fewer test failures without compromising the overall mission objectives.

The establishment of reliability requirements for different types of payloads and the decision as to whether to perform prototype or protoflight system level tests are not within the scope of this study; and, indeed, should be deferred until more definitive information is available on experiments and payloads. As the payload definition improves and definitive classes established, decision models need to be established and computerized parametric studies conducted to establish the bases for making these judgments.

CONCLUSIONS AND RECOMMENDATIONS

Conclusions

The results of this study indicate that significant cost savings can be realized by the use of shrouds for shuttle payloads, and that the thermal, contamination, and deployment problems can be solved in the design of such shrouds.

1. Available information on proposed experiment characteristics and mission requirements was assembled and general classifications formed. Based on the statistical distributions of experiment sizes and number of missions developed under Task A, it is concluded that approximately 95% of the total experiment population could be provided noise protection by practical shroud sizes of up to 9 meters long.
2. Literature and industry surveys were conducted to establish current test philosophies used throughout the industry, define test costs, and determine the differences in failure rates as related to the level of the random vibration environment.
3. Under Task C, a cost model was formulated and used to estimate the cost of environmental testing at the present acoustic levels and at achievable suppressed acoustic levels. The results indicate:
   a) The current range of test durations and test factors used can result in a factor of 4 in test program costs.
   b) If the cost penalty ratio is to be minimized (or made constant), the test factor used should decrease with increasing test duration.

c) The use of a relatively large test factor for experiments requiring short test durations does not impose a severe cost penalty and is advisable from the standpoint of maintaining the high reliability required for these types of experiments.

4. Under Task D, two different noise suppression concepts were developed, and a test program conducted on model shrouds for each concept. The results were compared to shroud configurations developed by other companies and agencies, and indicate:

a) Lightweight, practical shrouds can be developed which will provide from 5 dB to 10 dB attenuation for surface weights of approximately 6.3 Kg/m^2 (1.3 lbs/ft^2).

b) The double walled aluminum shroud provided the greatest noise reduction for a given weight, and injecting helium between the walls increased the noise reduction by approximately 5 dB.

c) The cost of the double walled aluminum design is several times that of the composite/foam concept.

5. In Task E, the shroud costs and the cost model were utilized to determine cost savings achievable for different classes, sizes, and numbers of IUS and pallet mounted payloads.

a) The test program cost savings is dependent upon the number and complexity of payloads involved, ranging from negative cost savings (the shroud cost) for single payloads to several million dollars for multiple payload test programs.

b) An example analysis was performed under an assumed set of conditions in which the cost savings for the total payload test

program was estimated to be $26.5 million dollars. We feel that this figure is conservatively low, since it does not include the cost savings resulting from decreased flight failures and reduction in testing if shrouds are used. On the other hand, the cost of actually including the shroud weight as part of the payload was not taken into account because of insufficient data; this effect, though significant and unconservative, is not expected to be large.

6. The final task in this study was the establishment of environmental requirements and recommended test philosophy directed towards minimizing costs for the shuttle experiment test program. In general, it was concluded that:

   a) It will be cost effective to obtain definition of the flight acoustic and vibration environments through a relatively extensive measurement program on the first few shuttle flights. Early definition of the environments with statistical confidence will minimize the uncertainty factors which are normally applied, thus reducing the test levels and achieving cost savings through minimizing test failures.

   b) Test factors applied to the environments should decrease with increasing number of missions (test durations).

   c) A relatively high test factor should be maintained for single mission payloads where high reliability is required.

   d) Reliability requirements should be reduced for multiple mission, repairable payloads.

e) The use of shrouds will reduce the number of system level qualification tests required with associated savings in dedicated test hardware.

Recommendations

The study has disclosed a number of areas which merit further investigation.

1. As additional, more definitive information becomes available on payloads/experiments, mission requirements and commonality of components, the payload classifications and configurations should be updated and a detailed assessment made of shroud configurations required to minimize the weight impact and increase payload cost savings through reduction in shroud costs. Smaller shroud sizes than the ones considered in this study may provide significant weight and cost improvements for a large number of payloads/experiments.
2. Additional tests and analyses of shroud configurations are required to determine the effect of different payload configurations on noise reduction characteristics, particularly with regard to the low frequency acoustic modes where severe notches appear in the noise reduction spectra. The shroud test program conducted at GSFC indicates that absorptive material at the shroud ends tends to alleviate this problem.
3. The current cost model should be improved to allow evaluation of the following parameters:
   a) Differences in reliability factors for different types of payloads.

b) Commonality of subsystems/components and the qualification of hardware through similarity/previous usage on other programs.

c) Improved failure rate data (if available).

d) Potential effects of elimination of system level tests at reduced acoustic levels.

e) Costs associated with flying the shroud weight.

4. Decision models should be developed and parametric studies conducted to determine the conditions for which either the protoflight or the prototype test is more cost effective for different types of payloads and mission requirements.

REFERENCES

1. Payload Descriptions, Volume I, Automated Payloads, NASA MSFC, Huntsville, Alabama, 1974.

2. Payload Descriptions, Volume II, Sortie Payloads, NASA MSFC, 1974.

3. Science and Engineering Directorate, Integrated Mission Planning - First Two Years of Shuttle Missions, NASA MSFC, Huntsville, Alabama.

4. C. V. Stahle and H. R. Gongloff, Final Report - Astronomy Sortie Vibration, Acoustics and Shock Program Planning, Phase I, G.E. Document No. 74SD4246, Contract NAS5-24022, General Electric, Space Systems Organization, Valley Forge Space Center, Pennsylvania, September 1974.

5. C. V. Stahle, Cost Effectiveness of Spacecraft Vibration Qualification Testing, Proceedings Inst. Env. Sci., April 1974.

6. J. H. Boeckel and A. R. Timmins, Test Plan Optimization for an Explorer-Size Spacecraft, NASA TND-5283, Goddard Space Flight Center, Greenbelt, Md., July 1969.

7. Anon., Saturn Component Failure Rates and Failure Rate Modifiers, NASA TMX-64619, NASA/MSFC, Huntsville, Alabama.

8. Anon., Final Report on Titan III Vehicle 10 Payload Acoustic Noise Attenuation Study, SSD-CR-66-148, Martin Marietta Corp., July 1966.

9. Young, J. P., "Cost Optimization of Spacecraft Test Levels", Proceedings of the Institute of Environmental Sciences, April, 1974.

10. R. W. Peverley, "The Effectiveness of Environment Acceptance Testing On the Apollo Spacecraft Program", Shock and Vibration Bulletin No. 43, Part 3, June 1973.

11. P. M. Morse, Vibration and Sound, McGraw-Hill Book Company, Inc., New York, New York, 1948.

12. F. J. On, Payload Effects on Shuttle Orbiter Bay Internal Acoustic Environment, Memorandum Report No. 751-35, Goddard Space Flight Center, Greenbelt, Maryland, 4 August 1975.

13. Anon., Space Shuttle Acoustic Protection Study, Bolt, Beranek and Newman, Canoga Park, California, Contract NAS5-22832, (in progress),

14. F. J. On, Ferrante, and Stahle, "Feasibility Study of an Acoustic Cover for Shuttle Payloads", Shock and Vibration Bulletin No. 46, The Shock and Vibration Information Center, October 1975.

15. IUS/TUG Payload Requirements Compatibility Study - Final Report, Vol. II, NASA/MSFC Contract NAS8-31013, MDAC and G. E. Corporation, May 1975.

16. "Acoustic Levels Inside the Spacelab Pallet/IUS/TUG Payload Shrouds", Minutes of the SPRAG Acoustic Ad Hoc Committee Meeting of June 25-26, 1975, MSFC.

17. Anon., Specification Vacuum Stability Requirements of Polymeric Material for Spacecraft Application, Lyndon B. Johnson Space Center, Houston, Texas, 9 September 1974.

18. Anon., ATM Material Control for Contamination Due to Outgassing", Rev. W, George C. Marshall Space Flight Center, Huntsville, Alabama, 1 March 1972.

ABBREVIATIONS AND ACRONYMS

USAF	United States Air Force
ATS-F	Applications Technology Satellite - F
ΔC	Cost Savings realized by using shroud
C_o	Fixed costs of shroud
C_L	Longitudinal wave velocity, m/sec
C_M	Average cost of modifying and replacing one component
C_P	Initial cost of payload
C_{RT}	Retest cost
C_S	Total cost of shroud
C_T	Initial test cost
CL	Confidence limit
dB	Decibel
ERTS	Earth resources technology satellite
f_R	Ring frequency, hertz
ft	Feet
g	Acceleration due to gravity
G	Test level in g's
GSFC	Goddard Space Flight Center
Hz	Hertz
IMP	Interplanetary Monitoring Platform
in.	Inch
IUS	Interim Upper stage
JSC	Johnson Space Center
k	Noise suppression factor
kg	Kilogram
lb	Pound
LRC	Langley Research Center
m	Meter
MDAC	McDonnell Douglas Astronautics Corporation
MMC	Martin Marietta Corporation
MSFC	Marshall Space Flight Center

ABBREVIATIONS AND ACRONYMS (continued)

NASA	National Aeronautics and Space Administration
N_G	Expected no. of components failures at test level G
N_P	Number of component failures
NQTF	Normalized qualification test factor
P/L	Payload
PSD	Power Spectral Density
psi	Pounds per square inch
RAE	Radio Astronomy Explorer
R.I.	Rockwell International
rms	Root mean square
sec	Second
SPL	Sound pressure level in dB re 20 $\mu N/m^2$
ST	Space telescope
STS	Space Transportation System
T	Total test exposure time, seconds
UPLF	Universal payload fairing
λ_G	Average constant failure rate
δC	Increase in test program cost

APPENDIX A

PAYLOAD CHARACTERISTICS

CONTENTS

INTRODUCTION

This appendix is a compilation of payload/experiment structural characteristics and mission requirements. The characteristics of payloads as defined by available integrated mission plans for the first 20 missions are presented in Table A-1. Tables A-2 through A-5 list the payload characteristics grouped according to major payload classifications; ie., pallet mounted, IUS-TUG, experiments flown in conjunction with IUS-TUG, and module (direct mounted) payloads. Experiment/component commonality matrices for three of the payload types are presented in Tables A-6, A-7 and A-8.

TABLE A-1. CHARACTERISTICS OF MISSIONS DEFINED BY AVAILABLE INTEGRATED MISSION PLANS

Missions and Associated Experiments	Weight Available for Shroud - Kg (lb)		Shroud Length Required - m (ft)		Shroud Diameter Required - m (ft)	
	Launch	Landing	Pallet	Module	Pallet	Module
MISSION NO. 3	19423 (42820)	8310 (18320)				
ST-01-A Long Duration Exposure Facility				9.1 (30.0)		6.4(14.0)
{Carry on Experiments / Engineering Data Package}			5.8(19.0)		4.0(13.1)	
MISSION NO. 8	25390 (55976)	7479 (16489)				
{LS-04-S Free Flying Teleoperator / LS-02-A Biomedical Experiment Scientific Satellite / OP-03-A Two Mini-Lageos Satellites}			6.3(20.6)		4.0(13.1)	
MISSION NO. 9	23381 (51546)	7972 (17575)				
HE-15-S Magnetic Spectrometer			5.5(18.0)		4.0(13.1)	
MISSION NO. 10	13709 (30223)	166 (367)				
{HE-11-S X-Ray Angular Structure / EO-703 High Speed Interferometer / SO-703 Solar Activity Growth Process / AP-04-A Gravity & Relativity Satellite}			9.0(29.5)		4.0(13.1)	

Notes:

{ } : EXPERIMENTS IN BRACKETS ON COMMON PALLET

TABLE A-1: CHARACTERISTICS OF MISSIONS DEFINED BY AVAILABLE INTEGRATED MISSION PLANS

Missions and Associated Experiments	Weight Available for Shroud - Kg (lb)		Shroud Length Required - m (ft)		Shroud Diameter Required - m (ft)	
	Launch	Landing	Pallet	Module	Pallet	Module
MISSION NO. 11	17291 (38120)	2737 (6035)				
{XST-001 Microwave Interferometer & Tracking Aid XST-004 Autonomous Navigation XST-006 Search & Rescue Aids XST-008 Imaging Radar}			4.9(16.0)		4.0(13.1)	
Advanced Technology Spacelab which contains the following:				6.9(22.5)		4.1(13.5)
XST-010 Lidar Measurement of Cirrus Clouds & Lower Stratospheric Aerosols						
XST-019 Ultraviolet Meteor Spectroscopy from Near Earth Orbit						
XST-020 Colony Growth in Zero-Gravity						
XST-021 Interpersonal Transfer of Microorganisms in Zero-Gravity						
XST-023 Electrical Characteristics of Cells						
XST-024 Special Properties of Biological Cells						

Notes:

{ }: EXPERIMENTS IN BRACKETS ON COMMON PALLET

TABLE A-1: CHARACTERISTICS OF MISSIONS DEFINED BY AVAILABLE INTEGRATED MISSION PLANS

Missions and Associated Experiments	Weight Available for Shroud - Kg (lb)		Shroud Length Required - m (ft)		Shroud Diameter Required - m (ft)	
	Launch	Landing	Pallet	Module	Pallet	Module
MISSION NO. 11 (Continued)						
XST-026 Zero Gravity Steam Generator XST-027 Sampling of Airborne Particles & Micro-organisms in Space Cabin Environment XST-029 Environmental Effects on Non-metallic Materials						
MISSION NO. 12	15981 (35232)	2113 (4657)				
LS-09-S Life Sciences Shuttle Laboratory				6.7(22.0)		4.1(13.3)
{DOD Space Experiment Satellite (SEXSAT) Teleoperator Bay Experiment}			4.9(16.1)		4.0(13.1)	
MISSION NO. 13	15910 (35076)	1339 (2953)				
{Large Fine Pointing Platform High Energy Solar Physics Cluster}			10.7(35.0)		4.0(13.1)	
The Large Fine Pointing Platform includes the following:						

Notes:

{ }: EXPERIMENTS IN BRACKETS ON COMMON PALLET

TABLE A-1: CHARACTERISTICS OF MISSIONS DEFINED BY AVAILABLE INTEGRATED MISSION PLANS

Missions and Associated Experiments	Weight Available for Shroud - Kg (lb)		Shroud Length Required - m (ft)		Shroud Diameter Required - m (ft)	
	Launch	Landing	Pallet	Module	Pallet	Module
MISSION NO. 13 (Continued)						
S0001 Externally Occulted Coronagraph S0003 Ultraviolet Spectrograph S0008 Grid Collimator Acquisition Photometer S0009 Modulation Collimator S0035 65-CM Photoheliograph S0036 Platform (Gimbal/Mount)						
The High Energy Solar Physics Cluster contains the following:						
S0011 Solid-State Flare Detector S0012 X-ray Burst Detector S0013 X-ray/Gamma-ray Spectrometer S0014 Gamma-ray Spectrometer S0015 Solar X-ray Polorimeter S0016 Bragg Reflection Crystal Polarimeter S0017 Solar Neutron Experiment S0018 High-Energy Gamma-ray and Neutron Detector S0019 Solar Gamma-ray Detector						
Notes:						

TABLE A-1: CHARACTERISTICS OF MISSIONS DEFINED BY AVAILABLE INTEGRATED MISSION PLANS

Missions and Associated Experiments	Weight Available for Shroud - Kg (lb)		Shroud Length Required - m (ft)		Shroud Diameter Required - m (ft)	
	Launch	Landing	Pallet	Module	Pallet	Module
MISSION NO. 14	15703 (34620)	1166 (2571)				
LS-02-A Biomedical Experiment Satellite			2.4(8.0)		4.0(13.1)	
LS-07-S Life Sciences Shuttle Laboratory				9.1(30.0)		4.3(14.1)
MISSION NO. 16	14373 (31688)	1222 (2694)				
HE-11-S High Energy Astrophysics Payload			4.3(14.1)		4.0(13.1)	
SO-03-A Solar Maximum Satellite			4.5(14.9)		4.0(13.1)	
MISSION NO. 18	14608 (32206)	258 (568)				
General Purpose Spacelab which contains the following:				4.6(15.1)		4.3(14.0)
XEO-044 Shuttle Imaging Microwave System						
XCN-007 Terrestrial RF Sources of Noise & Interference						
XOP-004 Multifrequency Propagation Experiment						

Notes:

TABLE A-1: CHARACTERISTICS OF MISSIONS DEFINED BY AVAILABLE INTEGRATED MISSION PLANS

Missions and Associated Experiments	Weight Available for Shroud - Kg (lb)		Shroud Length Required - m (ft)		Shroud Diameter Required - m (ft)	
	Launch	Landing	Pallet	Module	Pallet	Module
MISSION NO. 18 (Continued)						
XOP-005 Laser Ranging Experiment XOP-006 Laser Altimetry XOP-007 Multispectral Scanning Imagery XOP-008 Radar Altimetry XOP-010 Multifrequency Radar Ocean Imagery XOP-012 Combined Laser Experiment OP-03-A Mini-Lageos Satellites						
MISSION NO. 19	15531 (34240)	1852 (4083)				
General Purpose Spacelab which contains the following: XAP-410 Wave Characteristics XAP-420 Wave/Particle Interactions XAP-430 Plasma Interaction & Flow XAP-450 Global Emission Survey XAP-470 Magnetospheric Topology XAP-490 Interaction & Flow				4.6(15.1)		4.3(14.0)

Notes:

TABLE A-2: CHARACTERISTICS OF EXPERIMENTS

MOUNTED ON PALLETS

Experiments		Launch Weight -Kg (lb)	Length -m (ft)	Max. Diam. -m (ft)	Volume $-m^3(ft^3)$	Density $-Kg/m^3$ (lb/ft^3)	Flights per Experiment	No. of Components Common to Other Experiments/Number of Other Experiments They are Common to	Mission Number *
No.	Description								
AS-01-S	1.5M Telescope	3296 (7268)	4.6 (15.0)	2.4 (7.9)	20.7 (730)	160 (9.96)	15	6/1, 9/2	?
AS-03-S	Deep Sky UV Survey Telescope	3774 (8322)	6.0 (19.7)	2.2 (7.2)	22.8 (806)	165.4 (10.32)	8	9/2	?
AS-04-S	1m Diffraction Limited UV - Optical Telescope	1836 (4048)	4.0 (13.1)	3.7 (12.3)	44.1 (1557)	41.7 (2.6)	23		?
AS-05-S	Very Wide Field Galactic Camera	70 (154)	1.0 (3.3)	1.0 (3.3)	.8 (28)	89.1 (5.56)	2		?
AS-06-S	Calibration of Astronomical Fluxes	2190 (4829)	4.1 (13.5)	? ?	? ?	? ?	2		?
AS-07-S	Cometary Simulation	19244 (42543)	13.7 (45.0)	? ?	? ?	? ?	2	11/1	?
AS-08-S	Multipurpose 0.5m Telescope	554 (1222)	1.5 (4.9)	? ?	? ?	? ?	?	1/1	?
AS-09-S	30m 1R Interferometer	2601 (5735)	16.6 (54.5)	? ?	? ?	? ?	1		?
AS-10-S	Advanced XUV Telescope	426 (938)	1 (3.3)	? ?	? ?	? ?	?	2/1	?
AS-11-S	Polarimetric Experiments	252 (555)	1.5 (5.0)	? ?	? ?	? ?	1	2/1	?
AS-12-S	Meteoroid Simulation	2289 (5047)	6.1 (20.0)	?	?	?	?	11/1	?

Notes:

*See"Characteristics of Missions defined by available integrated mission plans" Matrix.

TABLE A-2: CHARACTERISTICS OF EXPERIMENTS

MOUNTED ON PALLETS

Experiments		Launch Weight -Kg (lb)	Length -m (ft)	Max. Diam. -m (ft)	Volume $-m^3(ft^3)$	Density $-Kg/m^3$ (lb/ft^3)	Flights per Experiment	No. of Components Common to Other Experiments/Number of Other Experiments They are Common to	Mission Number *
No.	Description								
AS-14-S	1m Uncooled IR Telescope	1545 (3407)	3 (9.8)	?	?	?	?		?
AS-15-S	3m Ambient Temperature IR Telescope	5326 (11744)	11 (36.1)	3.7 (12.1)	117.5 (4.50)	45.4 (2.83)	11	7/1,9/2	?
AS-18-S	1.5km IR Interferometer	5864 (12930)	9.2 (30.0)	?	?	?	?		?
AS-19-S	Selected Area Deep Sky Survey Telescope	1000 (2205)	3 (9.8)	?	?	?	?		?
AS-20-S	2.5m Cryogenically Cooled IR Telescope	4378 (9653)	4.6 (15.1)	?	?	?	?		?
AS-31-S	Combined AS-01, 03, 04, & -05-S	8009 (17660)	11.8 (38.7)	?	?	?	?		?
AS-41-S	Schwartzchild Camera	161.5 (356)	2.8 (9.2)	?	?	?	?		?
AS-42-S	Far UV Electronographic Schmidt Camera/Spectrograph	160 (353)	1.4 (4.5)	?	?	?	?		?
AS-43-S	UCB Black Brant Payload	291 (642)	.5 (1.6)	?	?	?	?	1/1	?
AS-44-S	XUV Concentrator/Detector Array	133 (293)	1 (3.3)	?	?	?	?		?
AS-45-S	Proportional Counter Array	62 (137)	1.6 (5.3)	?	?	?	?		?
AS-46-S	Wisconsin UV Photometry Experiment	98.1 (216)	1 (3.3)	?	?	?	?		?

Notes:

TABLE A-2: CHARACTERISTICS OF EXPERIMENTS

MOUNTED ON PALLETS

Experiments		Launch Weight -Kg (lb)	Length -m (ft)	Max. Diam. -m (ft)	Volume -m^3(ft^3)	Density -Kg/m^3 (lb/ft^3)	Flights per Experiment	No. of Components Common to Other Experiments/Number of Other Experiments They are Common to	Mission Number *
No.	Description								
AS-47-S	Attached Far 1R Spectrometer	170 (375)	1 (3.3)	?	?	?	?		?
AS-48-S	Aries/Shuttle UV Telescope	462 (1018)	3 (9.8)	?	?	?	?		?
AS-49-S	First UCB Black Brant Payload	273 (602)	.5 (1.6)	?	?	?	1	1/1	?
AS-50-S	UV/XUV Measurement (AS-04-S & AS-10-S)	2971 (6551)	5 (16.4)	?	?	?	?		?
AS-51-S	Combined 1R Payload (AS-01-S & AS-15-S)	9186 (20255)	15.6 (51.2)	?	?	?	?		?
AS-52-S	Combined UV Payload (AS-03-S & AS-04-S)	7017 (15472)	10 (32.8)	?	?	?	?		?
AS-61-S	Attached Far 1R Photometer (Wide Field of View)	145 (320)	1 (3.3)	?	?	?	?		?
AS-62-S	Cosmic Background Anisotropy	220 (485)	1 (3.3)	?	?	?	?		?
AS-01-R	LST Revisit	4400 (9702)	4 (13.1)	?	?	?	?		?
HE-11-S	X-Ray Angular Structure	5782 (12948)	6.1 (20)	4.3 (14.0)	87.1 (3076)	67.5 (4.21)	6		10,16
HE-12-S	High Inclination Cosmic Ray Survey	5190 (11444)	9.2 (30.0)	?	?	?	?		?
HE-13-S	X-Ray/Gamma-Ray Pallet	5034 (11100)	7 (23.0)	?	?	?	?		?

Notes:

TABLE A-2: CHARACTERISTICS OF EXPERIMENTS

MOUNTED ON PALLETS

Experiments		Launch Weight -Kg (lb)	Length -m (ft)	Max. Diam. -m (ft)	Volume -m^3(ft^3)	Density -Kg/m^3 (lb/ft^3)	Flights per Experiment	No. of Components Common to Other Experiments/Number of Other Experiments They are Common to	Mission Number *
No.	Description								
HE-14-S	Gamma-Ray Pallet	4687 (10335)	5 (16.4)	?	?	?	?		?
HE-15-S	Magnetic Spectrometer	4003 (8827)	4.6 (15.1)	4.6 (15.0)	75.5 (2667)	53.1 (3.31)	3		9
HE-16-S	High Energy Gamma-Ray Survey	6152 (13566)	4 (13.1)	?	?	?	?		?
HE-17-S	High Energy Cosmic-Ray Study	2000 (4410)	1 (3.3)	?	?	?	?		?
HE-18-S	Gamma-Ray Photometric Studies	6740 (14862)	2 (6.6)	?	?	?	?		?
HE-19-S	Low Energy X-Ray Telescope	1814 (4000)	3.5 (11.5)	?	?	?	?		?
HE-20-S	High Resolution X-Ray Telescope	4335 (9559)	3.0 (9.8)	?	?	?	?		?
HE-03R-S	Extended X-Ray Surveyer Revisit	4400 (9702)	4 (13.1)	?	?	?	?	6/1	?
HE-11R-S	Large High Energy Observatory D Revisit	4400 (9702)	4 (13.1)	?	?	?	?	6/1	?
SO-01-S	Dedicated Solar Sortie Mission	5619 (12390)	13.7 (44.9)	1.5 (4.8)	23.2 (821)	2420 (15.1)	?	11/1	?
SO-11-S	Solar Fine-Pointing Payload	3159 (7759)	8.8 (28.9)	1.5 (4.8)	14.9 (525)	235.6 (14.7)	5	11/1	?
SO-12-S	ATM Spacelab	11336 (24996)	6 (19.7)	?	?	?	?		?

Notes:

TABLE A-2: CHARACTERISTICS OF EXPERIMENTS

MOUNTED ON PALLETS

Experiments		Launch Weight -Kg (lb)	Length -m (ft)	Max. Diam. -m (ft)	Volume $-m^3(ft^3)$	Density $-Kg/m^3$ (lb/ft^3)	Flights per Experiment	No. of Components Common to Other Experiments/Number of Other Experiments They are Common to	Mission Number *
No.	Description								
AP-06-S	Atmospheric, Magnetospheric, & Plasmas in Space	5381 (11865)	7.6 (24.9)	4.0 (13.1)	94.9 (3352)	56.7 (3.54)	?		?
EO-05-S	Shuttle Imaging Microwave System	7432 (16388)	18.0 (59.1)	?	?	?	?		?
EO-06-S	Scanning Spectro Radiometer	520 (1147)	2.1 (7.0)	0.9 (3.0)	1.4 (49.0)	367.7 (23.5)	?		?
EO-07-S	Active Optical Scatterometer	442.6 (976)	2.0 (6.6)	?	?	?	?		?
OP-02-S	Multifrequency Radar Land Imagery	1470 (3241)	0.6 (2.0)	0.5 (1.5)	0.1 (3.0)	15967 (996.3)	?	9/1, 7/4, 2/2, 1/3	?
OP-03-S	Multifrequency Dual Polarized Radiometry	633.2 (1396)	3.0 (9.8)	2.1 (7.0)	9.8 (346)	64.6 (4.03)			
OP-04-S	Microwave Scatterometer	388 (855)	1.1 (3.6)	0.5 (1.6)	0.2 (7.6)	1797 (112.1)	?	7/4, 1/3	?
OP-05-S	Multispectral Scanning Imagery	1470 (3241)	0.6 (2.0)	0.7 (2.3)	0.2 (8.2)	6347 (396)	?	6/1, 7/4, 2/2	?
OP-06-S	Combined Laser Experiment	343 (757)	0.6 (2.0)	4.6 (15.0)	10.0 (354)	34.3 (2.14)	?	3/1, 7/4, 2/2, 1/3	?
SP-01-S	SPA No. 1 - Biological (Manned) (B+C)	2547 (5616)	1.3 (4.3)	1.3 (4.3)	17.3 (611)	147.3 (9.19)			
SP-02-S	SPA No. 2-Furnace (Manned) (F+C)	3524 (7770)	2.5 (8.0)	?	?	?	?	1/1, 1/10	?

Notes:

TABLE A-2: CHARACTERISTICS OF EXPERIMENTS

MOUNTED ON PALLETS

Experiments		Launch Weight -Kg (lb)	Length -m (ft)	Max. Diam. -m (ft)	Volume -m^3(ft^3)	Density -Kg/m^3 (lb/ft^3)	Flights per Experiment	No. of Components Common to Other Experiments/Number of Other Experiments They are Common to	Mission Number *
No.	Description								
SP-03-S	SPA No. 3 - Levitation (Manned)(C+C)	4104 (9049)	2.5 (8.0)	?	?	?	?	1/10	?
SP-04-S	SPA No. 4 - General Purpose (Manned) (G+C)	2325 (5127)	1.3 (4.3)	?	?	?	?	1/10, 1/3	?
SP-05-S	SPA No. 5 - Dedicated (Manned)(B+F+ L+G+C)	7085 (15622)	3.7 (12.1)	?	?	?	?	1/10, 1/3, 1/2	?
SP-12-S	SPA No. 12 - Automated Furnace	3187 (7027)	2.5 (8.0)	?	?	?	?	1/1, 2/2	?
SP-13-S	SPA No. 13 - Automated Levitation (LP+CP)	3801 (8381)	2.5 (8.0)	?	?	?	?	1/2, 1/3	?
SP-14-S	SPA No. 14 Manned & Automated (B+G+C+FP+LB)	6365 (14035)	2.5 (8.0)	4.1 (13.5)	31.5 (1114)	2020 (12.6)	10	2/2, 1/10,2/3,	?
SP-15-S	SPA No. 15 Automated Furnace/Levitation (FB+LB+CP)	4907 (10820	2.5 (8.0)	4.1 (13.5)	20.7 (732)	150.7 (9.4)	10	7/1, 1/2, 1/10, 1/3	?
SP-16-S	SPA No. 16 Biological/General (Manned)(B+B+C)	3119 (6877)	1.3 (4.3)	?	?	?	?		?
SP-19-S	SPA No. 19 Biological & Automated (B+C+FB+LB)	5793 (12774)	2.5 (8.0)	?	?	?	?	1/10, 2/3, 2/2	?
ST-08-S	Integrated Real Time Contamination Monitor	52.7 (116)	?	0.7 (2.3)	?	?	?	8/3	?
ST-09-S	Controlled Contamination Release	62.7 (138)	0.7 (2.3)	?	?	?	?		?

Notes:

TABLE A-2: CHARACTERISTICS OF EXPERIMENTS

MOUNTED ON PALLETS

Experiments		Launch Weight -Kg (lb)	Length -m (ft)	Max. Diam. -m (ft)	Volume -m^3(ft^3)	Density -Kg/m^3 (lb/ft^3)	Flights per Experiment	No. of Components Common to Other Experiments/Number of Other Experiments They are Common to	Mission Number *
No.	Description								
ST-11-S	Laser Information/Data Transmission	54.4 (120)	5 (16.4)	?	?	?	?		?
ST-13-S	Wake Shield Investigation	450 (992)	5 (16.4)	?	?	?	?		?
ST-21-S	ATL P/L No. 2 (Module + Pallet)	1353 (2983)	6 (19.7)	?	?	?	?	8/3,1/1	?
ST-22-S	ATL P/L No. 3 (Module + Pallet)	2330 (5138)	6 (19.7)	3.3 (10.8)	51.5 (1803)	45.7 (2.85)	?	22/1, 8/3,2/2	?
ST-23-S	ATL P/L No. 5 (Pallet Only)	3328 (7118)	15.0 (49.2)	4.6 (15.0)	246.1 (8691)	13.1 (.82)	?	7/1, 8/3, 2/2	?
CN-04-S	Terrestrial Sources of Noise & Interference	289 (637)	1.6 (5.3)	3.1 (10.0)	11.7 (414)	24.7 (1.54)	8		?
CN-05-S	Laser Communication Experimentation	389 (857)	1.8 (5.8)	1.5 (5.0)	3.3 (116)	118.3 (7.4)	6		?
CN-06-S	Communication Relay Tests	678 (1495)	3 (9.8)	?	?	?	?		?
CN-07-S	Large Reflector Deployment	1922 (4238)	15.0 (49.2)	?	?	?	?		?
CN-08-S	Open Traveling Wave Tube	121 (266)	0.5 (1.6)	?	?	?	?		?
CN-11-S	Stars & Pads Experimentation	112 (246)	1 (3.3)	?	?	?	?		?
CN-12-S	Interferometric Navigation & Surveillance Techniques	189 (417)	0.5 (1.6)	?	?	?	?		?

Notes:

TABLE A-3. CHARACTERISTICS OF TUG PAYLOADS

Missions and Associated Experiments		Weight Available for Shroud-Kg(lb)		Shroud Length Required - m (ft)
No.	Description	Launch	Landing	
T-1	DOD Mission, Two D-12 S/C	0(0)	5872(12946)	5.5(18.0)
T-2	DOD Mission, D-03 S/C	10470(23082)	10129(22331)	6.4(21.0)
T-3	PL-01-A Mars Surface Sample Return	0(0)	4007(8833)	7.3(24.0)
T-4	PL-18-A Encke Rendezvous	598(1318)	6912(15238)	6.2(20.2)
T-5	PL-11-A Pioneer Saturn/Uranus Flyby	1387(3057)	7701(16977)	3.1(10.2)
T-6	PL-13-A Pioneer Jupiter Probe	1387(3057)	7701(16977)	3.1(10.2)
T-7	PL-22-A Pioneer Saturn Probe	1387(3057)	7701(16977)	3.1(10.2)
T-8	AS-02-A Extra Coronal Lyman Alpha Explorer AP-03-A High Altitude Explorer	1183(2609)	7497(16529)	5.9(19.3)
T-9	PL-30-A Pioneer Venus Multiprobe (2 ea)	494(1088)	6808(15008)	2.0(6.7)
T-10	PL-03-A Pioneer Venus Multiprobe	14971(33006)	10644(23466)	2.0(6.7)
T-11	LU-01-A Lunar Orbiter	15166(33436)	10839(23896)	4.8(15.7)

Notes:

MISSIONS T-1 THROUGH T-39 ARE BASED ON "EXPENDABLE" TUG CONCEPT
MISSIONS T-40 THROUGH T-81 ARE BASED ON "REUSABLE" TUG CONCEPT

TABLE A-3: CHARACTERISTICS OF TUG PAYLOADS

Missions and Associated Experiments		Weight Available for Shroud-Kg(lb)		Shroud Length Required - m (ft)
No.	Description	Launch	Landing	
T-12	PL-07-A Venus Orbital Imaging Radar	0(0)	5843(12881)	5.6(18.4)
T-13	AP-02-A Medium Altitude Explorer	14705(32419)	10378(22873)	1.8(6.0)
T-14	EO-58-A Geosynchronous Operational Meteorological Satellite CN-56-A Foreign Communications Satellite A EO-09-A Synchronous Earth Observatory Satellite	8196(78068)	7855(17317)	8.3(17.4)
T-15	CN-51-A Intelsat CN-53-A U.S. Domsat "B"	726(1600)	7040(15520)	5.4(17.8)
T-16	CN-56-A Foreign Communications Satellite A CN-51-A Intelsat	9730(21450)	9389(20699)	5.0(16.6)
T-17	EO-57-A Geosynchronous Operational Meteorological Satellite CN-55-A Traffic Management Satellite CN-51-A Intelsat	9122(20111)	8782(19360)	7.4(24.4)
T-18	AP-05-A Environmental Perturbation Satellite - Mission	14525(32022)	10198(22482)	3.7(12.1)

Notes:

TABLE A-3: CHARACTERISTICS OF TUG PAYLOADS

Missions and Associated Experiments		Weight Available for Shroud-Kg(lb)		Shroud Length Required - m (ft)
No.	Description	Launch	Landing	
T-19	OP-06-A Magnetic Field Monitor Satellite AP-05-A Environmental Perturbation Satellite - Mission	14281(31484)	9954(21944)	4.0(13.0)
T-20	AP-01-A Upper Atmosphere Explorer	15116(33225)	10788(23785)	2.3(7.7)
T-21	EO-57-A Foreign Synchronous Meteorological Satellite EO-58-A Geosynchronous Operational Meteorological Satellite EO-09-A Synchronous Earth Observatory Satellite	8343(18393)	8002(17642)	8.3(27.4)
T-22	CN-52-A U.S. Domsat "A" CN-56-A Foreign Communications Satellite A CN-54-A Disaster Warning Satellite	14212(31332)	9885(21792)	8.8(28.8)
T-23	CN-55-A Traffic Management Satellite (2 ea) CN-52-A U.S. Domsat "A"	14543(32061)	10215(22521)	6.9(22.4)
T-24	EO-57-A Foreign Synchronous Meteorological Satellite	14174(31249)	9847(21709)	6.3(22.3)

Notes:

TABLE A-3: CHARACTERISTICS OF TUG PAYLOADS

Missions and Associated Experiments		Weight Available for Shroud-Kg(lb)		Shroud Length Required - m (ft)
No.	Description	Launch	Landing	
T-24	(Continued) EO-58-A Geosynchronous Operational Meteorological Satellite CN-52-A U.S. Domsat "A"			
T-25	CN-55-A Traffic Management Satellite OP-01-A Geopause	1535(3383)	7849(17303)	4.1(13.4)
T-26	EO-12-A Tiros "O"	1583(3491)	7586(16724)	4.1(13.4)
T-27	CN-58-A Geosynchronous Operational Meteorological Satellite (2 ea)	9892(21809)	9552(21058)	3.7(12.0)
T-28	DOD Mission, D-07 (8 ea)	7787(17168)	7447(16417)	10.7(35.0)
T-29	DOD Mission, D-10	14906(32862)	10579(23322)	6.7(22.0)
T-30	DOD Mission, D-05	14536(32046)	10209(22506)	9.1(30.0)
T-31	DOD Mission, D-09	14536(32046)	10209(22506)	5.0(17.0)
T-32	AS-05-A Advanced Radio Explorer (2 ea) CN-51-A Intelsat	609(1342)	6923(15262)	4.1(14.1)

Notes:

TABLE A-3: CHARACTERISTICS OF TUG PAYLOADS

Missions and Associated Experiments		Weight Available for Shroud-Kg(lb)		Shroud Length Required - m (ft)
No.	Description	Launch	Landing	
T-33	CN-51-A Intelsat CN-55-A Traffic Management Satellite	9751(21497)	9410(20746)	7.8(26.1)
T-34	CN-52-A U.S. Domsat "A" CN-51-A Intelsat CN-55-A Traffic Management Satellite	9037(19923)	8896(19172)	7.8(26.1)
T-35	EO-56-A Environmental Monitoring Satellite	1583(3491)	7552(16650)	3.7(12.2)
T-36	DOD Mission, S/C D-11 (2 ea)	8723(19231)	8382(18480)	6.1(20.0)
T-37	DOD Mission, S/C D-06	14860(32760)	10532(23220)	9.6(32.0)
T-38	DOD Mission, S/C D-04 (2 ea)	9361(20637)	9020(19886)	3.8(12.5)
T-39	DOD Mission, S/C D-02 S/C D-01 (2 ea)	9021(19887)	8680(19136)	8.6(28.0)
T-40	DOD Mission S/C D-04 (2 ea)	9361(20637)	9020(19886)	3.8(12.5)
T-41	DOD Mission S/C D-12	0(0)	5872(12946)	2.4(8.0)
T-42	DOD Mission S/C D-03	7817(17233)	7519(16576)	7.6(25.0)

Notes:

TABLE A-3: CHARACTERISTICS OF TUG PAYLOADS

Missions and Associated Experiments		Weight Available for Shroud-Kg(lb)		Shroud Length Required - m (ft)
No.	Description	Launch	Landing	
T-43	PL-11-A Pioneer Saturn/Uranus Flyby	271(597)	6585(14517)	3.1(10.1)
T-44	PL-13-A Pioneer Jupiter Probe	271(597)	6585(14517)	3.1(10.1)
T-45	PL-22-A Pioneer Saturn Probe	271(597)	6585(14517)	3.1(10.1)
T-46	PL-01-A Mars Surface Sample Return	0(0)	4007(8833)	7.3(24.0)
T-47	PL-18-A Encke Rendezvous	532(1172)	6912(15238)	6.1(20.0)
T-48	AS-05-A Advanced Radio Explorer (2 ea)	7463(16452)	7164(15795)	2.5(8.1)
T-49	PL-03-A Pioneer Venus Multiprobe	14971(33006)	10644(23466)	2.0(6.7)
T-50	LU-01-A Lunar Orbiter	15166(33436)	10839(23896)	4.8(15.7)
T-51	PL-07-A Venus Orbital Imaging Radar	0(0)	5843(12881)	5.6(18.4)
T-52	AS-02-A Extra Coronal Lynam Alpha Explorer PL-03-A Pioneer Venus Multiprobe	1183(2609)	7525(16589)	5.9(19.3)
T-53	PL-03-A Pioneer Venus Multiprobe (2 ea)	489(1079)	6808(15008)	2.0(6.7)

Notes:

TABLE A-3: CHARACTERISTICS OF TUG PAYLOADS

Missions and Associated Experiments		Weight Available for Shroud-Kg(lb)		Shroud Length Required - m (ft)
No.	Description	Launch	Landing	
T-54	EO-57-A Foreign Synchronous Meteorological Satellite CN-55-A Traffic Management Satellite CN-51-A Intelsat	9122(20111)	8781(19360)	7.4(25.8)
T-55	AP-05-A Environmental Perturbation Satellite, Mission	7552(16649)	7254(15992)	3.7(12.2)
T-56	OP-06-A Magnetic Field Monitor Satellite AP-05-A Environmental Perturbation Satellite	14280(31484)	9954(21944)	4.0(13.0)
T-57	AP-01-A Upper Atmosphere Explorer	15116(33325)	10789(23785)	2.3(7.7)
T-58	AP-02-A Medium Altitude Explorer CN-51-A Intelsat	9780(21561)	9439(20810)	4.5(14.9)
T-59	EO-58-A Geosynchronous Operational Meteorological Satellite CN-56-A Foreign Communications Satellite A EO-09-A Synchronous Earth Observatory Satellite	8196(18068)	7855(17317)	8.3(27.4)
T-60	CN-51-A Intelsat CN-53-A U.S. Domsat "B"	6079(13402)	5738(12651)	5.4(17.8)

Notes:

TABLE A-3: CHARACTERISTICS OF TUG PAYLOADS

Missions and Associated Experiments		Weight Available for Shroud-Kg(lb)		Shroud Length Required - m (ft)
No.	Description	Launch	Landing	
T-61	CN-56-A Foreign Communications Satellite A CN-51-A Intelsat	9730(21450)	9389(20699)	5.0(16.6)
T-62	DOD Mission S/C D-11 (2 ea)	8723(19231)	8382(18480)	6.1(20.0)
T-63	DOD Mission S/C D-06	7886(17386)	7588(16729)	9.8(32.0)
T-64	DOD Mission S/C D-02 S/C D-01 (2 ea)	9021(19887)	8680(19136)	8.6(28.0)
T-65	CN-55-A Traffic Management Satellite CN-52-A U.S. Domsat "A"	8024(17690)	7726(17033)	5.3(17.2)
T-66	OP-01-A Geopause	8265(18222)	7967(17565)	2.5(8.2)
T-67	EO-12-A Tiros "0"	1583(3491)	7586(16724)	4.1(13.3)
T-68	CN-58-A U.S. Domsat "C" (3 ea)	6349(13997)	6008(13246)	7.4(24.2)
T-69	EO-57-A Foreign Synchronous Meteorological Satellite EO-58-A Geosynchronous Operational Meteorological Satellite	8343(18393)	8002(17642)	8.3(27.4)

Notes:

TABLE A-3: CHARACTERISTICS OF TUG PAYLOADS

Missions and Associated Experiments		Weight Available for Shroud-Kg(lb)		Shroud Length Required - m (ft)
No.	Description	Launch	Landing	
T-69	(Continued) EO-09-A Synchronous Earth Observatory Satellite			
T-70	CN-52-A U.S. Domsat "A" CN-56-A Foreign Communications Satellite A CN-54-A Disaster Warning Satellite	7239(15959)	6941(15302)	8.8(28.8)
T-71	CN-55-A Traffic Management Satellite (2 ea) CN-52-A U.S. Domsat "A"	7569(16688)	7272(16031)	6.9(22.4)
T-72	EO-57-A Foreign Synchronous Meteorological Satellite EO-58-A Geosynchronous Operational Meteorological Satellite	7993(17621)	7695(16964)	3.1(10.3)
T-73	AS-05-A Advance Radio Explorer (2 ea)	5962(13144)	5621(12393)	2.5(8.1)
T-74	CN-55-A Traffic Management Satellite CN-51-A Intelsat	7098(15649)	6800(14992)	4.3(14.1)
T-75	CN-52-A U.S. Domsat "A" CN-51-A Intelsat CN-55-A Traffic Management Satellite	9037(19923)	8696(19172)	8.0(26.1)

Notes:

TABLE A-3: CHARACTERISTICS OF TUG PAYLOADS

Missions and Associated Experiments		Weight Available for Shroud-Kg(lb)		Shroud Length Required - m (ft)
No.	Description	Launch	Landing	
T-76	EO-56-A Environmental Monitoring Satellite	1583(3491)	7552(16650)	3.7(12.2)
T-77	DOD Mission S/C D-07 (8 ea)	7787(17168)	7447(16417)	3.7(12.0)
T-78	DOD Mission S/C D-10	10410(22951)	10112(22294)	10.7(35.0)
T-79	DOD Mission S/C D-05	7562(16672)	7264(16015)	6.7(22.0)
T-80	DOD Mission S/C D-09	7562(16672)	7264(16015)	9.1(30.0)

Notes:

TABLE A-4: CHARACTERISTICS OF EXPERIMENTS FLOWN IN CONJUNCTION WITH TUG

Experiments		Launch Weight -Kg (lb)	Length -m (ft)	Max. Diam. -m (ft)	Volume $-m^3(ft^3)$	Density $-Kg/m^3$ (lb/ft^3)	Flights per Experiment	No. of Components Common to Other Experiments/Number of Other Experiments They are Common to	Mission Number *
No.	Description								
AS-02-A	Extra Coronal Lyman Alpha Explorer	595 (1312)	4.1 (13.3)	1.8 (6.0)	10.7 (377)	55.6 (3.5)	1	1/10,1/12,1/13,6/18	T-8 T-52
AS-03-A	Cosmic Background Explorer	595 (1312)	3.1 (10.3)	1.8 (6.0)	8.2 (290)	72.4 (4.52)	1	1/10,1/12,1/13,6/18	?
AS-05-A	Advanced Radio Explorer	1199 (2644)	2.5 (8.1)	1.8 (6.0)	6.5 (228)	186 (11.6)	1		T-32 T-48 T-73
AS-16-A	Large Radio Observatory Array	1300 (2867)	5.2 (17.0)	3.3 (11.0)	45.4 (1602)	28.7 (1.79)	1		?
AP-01-A	Upper Atmosphere Explorer	909 (2004)	2.4 (7.7)	1.4 (4.5)	3.5 (122)	263 (16.4)	2	2/1,3/2,1/10,1/12, 1/13,6/18	T-20 T-57
AP-02-A	Medium Altitude Explorer	272 (599)	1.8 (6.0)	1.4 (4.5)	2.7 (95)	101.1 (6.31)	1	2/1,2/2,1/10,1/12, 1/13,6/18	T-13 T-58
AP-03-A	High Altitude Explorer	427 (941)	1.8 (6.0)	1.2 (4.0)	2.1 (75)	200 (12.5)	1	3 /2,1/10,1/12, 1/13,6/18	
AP-04-A	Gravity & Relativity Satellite-LEO	600 (1323)	3.6 (11.7)	2.7 (8.8)	20.1 (711)	29.8 1.86	1	1/12,1/13,6/18	
AP-05-A	Environmental Pertubation Satellite Mission A	1488 (3281)	3.7 (12.1)	2.1 (6.9)	12.8 (451)	116.5 (7.27)	1	1/2,1/12,1/13,6/18	T-16 T-19 T-55 T-56
AP-06-A	Gravity & Relativity Satellite-Solar	349 (770)	2.1 (6.9)	2.6 (8.5)	11.1 (393)	31.4 (1.96)	1		?

Notes:

*See "Characteristics of Tug Payloads" Matrix

TABLE A-4: CHARACTERISTICS OF EXPERIMFNTS FLOWN IN CONJUNCTION WITH TUG

Experiments		Launch Weight -Kg (lb)	Length -m (ft)	Max. Diam. -m (ft)	Volume -m^3(ft^3)	Density -Kg/m^3 (lb/ft^3)	Flights per Experiment	No. of Components Common to Other Experiments/Number of Other Experiments They are Common to	Mission Number *
No.	Description								
AP-07-A	Environmental Perturbation Satellite Mission B	3946 (8701)	4.6 (15.1)	3.0 (9.8)	32.5 (1148)	121.5 (7.58)	1		?
AP-08-A	Heliocentric & Interstellar Spacecraft	280 (617)	3.0 (9.8)	3.0 (9.8)	21.2 (748)	13.2 (.82)	1		?
EO-07-A	Advanced Synchronous Meteorological Satellite	1006 (2218)	2.9 (9.6)	4.2 (13.9)	41.1 (1450)	24.5 (1.53)	1		?
EO-09-A	Synchronous Earth Observatory Satellite	1531 (3376)	5.2 (17.1)	4.3 (14.1)	75.4 (2679)	20.2 (1.26)	?	1/12,1/13,6/18	T-14 T-21 T-59 T-69
EO-12-A	TIROS 'O'	2150 (4741)	4.1 (13.3)	3.1 (10.0)	29.6 (1044)	72.8 (4.56)	1	1/10,1/12,1/13,6/18	T-26 T-67
EO-56-A	Environmental Monitoring Satellite	2204 (4860)	10.0 (3.72)	3.1 (10.0)	.8 (27)	2866 (179)	?	1/10,1/12,1/13,6/18	T-35 T-76
EO-57-A	Foreign Synchronous Meteorology Satellite	257 (566)	3.1 (10.3)	1.9 (6.3)	9.0 (318)	28.5 (1.78)	?	8/1,1/10,1/12,1/13, 6/18	T-17 T-21 T-24 T-54 T-69 T-72
EO-58-A	Geosynchronous Operational Meteorological Satellite	257 (566)	3.1 (10.3)	1.9 (6.3)	9.0 (318)	28.5 (1.78)	?	8/1	T-14 T-21 T-24 T-27 T-59 T-69 T-72

Notes:

TABLE A-4: CHARACTERISTICS OF EXPERIMENTS FLOWN IN CONJUNCTION WITH TUG

Experiments		Launch Weight -Kg (lb)	Length -m (ft)	Max. Diam. -m (ft)	Volume -m^3 (ft^3)	Density -Kg/m^3 (lb/ft^3)	Flights per Experiment	No. of Components Common to Other Experiments/Number of Other Experiments They are Common to	Mission Number *
No.	Description								
EO-59-A	Geosynchronous Earth Resources Satellite	1531 (3376)	5.2 (17.1)	4.3 (14.1)	75.9 (2679)	20.2 (1.26)	?	3/1	?
EO-62-A	Foreign Synchronous Earth Observatory Satellite	1531 (3376)	5.2 (17.1)	4.3 (14.1)	75.9 (2679)	20.2 (1.26)	?	3/1	?
OP-01-A	Geopause	789 (1740)	2.5 (8.2)	2.0 (6.6)	7.8 (277)	100.6 (6.28)	1	6/18	T-25 T-66
OP-06-A	Magnetic Field Monitor Satellite	200 (441)	4.0 (13.0)	1.3 (4.3)	5.4 (192)	36.9 (2.3)	1	6/18	T-56
PL-01-A	Mars Surface Sample Return	4795 (10573)	7.3 (24.0)	4.3 (14.1)	106 (3749)	45.2 (2.82)	1	3/1	T-3 T-46
PL-02-A	Mars Satellite Sample Return	8402 (18526)	7.6 (24.9)	4.57 (15.0)	125 (4400)	67.5 (4.2)	1	3/1	?
PL-03-A	Pioneer Venus Multiprobe	769 (1696)	2.0 (6.7)	2.5 (8.3)	10.3 (363)	4.67 (74.9)	5	6/18	T-10 T-49 T-52 T-53
PL-07-A	Venus Orbital Imaging Radar	3770 (8313)	5.6 (18.4)	3.0 (9.8)	39.6 1399	95.2 (5.94)	1	1/7,1/11,1/13, 1/8 , 4/12	T-12 T-51
PL-08-A	Venus Buoyancy Probe	7429 (16381)	3.5 (11.5)	4.6 (15.0)	57.5 (2032)	129.2 (8.06)	1		?
PL-09-A	Mercury Orbiter	3125 (6891)	7.6 (24.9)	4.6 (15.0)	124.3 (4389)	25.2 (1.57)	1		?

Notes:

TABLE A-4: CHARACTERISTICS OF EXPERIMENTS FLOWN IN CONJUNCTION WITH TUG

Experiments		Launch Weight -Kg (lb)	Length -m (ft)	Max. Diam. -m (ft)	Volume -m^3(ft^3)	Density -Kg/m^3 (lb/ft^3)	Flights per Experiment	No. of Components Common to Other Experiments/Number of Other Experiments They are Common to	Mission Number *
No.	Description								
PL-10-A	Venus Large Lander	1690	5.0	4.6	82.4	20.5	1		?
		(3726)	(16.4)	(15.0)	(2911)	(1.28)			
PL-11-A	Pioneer Saturn/Uranus Flyby	477	3.1	2.7	18.4	26.0	1	6/2, 1/10, 1/12, 1/13,	T-5
		(1052)	(10.2)	(9.0)	(649)	(1.62)		6/18	T-43
PL-12-A	Mariner Jupiter Orbiter	1600	5.8	3.7	60.9	26.3	1	8/2	T-44
		(3528)	(19.0)	(12.0)	(2151)	(1.64)			
PL-13-A	Pioneer Jupiter Probe	477	3.1	2.7	18.4	26.0	1	14/2, 1/10, 1/12, 1/13,	T-6
		(1052)	(10.2)	(9.0)	(649)	(1.62)		6/18	
PL-14-A	Saturn Orbiter	1286	3.0	4.6	49.3	26.0	1		?
		(2836)	(9.8)	(15.0)	(1740)	(1.63)			
PL-15-A	Uranus Probe/Neptune Flyby	815	6.4	4.6	105.1	7.8	1		?
		(1797)	(21.0)	(15.0)	(3713)	(.484)			
PL-16-A	Ganymede Orbiter/Lander	4000	7.6	4.6	124.9	33.6	1		?
		(8820)	(24.9)	(15.0)	(4410)	(2.0)			
PL-18-A	Encke Rendezvous	2390	6.2	4.6	100.8	23.7	1	6/18	T-4
		(5270)	(20.2)	(15.0)	(3561)	(1.48)			T-48
PL-19-A	Halley Comet Flyby	580	3.0	3.0	21.2	27.4	1		?
		(1279)	(9.8)	(9.8)	(748)	(1.71)			
PL-20-A	Asteroid Rendezvous	2160	5.0	3.1	38.0	56.9	1		?
		(4673)	(16.4)	(10.2)	(1342)	(3.55)			
PL-22-A	Pioneer Saturn Probe	477	3.1	2.7	18.4	26.0	1	14/2, 1/10, 1/12, 1/13	T-7
		(1052)	(10.2)	(9.0)	(649)	(1.62)		6/18	T-45

Notes:

TABLE A-4: CHARACTERISTICS OF EXPERIMENTS

FLOWN IN CONJUNCTION WITH TUG

Experiments		Launch Weight -Kg (lb)	Length -m (ft)	Max. Diam. -m (ft)	Volume -m^3(ft^3)	Density -Kg/m^3 (lb/ft^3)	Flights per Experiment	No. of Components Common to Other Experiments/Number of Other Experiments They are Common to	Mission Number *
No.	Description								
CN-51-A	Intelsat	1472 (3246)	2.7 (8.9)	2.5 (8.2)	13.3 (468)	111.2 (6.94)	1	9/1	T-17 T-33 T-34 T-54 T-58 T-60 T-61 T-74 T-75
CN-52-A	U.S. Domsat 'A'	262 (577)	3.2 (10.5)	2.2 (7.2)	12.2 (430)	21.5 (1.34)	1		T-22 T-23 T-24 T-34 T-65 T-70 T-71 T-75
CN-53-A	U.S. Domsat 'B'	1472 (3246)	2.7 (8.9)	2.5 (8.2)	13.3 (468)	111.2 (6.94)	1	9/1	T-60
CN-54-A	Disaster Warning Satellite	583 (1299)	5.12 (16.8)	1.4 (4.6)	7.9 (278)	74.8 (4.67)	1		T-22 T-70
CN-55-A	Traffic Management Satellite	299 (658)	1.6 (5.2)	3.9 (12.7)	18.6 (658)	16.0 (1.0)	1		T-17 T-22 T-23

Notes:

T-65	T-25
T-71	T-33
T-74	T-34
T-75	T-54

TABLE A-4: CHARACTERISTICS OF EXPERIMENTS

FLOWN IN CONJUNCTION WITH TUG

Experiments		Launch Weight -Kg (lb)	Length -m (ft)	Max. Diam. -m (ft)	Volume -m^3(ft^3)	Density -Kg/m^3 (lb/ft^3)	Flights per Experiment	No. of Components Common to Other Experiments/Number of Other Experiments They are Common to	Mission Number *
No.	Description								
CN-56-A	Foreign Communications Satellite A	307.9 (679)	2.4 (7.7)	1.6 (5.3)	4.8 (168)	64.9 (4.05)	1		T-16 T-22 T-59 T-61 T-68 T-70
CN-58-A	U.S.Domsat 'C'	868 (1913)	3.7 (12.1)	2.2 (7.2)	13.8 (486)	63.1 (3.94)	1		?
CN-59-A	Communications R&D/Prototype Satellite	956.3 (2109)	6.0 (19.7)	3.4 (11.2)	54.8 (1935)	17.5 (1.09)	1		?
CN-06-A	Foreign Communications Satellite B	332 (732)	3.2 (10.5)	2.2 (7.2)	12.2 (431)	27.2 (1.7)	1		?
LU-01-A	Lunar Orbiter	839 (1850)	4.8 (15.7)	2.0 (6.7)	15.5 (547)	54.2 (3.38)	1	1/13, 6/18	T-11 T-50
LU-02-A	Lunar Rover	1380 (3043)	4.9 (16.2)	3.2 (10.6)	40.5 (1429)	34.1 (2.13)	1	6/1	?
lu-03-A	Lunar Halo Satellite	1120 (2470)	5.1 (16.7)	2.3 (7.6)	21.7 (765)	51.8 (3.23)	1	6/1	?
LU-04-A	Lunar Sample Return	2665 (5876)	4.9 (16.2)	3.2 (10.6)	40.5 (1430)	65.9 (4.11)	1		?

Notes:

TABLE A-5: CHARACTERISTICS OF MODULE TYPE EXPERIMENTS

Experiments		Launch Weight -Kg (lb)	Length -m (ft)	Max. Diam. -m (ft)	Volume -m^3(ft^3)	Density -Kg/m^3 (lb/ft^3)	Flights per Experiment	No. of Components Common to Other Experiments/Number of Other Experiments They are Common to	Mission Number *
No.	Description								
AS-01-A	Large Space Telescope	11340 (25005)	12.9 (42.3)	4.0 (13.1)	162 (5723)	70.0 (4.37)	3		?
AS-07-A	3m Ambient Temperature IR Telescope	8590 (18950)	12.2 (40.1)	4.6 (15.0)	205 (7233)	42.0 (2.62)	3	2/7	?
AS-11-A	1.5m IR Telescope	6045 (11329)	5.2 (17.1)	4.6 (15.0)	85.8 (3029)	70.5 (4.4)	?	2/7	?
AS-13-A	UV Survey Telescope	?	?	?	?	?	?	2/7	?
AS-14-A	1m UV-Optical Telescope	4001 (8822)	5.2 (17.4)	4.6 (15.0)	86.7 (3063)	46.2 (2.9)	?	2/7	?
AS-17-A	30m IR Interferometer	3490 (7695)	17.0 (53.9)	4.6 (15.0)	279 (9865)	12.5 (.78)	?	2/7	?
HE-01-A	Large X-Ray Telescope Facility	11869 (26171)	16.0 (52.5)	4.6 (15.0)	206 (7290)	57.5 (3.6)	1	15/1,2/7,1/8, 4/12,1/11,1/13	?
HE-03-A	Extended X-Ray Survey	8011 (17664)	5.7 (18.8)	4.6 (15.0)	94.0 (3320)	85.3 (5.3)	1	1/8,2/7,1/13,, 4/12,1/11	?
HE-05-A	High Latitude Cosmic-Ray Survey	7062 (11572)	9.2 (30.0)	4.6 (15.0)	150.0 (5296)	47.1 (2.94)	1	2/7	?
HE-07-A	Small High Energy Satellite	595 (1311)	2.6 (8.6)	1.8 (6.0)	4.8 (169)	123.9 (7.73)	1	1/13 4/12,1/11	
HE-08-A	Large High Energy Observatory A (Gamma-Ray)	8700 (19184)	5.2 (17.1)	4.6 (15.0)	85.5 (3021)	101.8 (6.35)	1	1/8,2/7,1/13 4/12,1/11	?
HE-09-A	Large High Energy Observatory B (Magnetic Spectrometer)	6255 (13792)	5.5 (18.0)	4.6 (15.0)	90.0 (3178)	69.6 (4.34)	1	1/8,2/7,1/13 4/12,1/11	?

Notes:

*See "Characteristics of Missions Defined by Available Integrated Mission Plans" Matrix

TABLE A-5: CHARACTERISTICS OF MODULE TYPE EXPERIMENTS

Experiments		Launch Weight -Kg (lb)	Length -m (ft)	Max. Diam. -m (ft)	Volume $-m^3(ft^3)$	Density $-Kg/m^3$ (lb/ft^3)	Flights per Experiment	No. of Components Common to Other Experiments/Number of Other Experiments They are Common to	Mission Number *
No.	Description								
HE-10-A	Large High Energy Observatory C (Nuclear Calorimeter)	5336 (11766)	5.5 (18.0)	4.6 (15.0)	90.0 (3180)	59.3 (3.7)	1	1/1	?
HE-11-A	Large High Energy Observatory D (1.2 m X-Ray Telescope)	6771 (14930)	10.2 (33.5)	4.6 (15.0)	168 (5925)	40.4 (2.52)	1	15/1,2/7,1/13, 4/12,1/11,1/8	?
HE-12-A	Cosmic Ray Laboratory	10332 (22782)	8.5 (28.0)	4.6 (15.0)	14.0 (4953)	73.7 (4.6)	1	2/7,1/1	?
SO-02-A	Large Solar Observatory	9825 (21664)	17.7 (58.1)	4.6 (15.0)	291 (10267)	33.8 (2111)	1		?
SO-03-A	Solar Maximum Satellite	761 (1678)	3.2 (10.5)	1.5 (5.0)	5.8 (206)	130.5 (8.14)	?	1/8,2/7,1/13 4/12,1/11	16
EO-08-A	Earth Observatory Satellite	3475 (7662)	11 36.1	3.1 (10.0)	80.4 (2838)	43.3 (2.7)	?	1/8,2/7,1/13,4/12 1/11	?
EO-10-A	Applications Explorer (Special Purpose Satellite)	141 (310)	1.1 (3.5)	0.9 (2.9)	0.6 (22)	2244 (14.0)	?		?
EO-61-A	Earth Resources Survey Operational Satellite	733 (614)	3.0 (10.0)	1.5 (5.0)	5.6 (196)	132.2 (8.25)	1	1/7,1/8,1/13 4/12	?
OP-02-A	Gravity Gradiometer	3277 (7266)	4.6 (15.1)	4.0 (13.1)	57.6 (2035)	56.9 (3.55)	1	1/13,4/12,1/11	?
OP-03-P	Mini-Lageos	204 (450)	?	0.5 (1.6)	?	?	?		8,18
OP-04-A	GRAVSAT	3086 (6805)	2.7 (8.9)	2.0 (6.6)	8.5 (301)	362.2 (22.6)	1	1/13,4/12,1/11	?

Notes:

TABLE A-5: CHARACTERISTICS OF MODULE TYPE EXPERIMENTS

Experiments		Launch Weight -Kg (lb)	Length -m (ft)	Max. Diam. -m (ft)	Volume $-m^3(ft^3)$	Density $-Kg/m^3$ (lb/ft^3)	Flights per Experiment	No. of Components Common to Other Experiments/Number of Other Experiments They are Common to	Mission Number *
No.	Description								
OP-05-A	Vector Magnetometer Satellite	141 (310)	4.0 (13.0)	1.3 (4.3)	5.4 (191)	26.0 (1.62)	1	1/13,4/12,1/11	?
OP-07-A	SEASAT-B	440 (2073)	4.6 (15.0)	4.0 (13.0)	56.4 (1993)	16.7 (1.04)	1	1/13	?
OP-51-A	Global Earth & Ocean Monitor System	?	?	?	?	?	?		?
SP-01-A	Space Processing Free-Flyer	6059 (13360)	3.4 (11.3)	4.3 (14.0)	49.2 (1739)	123.1 (7.68)	?		?
LS-02-A	Biomedical Experiment Scientific Satellite	1814 (4000)	2.9 (9.5)	3.7 (12.0)	30.4 (1075)	59.6 (3.72)	?		?
ST-01-A	Long Duration Exposure Facility	3856 (8502)	9.3 (30.3)	4.3 (14.2)	136.0 (4803)	28.4 (1.77	6		3
SP-21-S	SPA No. 21 Minimum Biological (B + C)	926 (2042)	?	?	?	?	?		?
SP-22-S	SPA No. 22 Minimum Furnace (Manned)	829 (1828)	?	?	?	?	?		?
SP-23-S	SPA No. 23 Minimum General (G+C)	748 (1649)	?	?	?	?	?		?
SP-24-S	SPA No. 24 Minimum Levitation (Manned)	930 (2051)	?	?	?	?	?		?
LS-09-S	Life Sciences Shuttle Laboratory	2846 (6275)	?	4.1 (13.5)	?	?	?		?

Notes:

TABLE A-5: CHARACTERISTICS OF MODULE TYPE EXPERIMENTS

Experiments		Launch Weight -Kg (lb)	Length -m (ft)	Max. Diam. -m (ft)	Volume $-m^3(ft^3)$	Density $-Kg/m^3$ (lb/ft^3)	Flights per Experiment	No. of Components Common to Other Experiments/Number of Other Experiments They are Common to	Mission Number *
No.	Description								
ST-05-S	Superfluid He + Particle/Drop Positioning (FACIL. No. 2)	440 (970)	?	?	?	?	?		?
ST-06-S	Fluid Physics + Heat Transfer (FACIL. No. 3)	622 (1371)	?	?	?	?	?		?
CN-13-S	Shuttle Navigation Via Geosynchronous Satellite	60 (132)	?	?	?	?	?		?

Notes:

TABLE A-6: EXPERIMENT/COMPONENT COMMONALITY MATRIX FOR PALLET MOUNTED UNITS

COMPONENTS		EXPERIMENTS																
NUMBER	DESCRIPTION	OP-02-S	OP-03-S	OP-04-S	OP-05-S	OP-06-S	SP-01-S	SP-02-S	SP-12-S	SP-13-S	SP-14-S	SP-15-S	SP-19-S	ST-08-S	ST-21-S	ST-22-S	ST-23-S
OP060	Antenna	X			X												
OP061	Transmitter	X			X												
OP062	Receiver	X			X												
OP065	Power Supply	X			X												
OP076	Gimball & Optical Assy.	X			X												
OP077	Electronics Package	X			X												
OP085	Optical Package "A"	X	X	X	X	X											
OP086	Optical Package "B"	X	X	X	X	X											
OP087	Optical Package "C"	X	X	X	X	X											
OP088	Optical Package "O"	X	X	X	X	X											
OP089	Electronics Module	X	X	X	X	X											
OP097	Gimbal & Camera Assy.	X			X	X											
OP094	Gimbal Servo	X			X	X											
OP098	Optical Contamination Monitor Gage	X				X											
OP099	Contamination Monitor Gage	X				X											
OP100	Mass Spectrometer Sensor	X				X											
OP102	Observation Telescope/Camera	X	X	X	X	X											
OP103	Servo Electronics	X	X	X	X	X											
OP105	Support Equipment Control Unit	X	X	X		X											
SP-101	Fluid Cooling/Refrigeration						X				X						
SP-902	Fuel Cells						X					X					
SP-907	Inverter-400 Hz						X					X					
SP-600	Furnace Subelement							X				X					
SP-701	Automated Furnace								X		X		X				
SP-800	Automated Core								X	X		X					

TABLE A-6: EXPERIMENT/COMPONENT COMMONALITY MATRIX FOR PALLET MOUNTED UNITS

COMPONENTS		EXPERIMENTS															
NUMBER	DESCRIPTION	OP-02-S	OP-03-S	OP-04-S	OP-05-S	OP-06-S	SP-01-S	SP-02-S	SP-12-S	SP-13-S	SP-14-S	SP-15-S	SP-19-S	ST-08-S	ST-21-S	ST-22-S	ST-23-S
SP-700	Automated Levitation									X	X	X	X				
ST-246	Optical Effects Module													X	X	X	X
ST-247	Particle Spectrometer													X	X	X	X
ST-248	Mass Spectrometer													X	X	X	X
ST-249	Quartz Crystal Microbalance													X	X	X	X
ST-250	Active Cleaning													X	X	X	X
ST-251	Multiplexer													X	X	X	X
ST-252	Command Decoder													X	X	X	X
ST-253	Tray													X	X	X	X
ST-028	Camera, TV														X	X	
ST-076	Photomultiplier Meteor Detector															X	X
ST-073	Spectrograph, Far U-V															X	X
ST-074	Electronographic Spectrograph															X	X
ST-075	Spectrograph Panchromatic															X	X
ST-112	Sample Arrays															X	X
ST-113	Extendable Boom															X	X
ST-241	Tray Cover w/Motor															X	X

TABLE A-6: EXPERIMENT/COMPONENT COMMONALITY MATRIX FOR PALLET MOUNTED UNITS

COMPONENTS		EXPERIMENTS																
NUMBER	DESCRIPTION	SP-01-S	SP-02-S	SP-03-S	SP-04-S	SP-05-S	SP-14-S	SP-15-S	SP-19-S	SP-21-S	SP-22-S	SP-23-S	SP-24-S	SP-12-S	SP-13-S	SP-21-S	ST-22-S	ST-23-S
SP-903	Liquid Oxygen Bottle	X						X										
SP-904	Liquid Hydrogen Bottle	X						X										
SP-905	Fuel Cell Controls	X						X										
SP-906	F.C. Water Storage Bottle	X						X										
SP-850	Core Sub-Element		X	X	X	X	X	X	X	X	X	X	X					
SP-400	General Purpose Sub-Element				X	X	X		X									
SP-100	Biological Sub-Element					X	X		X									
?	Control Console													X	X			
ST-026	Monitor, TV															X	X	
ST-045	Gas Source															X	X	
ST-046	Aerosol Generator															X	X	
ST-047	Ion Generator															X	X	
ST-048	Water Vapor Source															X	X	
ST-049	Light Source															X	X	
ST-050	Chamber, Environmental															X	X	
ST-051	Microscope															X	X	
ST-052	Sensors															X	X	
ST-079	Tube Holder															X	X	
ST-080	Refrigerator															X	X	X
ST-081	Container, Experiment																	
ST-083	Incubator															X	X	
ST-087	Microscope, Camera															X	X	
ST-035	Data Processing Equipment															X	X	
ST-105	Air Sample Unit															X	X	X
ST-107	Timer															X	X	

TABLE A-6: EXPERIMENT/COMPONENT COMMONALITY MATRIX FOR PALLET MOUNTED UNITS

COMPONENTS		EXPERIMENTS														
NUMBER	DESCRIPTION	AS-01-S	AS-03-S	AS-07-S	AS-08-S	AS-10-S	AS-11-S	AS-12-S	AS-15-S	AS-19-S	AS-43-S	AS-49-S	HE-03-S	HE-11R-S	SO-01-S	SO-11-S
AS-008	Chamber, Selector, Multiple Instrument, LHe Cooled	X							X							
AS-009	Unit, Electronics, Checkout, Test, Control	X							X							
AS-010	Unit, Recycling, LHe	X							X							
AS-013	Computer Digital	X	X						X							
AS-014	Display, Malfunction	X	X						X							
AS-015	Panel, Indicators/Switches, Data Flow	X	X						X							
AS-016	Panel, Envr/Power, Indicators, Switches	X							X							
AS-017	Panel, Monitor/Control, Cryogens	X							X							
AS-018	Panel, Control, Fine Pointing, Overide	X	X						X							
AS-019	Keyboard, Computer, Input	X	X						X							
AS-020	Tracker/Field Monitor & Guide Star Sensors	X	X						X							
AS-021	Unit, Electronics, Guide Star Trackers	X	X						X							
AS-022	Multiplexer/Demultiplexer, High Speed	X	X						X							
AS-023	Memory Unit, Disc File	X	X						X							
AS-024	Unit, Electronics, Telescope Control	X							X							

TABLE A-6: EXPERIMENT/COMPONENT COMMONALITY MATRIX FOR PALLET MOUNTED UNITS

COMPONENTS		EXPERIMENTS														
NUMBER	DESCRIPTION	AS-01-S	AS-03-S	AS-07-S	AS-08-S	AS-10-S	AS-11-S	AS-12-S	AS-15-S	AS-19-S	AS-43-S	AS-49-S	HE-03-S	HE-11R-S	SO-01-S	SO-11-S
AS-025	Disc Pack			X				X								
?	XUV Telescope Filter Photometer			X				X								
?	XUV Telescope Grating Spectrometer			X				X								
?	UV Spectrometer			X				X								
?	Visible Spectrometer			X				X								
?	Near IR Spectrometer			X				X								
?	IR Interferometer Spectrometer			X				X								
?	Far IR Spectrometer			X				X								
?	UV Telescope Camera			X				X								
?	TV Camera (10 Filters)			X				X								
?	Still Camera (10 Filters)			X				X								
?	Guide Star Tracker				X				X							
?	Control Display Assembly					X	X									
?	Black Brant Vehicle					X	X									
?	X-Ray Proportional Counters										X	X				
?	Assembly, Service & Storage												X	X		
?	Pointing Component Replacement Kit												X	X		
?	Instrument Replacement Kit												X	X		
?	SSM Component Replacement Kit												X	X		
?	Checkout/Display/Control Assy.												X	X		

TABLE A-6: EXPERIMENT/COMPONENT COMMONALITY MATRIX FOR PALLET MOUNTED UNITS

COMPONENTS		EXPERIMENTS													
NUMBER	DESCRIPTION	AS-01-S	AS-03-S	AS-07-S	AS-08-S	AS-10-S	AS-11-S	AS-12-S	AS-15-S	AS-19-S	AS-43-S	AS-49-S	HE-03-S	HE-11R-S	SO-01-S	SO-11-S
SO-001	Coronagraph, Externally Occulted														X	X
SO-002	Photoheliograph, 100-CM														X	X
SO-003	Spectrograph, Ultraviolet														X	X
SO-004	Spectroheliometer, Extreme UV														X	X
SO-005	Spectrometer/Spectroheliograph														X	X
SO-007	Spectrometer/Spectroheliograph Soft X-Ray														X	X
SO-008	Photometer, Grid Collimator Acquisition														X	X
SO-009	Collimator, Modulation														X	X
SO-020	Telescope/Spectrograph, Soft X-Ray														X	X
SO-030	Mount, Coronagraph														X	X
SO-055	Tape Recorder and Magazine														X	X

TABLE A-7: EXPERIMENT/COMPONENT COMMONALITY MATRIX FOR MODULE MOUNTED COMPONENTS

COMPONENTS		EXPERIMENTS																			
NUMBER	DESCRIPTION	AS-07-A	AS-11-A	AS-13-A	AS-14-A	AS-17-A	HE-01-A	HE-03-A	HE-05-A	HE-07-A	HE-08-A	HE-09-A	HE-10-A	HE-11-A	HE-12-A	SO-03-A	EO-08-A	EO-61-A	OP-02-A	OP-04-A	OP-05-A	OP-07-A	PL-07-A
SS001	Structure, Mechanisms						X	X		X	X	X	X		X	X	X	X	X	X		X
SS002	Environmental Control						X	X		X	X	X	X		X	X	X	X	X	X		X
SS003	Guidance, Navigation, Stabilization						X	X		X	X	X	X		X	X	X	X	X	X	X	X
SS004	Propulsion						X	X			X	X	X		X	X	X					X
SS005	Kick Motor						X	X			X	X	X		X	X	X					X
SS006	Attitude Control						X	X		X	X	X	X		X	X	X		X	X	X	X
SS007	Telemetry, Tracking Command						X	X		X	X	X	X		X	X	X	X	X	X		X
SS008	Electrical						X	X		X	X	X	X		X	X	X	X	X	X		X
SS009	Other						X	X			X	X	X		X	X	X					
?	Spacecraft Support Subsystems Module	X	X	X	X	X			X				X		X							
?	Control Display & Electronics	X	X	X	X	X			X				X		X							
HE106	Mounting, Instrument, Including Selector Assy						X						X									
HE101	Field Monitor Camera						X						X									
HE103	Star Guide Trackers						X						X									
HE105	Aspect Sensor Optics						X						X									
HE111	Counter, Proportional Array, Position Sensing						X						X									
HE121	Converter/Intensifier, X-Ray						X						X									
HE131	Crystal X-Ray Spectrometer						X						X									
HE141	Maximum Sensitivity Detector						X						X									
HE143	X-Ray Transmission Grating						X						X									
HE155	Lithium Hydride Polarimeter						X						X									
HE102	Field Monitor Electronics						X						X									
HE104A	Star Guide Tracker Electronics						X						X									
HE112	Prop Counter Electronics						X						X									
HE122	Electronics, Converter Intensifier						X						X									
HE132	Crystal Electronics Spectrometer						X						X									
?	Nuclear Calorimeter												X		X							

TABLE A-7: EXPERIMENT/COMPONENT COMMONALITY MATRIX FOR MODULE MOUNTED UNITS

COMPONENTS		EXPERIMENTS			
NUMBER	DESCRIPTION	OP-02-S	OP-05-S	SP-01-S	SP-14-S
OP063	Film Recorder	X	X		
SP-104	Laser Optical Scattering Monitor			X	X
SP-105	UV-Vis. Spectrometer			X	X
SP-106	Dye Laser/Flash Lamp			X	X
SP-107	Retro-Reconstruction Holimicroscope			X	X
SP-108	Recruiting Fluid Incubator			X	X
SP-109	Dialysis Unit			X	X
SP-110	Pump Metering			X	X
SP-111	Continuous Flow Electrophoretic Column			X	X
SP-112	Stationary Electrophoresis Column			X	X
SP-113	Gas Elimination System			X	X
SP-114	Electrolyte Supply Tank			X	X
SP-115	PH Monitor			X	X
SP-116	Fraction Collection System			X	X
SP-117	Flowmeter			X	X
SP-118	Lyophilization Unit			X	X
SP-119	Oxygen Analyzer			X	X
SP-120	Specimen Supply Tank			X	X
SP-121	Power Conditioning Unit (5Kv)			X	X
SP-122	Dark Field Illuminator			X	X
SP-123	Refrigerator			X	X

TABLE A-7: EXPERIMENT/COMPONENT COMMONALITY MATRIX FOR MODULE MOUNTED UNITS

COMPONENTS		EXPERIMENTS			
NUMBER	DESCRIPTION	OP-02-S	OP-05-S	SP-01-S	SP-14-S
SP-124	Freezer			X	X
SP-125	Dewar			X	X
SP-126	Liquid Waste Tank			X	X
SP-127	Molecular Sieve			X	X
SP-129	Coolant Supply Tank			X	X
SP-130	Glove Box			X	X
SP-131	Isoelectric Focusing Unit			X	X
SP-501	Digital Clock			X	X
SP-502	Scanner/Programmer			X	X
SP-503	Signal Conditioner			X	X
SP-504	Digital Voltmeter			X	X
SP-505	Set Point Controller			X	X
SP-506	Processor			X	X
SP-507	Input/Output Stage			X	X
SP-508	Operator Control Unit			X	X
SP-509	Printer (Output)			X	X
SP-510	Fuel Supply System			X	X
SP-511	Teleprinter			X	X
SP-512	Digital Storage			X	X
SP-513	SCR Controller			X	X
SP-514	Multiplexer A/D Converter			X	X
SP-515	Tape Input			X	X
SP-516	Storage Peripheral			X	X

TABLE A-7: EXPERIMENT/COMPONENT COMMONALITY MATRIX FOR MODULE MOUNTED UNITS

COMPONENTS		EXPERIMENTS			
NUMBER	DESCRIPTION	OP-02-S	OP-05-S	SP-01-S	SP-14-S
SP-517	CCTV Camera			X	X
SP-518	CCTV Control Unit			X	X
SP-519	CCTV Monitor			X	X
SP-520	CCTV Frame Storage Unit			X	X
SP-521	CCTV Slow Scan Synchr. Unit			X	X
SP-522	CCTV Automatic Processor			X	X
SP-523	Oscilloscope			X	X
SP-524	Racks/Support Structures			X	X
SP-525	Cabling			X	X

TABLE A-8: EXPERIMENT/COMPONENT COMMONALITY MATRIX FOR MODULE-TUG MOUNTED COMPONENTS

COMPONENTS		EXPERIMENTS																										
NUMBER	DESCRIPTION	AS-02-A	AS-03-A	AS-16-A	AP-01-A	AP-02-A	AP-03-A	AP-04-A	AP-05-A	EO-09-A	EO-12-A	EO-56-A	EO-57-A	EO-58-A	EO-59-A	EO-62-A	OP-01-A	OP-06-A	PL-01-A	PL-02-A	PL-03-A	PL-11-A	PL-13-A	PL-18-A	PL-22-A	CN-51-A	CN-53-A	LU-01-A	LU-02-A	LU-03-A	PL-12-A
SS001	Structure Mechanisms	X	X		X	X	X	X	X	X	X	X	X				X	X			X	X	X	X	X			X			
SS002	Environmental Control	X	X		X	X	X	X	X	X	X	X	X				X	X			X	X	X	X	X			X			
SS003	Guidance, Navigation, Stabilization	X	X		X	X	X	X	X	X	X	X	X				X	X			X	X	X	X	X			X			
SS004	Propulsion	X	X		X	X	X	X	X	X	X	X										X	X		X			X			
SS005	Kick Motor	X	X		X	X	X	X	X	X	X	X										X	X		X						
SS006	Attitude Control	X	X		X	X	X	X	X	X	X	X	X				X	X			X	X	X	X	X			X			
SS007	Telemetry, Tracking Command	X	X		X	X	X	X	X	X	X	X	X				X	X			X	X	X	X	X			X			
SS008	Electrical	X	X		X	X	X	X	X	X	X	X	X				X	X			X	X	X	X	X			X			
SS009	Other	X	X		X	X	X				X	X	X									X	X		X						
AP-003	VLF Receiver W/Antenna				X		X		X																						
AP-004	Mass Spectrometer				X	X																									
AP-006	Electrical Field Detector				X	X	X																								
AP-007	Magnetometer				X	X	X																								
AP-008	Drag Analyzer				X	X																									
EO-053	Visible Infrared Spin-Scan Radiometer/Sounder												X	X																	
EO-054	VISSR Auxiliary Electronics Module												X	X																	
EO-055	Magnetometer Sensor Assy												X	X																	
EO-056	Magnetometer Data Handling Assy												X	X																	
EO-057	X-Ray Sensor Telescope & Positioner												X	X																	
EO-058	X-Ray Sensor Data Handling Assy												X	X																	

TABLE A-8: EXPERIMENT/COMPONENT COMMONALITY MATRIX FOR MODULE-TUG MOUNTED COMPONENTS

COMPONENTS		EXPERIMENTS																															
NUMBER	DESCRIPTION	AS-02-A	AS-03-A	AS-16-A	AP-01-A	AP-02-A	AP-03-A	AP-04-A	AP-05-A	EO-09-A	EO-12-A	EO-56-A	EO-57-A	EO-58-A	EO-59-A	EO-62-A	OP-01-A	OP-06-A	PL-01-A	PL-02-A	PL-03-A	PL-11-A	PL-13-A	PL-18-A	PL-22-A	CN-51-A	CN-53-A	LU-01-A	LU-02-A	LU-03-A	PL-12-A
EO-059	Solar Energetic Particle Counter												X	X																			
EO-060	Solar Energetic Particle Sensor Data Handling Assy												X	X																			
?	Telescope, Cassengrain, 1.5 Meter Objective														X	X																	
?	Sensor Assy														X	X																	
?	Data Collection System														X	X																	
?	Mars Orbiter Vehicle Subsys																		X	X													
?	Earth Return Vehicle Subsys																		X	X													
?	Earth Entry Capsule Subsystem																		X	X													
PL-125	Mass Spectrometer, Neutral																					X	X		X								
PL-126	Gauge, Temperature																					X	X		X								
PL-127	Gauge , Pressure																					X	X		X								
PL-128	Nephelometer																					X	X		X								
PL-129	Accelerometer																					X	X		X								
PL-130	Magnetometer																					X	X		X								
PL-131	Analyzer, Solar Wind																						X		X								X
PL-132	Detector, Charged Particle																						X		X								X
PL-133	Radiometer, IR																						X		X								X
PL-134	Spectrometer, IR																						X		X								X
PL-135	Photometer, UV																						X		X								X
PL-136	Camera, Line Scan (2)																						X		X								X
PL-137	Detector, RF Noise																						X		X								X
PL-138	Detector,Micrometeroid																						X		X								X

TABLE A-8: EXPERIMENT/COMPONENT COMMONALITY MATRIX FOR MODULE-TUG MOUNTED COMPONENTS

COMPONENTS		EXPERIMENTS																								
NUMBER	DESCRIPTION	AS-02-A	AS-03-A	AS-16-A	AP-01-A	AP-02-A	AP-03-A	AP-04-A	AP-05-A	EO-09-A	EO-12-A	EO-56-A	EO-57-A	EO-58-A	EO-59-A	EO-62-A	OP-01-A	OP-06-A	PL-01-A	PL-02-A	PL-03-A	PL-11-A	PL-13-A	PL-18-A	PL-22-A	CN-51-A	CN-53-A	LU-01-A	LU-02-A	LU-03-A	PL-12-A
CN-028	Transceiver, 4/6 GHz, 24 Channel																								X	X				
CN-029	Transceiver, 12/13 GHz, 24 Channel																								X	X				
CN-030	Antenna, 6 GHz Receiver																								X	X				
CN-031	Antenna, 4 GHz Transmitter																								X	X				
CN-032	Antenna, 13 GHz Receiver																								X	X				
CN-033	Antenna, 13 GHz Receiver (2 Horn Feed)																								X	X				
CN-034	Antenna, 12 GHz Transmitter																								X	X				
CN-035	Antenna, 12 GHz Transmitter																								X	X				
CN-036	Antenna, Beacon 12 GHz (Small Horn)																								X	X				
?	Imaging System																											X	X	
?	Surface Sampler																											X	X	
?	Sample Processing & Distribution Systems																											X	X	
?	X-Ray Diffractometer																											X	X	
?	X-Ray Spectrometer																											X	X	
?	Rover																											X	X	

APPENDIX B

STS PAYLOAD SHROUD ACOUSTIC TEST

CONTENTS

CONTENTS (cont'd)

CONTENTS (cont'd)

1.0 SCOPE

1.1 Purpose - This report presents a description of acoustic tests performed on two STS payload shroud simulators. Also presented are the test data, test objective, test configuration, facility description and test summary.

1.2 Summary - The acoustic tests were performed during the period extending from 14 November through 26 November 1975. The test program was performed at the Martin Marietta Corporation Acoustic Vibration Facility in Denver, Colorado. Included in this appendix are composite plots of all the transducer data and noise reduction plots of the microphone data.

2.0 ACOUSTIC TEST DESCRIPTION

2.1 Test Objective - The objective of this test was to subject the test specimen to a uniform acoustic sound field, measure the noise attenuation characteristics and obtain the structural response of the specimen.

2.2 Specimen/Test Configurations - The test specimen consisted of a composite fiberglass shroud and a double bulkhead aluminum shroud. Each specimen was cylindrical in shape and the ends were capped with plywood. Photographs of each specimen are presented in Figures 1 and 2 along with details concerning each specimen arrangement.

The test specimen were suspended inside the acoustic shroud with nylon rope. Six control microphones were placed externally around the specimen and five monitor microphones were located inside the specimen. Four accelerometers, three external and one internal, were located on the composite shroud and strain gages (4 each) were located on external and internal panels of the aluminum shroud. A mechanical vacuum pump was used to provide differential pressure test conditions and a regulated helium supply was used for the helium test condition. Transducer locations and the general test configuration are depicted in Figures 3 and 4 respectively.

2.3 Facility Description - The tests described in this document were conducted in the Acoustic Vibration Laboratory acoustic facility which utilizes an acoustic shroud with two Wyle WAS-3000 acoustic transducers which are coupled to the shroud by acoustic horns, top and bottom. The transducers are operated with a continuous gaseous nitrogen supply.

2.3.1 Control System - The acoustic input was controlled by the average of six external microphones. The control of this average was accomplished utilizing a General Radio one-third octave spectrum equalizer/analyzer system.

2.3.2 Data Acquisition/Reduction System - The data was acquired and analyzed following each acoustic test at the rate of two transducers per exposure. Microphone data was analyzed with a General Radio one-third octave spectrum analyzer and accelerometer, strain gage and selected microphone data were analyzed with a Time Data 1923 digital analysis system. Unholtz-Dickie charge amplifiers were used to signal condition microphone and accelerometer data and a Martin bridge balance voltage divider system was used for strain gage signal conditioning utilizing Dana amplifiers. Standard, miniature crystal accelerometers, crystal microphones and 350 ohm strain gages were used to measure the surrounding acoustics and structural response of the specimen.

2.4 Test Summary - In order to accomplish the stated objectives of the test, each specimen was subjected to an acoustic level of 140 dB overall for a minimum period of 60 seconds. This exposure was repeated sufficiently to acquire and analyze all the required data for the various test conditions identified in Section 2.4.4.

2.4.1 Test Procedure - The performance of each acoustic test was implemented by verifying the spectrum shape and setting the overall level on a B&K rms meter.

2.4.2 Instrumentation - 11 microphones and 4 accelerometers were used for the composite shroud tests, and 11 microphones and 8 strain gages were used for the aluminum shroud tests. Locations of these transducers are shown in Figures 3 and 4 respectively.

2.4.3 Data Summary - One-third octave spectrum analysis data was obtained for the external and internal microphones during all test conditions. 8 Hz bandwidth analysis was performed on the internal microphones for both the composite and aluminum shroud ambient test conditions. Also, 8 Hz analysis was performed on accelerometer and strain gage data for all test conditions. In addition, static strain gage data was obtained for the aluminum shroud (ΔP = 0.7 psi) test condition. Composite plots of the foregoing data are presented, herein, along with noise reduction plots and noise reduction comparison plots.

2.4.4 Test Conditions - The following test conditions were imposed on the subject shroud simulators during acoustic testing.

Composite Shroud

Ambient Condition - The shroud was capped and local ambient pressure conditions existed internally.

ΔP = 2.6 psi - A vacuum pump continuously pumped during acoustic testing creating a differential pressure of 2.6 psi. The vacuum was created in the interior of the shroud.

Aluminum Shroud

Ambient Condition - The shroud was capped and local ambient pressure conditions existed internal to the shroud.

$\Delta P = 0.7$ psi - A vacuum pump continuously pumped during acoustic exposure causing a differential pressure of 0.7 psi. The vacuum was created between the inner and outer bulkhead of the shroud.

0.2 psi Helium - Helium was continuously forced through the space between the bulkheads which displaced the air during acoustic testing.

3.0 SUMMARY OF RESULTS

The acoustic test was successfully completed with the data indicating the following variation between the ambient test condition and the various pressure conditions.

3.1 Composite Shroud Tests - A comparison of Figures 8B and 14B indicates a 1 to 3 dB increase in noise reduction for the 2.6 psi condition in the frequency range below 80 Hz. In addition, no significant change in structural response is shown from the accelerometer data, Figures 9B and 15B.

*3.2 Aluminum Shroud Tests - A review of the microphone data summarized in Figures 27B and 34B shows the changes in noise reduction for the 0.7 psi condition and the 0.2 psi Helium condition. A larger change is observed for the Helium case.

A significant change in response characteristics of the external panel is indicated from a comparison of Figures 20B and 28B due largely to the static deflection of the panel for the 0.7 psi condition.

A comparison of the response of the internal panel strain gages indicates a 16 Hz increase in the first circumferential structural resonance of the panel for the 0.7 psi condition (see Figures 21B and 29B, strain gages 6 and 8).

The structural response characteristics for the external and internal panels remained essentially the same for the 0.2 psi Helium condition (see Figures 21B, 35B and 36B).

---

* Note: Test data contained a 60 Hz noise component which obscurred structural response data and was deleted from the composite plots (Figures 28B, 29B, 35B and 36B).

Table 1B . Static Strain $\Delta P = 0.7$ psi - Aluminum Shroud

Panel	Strain Gage No.	Total* Static Strain (μ s)
External	1	399
	2	-1447
	3	28.2
	4	2362
Internal	5	-44
	6	58
	7	-50
	8	165

* + Tension
- Compression

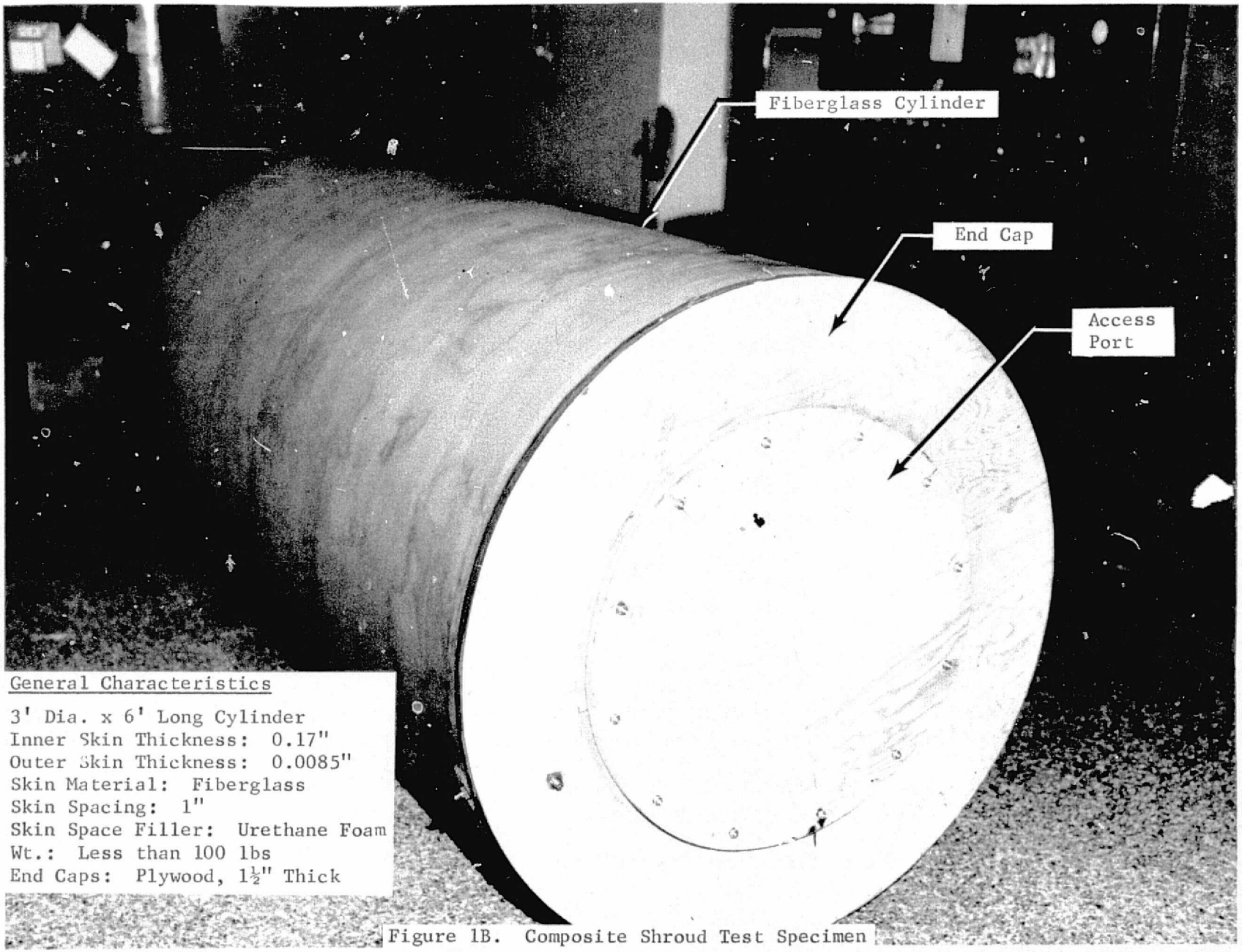

General Characteristics

3' Dia. x 6' Long Cylinder
Inner Skin Thickness: 0.17"
Outer Skin Thickness: 0.0085"
Skin Material: Fiberglass
Skin Spacing: 1"
Skin Space Filler: Urethane Foam
Wt.: Less than 100 lbs
End Caps: Plywood, 1½" Thick

Figure 1B. Composite Shroud Test Specimen

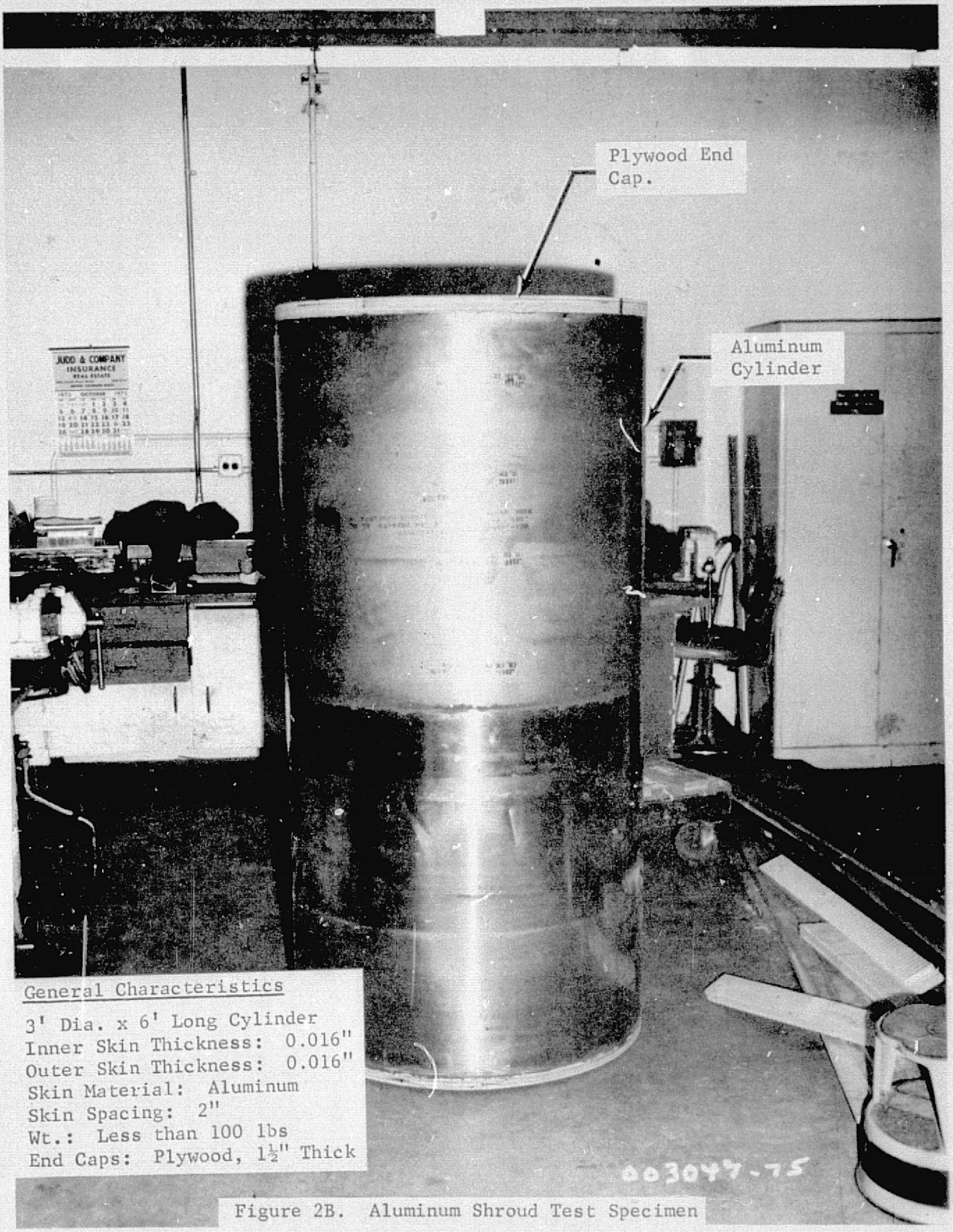

Figure 2B. Aluminum Shroud Test Specimen

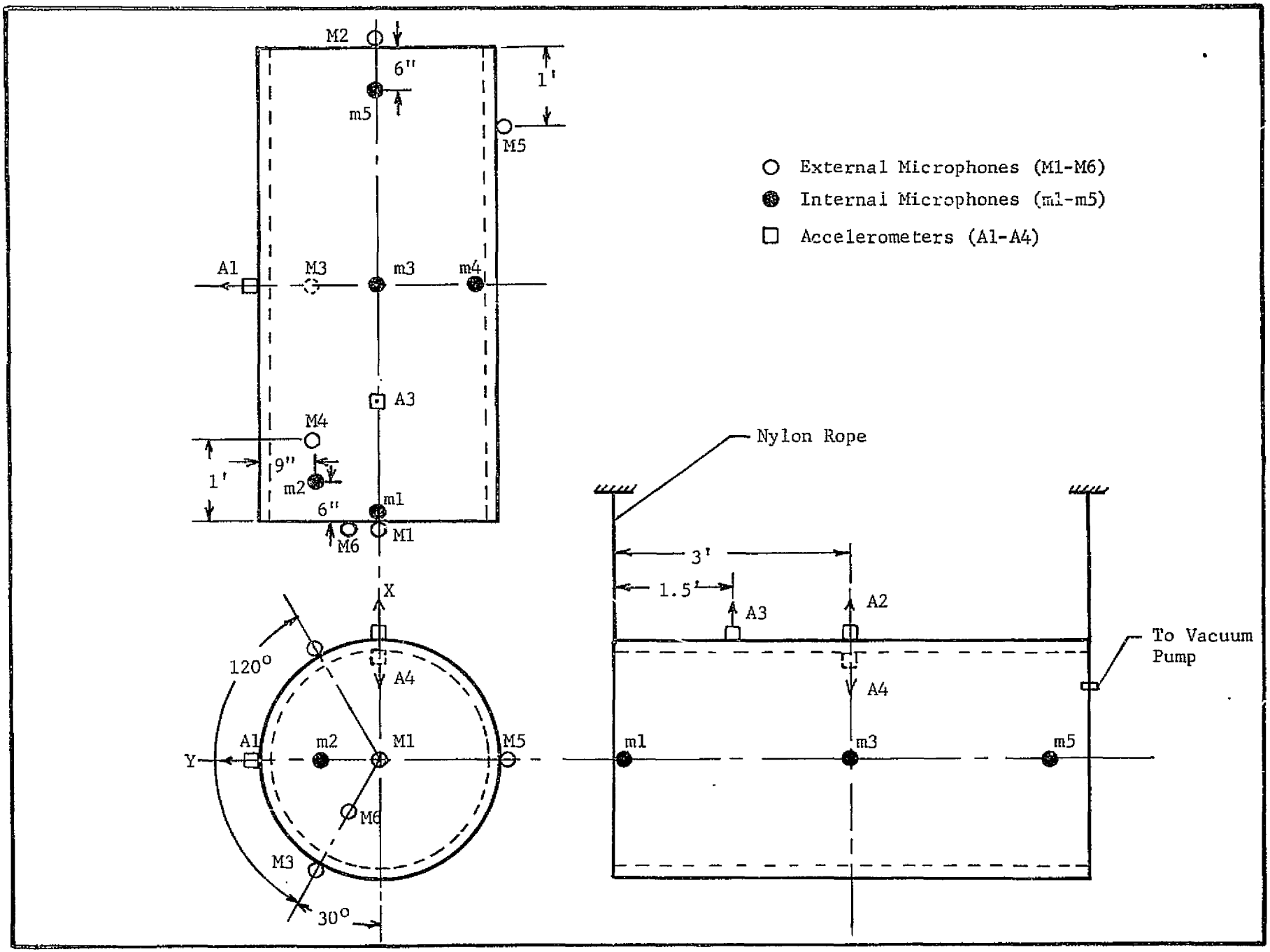

Figure 3B. Composite Shroud Test Setup

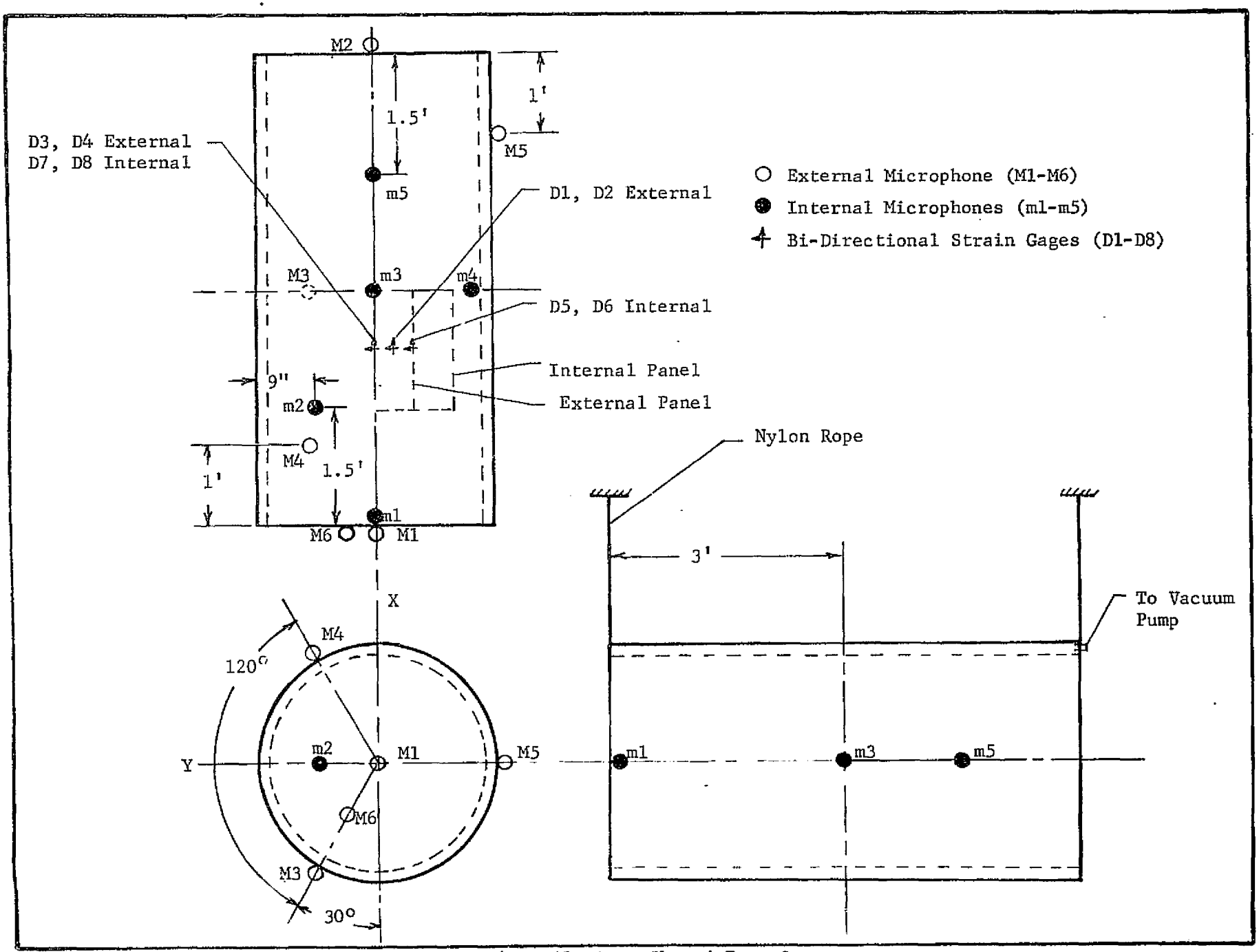

Figure 4B. Aluminum Shroud Test Setup

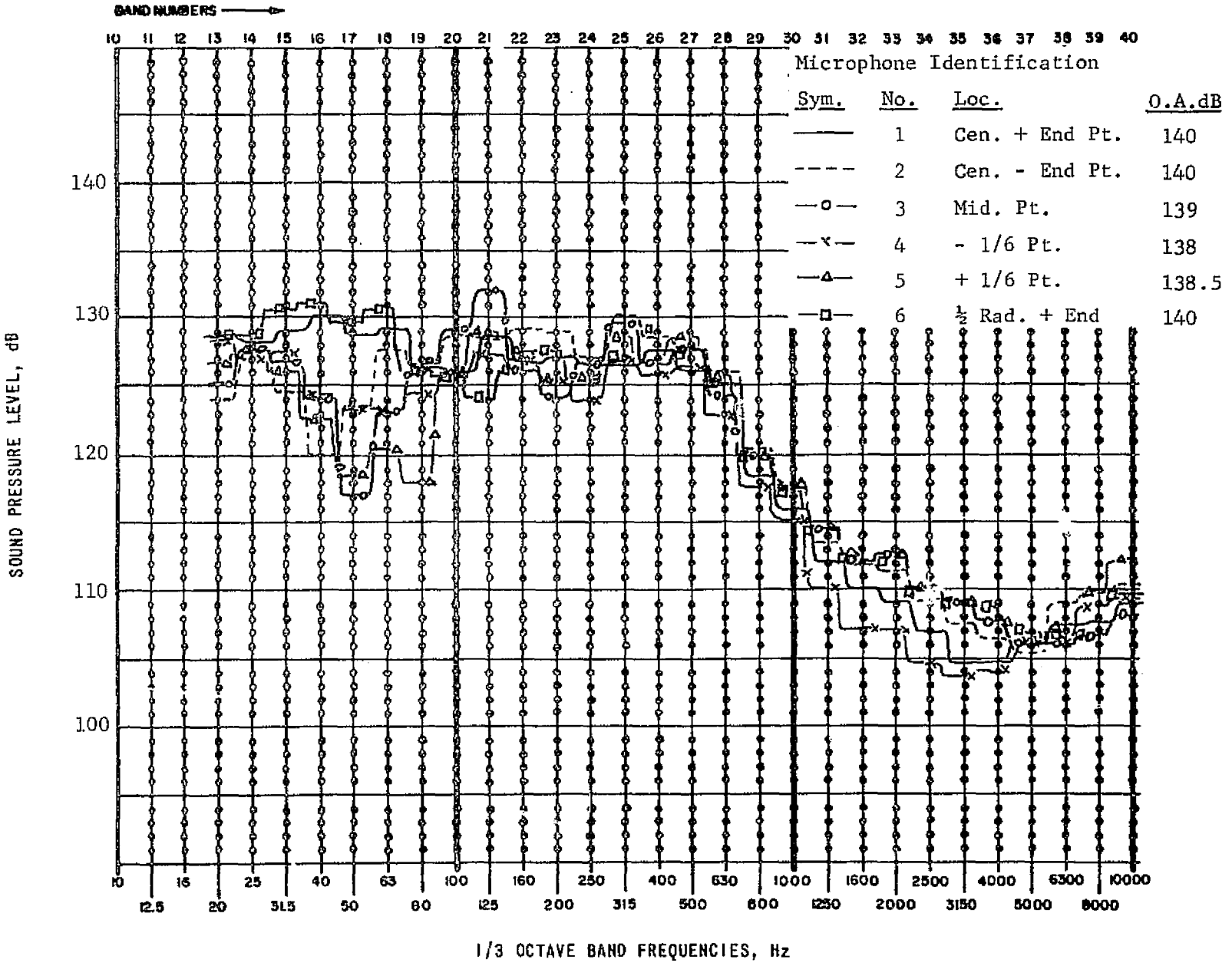

Figure 5B . Composite External Microphone Data - Composite Shroud, Ambient Condition

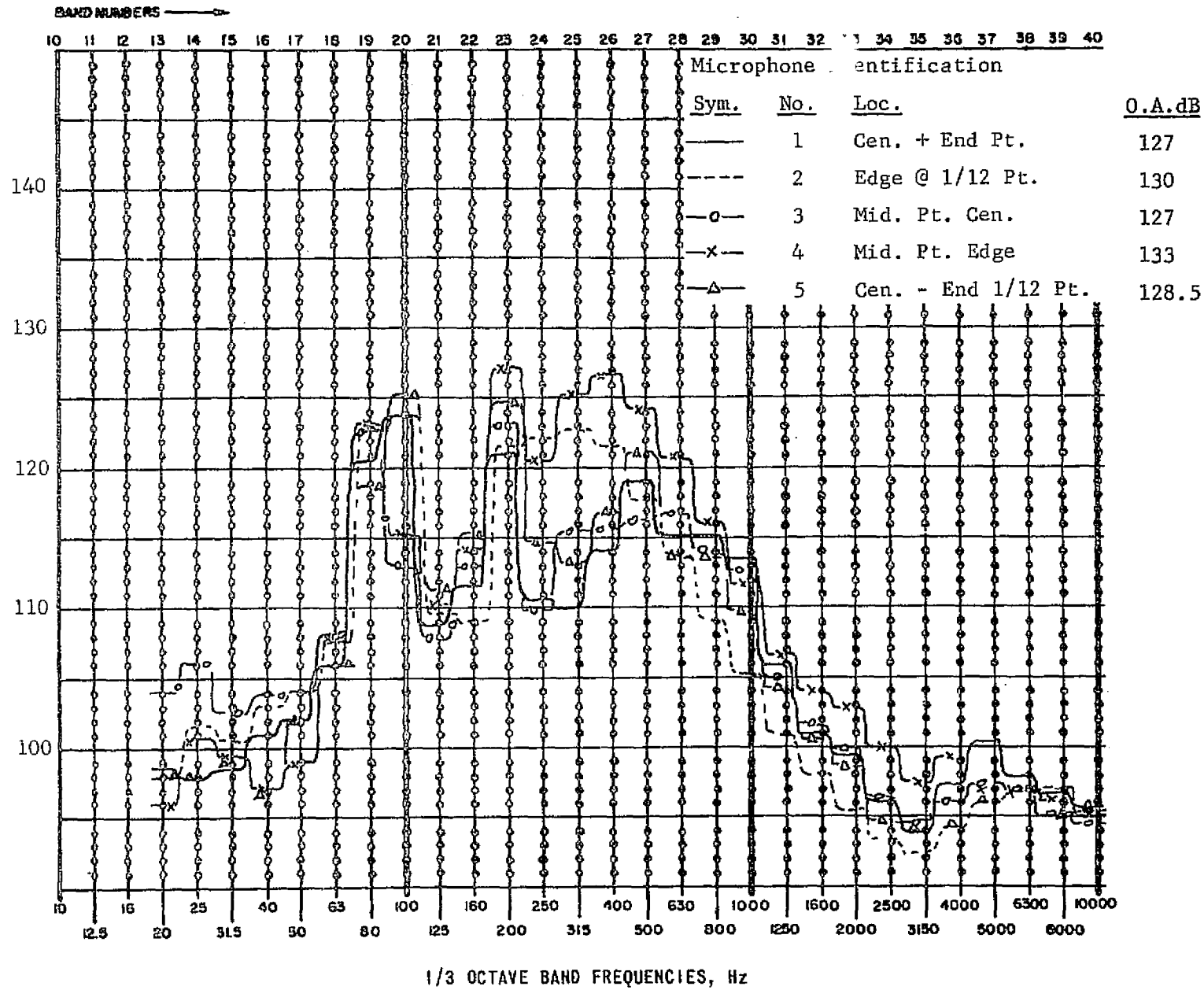

Figure 6B . Composite Internal Microphone Data - Composite Shroud, Ambient Condition

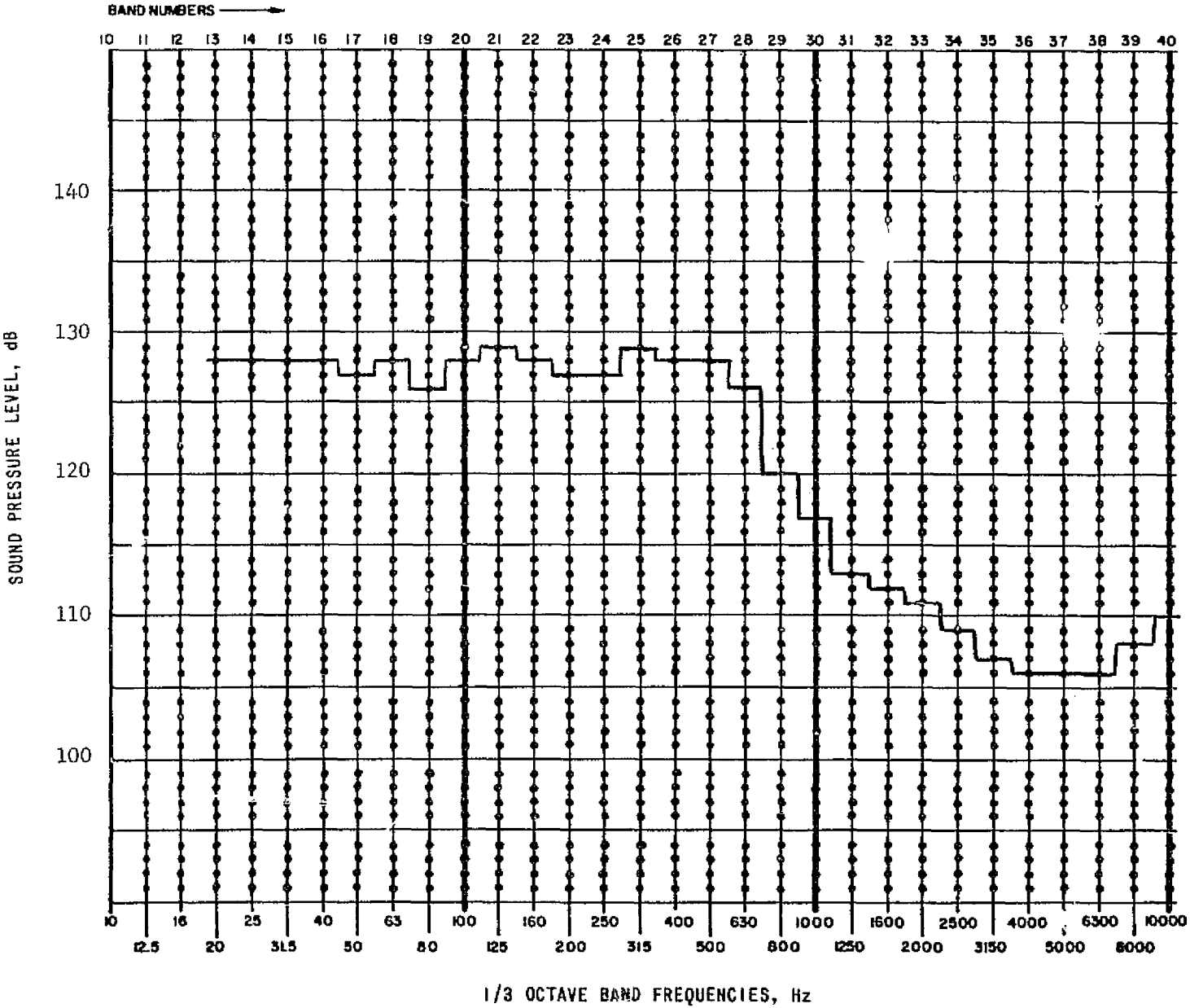

Figure 7B. Average of External Microphone Data - Composite Shroud, Ambient Condition, 140 dB

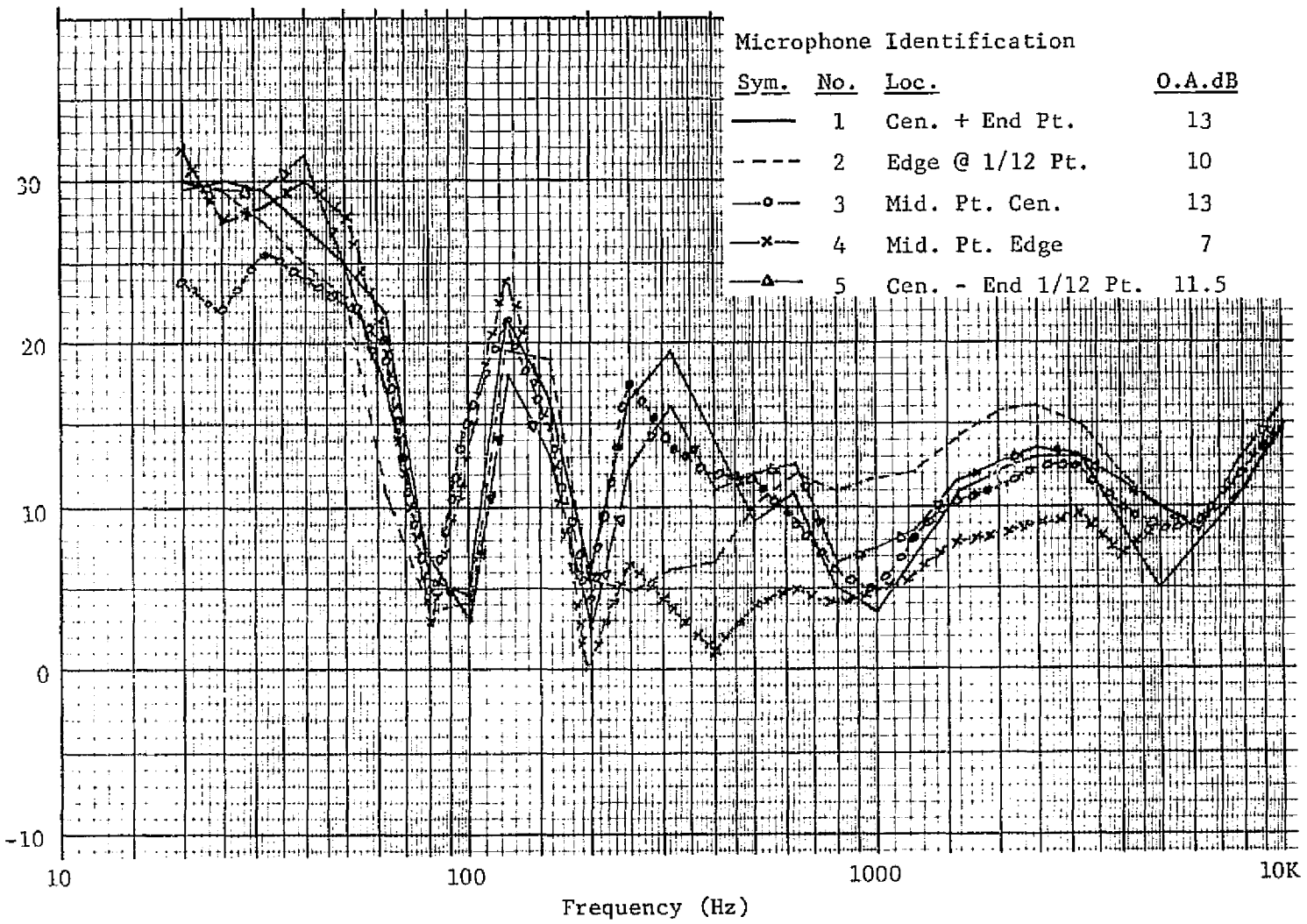

Figure 8B . Noise Reduction for Composite Shroud - Ambient Condition

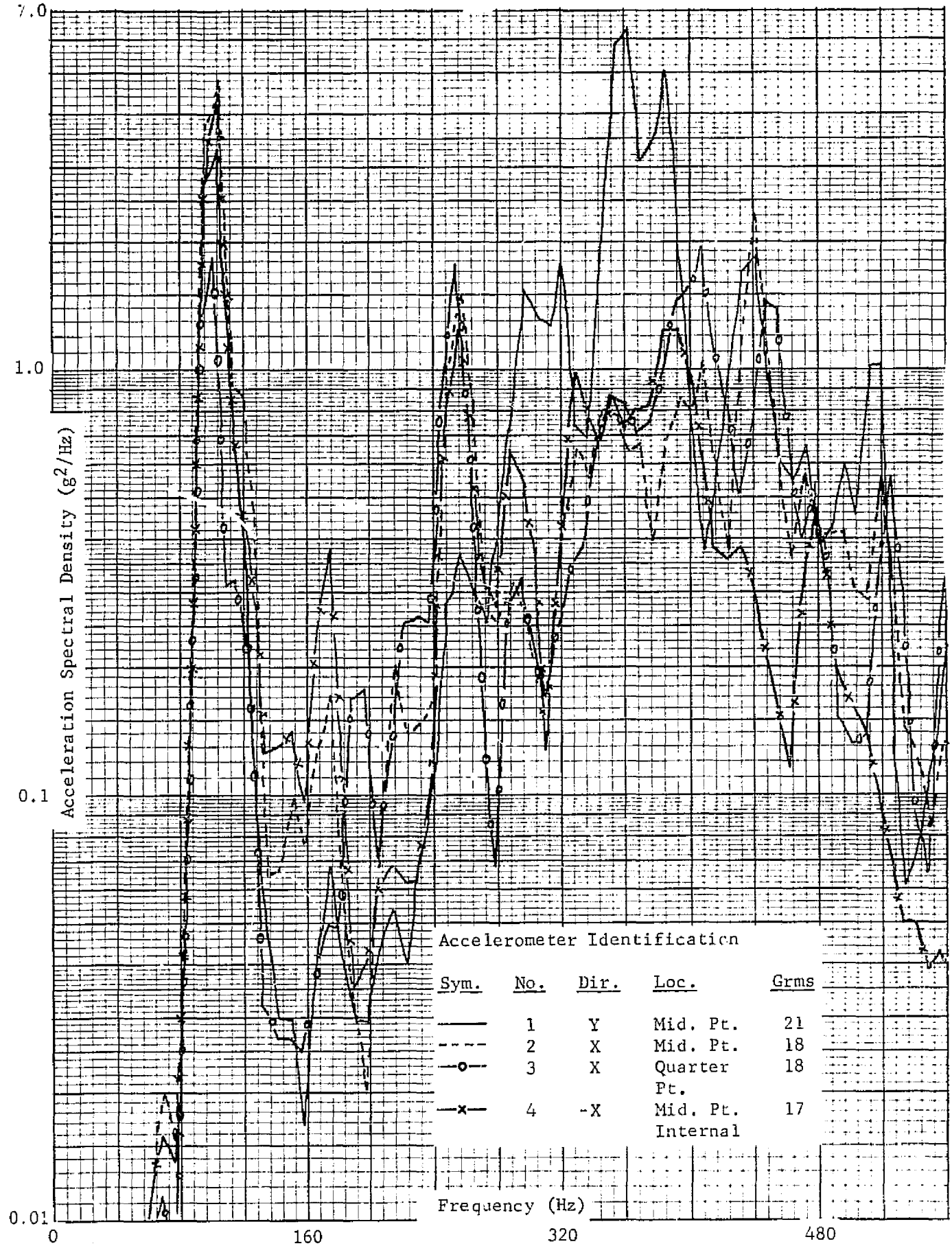

Figure 9B. Composite Accelerometer Data - Composite Shroud, Ambient Condition

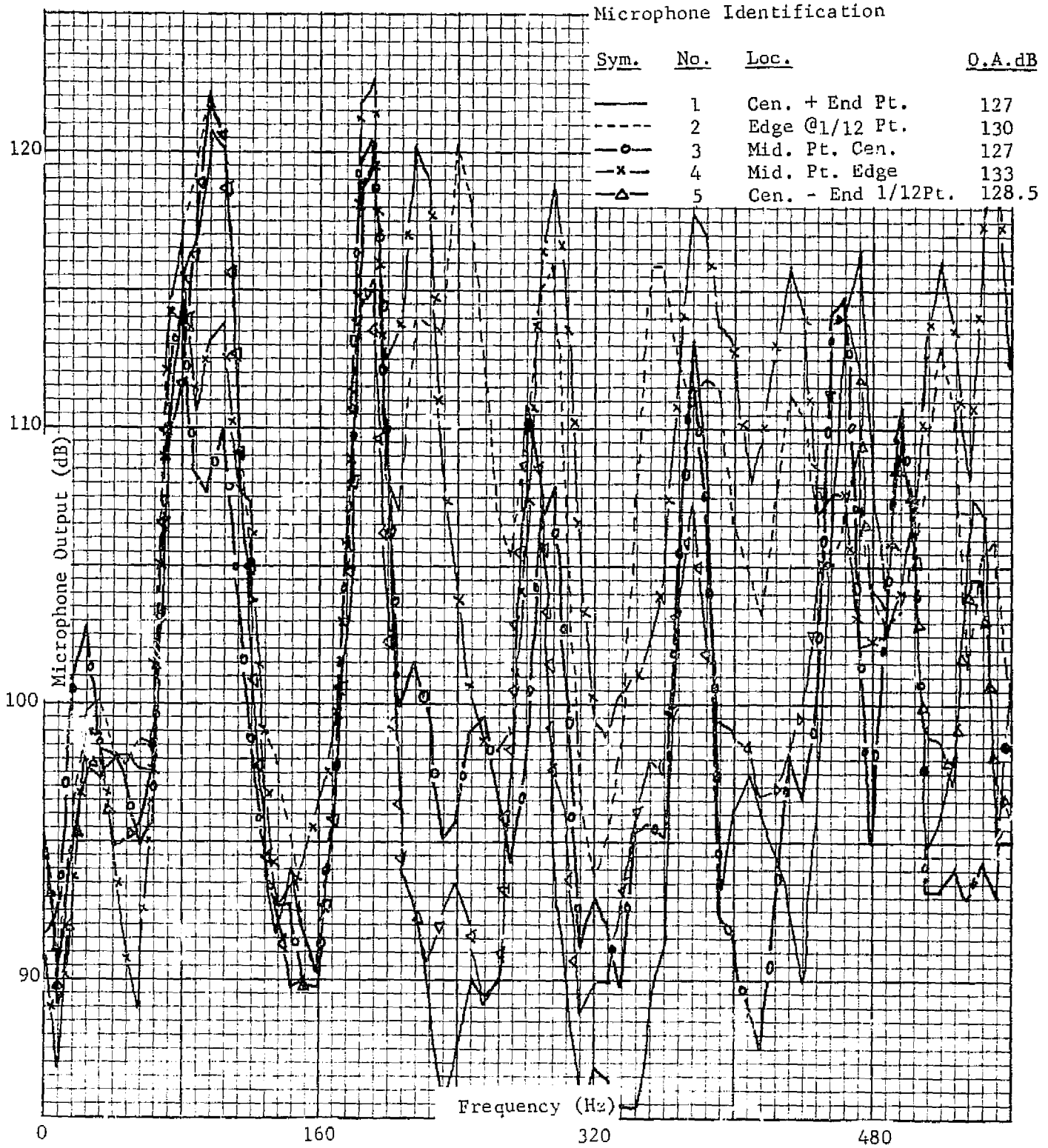

Figure10B. Composite Internal Microphone Data - Composite Shroud, Ambient Condition

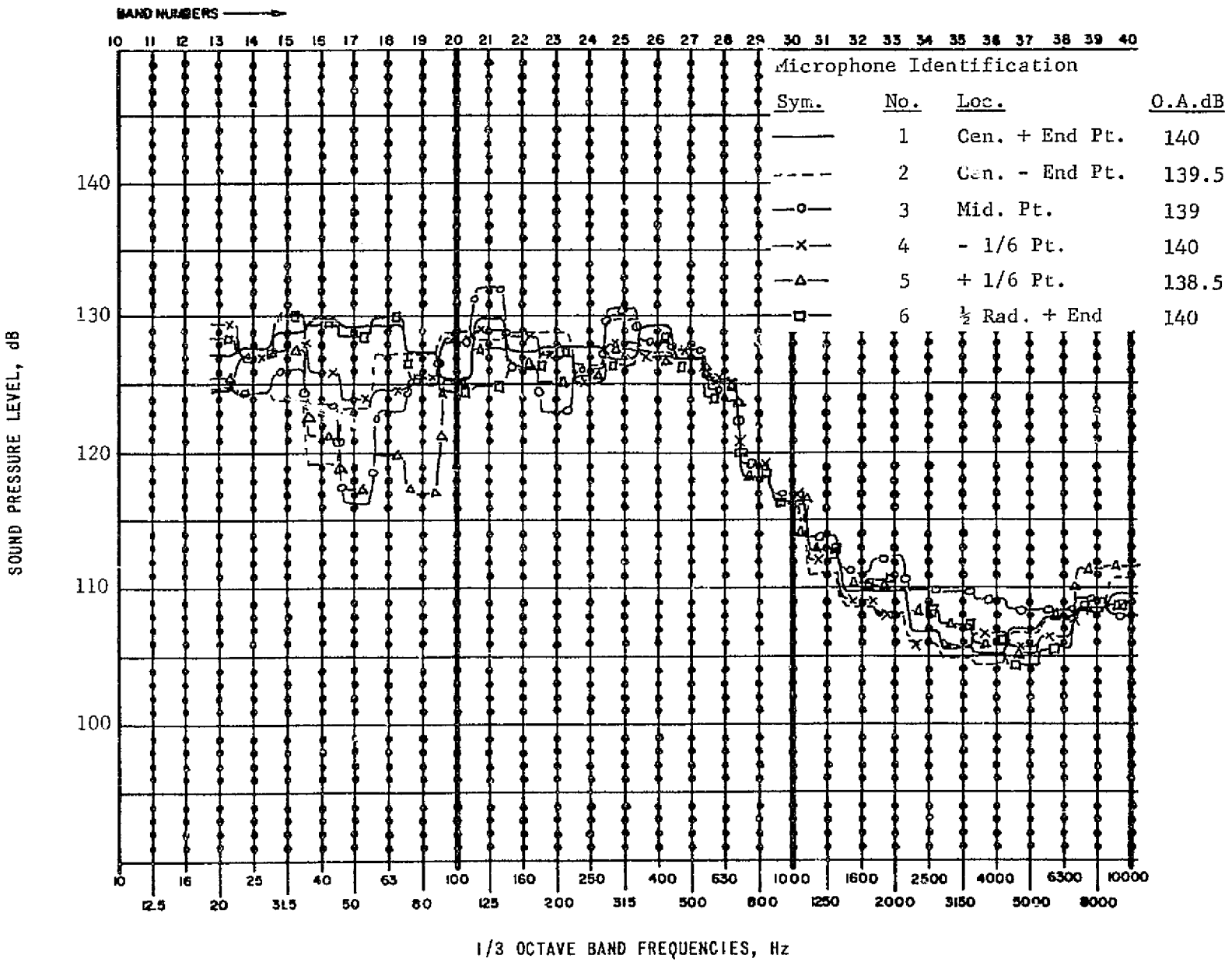

Figure 11B. Composite External Microphone Data - Composite Shroud, $\Delta P = 2.6$ psi

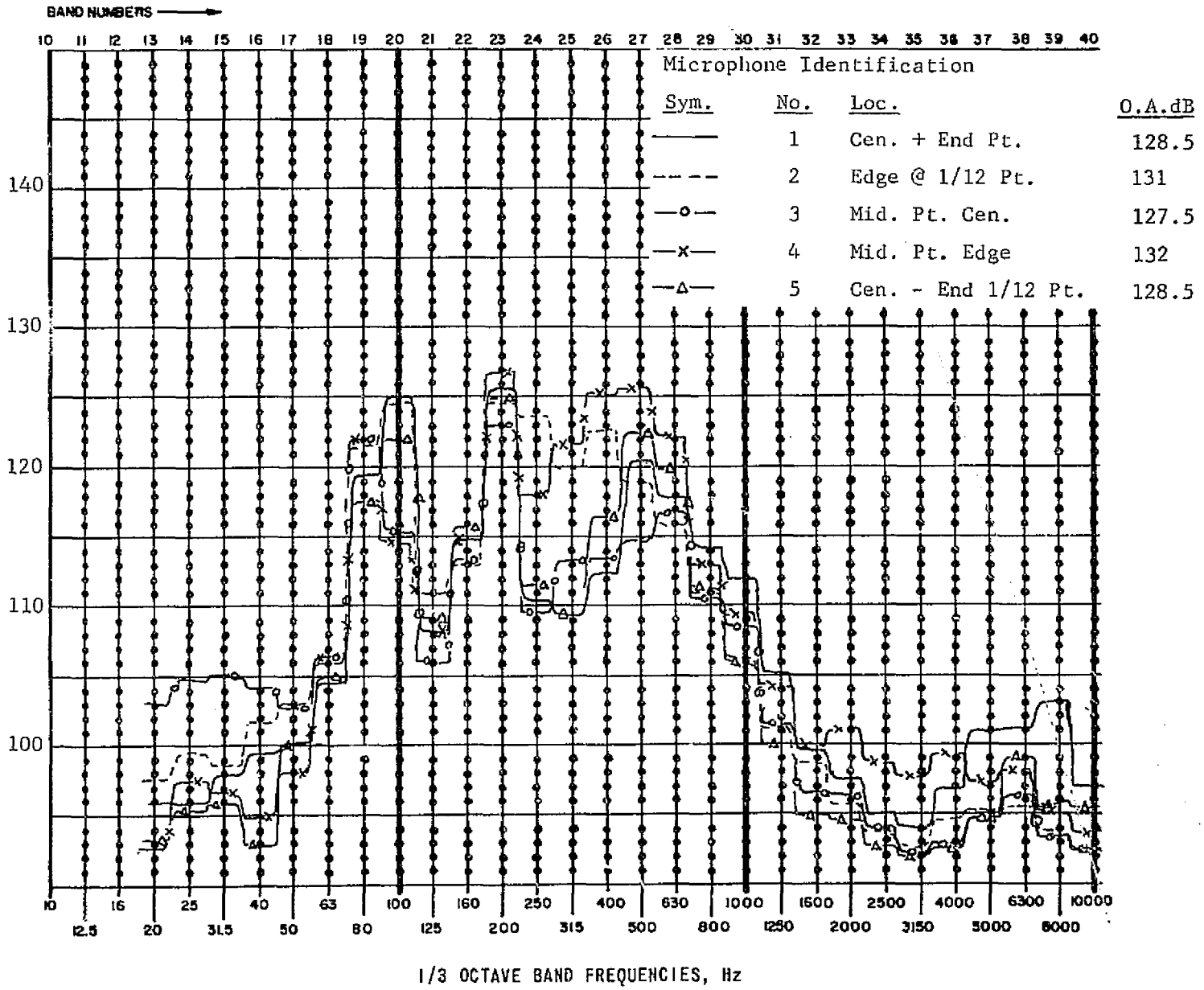

Figure 12B. Composite Internal Microphone Data - Composite Shroud, $\Delta P = 2.6$ psi

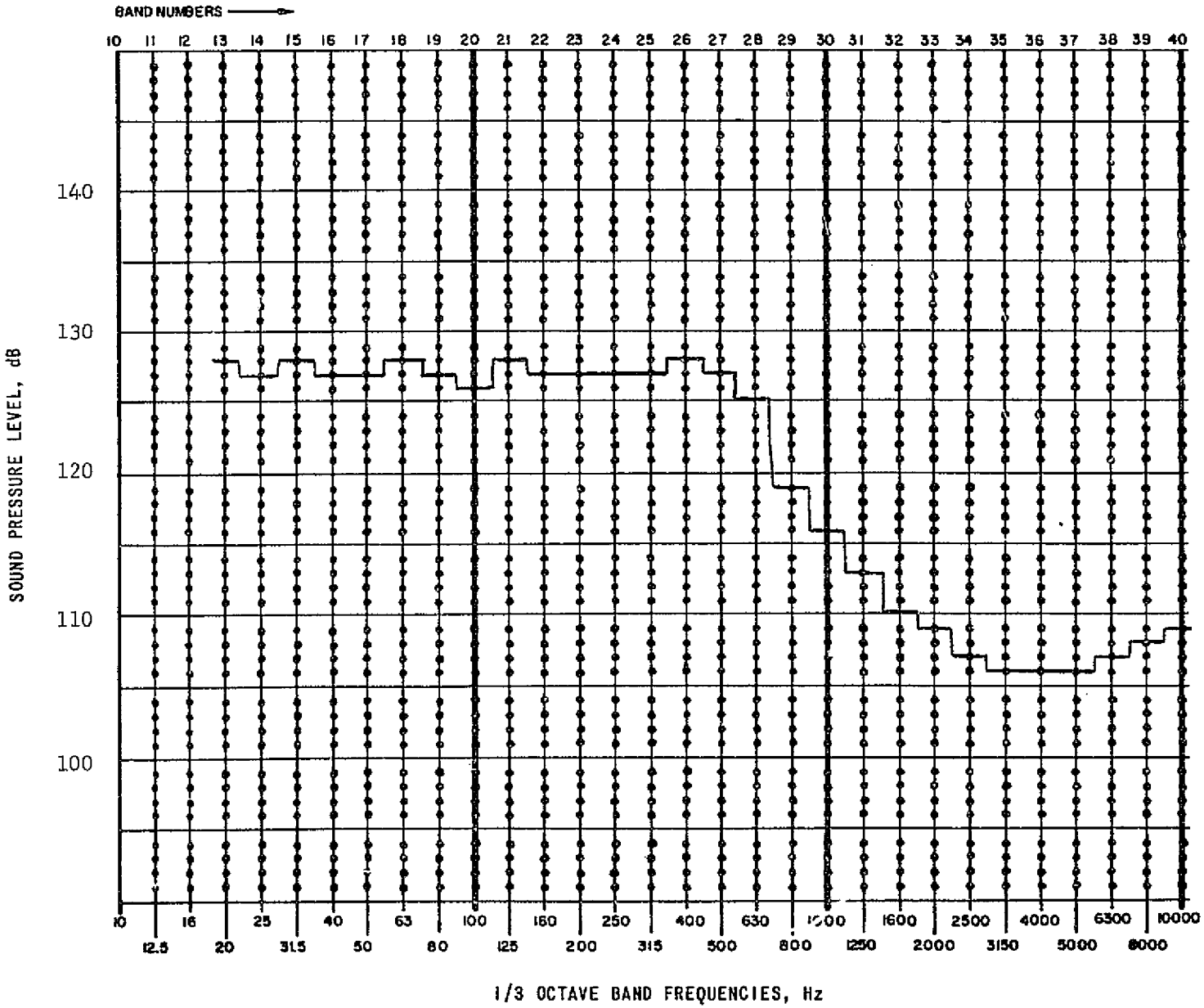

Figure 13B. Average of External Microphone Data - Composite Shroud, $\Delta P = 2.6$ psi, 140 dB Overall

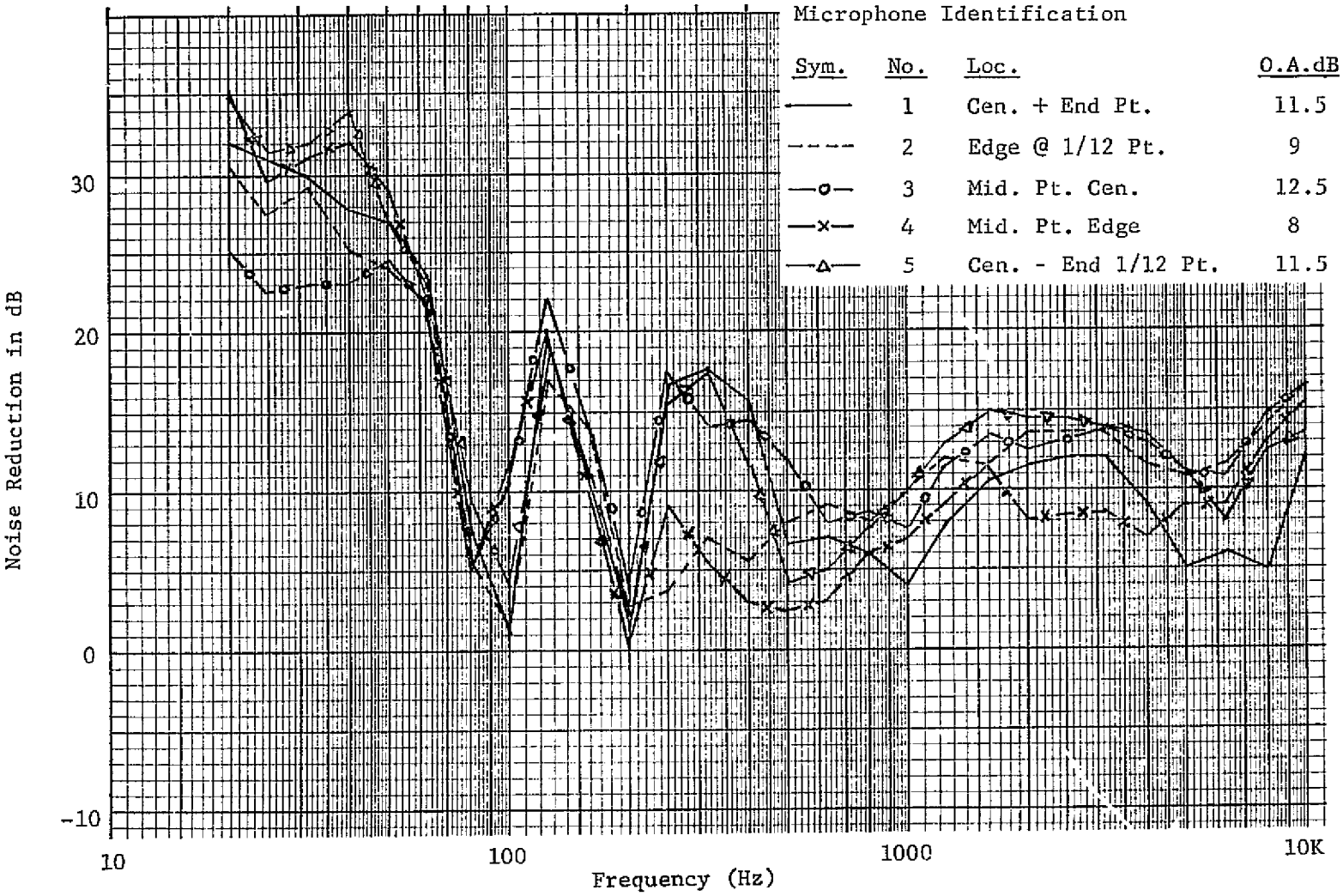

Figure 14B. Noise Reduction for Composite Shroud - $\Delta P = 2.6$ p.s.i.

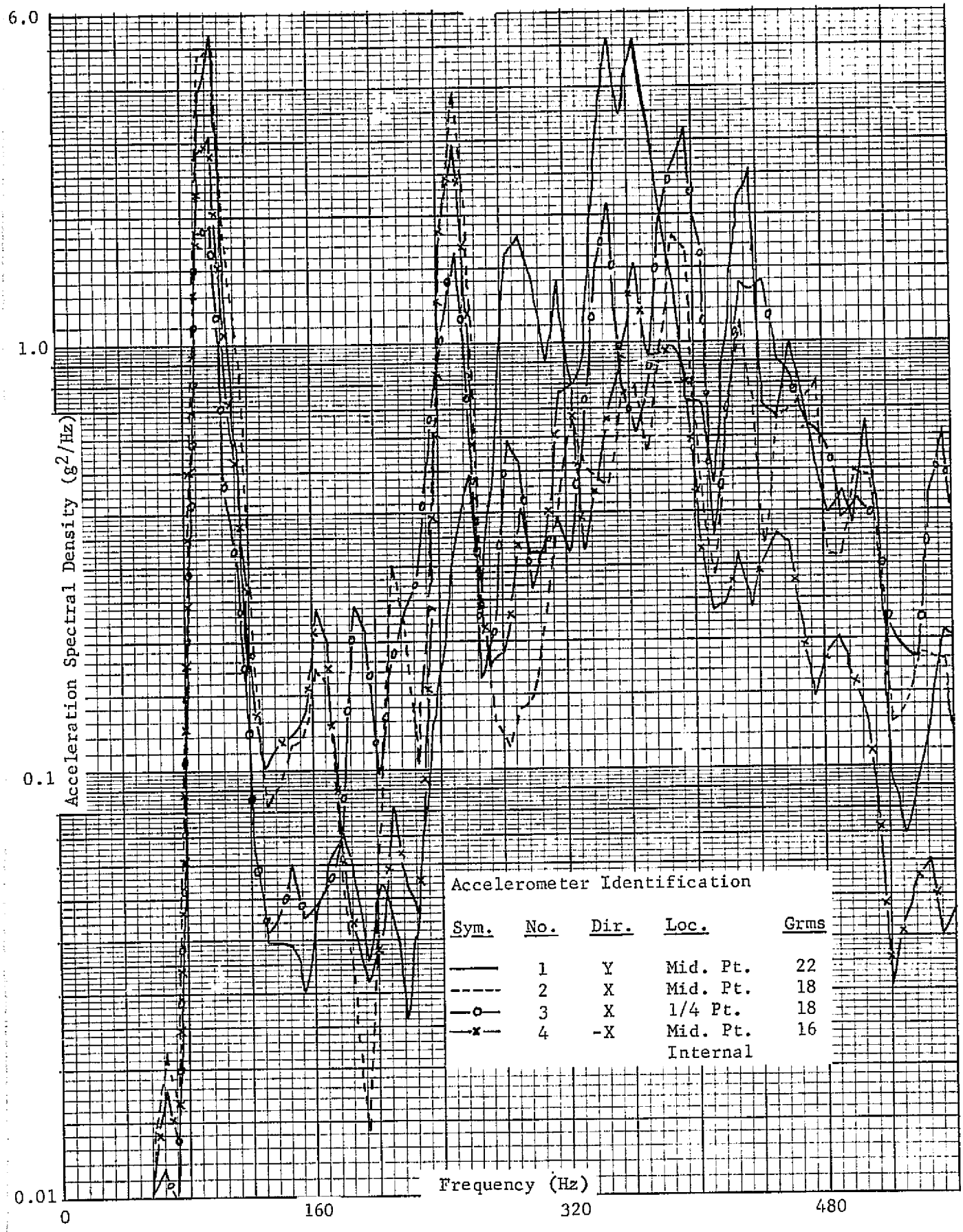

Figure 15B. Composite Accelerometer Data, Composite Shroud, ΔP = 2.6 psi

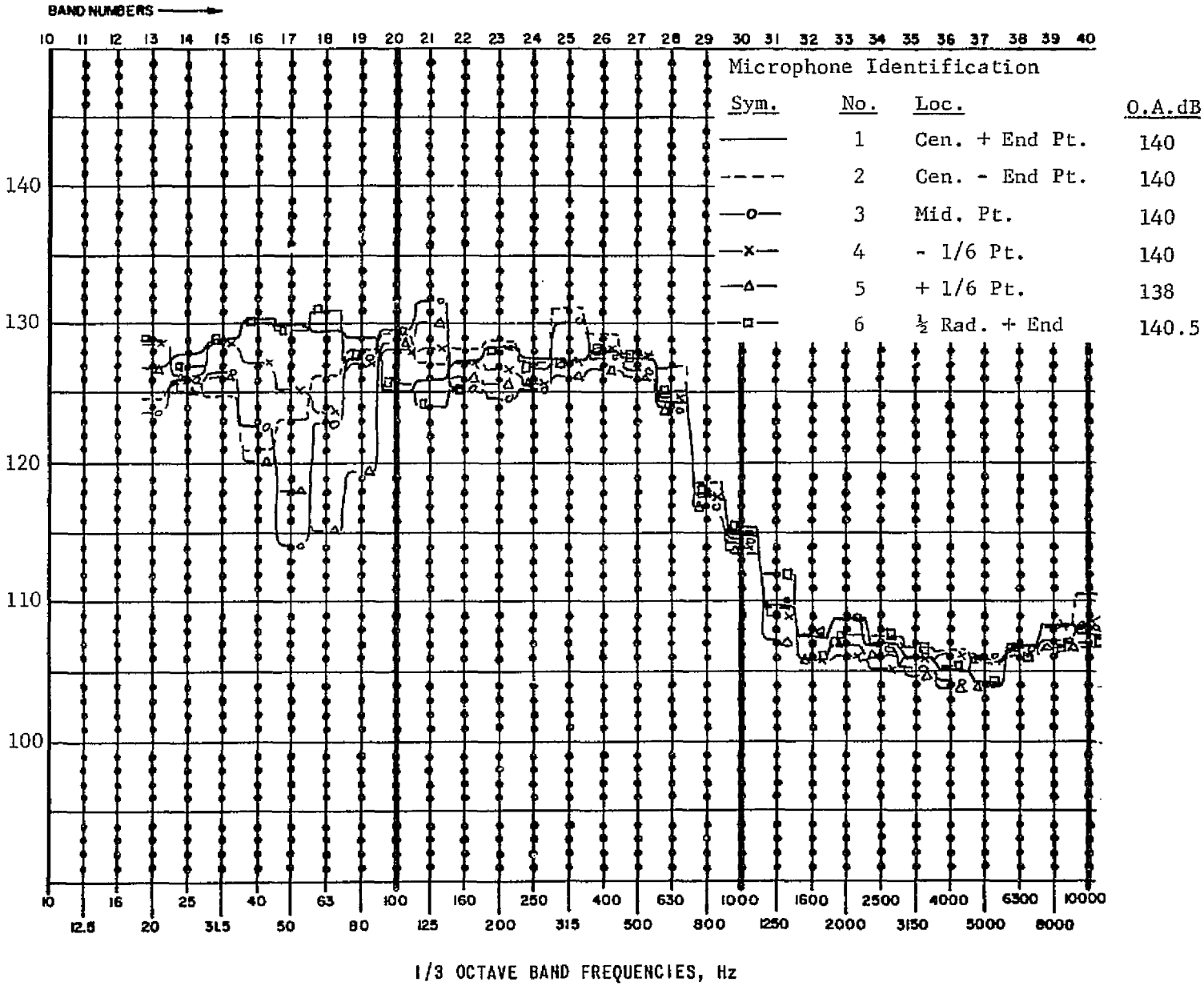

Figure 16B. Composite External Microphone Data - Aluminum Shroud, Ambient Condition

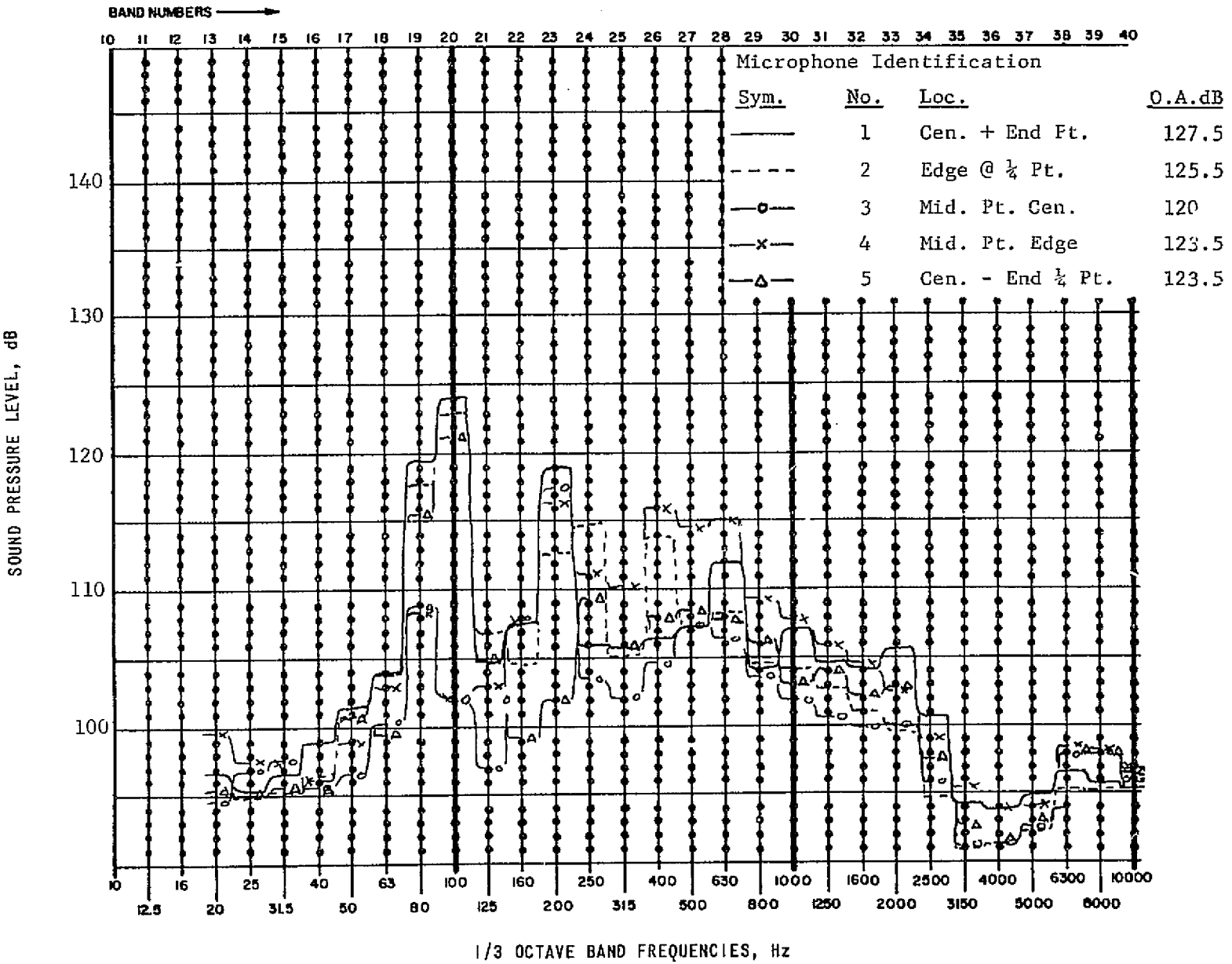

Figure 17B. Composite Internal Microphone Data - Aluminum Shroud, Ambient Condition

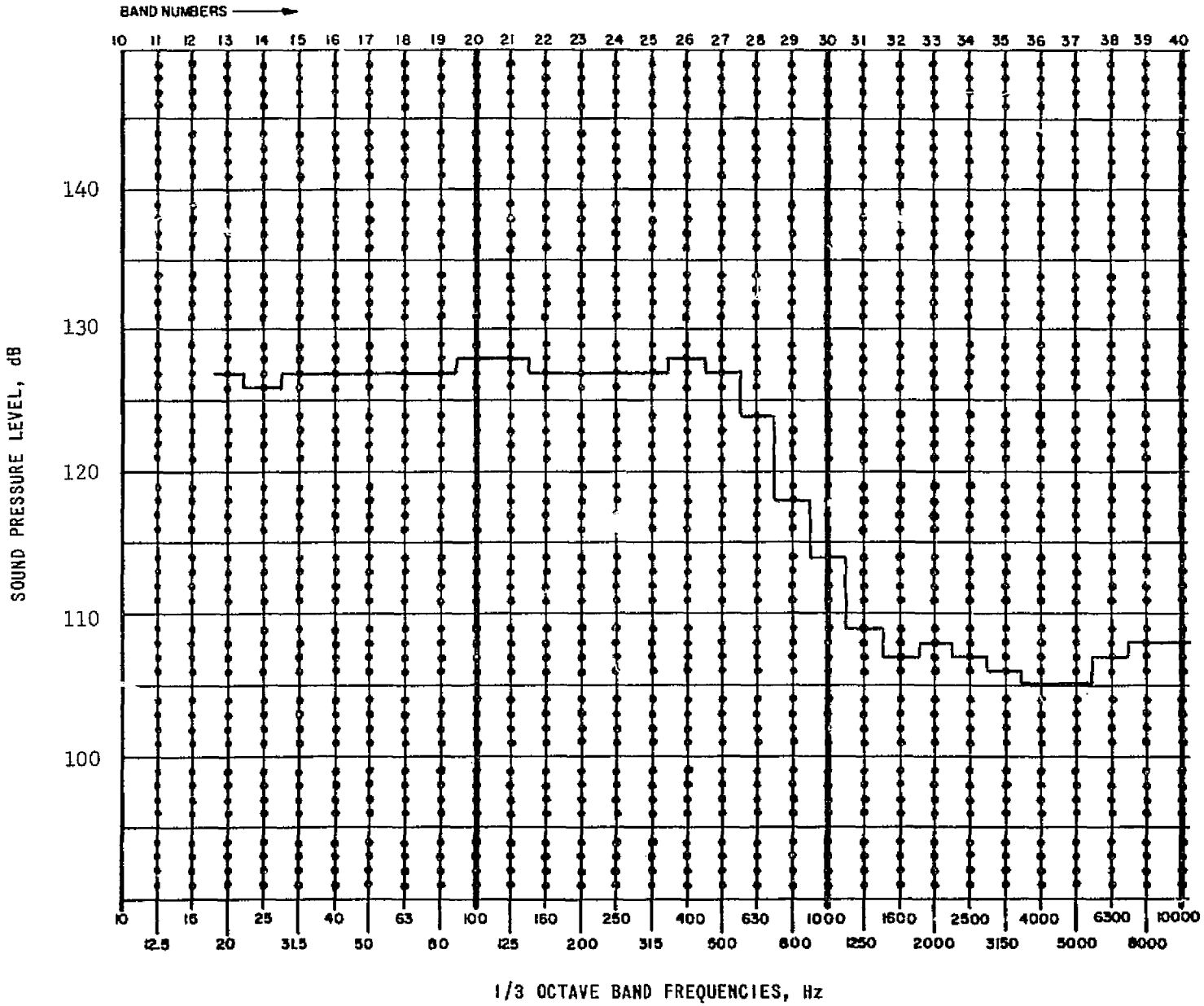

Figure 18B. Average of External Microphone Data - Aluminum Shroud, Ambient Condition, 140 dB Overall

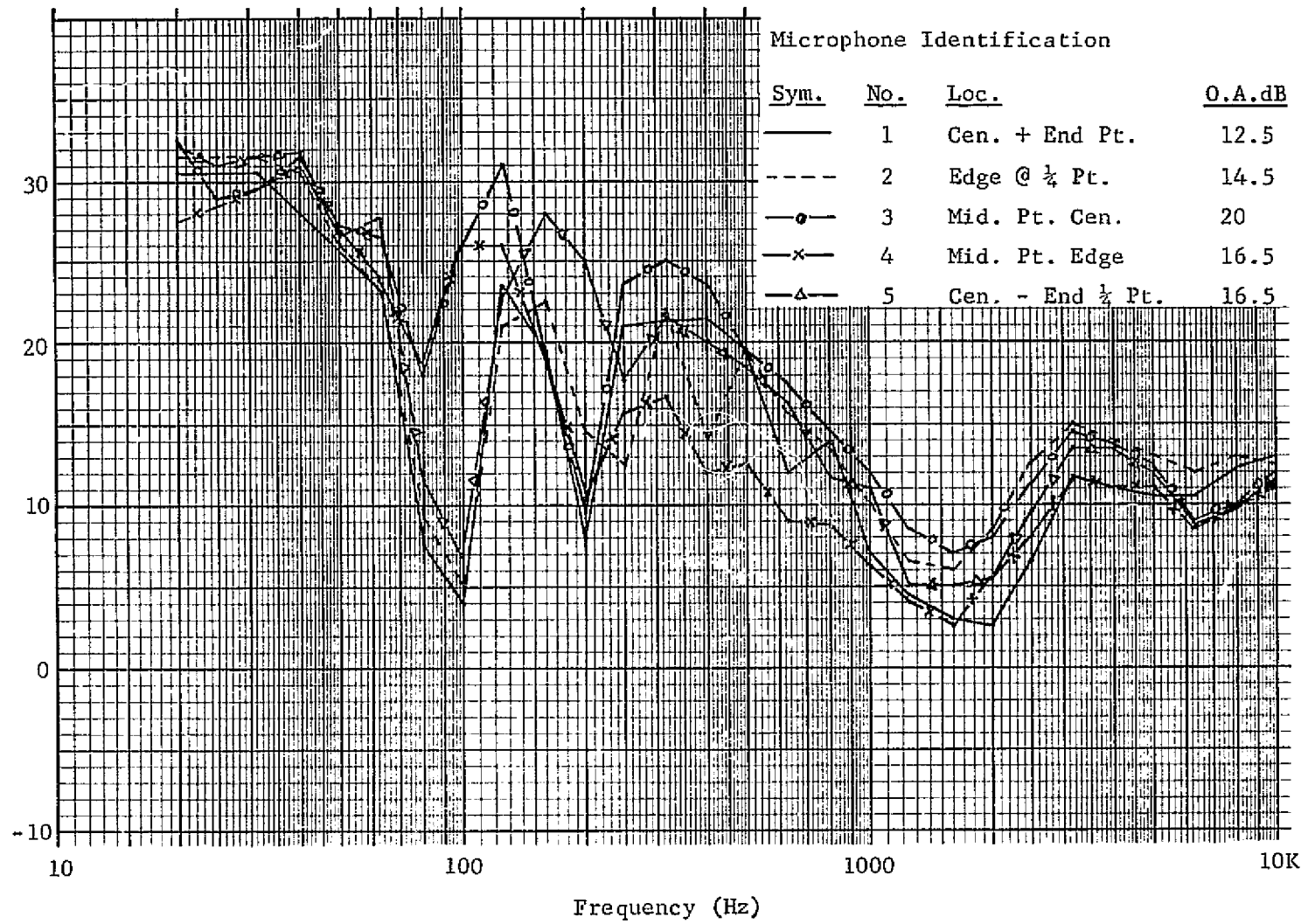

Figure 19B. Noise Reduction for Aluminum Shroud - Ambient Condition

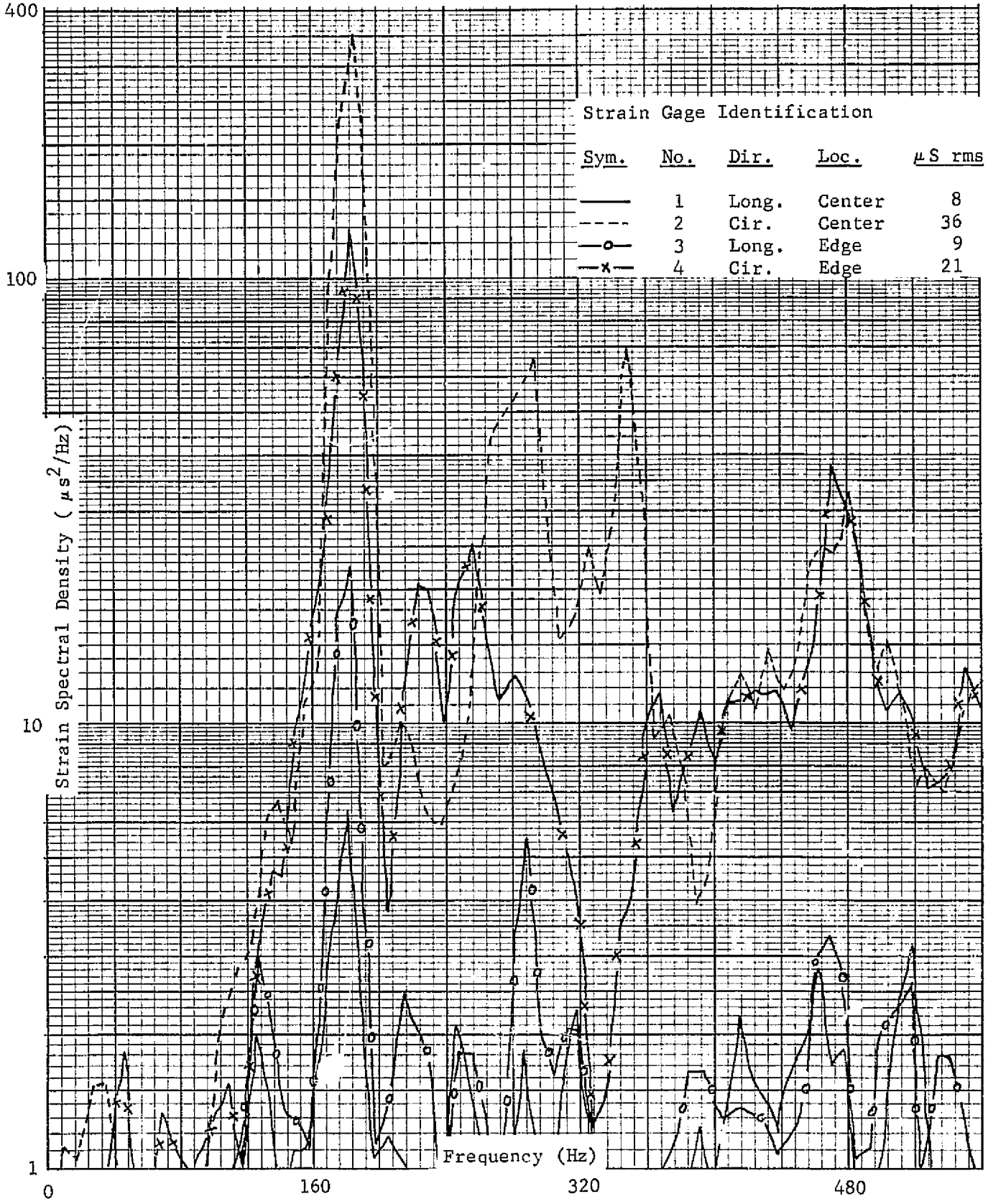

Figure 20B. Composite Strain Gage Data - Aluminum Shroud, Ambient Condition, External Panel

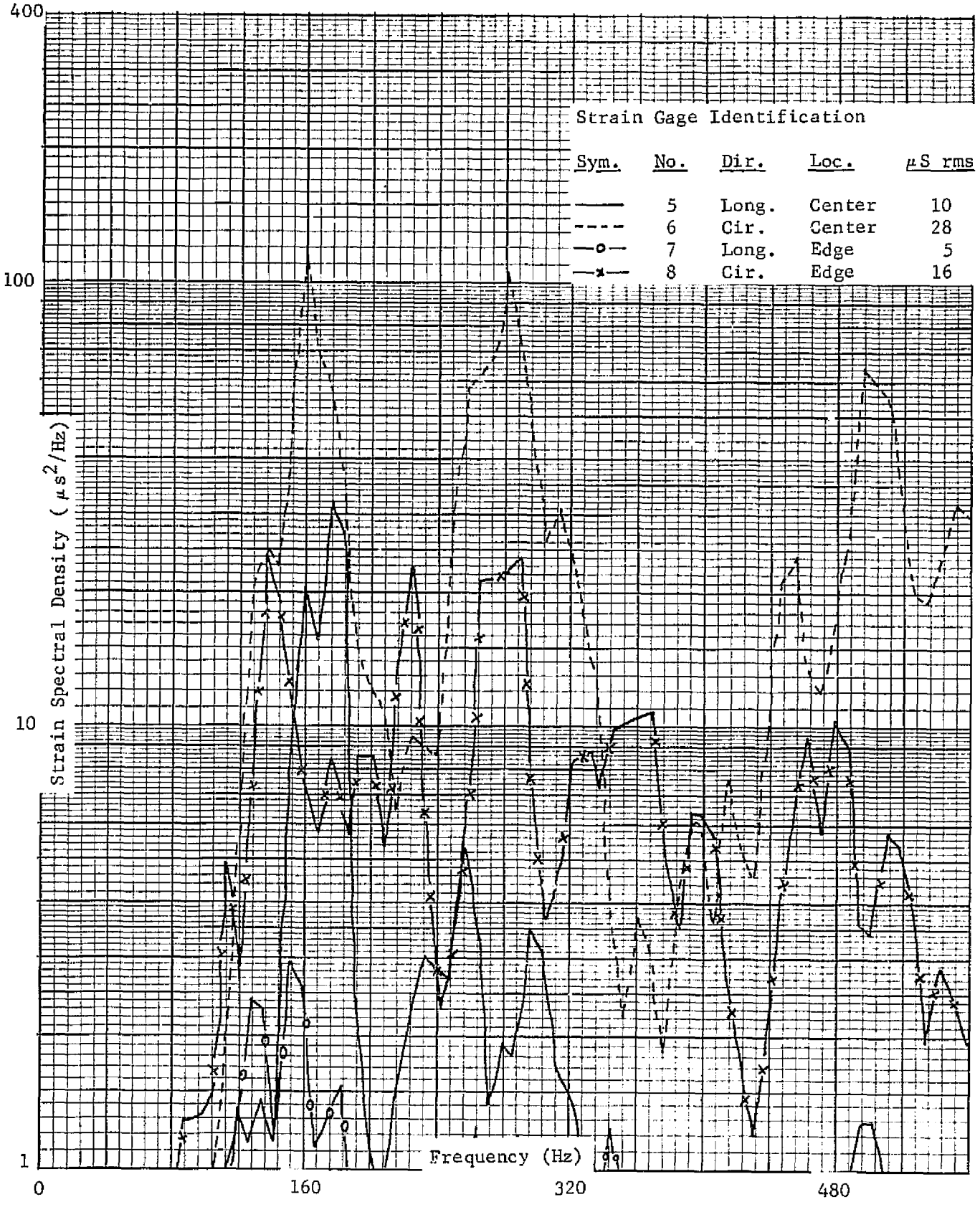

Figure 21B. Composite Strain Gage Data - Aluminum Shroud, Ambient Condition, Internal Panel

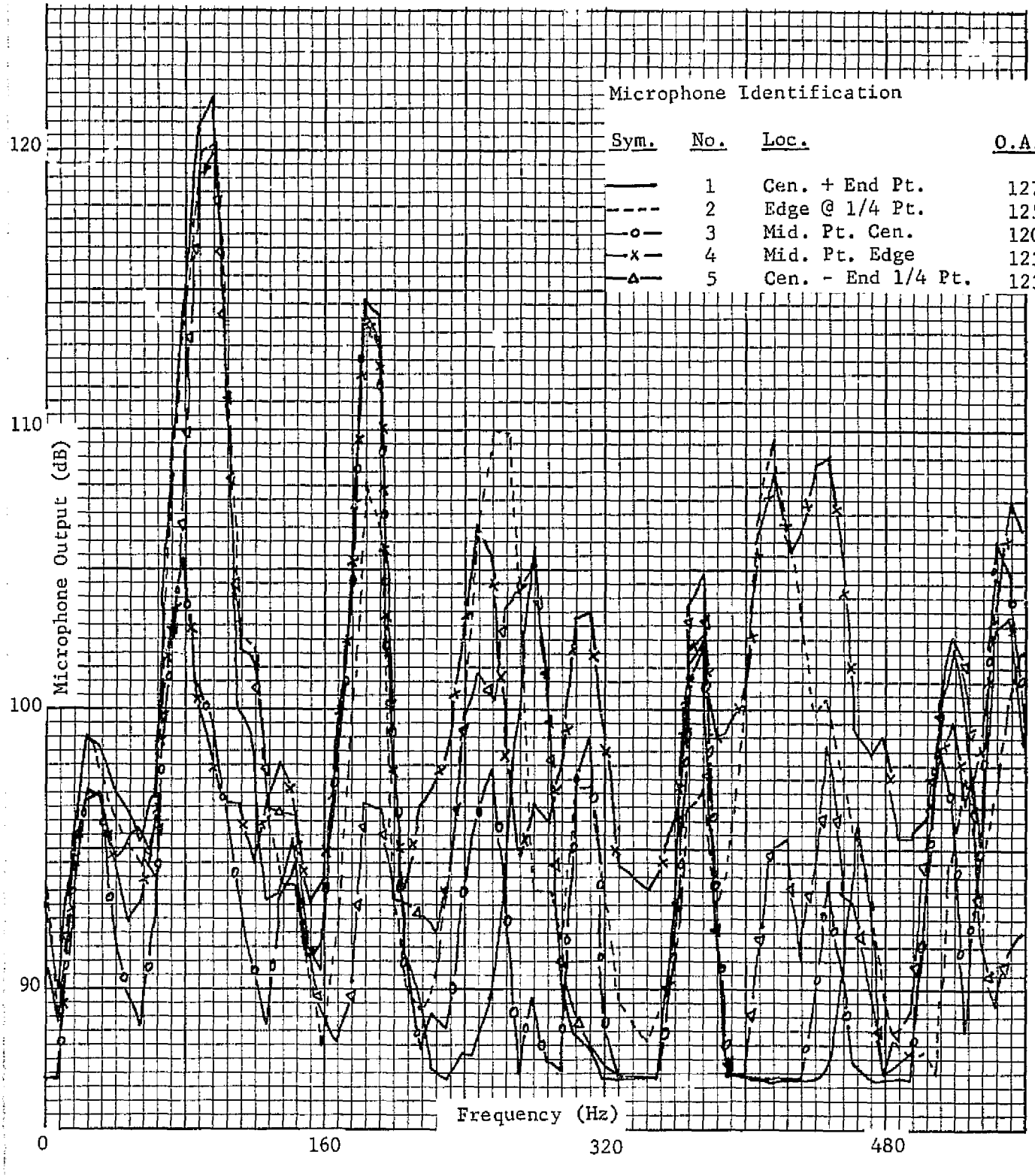

Figure 22B. Composite Internal Microphone Data - Aluminum Shroud, Ambient Condition

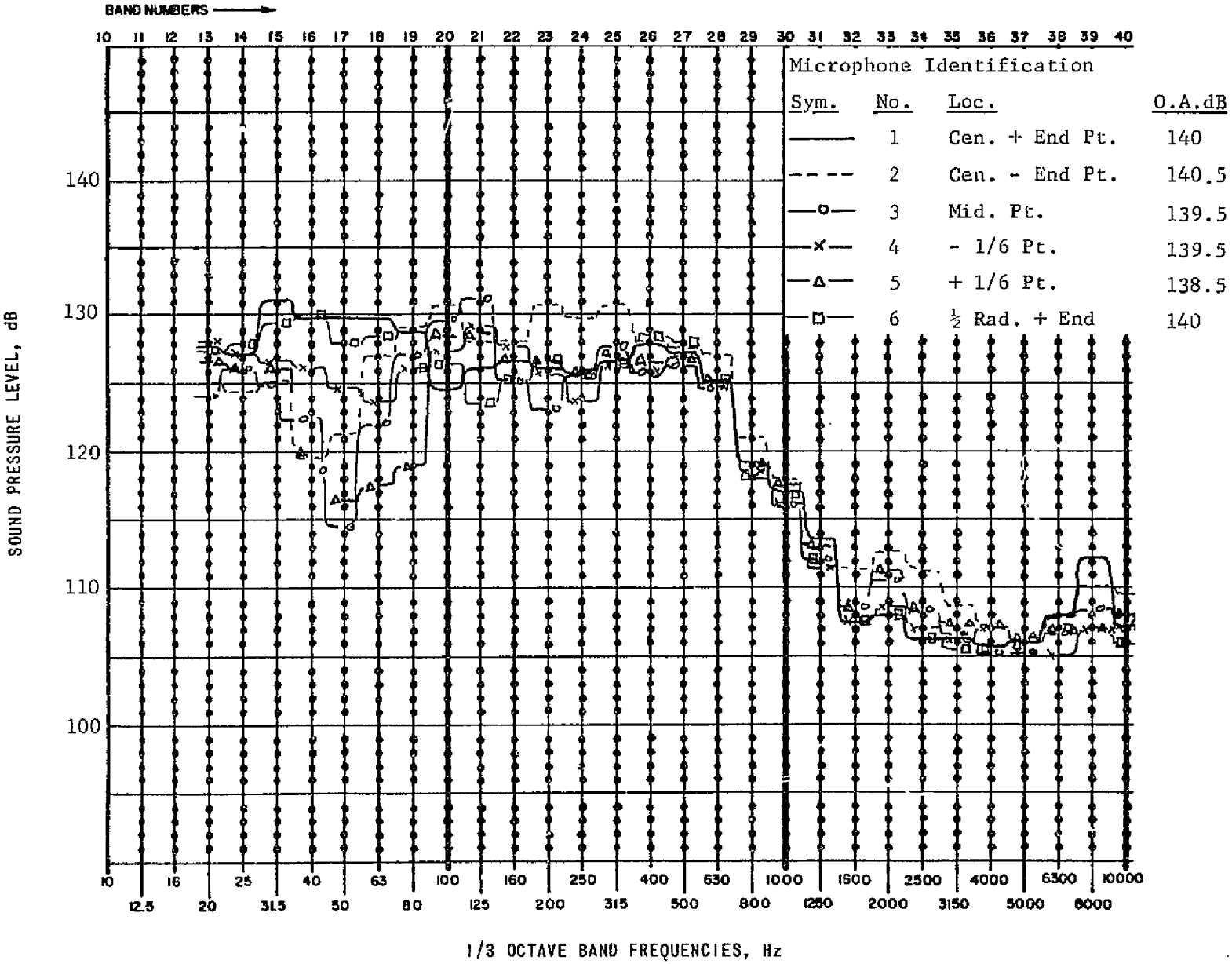

Figure 23B . Composite External Microphone Data - Aluminum Shroud, $\Delta P = 0.7$ psi

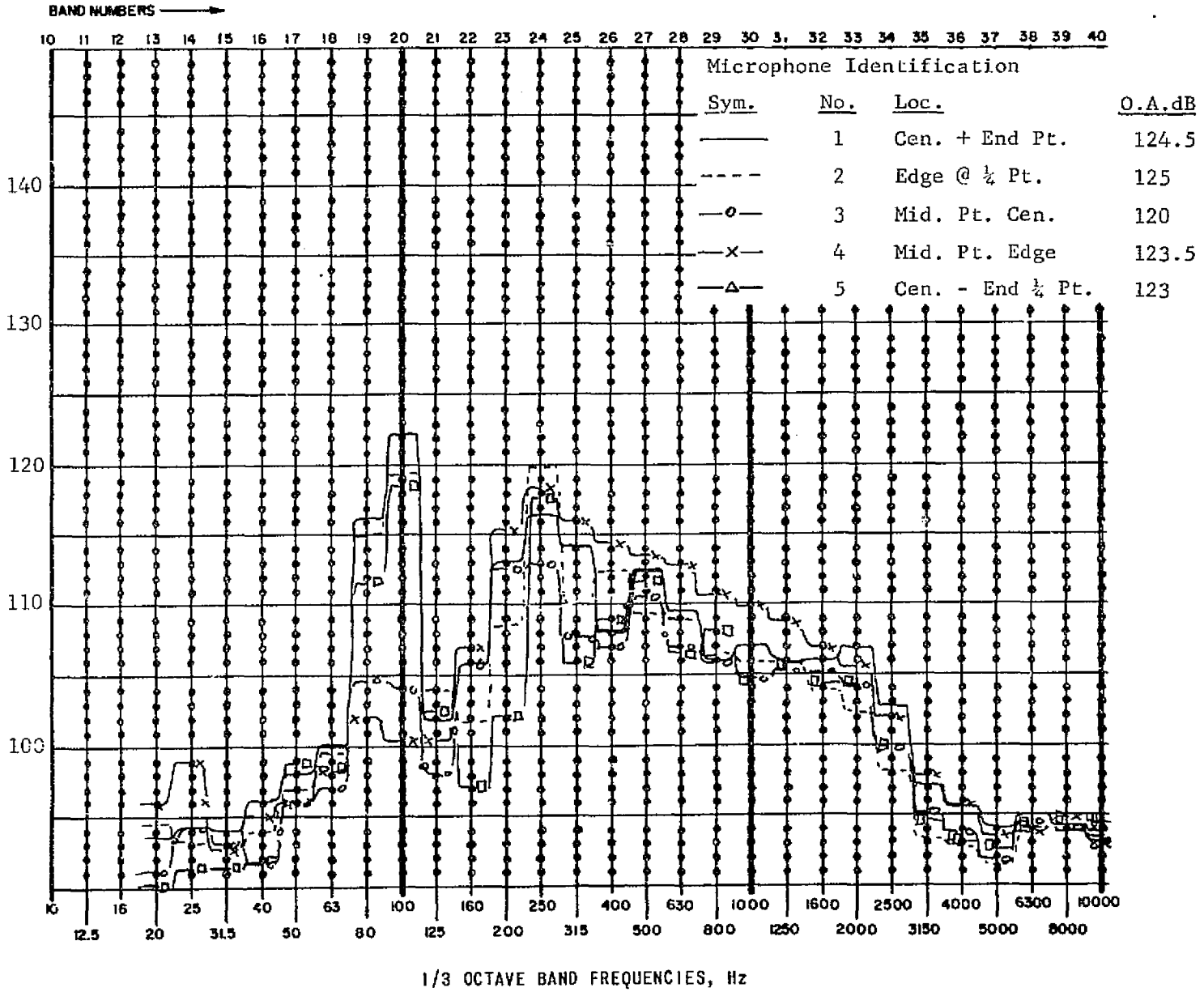

Figure 24B. Composite Internal Microphore Data - Aluminum Shroud, $\Delta P = 0.7$ psi

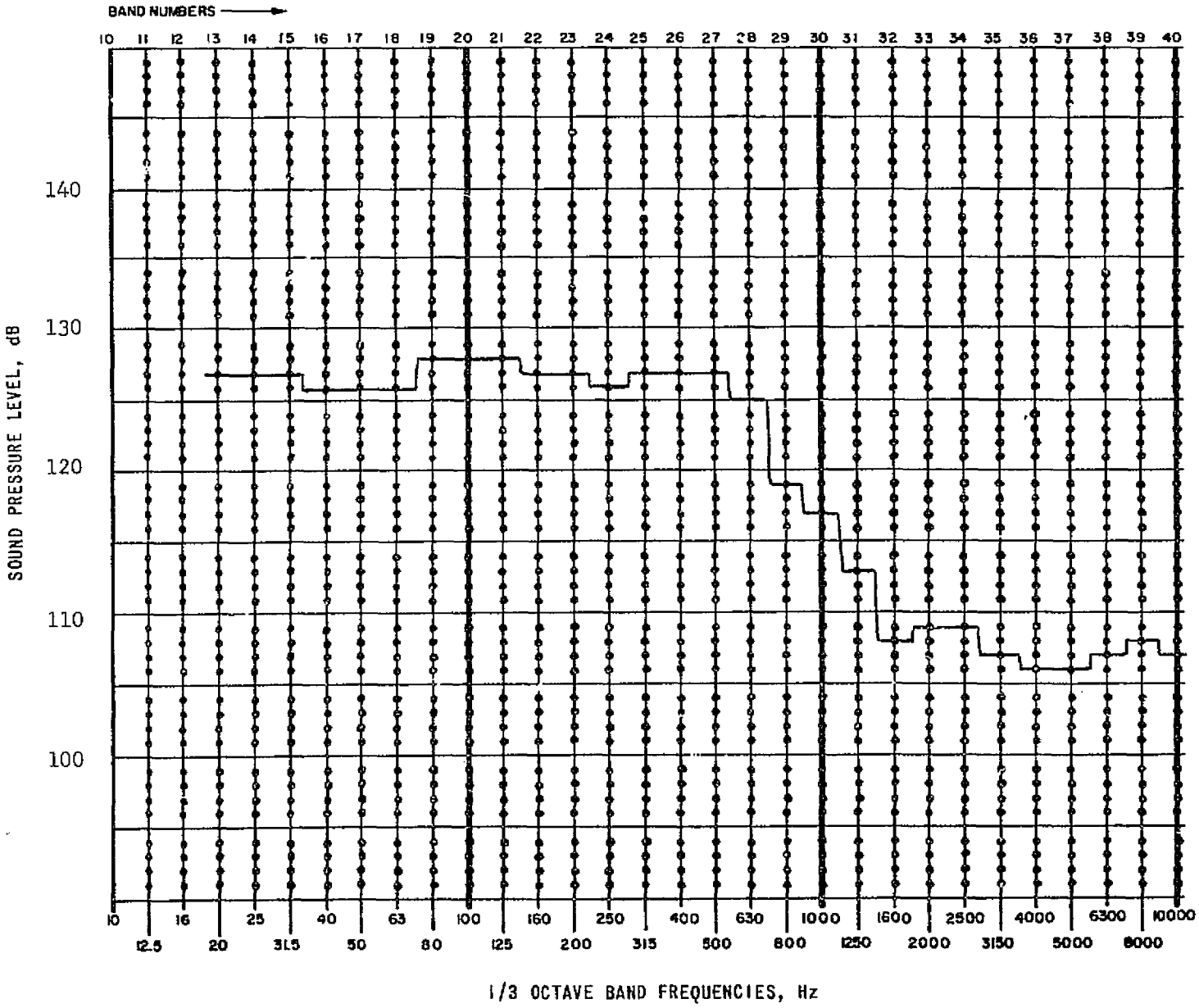

Figure 25B. Average of External Microphone Data - Aluminum Shroud, ΔP = 0.7 psi, 140 dB Overall

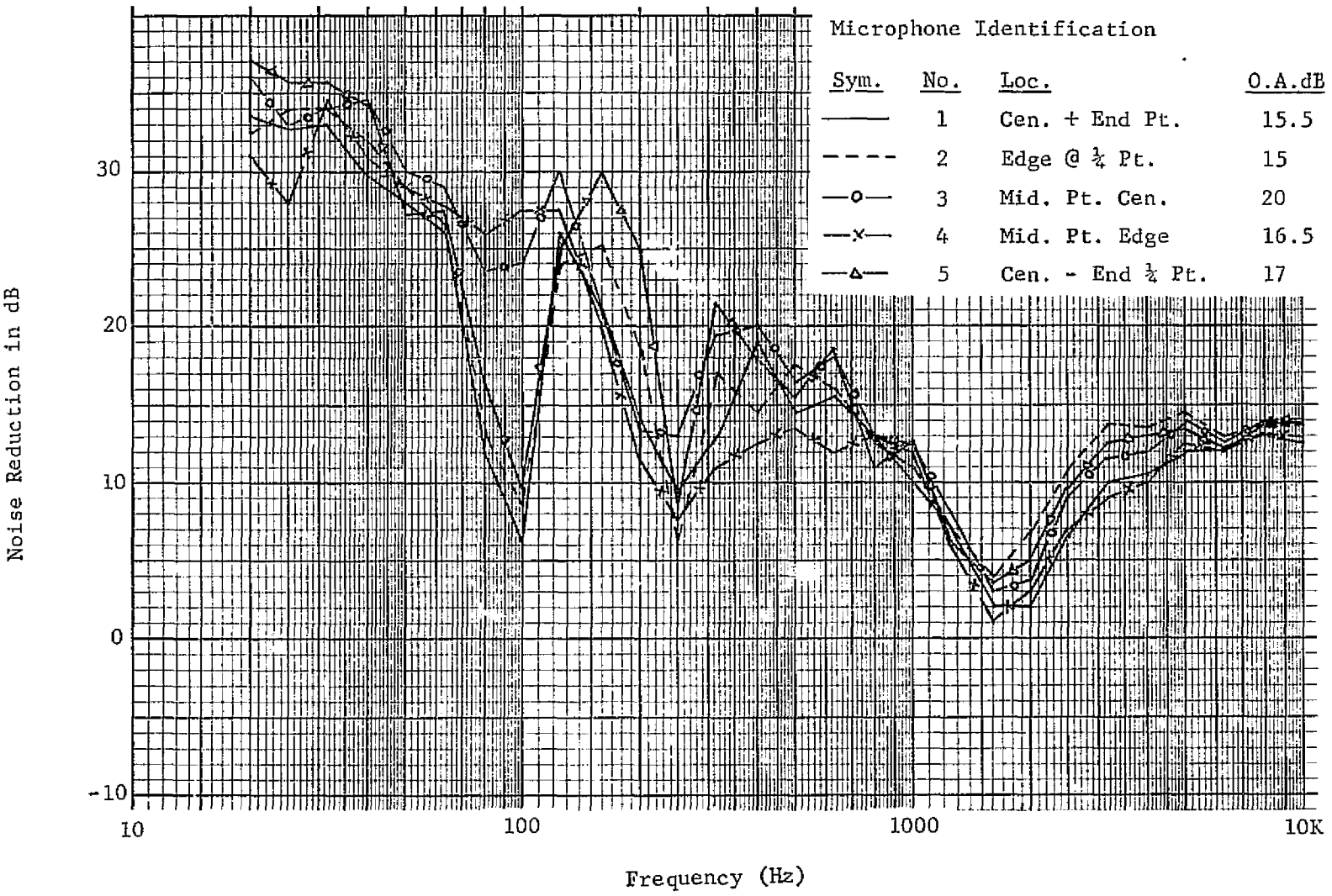

Figure 26B. Noise Reduction for Aluminum Shroud - $\Delta P = 0.7$ p.s.i.

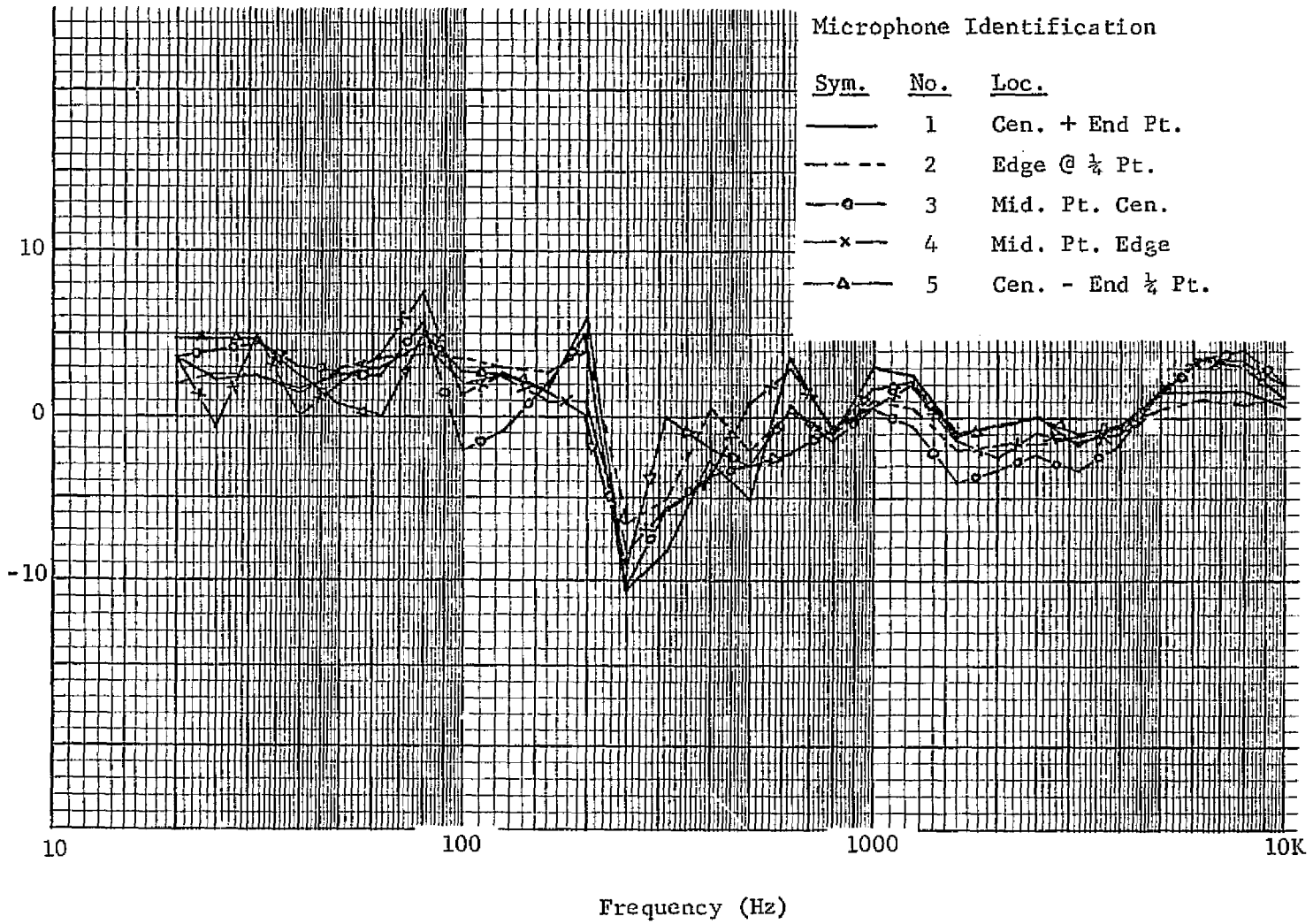

Figure 27B. Comparison of Aluminum Shroud Noise Reduction Data - (0.7 psi Minus Ambient Condition Data)

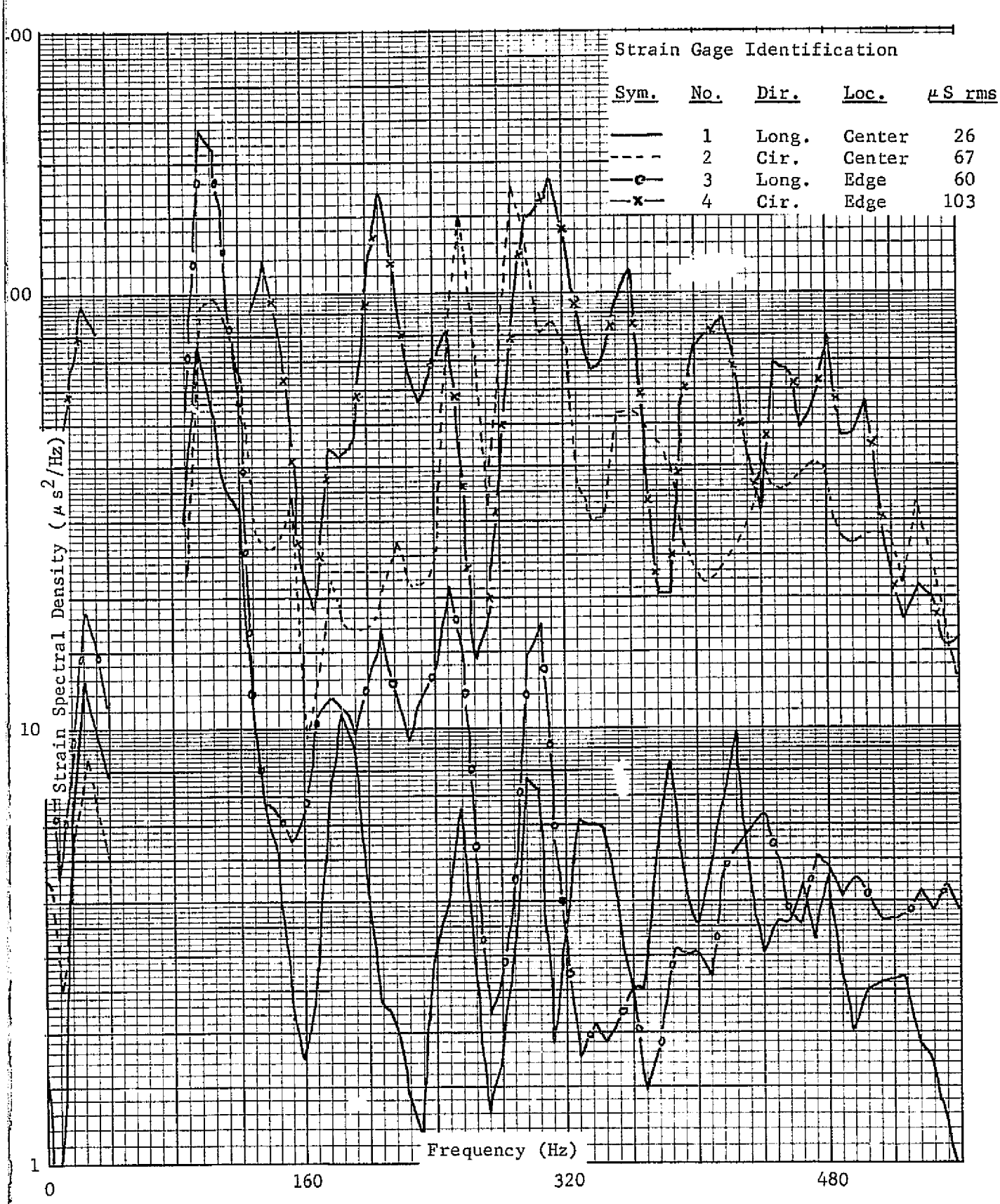

Figure 28B. Composite Strain Gage Data - Aluminum Shroud, $\Delta P = 0.7$ psi, External Panel

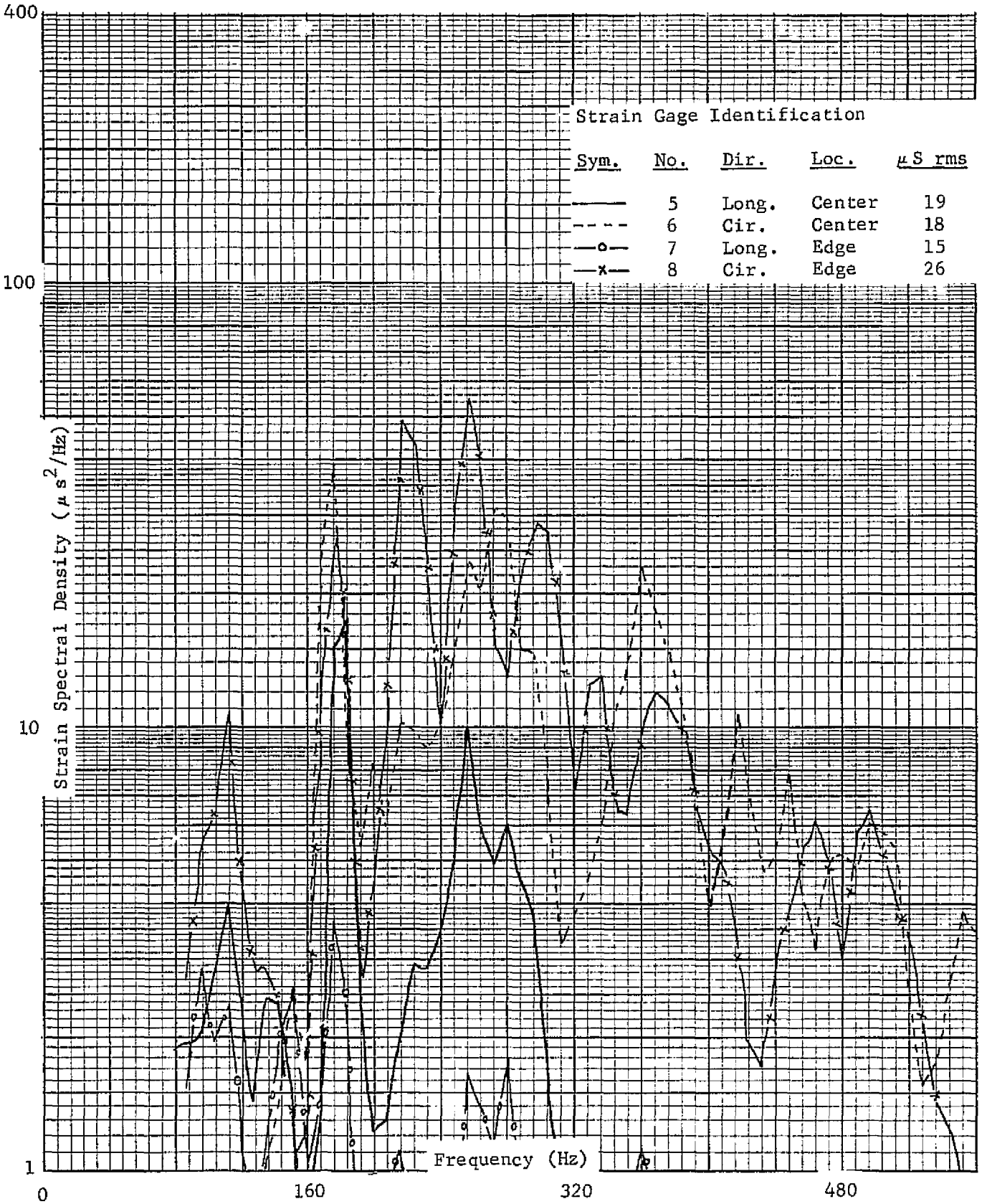

Figure 29B. Composite Strain Gage Data - Aluminum Shroud, $\Delta P = 0.7$ psi, Internal Panel

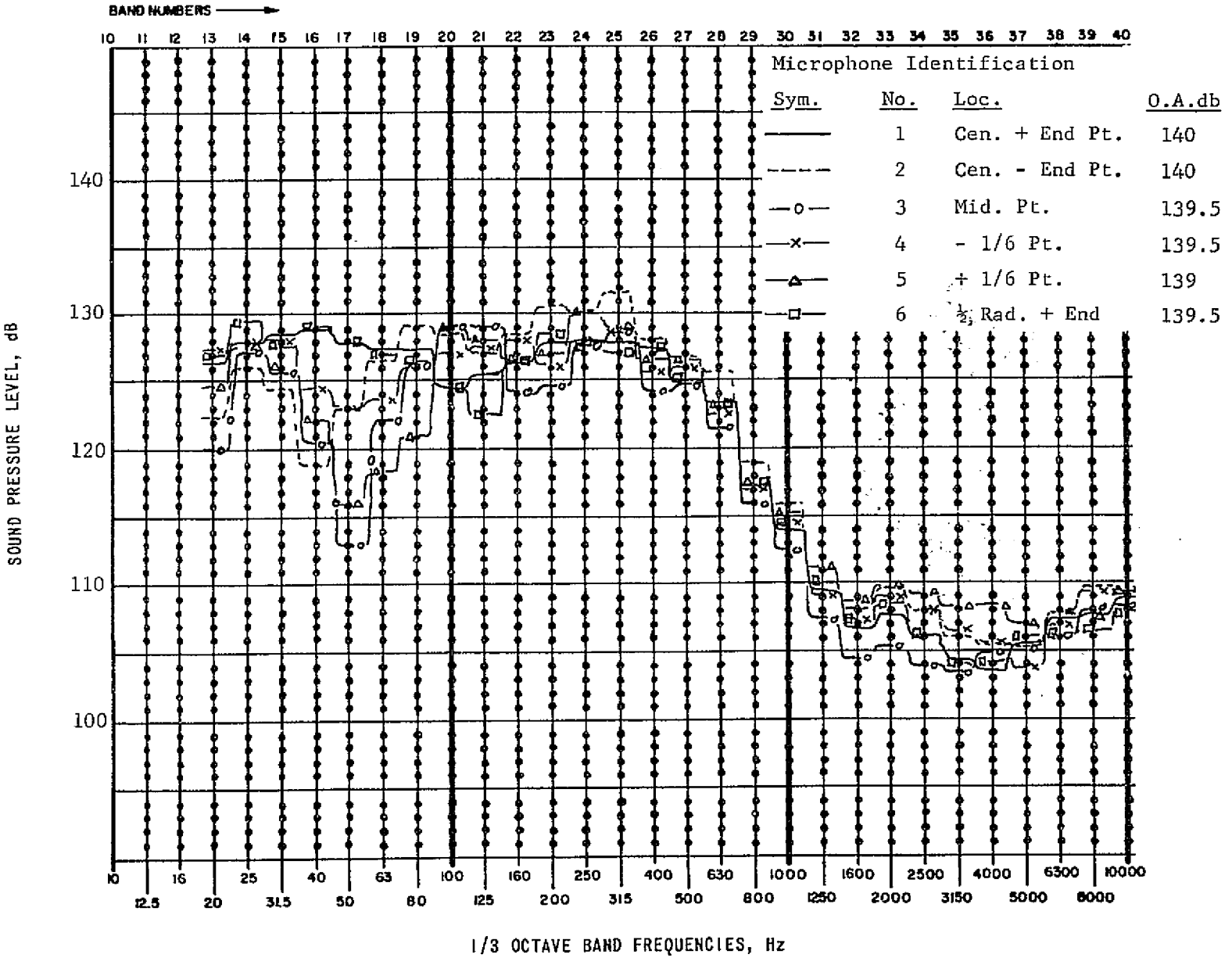

Figure 30B. Composite External Microphone Data - Aluminum Shroud, 0.2 psi Helium

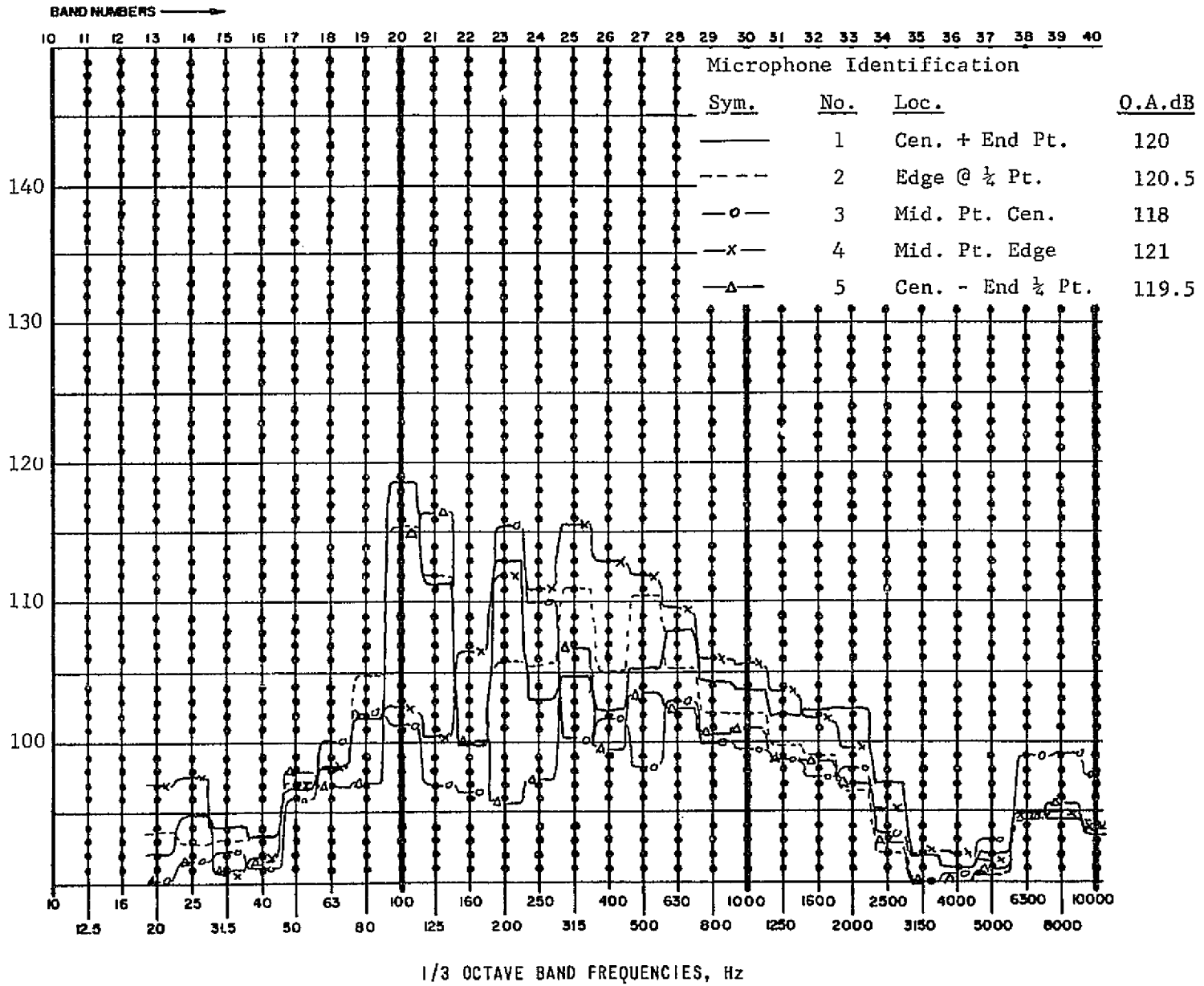

Figure 31B. Composite Internal Microphone Data - Aluminum Shroud, 0.2 psi Helium

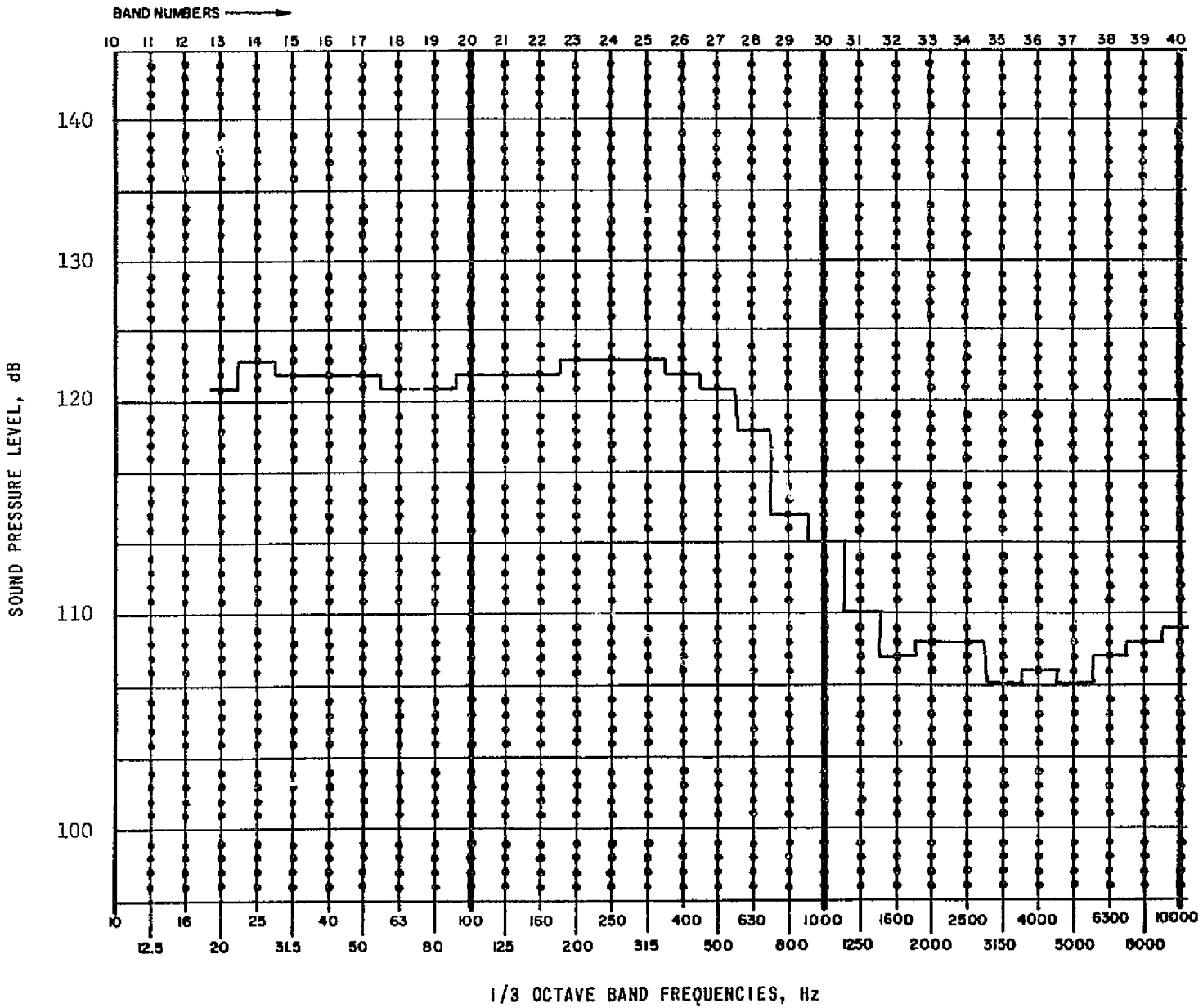

Figure 32B. Average of External Microphone Data - Aluminum Shroud, 0.2 psi Helium, 140 dB Overall

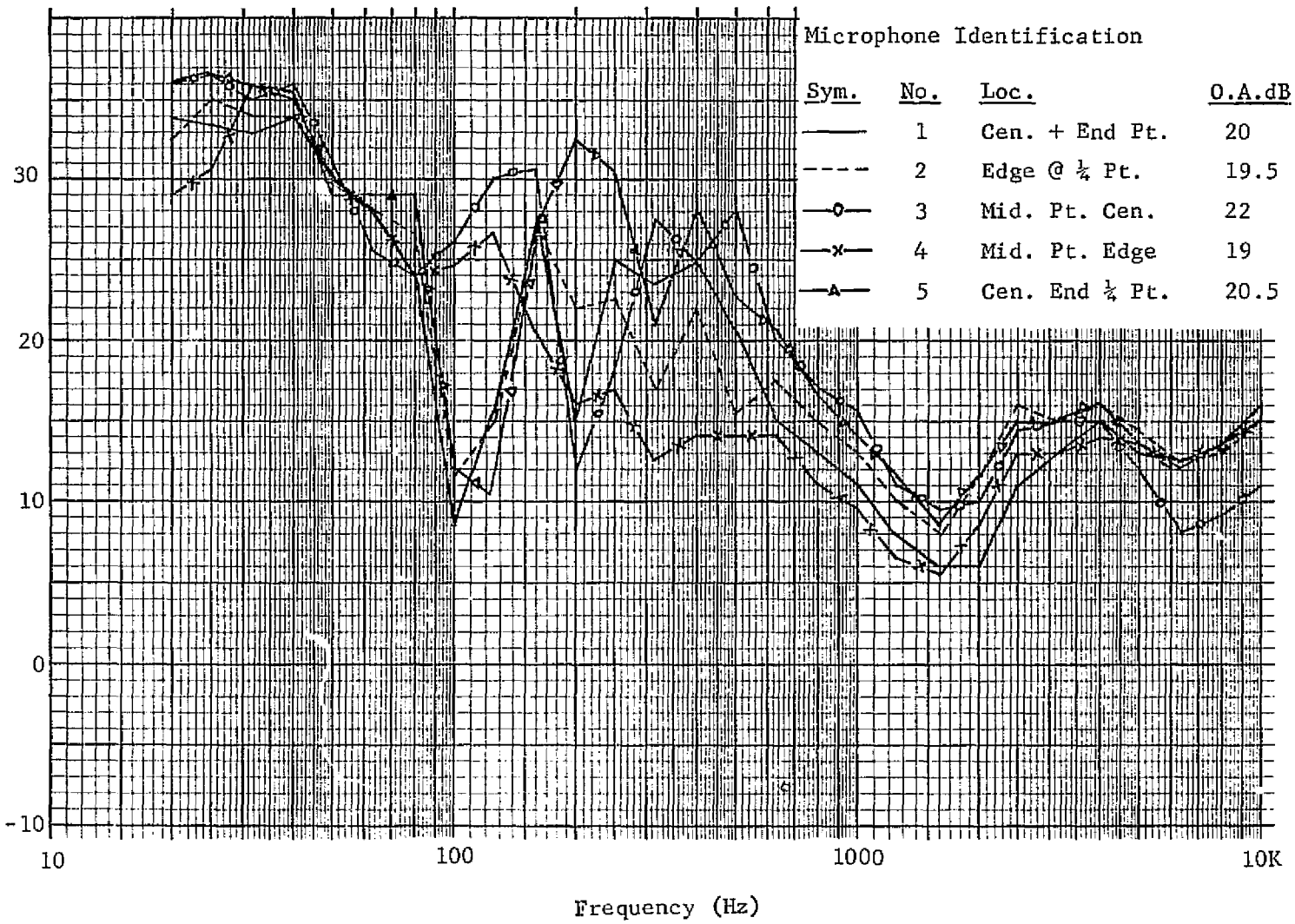

Figure 33B . Noise Reduction for Aluminum Shroud - 0.2 psi Helium Condition

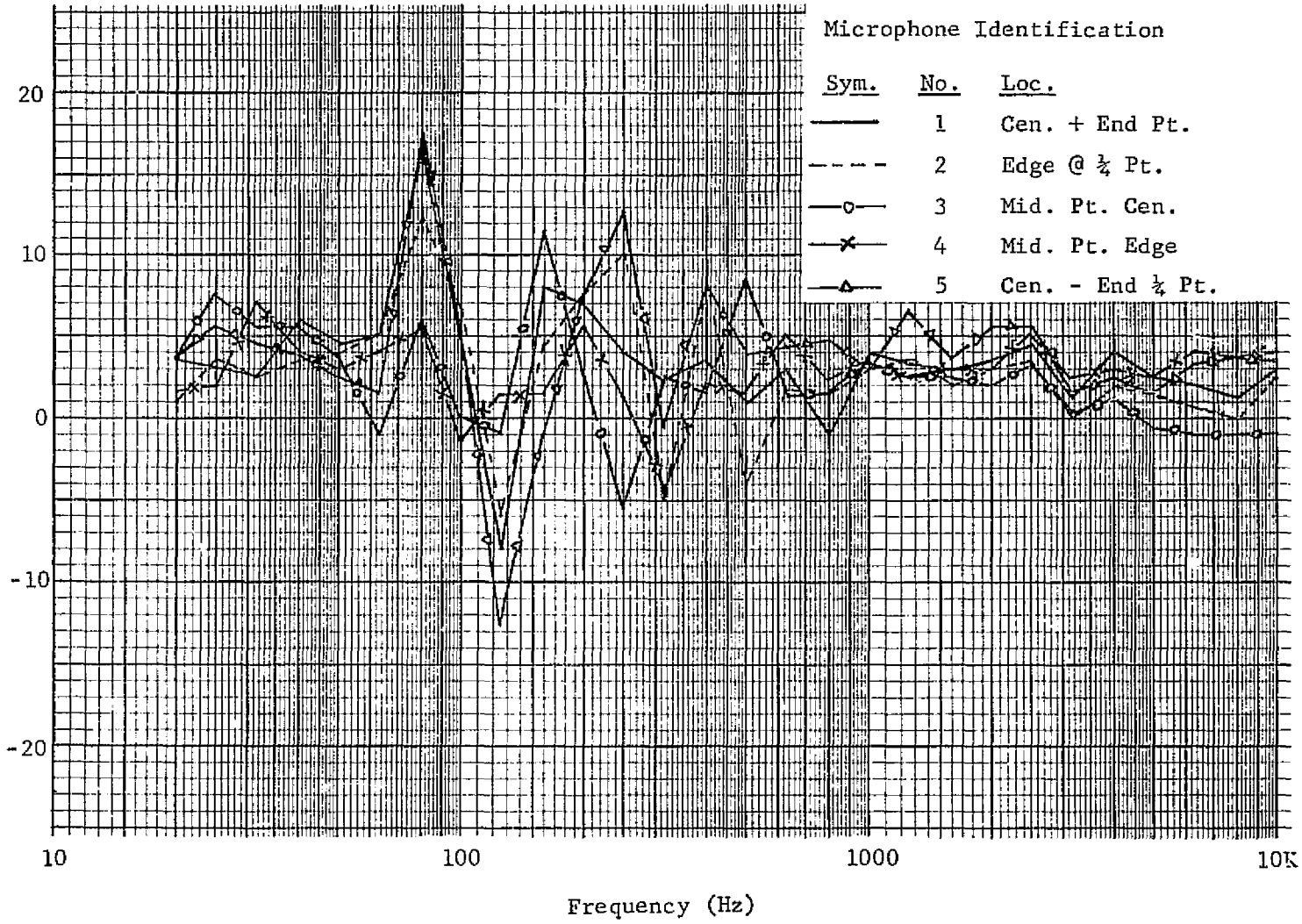

Figure 34B. Comparison of Aluminum Shroud Noise Reduction Data - (0.2 psi Helium Minus Ambient Condition Data)

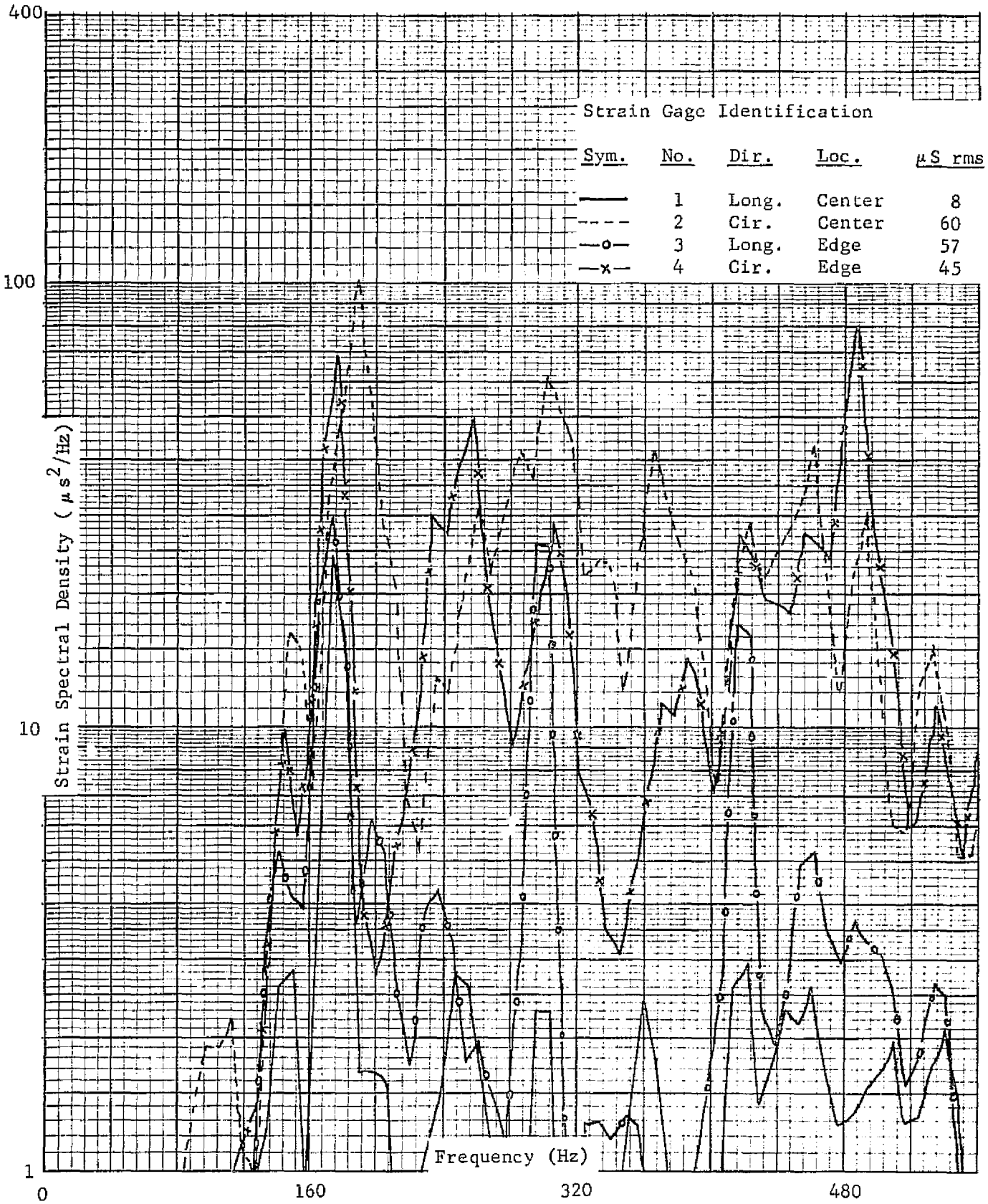

Figure 35B. Composite Strain Gage Data - Aluminum Shroud, 0.2 psi Helium, External Panel

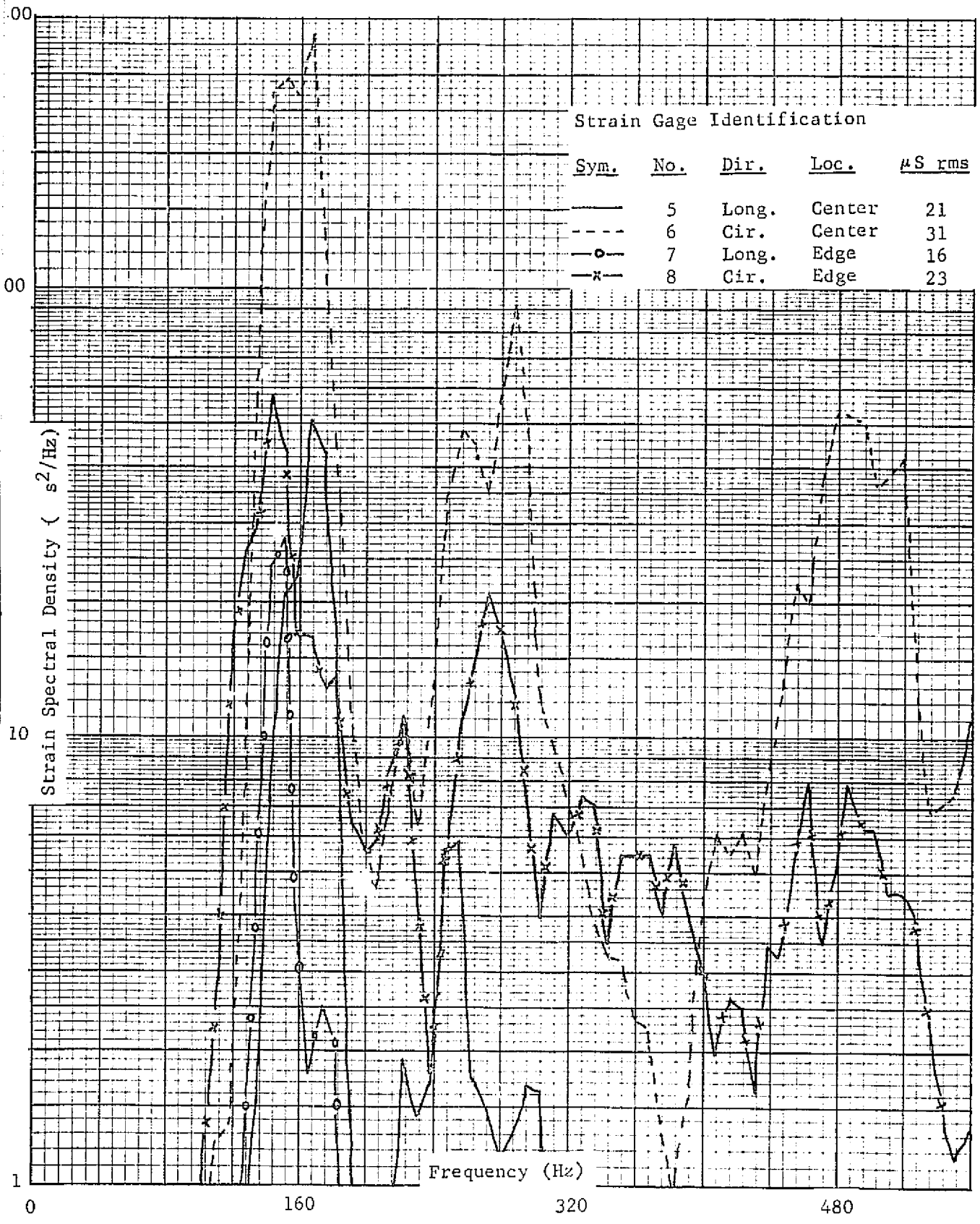

Figure 36B. Composite Strain Gage Data - Aluminum Shroud, 0.2 psi Helium, Internal Panel